

Dissertation zur Erlangung des Doktorgrades
der Fakultät für Chemie und Pharmazie
der Ludwig-Maximilians-Universität München

**SYNTHESIS AND INVESTIGATION OF
NEW FLUOROMETHYLATING
AGENTS AND THEIR IMPACT ON
FORMING ENERGETIC MATERIALS**



Marco Reichel

aus

München, Deutschland

2020

Erklärung

Diese Dissertation wurde im Sinne von § 7 der Promotionsordnung vom 28. November 2011 von Herrn Professor Dr. Konstantin L. Karaghiosoff betreut.

Eidesstattliche Versicherung

Diese Dissertation wurde eigenständig und ohne unerlaubte Hilfsmittel erarbeitet.

München, den 20.02.2020

MARCO REICHEL

Dissertation eingereicht am:	20.02.2020
1. Gutachter:	Prof. Dr. Konstantin L. Karaghiosoff
2. Gutachter:	Prof. Dr. Thomas M. Klapötke
Mündliche Prüfung am:	20.04.2020

Dedicated to my parents and family

Der Blauwal

*Dieser so monstergroße Wal,
hüpft und springt wie ein Delfin.
Sympathisch ist er allemal
und viele Menschen lieben ihn.*

Heidi Schmitt-Lermann



Acknowledgement

First of all, I would like to thank my doctor father, Prof. Dr. Konstantin L. Karaghiosoff, for giving me the opportunity doing my Ph.D. in his research group. I am very grateful that I have been given freedom in the field of research. Further I want to thank Prof. Dr. Konstantin L. Karaghiosoff for my given possibility to participate at several conferences and workshops. I would also express my gratitude for financial support to him. Prof. Dr. Karaghiosoff is one of the most cordial professors with great intellect and vision I have ever met. It was an honor to be able to do my Ph.D. under his guidance. Thank you for the enriching time and for your friendship!

Secondly, I would like to thank Prof. Dr. Thomas M. Klapötke for the friendly reception in his chair, the confidence and the support he gave to me. I would also like to express my sincere thanks for taking over the second review of this thesis.

I also owe great gratitude to Prof. Dr. Andreas Kornath, without whom this work would not have been possible. Thank you for the great efforts you have made to write proposals together with us. Also thanks for the always enjoyable and generous excursions that we have undertaken.

In addition, special thanks go to AOR Dr. Burkhard Krumm to whom I am most grateful for the corrections of several papers and his patience. To Dr. Burkhard Krumm I would like to express my sincere thanks for the great help in writing proposals and in arranging an extremely successful cooperation between the university of Bielefeld.

My thanks also go to AOR Dr. Jörg Stierstorfer, who helped me with calculations and with whom a good knowledge transfer regarding tetrazolates resulted.

At this point I would also like to thank my cooperation partners Prof. Dr. Norbert Mitzel, Dr. Jan Schwabedissen, Dr. Yuri Vishnevskiy, Dr. Sebastian Blomeyer and Dr. Hans-Georg Stammer for the good and successful cooperation.

I thank Dr. Marc Andre Althoff for the informative excursions and the interesting and instructive training at the Bundeswehr in Sonnthofen, which he led. Furthermore, for the friendly conversations, the amusing evenings at conferences and the possibility to work with him.

Once again I would like to thank F-Select GmbH especially for the successful cooperation over many years and the industrial donations without which the topic of this dissertation would not have been possible.

I would like to thank Ms. Irene Scheckenbach, who with her thoughtful and warm manner is an enrichment for the research group.

I want to express my gratitude firstly to the members of the research group of Prof. Dr. Karaghiosoff. To M.Sc. Mara Egenhöfer, I thank you from the bottom of my heart for the wonderful time we spent together. As so often the time is unfortunately always too short, but I will always carry the beautiful moments in my heart. You know best, there are no words that

could express my deepest gratitude for this. So I remain with these words: I am proud of you and I hope to see you again! ···

Further I would like to thank M.Sc. Christin Kirst for her tireless efforts to write proposals with me. Thank you for the time and effort you took on me to help me! Also thank you for the funny moments we shared together. Thanks for all.

I thank M.Sc. Sarah Linert for her empathy in difficult moments and for the funny moments that have always arisen having you as our group member. Thanks also for the support which I could experience from you.

My gratitude goes secondly also to all members of the research group of Prof. Dr. Thomas M. Klapötke. To the former (Dr. Martin Härtel, Dr. Johann Glück, Dr. Marc Bölter, Dr. Thomas Reith) and current (M.Sc. Anne Friedrichs, M.Sc. Cornelia Unger, M.Sc. Teresa Küblböck, M.Sc. Maximilian Wurzenberger, M.Sc. Moritz Kofen, M.Sc. Alicia Dufter, M.Sc. Dominik Dosch, M.Sc. Greta Bikelyte, M.Sc. Max Born, B.Sc. Michael Gruhne, M.Sc. Alexander Harter, M.Sc. Stefanie Heimsch, M.Sc. Marcel Holler, B.Sc. Marcus Lommel, M.Sc. Elena Reinhardt, M.Sc. Maurus Völkl) members. Thanks for your support with measurements, graphic design, for the hospitality after our storage fire, the nice evenings together and for the nice and funny conversations we had together. Thank you for making the work a pleasure.

A special thanks goes to Dr. Ivan Gospodinov. Thank you for the great discussions regarding synthetic work and thank you for your friendship!

Also I want to express my gratitude to M.Sc. Anne Friedrich for being a great and friendly colleague.

M.Sc. Dominik Dosch is thanked for the successful cooperation and for the excursion to the swabian language.

In addition, I am grateful to M.Sc. Thomas Schnappinger for helping me with any calculation problems and giving me solutions.

Stefan Huber is thanked for his friendly and so helpful manner regarding the sensitivity measurements, joining the ABC-Abwehr team and in general for the nice conversations.

In this context I would like to thank my bachelor-, “F-” and master students, by name Freddy Saunders, Hannes Dettlaf, Fabian Huck, Laura Huber, Maximilian Mader, Eduard Wöllner, Martin Obermeier, Alexander Harter, Michael Mertens, Lukas Nusser, Sami Sile, Philipp Schmidt, Nathalie Kurle, Patrick Schüller, Christoph Seifert, Timotheus Hohl, Erol Ceylan, Nina Gordon, Alexander Gisnapp and Kevin Stuke who helped me during my synthetic work.

I would like to thank my friends here as well. I would especially like to mention Gabi Wagenstetter, Annette Brandl, Thomas Schnappinger and Maximilian Netter. Thank you for your friendship and your support in all situations of life!

Finally, I would like to thank my family from the bottom of my heart! Without your support this work would not have been possible! I thank my mother for her incredible patience with me. Thanks for all you had to endure through me. Without you, I wouldn't have become a person I am today! I thank my father who taught me everything I am. Thank you for dedicating all of

your energies to me in all areas of my life. Even without you, I would never have been as successful as I am allowed to be today. Furthermore, I would like to thank my sister. Thank you for your organizational talent and your empathy, when I just missed the head to anything and thank you for your warm-hearted good nature! I am also grateful for Helmut. With you I have won not only a good friend but also a brother. Thanks that you were always at my side and always cheered me up. Thank you for the beautiful and funny time! Furthermore, I would like to thank my grandparents. You became like second parents for me, who taught me with your wisdom and life experience what it means to become a diligent, honorable and righteous person. Thank you for the wonderful time together which I will never forget! I also thank my uncle and aunt, as well as my cousins with whom I was always allowed to spend a great time. Byoungmoo, I also want to thank you for being like a second dad to me. It is a blessing to have a friend like you, who is an inherent part of the family! And I always consider, 50% of the Nobel Prize ... I am also grateful to be able to number Wolfgang and Erika to our family, with whom we had such beautiful and amusing evenings together, which were so necessary to be able to switch off.

Finally, I would like to thank Flauschiwauschi Emma. Thank you for taking away my fears of dogs, for being open for caresses and for the nice time out you took me for a walk. There can never be a better dog!

Thank you!

Table of Content

1 Introduction	1
1.1 Overview	1
1.1.1 Magic of Fluorine	1
1.1.2 Organofluorine Compounds.....	2
1.1.3 References.....	4
1.2 Reagents for Selective Fluoromethylation – a Challenge in Organofluorine Chemistry.....	5
1.2.1 Introduction.....	6
1.2.1.1 General Overview	6
1.2.1.2 Historical Overview of Monofluoromethylating Reagents.....	9
1.2.2 Agents for Direct Monofluoromethylation	9
1.2.2.1 Electrophilic Monofluoromethylation.....	9
1.2.2.1.1 Fluoromethyl Halides	9
1.2.2.1.2 Fluoromethyl Sulfonates	12
1.2.2.1.3 <i>S</i> -(Monofluoromethyl)diarylsulfonium Tetrafluoroborate.....	13
1.2.2.1.4 <i>N,N</i> -(Dimethylamino)- <i>S</i> -phenyl- <i>S</i> -monofluoromethyl phenyloxosulfonium Triflate.....	13
1.2.2.1.5 Monofluoromethyl-substituted Sulfonium Ylids	14
1.2.2.2 Nucleophilic Monofluoromethylation.....	14
1.2.2.3 Radical Monofluoromethylation	15
1.2.2.3.1 <i>N</i> -Tosyl- <i>S</i> -fluoromethyl- <i>S</i> -phenylsulfoximine.....	15
1.2.2.3.2 Fluoromethylsulfonyl Chloride	16
1.2.2.3.3 Metal Fluoromethyl Sulfinates.....	16
1.2.2.3.4 Monofluoromethyl Sulfones.....	17
1.2.3 Indirect Monofluoromethylation.....	18
1.2.3.1 Nucleophilic Precursors	18
1.2.3.1.1 Fluoromalonates	18
1.2.3.1.2 Fluoromethylphenylsulfone and Related Compounds	19
1.2.3.1.3 Fluorobis(phenylsulfonyl)methane	21
1.2.3.1.4 2-Fluoro-1,3-benzothiole-1,1,3,3-tetraoxide	23
1.2.3.2 Phosphorus Containing Fluoromethylating Reagents.....	24
1.2.4 Conclusion	25
1.2.5 Acknowledgement	25

1.2.6 References.....	25
1.3 Objectives	31
2 Summary and Conclusion	32
3 Fluoromethyltriflate: Magic Fluoromethyls Little Brother	41
3.1 Introduction	41
3.2 Results and Discussion	42
3.3 Conclusion.....	50
3.4 Acknowledgement.....	50
3.5 Experimental Section.....	50
3.5.1 General Procedure.....	50
3.5.2 Preparation	51
3.6 References	57
3.7 Supporting Information	60
4 Fluoromethyl 2,4,6 trinitrobenzenesulfonate: A New Electrophilic Monofluoromethylating Reagent.....	62
4.1 Introduction	62
4.2 Results and Discussion	63
4.3 Conclusion.....	70
4.4 Acknowledgement.....	71
4.5 Experimental Section.....	71
4.5.1 General Procedure.....	71
4.5.2 Preparation	71
4.6 References.....	78
4.7 Supporting Information	79
5 The Correlation Between Structure and Energetic Properties of Three Nitroaromatic Compounds: Bis(2,4-dinitrophenyl) Ether, Bis(2,4,6-trinitrophenyl) Ether and Bis(2,4,6-trinitrophenyl) Thioether	83
5.1 Introduction	83
5.2 Results and Discussion	84
5.2.1 Synthesis and Properties	84
5.2.2 Structure Property Relationship.....	85
5.2.3 Energetic Properties	88
5.3 Conclusion.....	89
5.4 Acknowledgement.....	89

5.5 Experimental Section.....	89
5.5.1 General Procedure.....	89
5.5.2 Preparation	90
5.6 References	91
5.7 Supporting Information	93
6 Preparation and Investigation of Fluoromethyl Azide and Chalcogenocyanates	94
6.1 Introduction	95
6.2 Results and Discussion	95
6.3 Conclusion.....	99
6.4 Acknowledgement.....	99
6.5 Experimental Section.....	100
6.5.1 General Procedure.....	100
6.5.2 Preparation	100
6.6 References	102
7 Releasing the “Beast”: Direct, Silver Catalyzed Electrophile Monofluoromethylation	103
7.1 Introduction	104
7.2 Results and Discussion	105
7.3 Conclusion.....	110
7.4 Acknowledgement.....	111
7.5 Experimental Section.....	111
7.5.1 General Procedure.....	111
7.5.2 Preparation	111
7.6 References	115
7.7 Supporting Information	116
8 Synthesis and Investigation of Quarternary Phosphonium Salts Containing the Bioisoster - CH ₂ F Moiety	117
8.1 Introduction	117
8.2 Results and Discussion	118
8.3 Conclusion.....	129
8.4 Acknowledgement.....	129
8.5 Experimental Section.....	129
8.5.1 General Procedure.....	129
8.5.2 Synthesis and Characterization.....	130
8.6 References	133

8.7 Supporting Information	135
9 Synthesis and Properties of the Fluoromethylating Agent – (Fluoromethyl)triphenylphosphonium Iodide	137
9.1 Introduction	137
9.2 Results and Discussion	139
9.2.1 Synthesis and Properties	139
9.2.2 Crystal Structure	140
9.2.3 Vibrational Spectra	142
9.3 Conclusion	142
9.4 Acknowledgement	143
9.5 Experimental Section.....	143
9.5.1 General Procedures	143
9.5.2 Preparation	144
9.6 References	145
9.7 Supporting Information	146
10 <i>O,O</i> -Diethyl <i>O</i> -[2-(dimethylamino)ethyl] Phosphorothioate: Structural Evidence of the Decomposition Product and its Oxalate Salt	147
10.1 Introduction	148
10.2 Results and Discussion	149
10.2.1 Synthesis	149
10.2.2 NMR Spectroscopy	150
10.2.3 Vibrational Spectroscopy	150
10.2.4 Mass Spectrometry.....	151
10.3 Molecular and Crystal Structure.....	151
10.3.1 Compound 2.....	151
10.3.2 Compound 3.....	154
10.4 Conclusion	156
10.5 Acknowledgement	156
10.6 Experimental Section.....	156
10.6.1 General Procedure.....	156
10.6.2 Preparation	157
10.7 References	159
11 Synthesis and Investigation of Highly Energetic and Shock-sensitive Fluoromethyl Perchlorate	161

11.1 Introduction	161
11.2 Results and Discussion	162
11.2.1 Synthesis	162
11.2.2 NMR Spectroscopy	162
11.2.3 IR Spectroscopy	163
11.2.4 Mass Spectrometry.....	164
11.2.5 Energetic Properties	164
11.3 Acknowledgement	165
11.4 Experimental Section.....	165
11.4.1 General Procedures	165
11.4.2 Preparation	166
11.5 References	166
12 Solid/Gas Phase Structures and Energetic Properties of the Dangerous Methyl and Fluoromethyl Nitrates.....	169
12.1 Introduction	169
12.2 Results and Discussion	170
12.2.1 Synthesis	170
12.2.2 NMR Spectroscopy	170
12.2.3 Vibrational Spectroscopy	171
12.2.4 Structural Properties.....	171
12.2.5 Energetic Properties	173
12.3 Conclusion	175
12.4 Acknowledgement	176
12.5 Experimental Section.....	176
12.5.1 General Procedures	176
12.5.2 Preparation	176
12.6 References	177
12.7 Supporting Information	180
12.7.1 Crystal Growth.....	180
12.7.2 Structure Refinement Data.....	180
12.7.3 References.....	181
12.7.4 Gas-phase Electron Diffraction.....	182
12.7.4.1 General Information	182
12.7.4.2 Structural Analysis of MN	183

12.7.4.3 Structural analysis of FMN	184
12.7.4.4 References	185
13 Monofluoromethylated Nitrogen Rich Heterocycles: Synthesis, Characterization and Fluorination Effect.....	185
13.1 Introduction	186
13.2 Results and Discussion	187
13.3 Conclusion	196
13.4 Acknowledgement	196
13.5 Experimental Section.....	196
13.5.1 General Procedure.....	196
13.5.2 Preparation	197
13.6 References	199
13.7 Supporting Information	201
14 Appendix	204
14.1 List of Abbreviations	204
14.2 Computations.....	205
14.3 References	206
14.4 List of Publications	206
14.5 List of Presentations	207

1 Introduction

1.1 Overview

1.1.1 Magic of Fluorine

“Fluorine is a small atom with a big ego” – this statement^[1] is well founded. The *magic of fluorine* is often used in context with its unique properties and the quite different behavior of fluorine containing compounds, as compared to the corresponding fluorine free analogues.^[1] However, this difference is less due to magic, but is the consequence of three main reasons:^[2]

- 1) combination of high electronegativity with moderate size
- 2) perfect match of 2s / 2p orbitals with the orbitals of carbon
- 3) extremely low polarizability

Thus, as a consequence the introduction of one or more fluorine atoms into naturally occurring molecules will result in different physical, chemical and biological properties.^[3] Fluorine is the most electronegative element (χ : 3.98), which makes the carbon fluorine bond highly polar with a typical dipole moment of about 1.4 D.^[2] This affects the electrostatic environment and changes (or even inverts) the chemical reactivity of the molecule. For example, hydrocarbon systems like benzene can react with electrophiles to form substituted benzenes. In contrast perfluorobenzene can only be substituted using nucleophiles. Depending on the number of fluorine atoms introduced into a compound, it can be made more polar (semi fluorinated compounds) or less polar (perfluorinated compounds) with the dipoles compensating each other.^[3]

The large positive charge of the fluorine nucleus and the weak shielding effects by inner shell electrons cause a stabilization of the valence orbitals of fluorine (2s, 2p) (Figure 1).^[1]

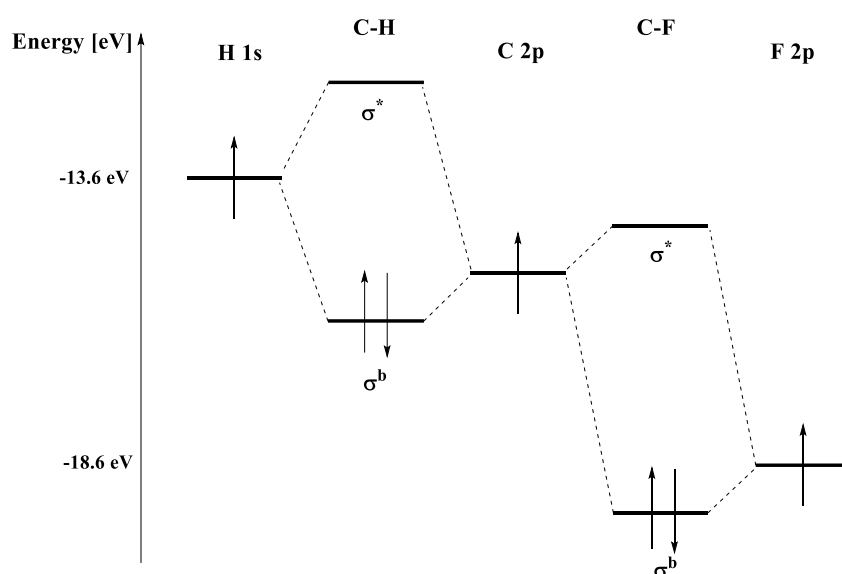


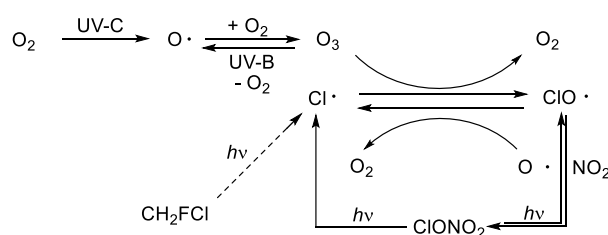
Figure 1: Molecular Orbital (MO) diagram for the C-H and C-F bond.

Due to the high electronegativity of fluorine its 2p orbitals are stabilized by about 5 eV with respect to the 1s orbital of hydrogen, resulting in energetically lower HOMO and LUMO orbitals for C-F compounds as compared to corresponding C-H analogues (Figure 1). This indicates for fluorine compounds a higher reactivity towards a reducing agent (accepting an electron in the LUMO) and a lower reactivity towards an oxidizing agent (donating an electron from the HOMO).^[1]

Fluorine atoms, which possess three pairs of negatively charged electrons, act due to their extremely low polarizability – particularly in perfluorinated systems – like a protective shield and shields the carbon backbone from chemical attack.^[2-3] Another consequence of the low polarizability are very weak intermolecular dispersion interactions in perfluorocarbons.^[2] Concerning the physical properties, fluorination mainly affects the boiling point (decreased), the surface tension (decreased), the lipophilicity (increased), the miscibility and the ability to dissolve gases. The latter two properties follow the rule “*similia similibus solvuntur*” and depend on the polarity of the specific compound.^[1] regarding the chemical properties, the high stability of the C-F bond is most important. Fluorine containing organic compounds are quite stable against nucleophilic attacks. Also the dramatic increase of the pK_a value in comparing fluorine containing and fluorine free carbonic acids (for example acetic acid: $pK_a = 4.76$; triflic acid: $pK_a = 0.52$) is substantial.^[1] Regarding the biological properties introduction of fluorine mainly affects the binding affinity of the molecules to proteins (increased) and the metabolic stability (increased).^[4] In addition the bioisosteric relationship of a fluorine atom to various functional groups (H, OH, NH₂, CH₃, NO₂) is of considerable importance.^[5] All these beneficial effects discussed above have been used by mankind for several decades to produce crystals, dyes, surfactants, membranes, polymers, pharmaceuticals and agrochemicals with special and unique properties.^[6]

1.1.2 Organofluorine Compounds

The first class of organofluorine compounds which were industrially applied in the beginning of the 1930s were chlorofluorocarbons (CFC). These compounds are highly volatile, non-toxic, non-flammable and display the ideal properties of refrigerants. In fact, this possibility was recognized early and halofluorocarbons were widely used in various freezers (HFC-22; CHClF₂), fridges (HFC-134a; CF₃CH₂F), air conditioning systems (CFC-12; CCl₂F₂) and fire extinguishers (Halon 1211; CBrClF₂). Thus, at peak times, about one million tons per year of the so called *Frions* were produced. However, as early as 1974, physicists warned that the accumulation of persistent CFCs in the atmosphere would lead to a significant decrease in ozone concentration (Scheme 1).^[2,7]



Scheme 1: Filtering of the UV-C and UV-B radiation by ozone molecules and the ozone depleting cycle caused by CFCs.

Since the ozone hole above the Antarctic has been occurring annually since the early 1980s and due to the clear cause of this phenomenon, quick action was required.^[2] By the decision documented in the Montreal Protocol in 1987 the use of ozone-depleting compounds was severely restricted and is currently phased out.^[2,8] Much effort has been invested to develop new non ozone-depleting materials to replace the ozone-damaging compounds. Fluorinated ethers seem to be suitable alternatives (E143a; CF_3OCH_3 or E134; $\text{CHF}_2\text{OCHF}_2$).^[2] The strong regulation of these substances, resulted 2012 for the first time in a small reduction of the hole in the ozone layer. A comparison of the size of the ozone hole in 2000 and 2018 is shown in Figure 3.^[9]

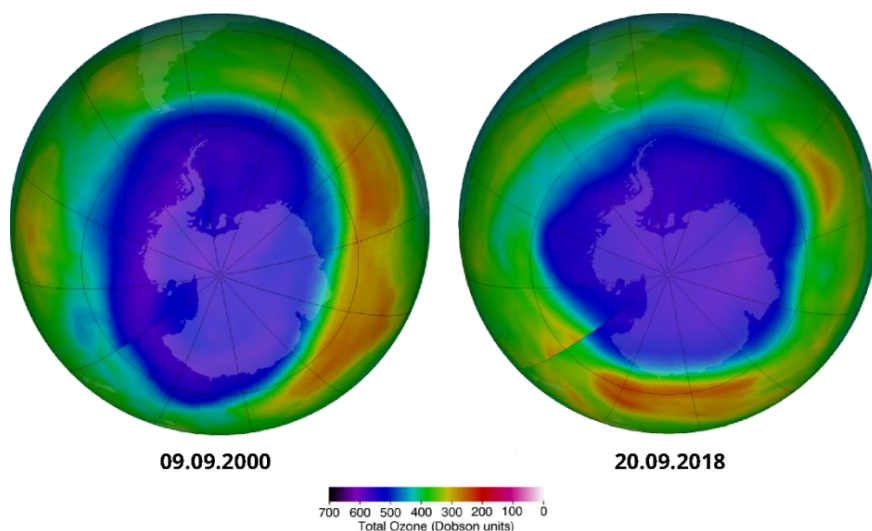


Figure 3: Ozone hole over the Antarctic. Ozone concentration in Dobson unit. One Dobson unit is referred to the number of ozone molecules that are required to form a 0.01 mm thick pure ozone layer at 0 °C and 1 atm.

The discovery of polytetrafluoroethylene (PTFE) and polytrifluoroethylene (Kel-F) in the 1940s marked the beginning of another era of organofluorine compounds. PTFE seals in combination with compressed nickel powder diffusion barriers enabled the separation of the extremely aggressive uranium hexafluorides $^{235}\text{UF}_6$ and $^{238}\text{UF}_6$ within the Manhattan Project and were fundamental for the construction of a nuclear bomb.^[2] Meanwhile PTFE, Kel-F or other perfluorinated organic substances are used for various applications such as Goretex protective clothing, kitchenware (Teflon Pan), furniture (Scotchgard), in space shuttle seals, in extinguishing foam (perfluoroactanoic acid) and many more.^[2] Currently, however, these extinguishing agents are severely criticized because they are very persistent and bioaccumulative.^[10]

In 1950 the era of fluoropharmaceuticals and fluorine containing agrochemicals began. Today about 20 % of all pharmaceuticals and 30-40 % of all agrochemicals contain fluorine (Figure 4).^[11]

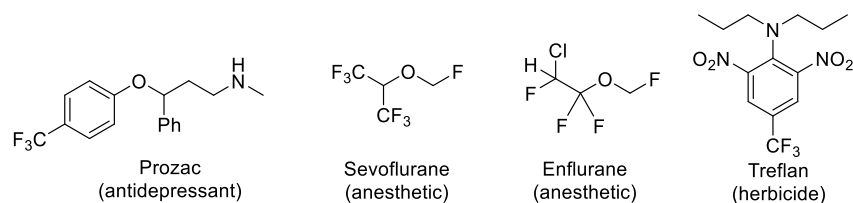


Figure 4: Selected fluorine containing pharmaceuticals and agrochemicals.

Not only ^{19}F pharmaceuticals, but also ^{18}F labeled radiopharmaceuticals are in the focus of interest. Fluorine-18 has a half lifetime of 109.7 min and is utilized as β^+ - emitter in positron emission tomography (PET). Frequently used representatives are for example fluoro-desoxyglucose or fluoro-L-dopa (Figure 5).^[2-3]

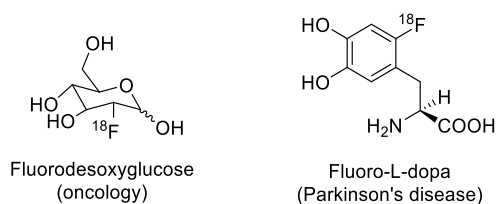


Figure 5: Examples of ^{18}F labeled radiopharmaceuticals.

Mechanisms of action are different. A tumor, for example, has a high glucose requirement. In the case of fluorodesoxyglucose, ^{18}F labeled glucose is accumulated due to the high metabolic stability caused by substitution with fluorine in the tumor. Because of the positron emission during the decay of ^{18}F to ^{18}O the tumor can be visualized in the PET.^[2]

Other important applications of organofluorine compounds were discovered in 1980 (gases for plasma etching processes and cleaning fluids for the semiconductor industry), 1990 (liquid crystals for LCD displays) and 2000 (fluorinated photoresistants).^[2] However, the pharmaceutical sector remains one of the most important industries using organofluorine compounds. In the field of fluorine containing pharmaceuticals, derivatives with fluorine containing alkyl substituents are of particular interest. In fact the introduction of a fluoroalkyl group in drug design has become a routine practice and the high demand of such building blocks motivated the development of a series of fluoroalkylating agents.^[12] The fluoromethyl (CH_2F) group is particularly important.^[5,13] However, the number of suitable direct electrophilic monofluoromethylating agents is limited.^[12, 14]

1.1.3 References

- [1] K. Uneyama, *Organofluorine Chemistry*, Wiley, **2008**.
- [2] P. Kirsch, *Modern Fluoroorganic Chemistry. Synthesis, Reactivity, Applications*, WILEY-VCH, **2004**.
- [3] G. Sandford *Philos. Trans. R. Soc., A* **2000**, 358, 455–471.
- [4] T. Liang, C. N. Neumann, T. Ritter *Angew. Chem., Int. Ed.* **2013**, 52, 8214–8264.
- [5] a) N. A. Meanwell *J. Med. Chem.* **2018**, 61, 5822–5880; b) N. A. Meanwell *J. Med. Chem.* **2011**, 54, 2529–2591.
- [6] R. Berger, G. Resnati, P. Mentrangolo, E. Weber, J. Hulliger *Chem. Soc. Rev.* **2011**, 40, 3496–3508.

- [7] M. J. Molina, F. S. Rowland *Nature* **1974**, *249*, 819.
- [8] EU, 1005/2009/EG, **2009**.
- [9] <https://www.eea.europa.eu/data-and-maps/figures/maximum-ozone-hole-area-in-6> (22.10.2019).
- [10] G. B. Post, P. D. Cohn, K. R. Cooper *Environ. Res.* **2012**, *116*, 93–117.
- [11] M. Reichel, J. Martens, E. Woellner, L. Huber, A. Kornath, K. Karaghiosoff *Eur. J. Inorg. Chem.* **2019**, *2019*, 2530–2534.
- [12] Y. Liu, L. Lu, Q. Shen *Angew. Chem., Int. Ed.* **2017**, *56*, 9930–9934.
- [13] a) G. A. Showell, J. S. Mills, *Drug Discovery Today* **2003**, *8*, 551–556; b) S. Zhang, Y. Zhang, Y. Ji, H. Li, W. Wang, *Chem. Commun. (Cambridge, U. K.)* **2009**, 4886–4888; c) Y. Zhou, J. Wang, Z. Gu, S. Wang, W. Zhu, J. L. Acena, V. A. Soloshonok, K. Izawa, H. Liu, *Chem. Rev. (Washington, DC, U. S.)* **2016**, *116*, 422–518.
- [14] J. Hu, W. Zhang, F. Wang, *Chem. Commun. (Cambridge, U. K.)* **2009**, 7465–7478.

1.2 Reagents for Selective Fluoromethylation – a Challenge in Organofluorine Chemistry

Marco Reichel, Konstantin Karaghiosoff

Accepted in *Angewandte Chemie*

DOI: 10.1002/anie.201913175



Abstract: The introduction of a monofluoromethyl moiety has undoubtedly become a very important area of research in recent years. Due to the beneficial effects of organofluorine compounds - such as their metabolic stability - the incorporation of the CH₂F group as a bioisosteric substitute for various functional groups is an attractive strategy for the discovery of new pharmaceuticals. Furthermore, the monofluoromethyl unit is also widely used in agrochemistry, in pharmaceutical chemistry and in fine chemicals. The problems associated with climate change and the growing need for environmentally friendly industrial processes means that alternatives to the frequently used CFC and HFBC fluoromethylating agents (CH₂FCl and CH₂FBr) are urgently needed and also required by the Montreal Protocol. This has recently prompted many researchers to develop alternative fluoromethylating agents. This article summarizes both the classical and new generation of fluoromethylating agents. Reagents which act *via* electrophilic, nucleophilic and radical pathways are discussed, in addition to their precursors.

1.2.1 Introduction

1.2.1.1 General Overview

Fluorine occurs abundantly in nature as fluorspar and fluorapatite.^[1] Despite these widespread natural resources, only one enzyme exists which has been confirmed as being able to perform fluorination: the fluorinase. However, current research suggests that there might be at least one more enzyme able to perform fluorination.^[2] Perhaps surprisingly, from an estimated 130,000 natural products, there are only 5 naturally occurring organofluorine compounds present in plants, bacteria or animals (Figure 1).^[1-2]

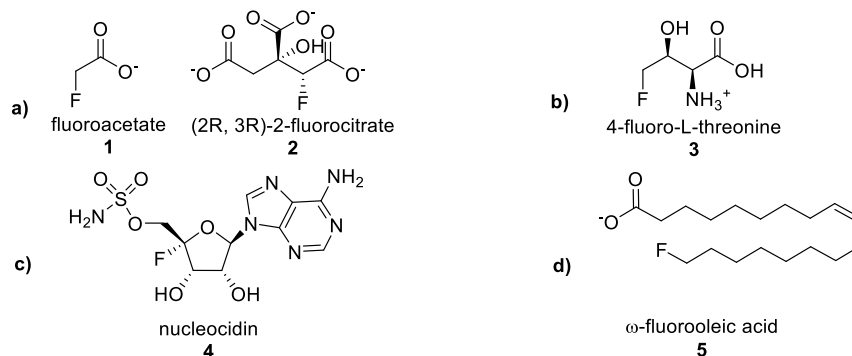


Figure 1: The five naturally occurring organofluorine compounds, which are found in plants, animals or bacteria; a) *Dichapetalum cymosum* b) *Streptomyces cattleya* c) *Streptomyces calvus* d) *Dichapetalum toxicarium*.

Fluoroacetate is the most common of the naturally occurring organofluorine compounds and occurs in about 40, mostly poisonous plants in the southern and tropical regions of Africa, Australia and Brazil.^[2-3] When it is considered that organofluorine compounds are almost absent in nature, it is remarkable that 20 % of all pharmaceuticals and 30 – 40 % of all agrochemicals contain fluorine.^[4] The reason for this is simple and can be clearly illustrated by considering the toxicity of *Dichapetalum cymosum*. After the incorporation of fluoroacetate, the C-F bond prevents the conversion of this compound in the citrate cycle to isocitrate and

stops, forming trans-aconitate instead of cis-aconitate, the citrate cycle.^[3b] The unique chemical, physical, biological properties and metabolic stability of organofluorine compounds makes them particularly interesting for the pharmaceutical and agricultural industries.^[5] These features make the monofluoromethyl group highly versatile as a bioisosteric unit for a series of functional groups occurring in biological systems (Figure 2).^[6]

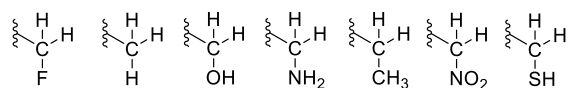


Figure 2: Selected functional groups to which the $-\text{CH}_2\text{F}$ moiety is bioisosteric.

This bioisosterism combined with the enhanced metabolic stability, bioavailability, lipophilicity and membrane permeability imparted by the fluorine substituent, allows efficient drug design.^[7] As a result, a variety of monofluoromethylated drugs and inhibitors have been developed (Figure 3). For instance, Afloqualone (**6**) is a muscle-relaxant and sedative with clinical use. Sevofluran (**7**) is a volatile anaesthetic with great significance in paediatric anaesthesia due to its good hypnotic but only weak analgesic and muscle relaxing properties. Fluticasone propionateTM (**8**) – a widely used drug against inflammatory diseases and as an analgesic in the treatment of certain cancers – is one of the industrially most important drugs.^[7b, 8] In addition to these well-established drugs, a number of inhibitors are also being tested.^[6a, 9]

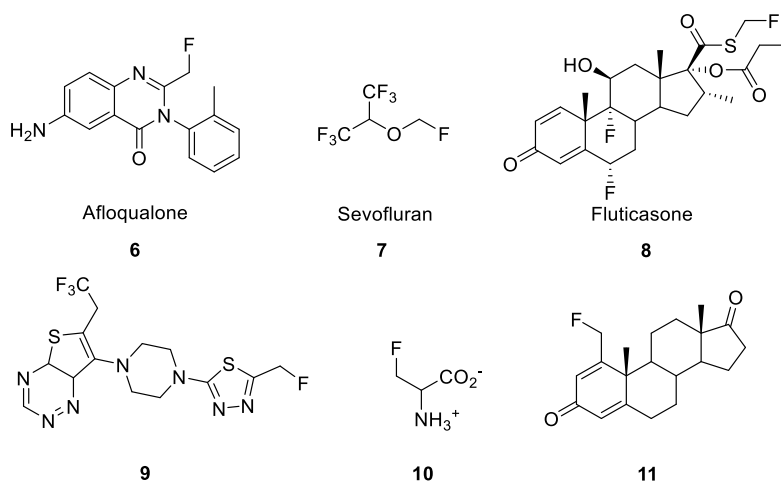


Figure 3: Selected drugs and inhibitors containing a fluoromethyl group.

Compound **9**, is an inhibitor for the tumor suppressor protein menin. The β -fluorinated amino acid **10** acts as so-called “suicide substrate”, which can deactivate decarboxylase enzymes and can be used against Parkinson’s disease. The androsta-1,4-diene-3,17-dione **11** acts as an aromatase inhibitor and is suitable for the treatment of estrogen-dependent diseases such as anovulatory infertility, prostate hyperplasia, breast cancer, and many more.^[6a, 9] The compounds CH_2FBr (HFBKW-31) and CH_2FCl (HFCKW-31) are frequently used on a large scale in industry for synthesis^[10] - even though these compounds have ozone depleting potentials.^[11] Since these substances are going to be subject to successive banning under the Montreal Protocol, and the handling of these chemicals will be accompanied by increasingly stricter rules,^[11b] alternative fluoromethylating agents are urgently needed. Although a fluoromethyl group can be generated by introducing fluorine in place of a suitable functional group^[12] or by direct monofluorination^[13] the majority of synthetic procedures use a fluoromethylating agent

instead, which can directly transfer a CH₂F group.^[14] A further method starts with a precursor compound which formally transfers a "CFR₂" unit (R = SO₂Ar or others) to the substrate in the initial step, and which subsequently gives the desired CH₂F group after work-up.^[7a] Fluoromethylation chemistry before 2009 has been nicely reviewed by *Hu* and co-workers.^[7a] In addition overview articles focused on fluorine containing functional groups^[5b], difluoro and fluoromethylation,^[14] transition metal mediated di- and monofluoroalkylations^[15], sulfur based fluorination and fluoroalkylation reagents^[16] and on shelf-stable reagents for fluoro-functionalization reactions^[17] have been published. This article gives an overview over the reagents used for the specific introduction of the CH₂F group in organic compounds. Classical monofluoromethylating agents as well as newly developed reagents have been considered (Figure 4). The literature has been covered until the end of 2019.

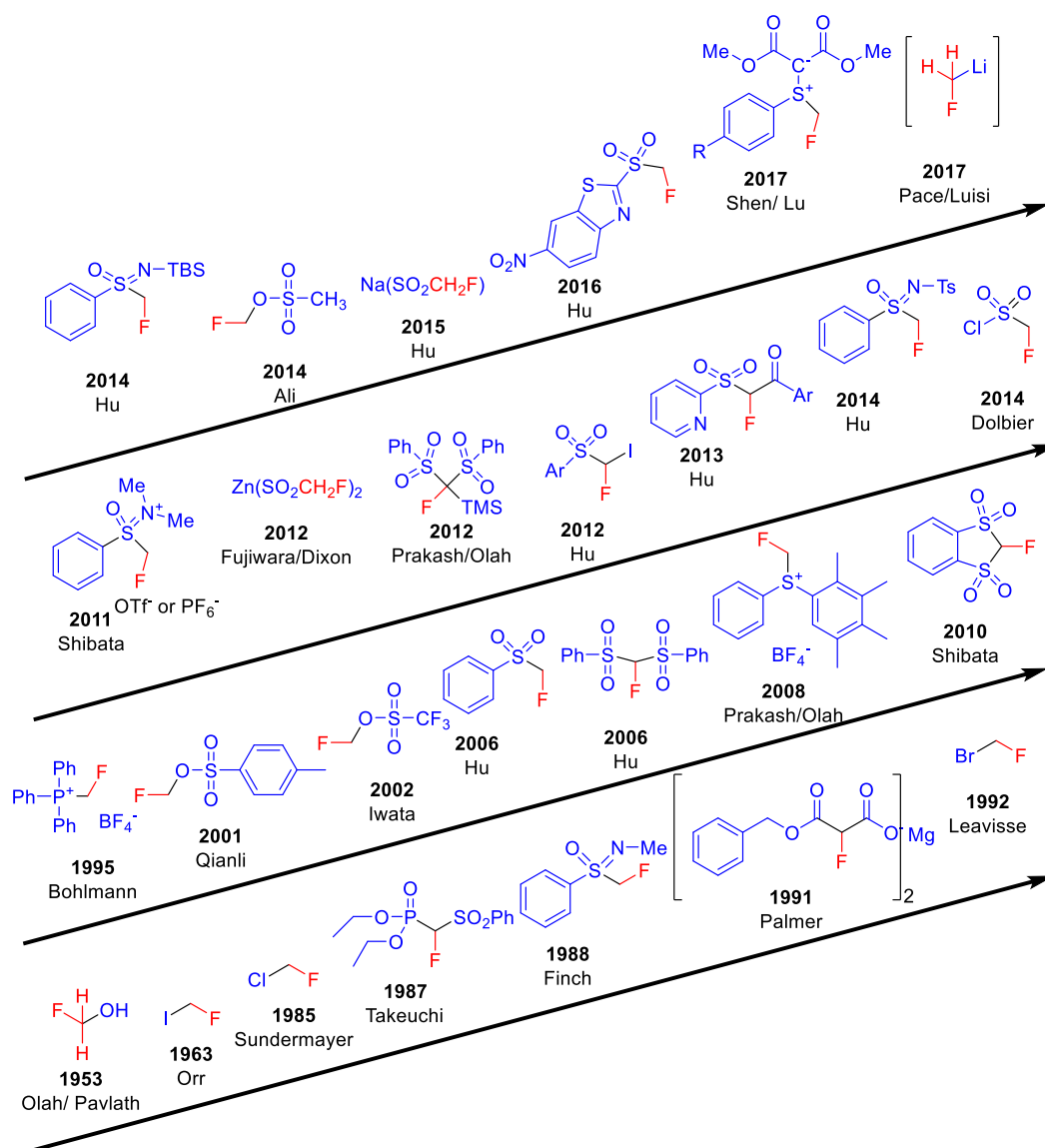


Figure 4: Historical overview on monofluoromethylating reagents and year of their first use as CH₂F transferring agent.

Reagents have been classified considering their ability to either directly transfer the CH₂F group in electrophilic, nucleophilic and radical fluoromethylation reactions, or to act as suitable precursors generating CH₂F after proper workup. Introduction of CH₂F based on transition metal mediated cross coupling reactions is discussed in the section of the corresponding reagent.

1.2.1.2 Historical Overview of Monofluoromethylating Reagents

The number of monofluoromethylating reagents has almost doubled within the last 10 years (Figure 4), reflecting a dramatic development in this field. Particularly active in this area has been the group of *Hu* and co-workers, providing eight of the reagents. Starting with simple compounds like fluoromethanol and the fluoromethyl halides CH₂FX (X = Cl, Br, I) more sophisticated and efficient reagents applicable to a broad range of substrates have been developed with time. Efforts were focused on the introduction of better leaving groups as compared to the halides and on fluoromethylating reagents acting as nucleophiles – the generation of CH₂FLi being certainly a highlight – or by a radical pathway. In the last 10 years in particular reagents and synthetic protocols for radical fluoromethylation as well as for CH₂F introduction through transition metal mediated cross coupling – mainly but not exclusively based on fluoromethyl halides – were developed.

1.2.2 Agents for Direct Monofluoromethylation

1.2.2.1 Electrophilic Monofluoromethylation

Fluoromethanol was the first reagent to be used for the electrophilic introduction of CH₂F. *Prakash* and *Pavilath* reported 1953 the formation of fluoromethyl substituted arenes on reaction with FCH₂OH in the presence of a Lewis acid (ZnCl₂).^[18] Recently it has been used for the fluoromethylation of special alcohols.^[19]

1.2.2.1.1 Fluoromethyl Halides

Fluoromethyl halides CH₂FX (X = Cl, Br, I) are all volatile, which represents a challenge when using these compounds. Nonetheless, this property is also an advantage, since this volatility allows an excess of the reagents to be readily separated from the product. In general, CH₂FX halides are weak fluoromethylating agents. Fluoromethylation *via* an S_N2 reaction mechanism is more difficult than the analogous methylation with a methyl halide.^[5b, 20] The α-fluorine effect is responsible for this behavior (Figure 5).^[21]

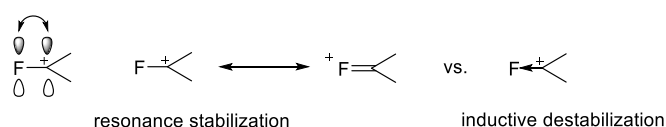
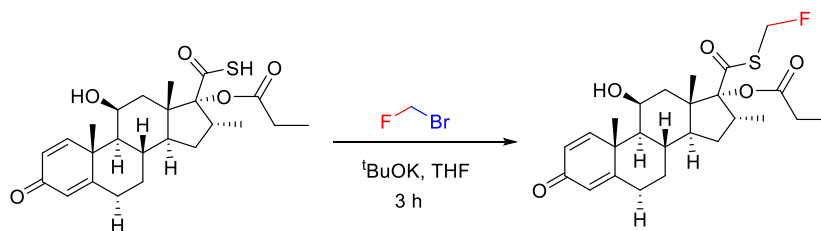


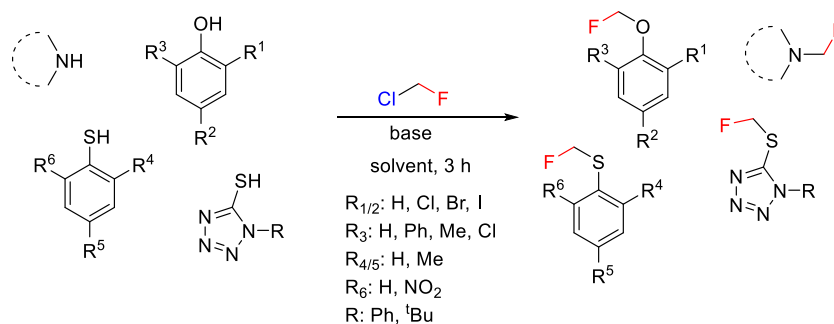
Figure 5: α-Fluorine effect.

A fluorine atom in the α-position stabilizes a positive charge by π-donation. This effect is so strong, that the destabilizing inductive effect can effectively be ignored and an S_N2 reaction can only take place if a good leaving group is present at the CH₂F moiety.^[21b, 21c] Thus, the reactivity

of CH₂FX halides increases in the order Cl < Br < I. However, some reactions such as the electrophilic fluoromethylation of carbon nucleophiles, as well as CH₂F transfer to weak nucleophiles are problematic.^[22] The fluoromethylating strength of CH₂FX can be increased considerably if silver cations are present to bind the halide^[21b, 23] making the fluoromethylation of weak nucleophiles like NO₃⁻^[23] and ClO₄⁻^[21b] possible. Initially CH₂FI (Orr^[24], 1963) and later CH₂FBr (Leavisse^[25], 1992) and CH₂FCl (Sundermayer^[26], 1985) were used for the fluoromethylation of a large number of substrates.^[25-27] The alkylation of a series of oxygen, sulfur, nitrogen, and carbon nucleophiles by fluoromethyl halides has been described.^[7a] Moreover fluoromethyl halides are often used as starting materials to develop more efficient fluoromethylating agents (Figure 6).^[28] The first fluoromethylated compounds acting as aromatase inhibitors, or compounds with anabolic properties were prepared using CH₂FI and CH₂FBr.^[24, 25] A series of ¹⁸F labeled fluoromethyl containing compounds, which are frequently used for Positron Emission Tomography (PET) imaging have been prepared employing CH₂¹⁸FBr.^[29] One of the most important applications of CH₂FBr is its use in the last step of the synthesis of FluticasoneTM,^[30] which involves fluoromethylation of a thiocarboxylate precursor at the sulfur atom (Scheme 1). Fluoroiodomethane^[27c-e, 31] and monosubstituted derivatives CHRFI^[27f, 27g] and CHRFB^[27f-h] have been used in several cases to introduce the CH₂F or CHRf group. The first systematic studies on the fluoromethylation of phenols, thiophenols, imidazoles and indoles with CH₂FCl (Scheme 2) have been reported in 2007 by Hu and co-workers.^[5b, 22]



Scheme 1: Fluoromethylation step of the synthesis of FluticasoneTM.



Scheme 2: Fluoromethylation of various *O*, *N* and *S* nucleophiles with CH₂FCl.

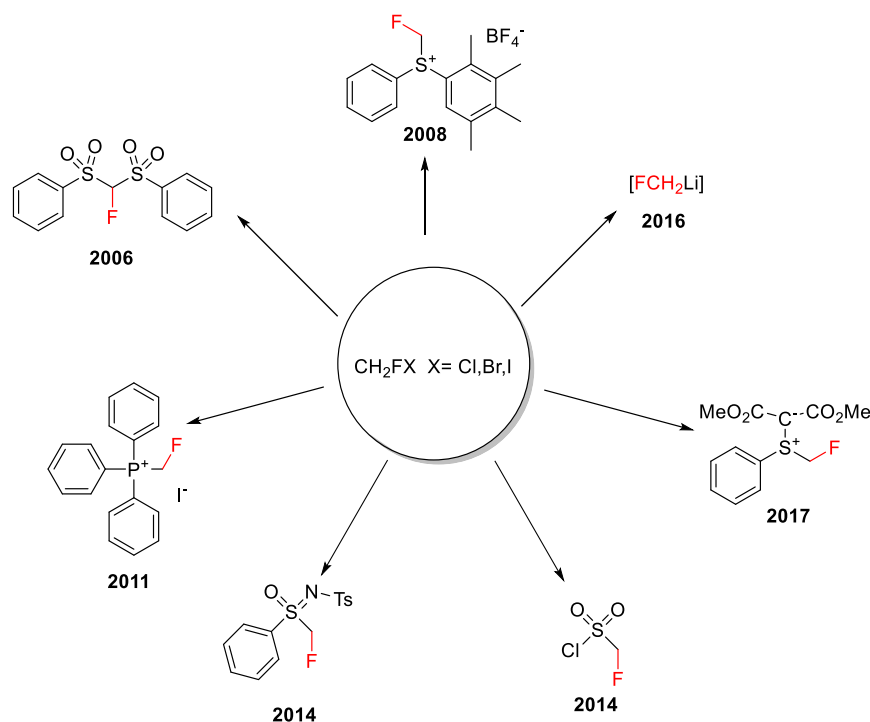
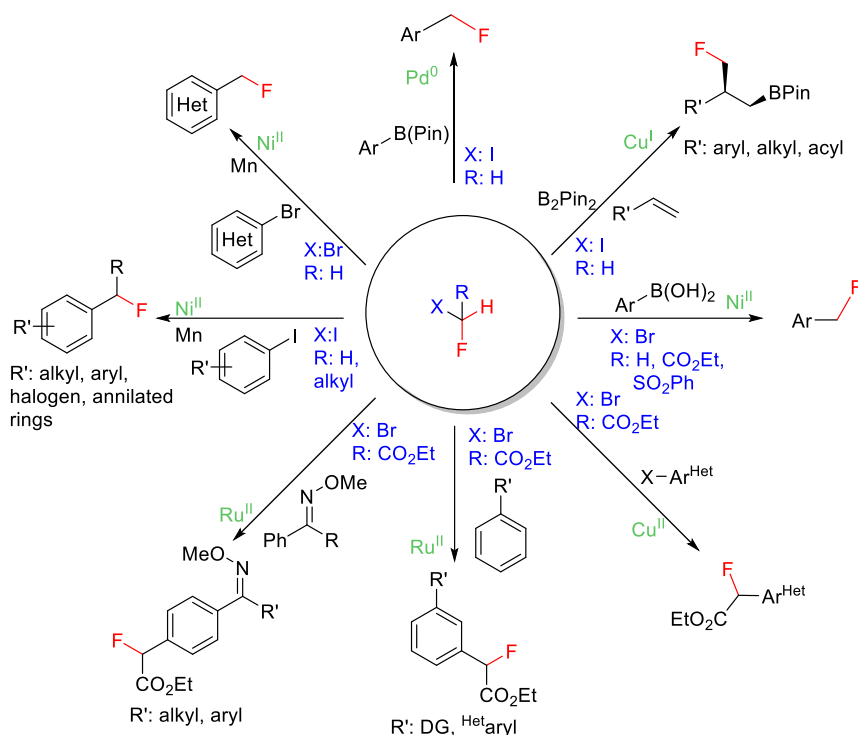


Figure 6: Selected strong fluoromethylating agents, derived from fluoromethyl halides and year of their first application as CH_2F transferring agent.

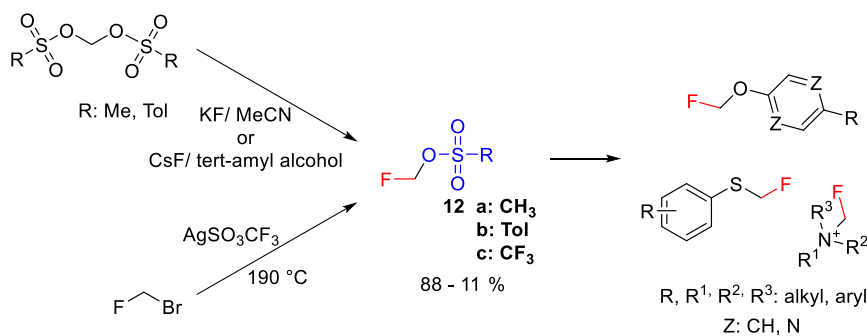
In the last 10 years several transition metal mediated fluoromethylation reactions starting from fluoromethyl halides CH_2FX ($\text{X} = \text{Br}, \text{I}$) or at carbon monosubstituted derivatives thereof have been developed (Scheme 3). All these syntheses involve C-C bond formation. Thus aryl boronic esters or aryl boronic acids can be converted to the corresponding fluoromethyl derivatives by coupling with CH_2FI , CH_2FBr or CHRFBr ($\text{R} = \text{CO}_2\text{Et}, \text{SO}_2\text{Ph}$) in Pd(0) (*Suzuki*^[27i], *Hu*^[27c], *Qing*^[32]) Cu(I) (*Qing*^[27e]) or Ni(II) (*Zhang*^[27b], *X.-S. Wang*^[27f]) catalyzed reactions, respectively. Ni(II) in combination with Mn has been used to promote the introduction of CH_2F (*X.-S. Wang*^[27a]) and CHRF ($\text{R} = \text{alkyl}$) (*X.-S. Wang*^[27g]) in heteroarenes and arenes starting from suitable heteroarene bromides and arene iodides by reductive cross coupling. The $\text{CH}(\text{CO}_2\text{Et})\text{F}$ group has been introduced in *p*- (*Zhao*^[33]) or *m*-position (*G.-W. Wang*^[27l], *Ackermann*^[27m]) by Ru(II) catalyzed reaction of $\text{CH}_2\text{F}(\text{CO}_2\text{Et})$ with corresponding methoxy phenyl ketoximes or monosubstituted phenyl derivatives, respectively. It has been shown (*Wu*^[27m]), that 8-aminoquinolines react with $\text{CHF}(\text{CO}_2\text{Et})\text{Br}$ in the presence of Cu(II) and $\text{HP}(\text{O})(\text{OMe})_2$ to give the corresponding $\text{CHF}(\text{CO}_2\text{Et})$ substituted derivatives. It is noteworthy, that the known fluoromethyl pseudohalides CH_2FX ($\text{X} = \text{CN}$ ^[34], NCO ^[35], N_3 ^[36]) have not yet been used as fluoromethylating agents.



Scheme 3: Transition metal mediated introduction of CH₂F starting from fluoromethyl halides and monosubstituted derivatives.

1.2.2.1.2 Fluoromethyl Sulfonates

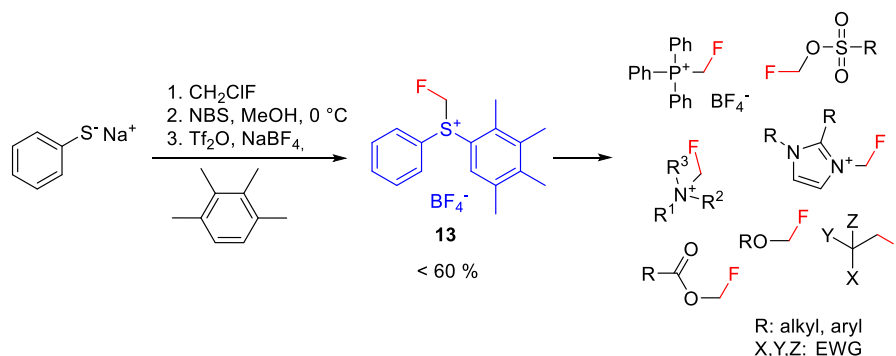
Fluoromethyl sulfonates **12a** (Ali, 2014)^[37], **12b** (Qianli, 2001)^[281], **12c** (Iwata, 2002)^[38] have been used to introduce CH₂F in a series of compounds at oxygen, sulfur and nitrogen atoms (Scheme 4).^[7a] The main and most important application of these reagents is in the synthesis of ¹⁸F labeled fluoromethyl compounds to enable PET imaging.^[39] Fluoromethyl sulfonates **12a,b** have been prepared starting from bis(mesyloxy) and bis(tosyloxy) methane and introducing fluorine by reaction with KF.^[40] The synthesis of **12b** has been considerably improved^[41] and is almost quantitative when CsF in *tert*-amyl alcohol is used to introduce fluorine.^[12] Fluoromethyl triflate **12c** has been obtained from CH₂FBr and silver triflate^[38, 39b]; quite harsh conditions are required, however.^[28d] Since 2009, the use of these reagents has greatly increased, and more non-¹⁸F-labeled compounds were synthesized in a targeted manner.^[28h, 42]



Scheme 4: Alkylation with fluoromethyl sulfonates.

1.2.2.1.3 *S*-(Monofluoromethyl)diarylsulfonium Tetrafluoroborate

In 2008, *Prakash* and *Olah* developed a powerful fluoromethylating agent which can be successfully applied to achieve the fluoromethylation of numerous nucleophiles (Scheme 5). The fluoromethylsulfonium salt **13** is obtained in a three step synthesis with an overall yield of 60 %.^[28b] Interestingly, the first step – the synthesis of the fluoromethyl phenyl thioether – is reported with better yields in the literature.^[5b] The sulfonium salt **13** is a moisture insensitive solid which is stable for several months in the solid state and is also stable in acetonitrile solution. However, in DMF and THF decomposition occurs.^[28b]

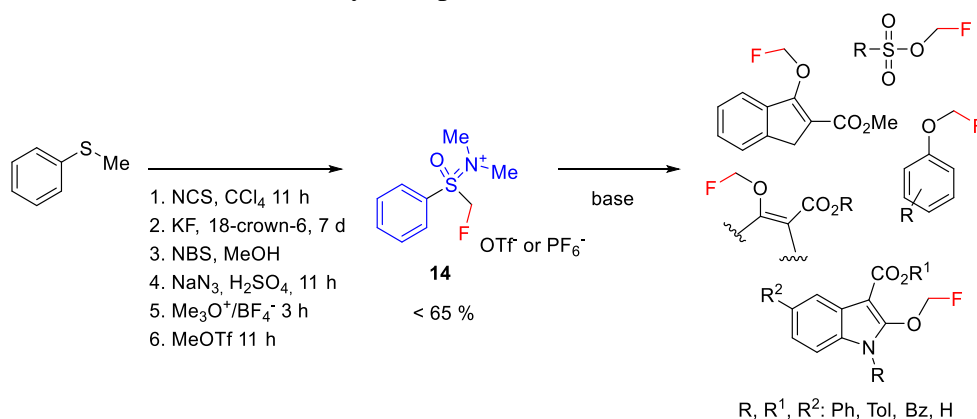


Scheme 5: Fluoromethylation with **13**.

Substrates which possess heteroatoms as nucleophilic centers are readily fluoromethylated on reaction with **13**. In particular, fluoromethyl sulfonates can be prepared under mild conditions using the sulfonium salt **13**. However its application to carbon nucleophiles remains so far limited to only a few compounds.^[28b]

1.2.2.1.4 *N,N*-(Dimethylamino)-*S*-phenyl-*S*-monofluoromethyl phenyloxosulfonium Triflate

A very effective fluoromethylating reagent was developed 2011 by *Shibata* and co-workers.^[43] It shows a pronounced preference for fluoroalkylation at oxygen atoms, which provides a synthetic approach for the preparation of monofluoromethyl ethers. This methodology was applied to a number of 1,3 dicarbonyl compounds.



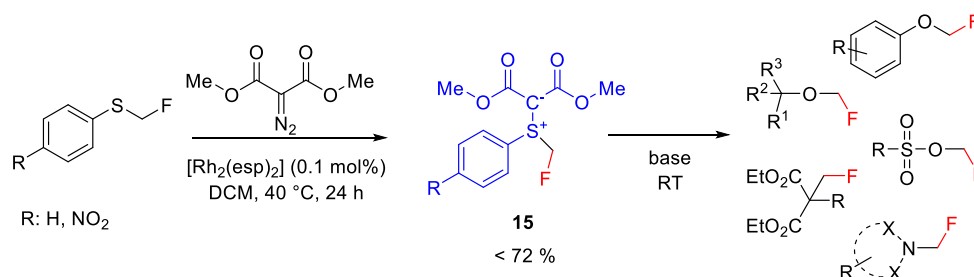
Scheme 6: *O*-Fluoromethylation of selected compounds.

It is a regioselective reagent for β -ketoesters and was successful also in the fluoromethylation of carboxylic and sulfonic acids, oxindole derivatives and phenols, as well as naphthols (Scheme 6).^[17, 43] A disadvantage of this reagent is its tedious, multi-step synthesis. However, if a modified procedure from the literature is used to simplify the synthesis of the fluoromethyl phenyl thioether intermediate,^[44] the overall synthesis time can be reduced substantially from almost 9 days to 1.5 days.^[28b, 43] The reagent **14** is a solid which is easy to handle and can be stored.^[43] Although *O*-alkylation can also be performed well with other reagents, the *E/Z* stereoselectivity of **14** is particularly noteworthy. The *O*-regiospecificity of **14** was explained by a radical-like mechanism involving an SET process.^[45] However, *Shen* et al. reported that alcohols did not react with this reagent under the conditions applied.^[28d]

1.2.2.1.5 Monofluoromethyl-substituted Sulfonium Ylids

Completing the series of difluoromethyl- and trifluoromethyl-substituted sulfonium ylids, *Shen* and *Lu* reported in 2017 the missing monofluoromethyl sulfonium ylid **15**, which was structurally characterized using single crystal X-ray diffraction. Reagent **15** is a stable solid and can be stored at least for one month at ambient temperature on the bench without notable decomposition, and can be prepared in a straightforward synthesis in good yields.^[28d]

The ylide **15** was found to be a very effective reagent for the electrophilic fluoromethylation of primary, secondary and tertiary alcohols, as well as of malonic acid derivatives.^[28d] It was shown that **15** is a strong alkylating agent. Thus, the conversion of sulfonic acids, carboxylic acids, phenols, amides and *N*-heteroarenes to the corresponding fluoromethyl derivatives takes place readily under mild conditions (Scheme 7).^[28d]



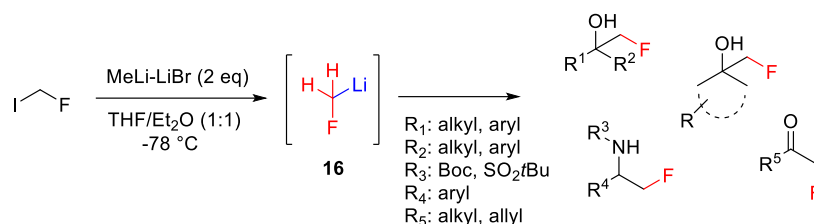
Scheme 7: *C*, *N* and *O* fluoromethylation with sulfonium ylide **15**.

Although **15** is a strong alkylating agent, reaction of **15** with carbon nucleophiles with formation of C-CH₂F bonds is problematic, and can only be applied to special substrates.^[28d]

1.2.2.2 Nucleophilic Monofluoromethylation

Due to their high instability, organometallic reagents such as fluoromethyl lithium or the corresponding Grignard compounds belong to the most difficult areas of research on nucleophilic monofluoromethylating agents.^[7a] In 2017, *Pace* and *Luisi* achieved a great breakthrough in this field. They reported the generation and use of fluoromethyl lithium which was the first and still only direct nucleophilic monofluoromethylation reagent (Scheme 8).^[46] In order to perform reactions with this unstable species it is important to stick strictly to the reaction conditions,^[46] as the generation of **16** only succeeds adding MeLi · LiBr in a molar

ratio of 2 : 1.5 to the substrate. Furthermore, the reaction has to be quenched and a solvent mixture of THF:Et₂O (1:1) has to be used.^[46]



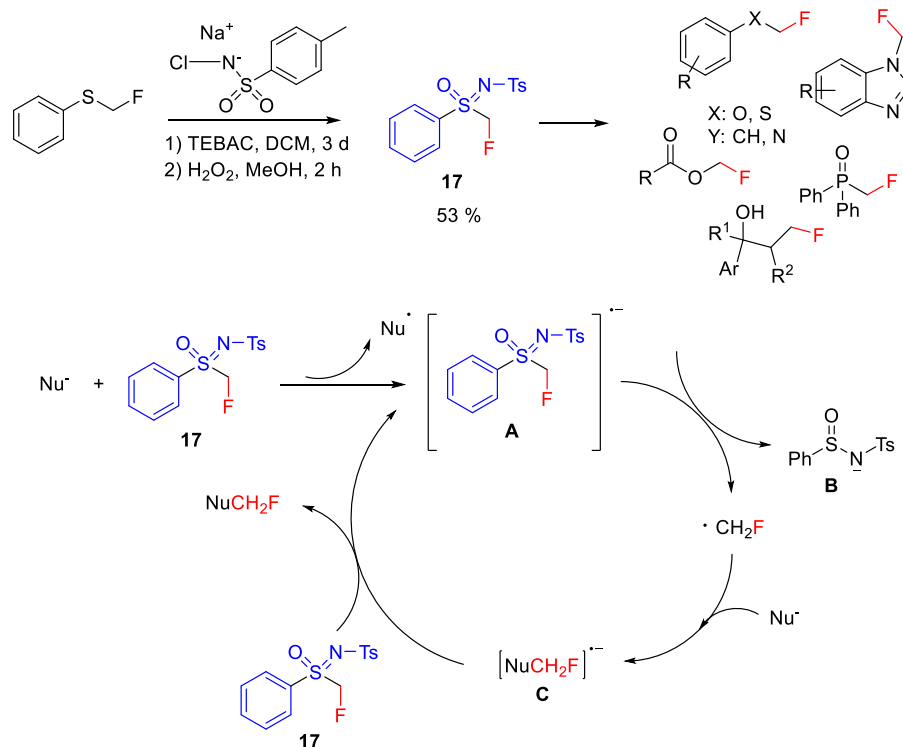
Scheme 8: Nucleophilic fluoromethylation with fluoromethyl lithium **16**.

Unfortunately, reagent **16** cannot be isolated at room temperature – in contrast to MeLi - since decomposition occurs very quickly, most probably by elimination of LiF.

1.2.2.3 Radical Monofluoromethylation

1.2.2.3.1 *N*-Tosyl-*S*-fluoromethyl-*S*-phenylsulfoximine

Until about 10 years ago a free radical monofluoromethylation was unknown.^[7a] In 2014, *Hu* and co-workers described the sulphur-containing reagent **17**, which is able to transfer the fluoromethyl radical group to a substrate (Scheme 9).^[28e, 47]



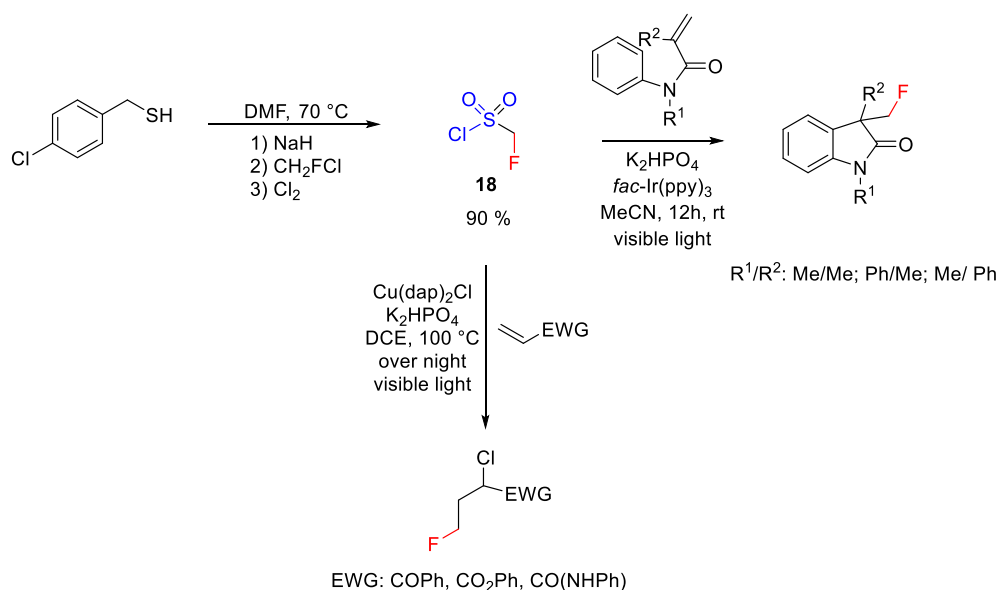
Scheme 9: Radical fluoromethylation of selected *O*, *S*, *N*, *P* compounds with **17** and the proposed reaction mechanism.

Various compounds were fluoromethylated at *O*, *S*, *N* or *P* with good yields using sulfoximine **17**. The range of applications of **17** was extended by *Akita* et al. to *C*-fluoromethylation of alkenes by using strongly reducing photoredox catalysts.^[13a] Despite the time consuming (3 d) synthesis of **17** and the only moderate yield, an important advantage of this reagent is its

stability. At room temperature, **17** is a crystalline solid, which has been characterized by single crystal X-ray diffraction and which does not decompose even on storage in air for one year.^[47]

1.2.2.3.2 Fluoromethylsulfonyl Chloride

Concurrent with the development of the sulfoximine **17**, in 2014 *Dolbier* and co-workers developed the photoredox catalyzed tandem radical cyclization of *N*-aryl acrylamides to form fluorinated 3,3-disubstituted 2-oxindoles using an iridium catalyst and fluoromethylsulfonyl chloride as the CH₂F source (Scheme 10).^[28j]

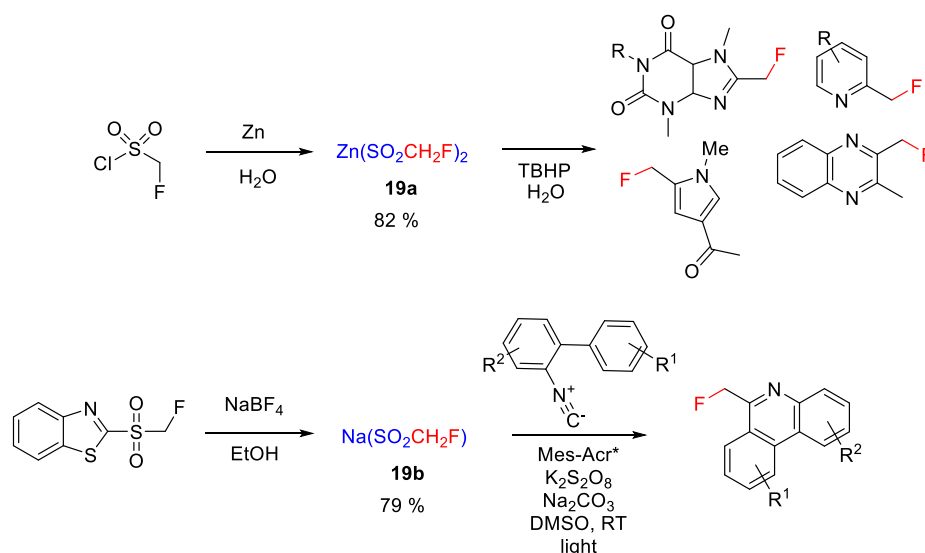


Scheme 10: Radical fluoromethylation of *N*-aryl acrylamides with **18**.

The sulfonyl chloride **18** (colorless oil) is readily obtained starting from 4-chloro benzyl thiol in three steps in excellent yield (90 %). In the cases of *N*-phenyl acryl amide and electron deficient alkenes, instead of cyclization occurring, a formal addition of chlorine and CH₂F to the C=C double bond takes place yielding saturated derivatives with a terminal fluoromethyl group (Scheme 10). The reaction is catalyzed by Cu and is induced by visible light. Both reactions also occur with CHF₂ or CF₃ substituents in place of CH₂F.^[28c] However, although the yields of the fluoroalkylated products are good, application of this reagent still remains limited at the present time.

1.2.2.3.3 Metal Fluoromethyl Sulfinates

In 2012, *Fujiwara* and *Dixon* described a radical fluoromethylation using the zinc fluoromethyl sulfinate **19a**.^[48] This reagent enables the C-H functionalization of diverse heterocycles by introducing a fluoromethyl group (Scheme 11).

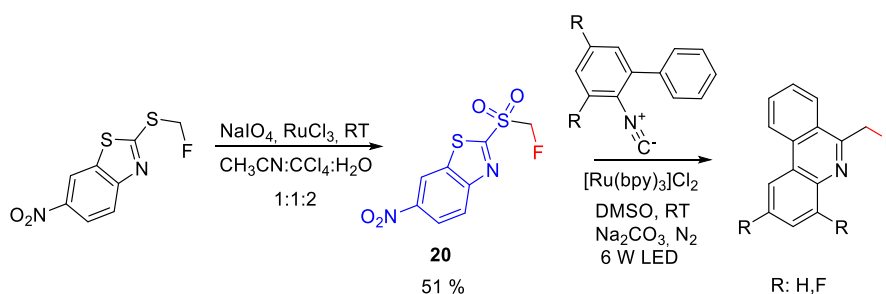


Scheme 11: Free radical fluoromethylation of selected heterocycles.

In 2015, *Hu* and co-workers developed a large scale synthesis for sodium sulfinate **19b** and used it for radical monofluoromethylation reactions.^[49] Later in 2017, *Liu* et al. demonstrated that sodium sulfinate **19b** is a suitable reagent for the transition metal free radical fluoroalkylation of isocyanides to form phenanthridines.^[50] Coumarin derivatives with a CH_2F group have been prepared very recently by *Li* et al. starting from alkoxynates by a silver catalyzed cascade monofluoromethylation with **19b**.^[51] The zinc sulfinate **19a** has also been widely used for the synthesis of bioactive compounds,^[48] and is remarkable because of its simple and straightforward synthesis. Compound **19a** has been isolated as a colorless solid and is stable at room temperature. However, the synthesis of the sodium salt, starting from a heteroaryl sulfone, is much simpler.^[49]

1.2.2.3.4 Monofluoromethyl Sulfones

In 2016, *Hu* et al. reported the photoredox synthesis of fluoromethyl substituted phenanthridines catalyzed by visible light, by reaction of suitable isocyanides with the fluoromethyl sulfone **20**.^[52] A high redox potential of the fluoromethyl sulfone is essential for a successful fluoromethylation. An irradiation time of 48h is required (Scheme 12).^[12-15, 17, 53]



Scheme 12: Metal mediated radical fluoromethylation of isocyanides.

The fluoromethylating reagent **20** is isolated in the last step in moderate yield as a colorless, air stable solid, which makes it easy to handle. Its overall synthesis, however, includes several steps and requires the use of CH_2FCl as the source of the fluoromethyl group.^[12-15, 17, 53]

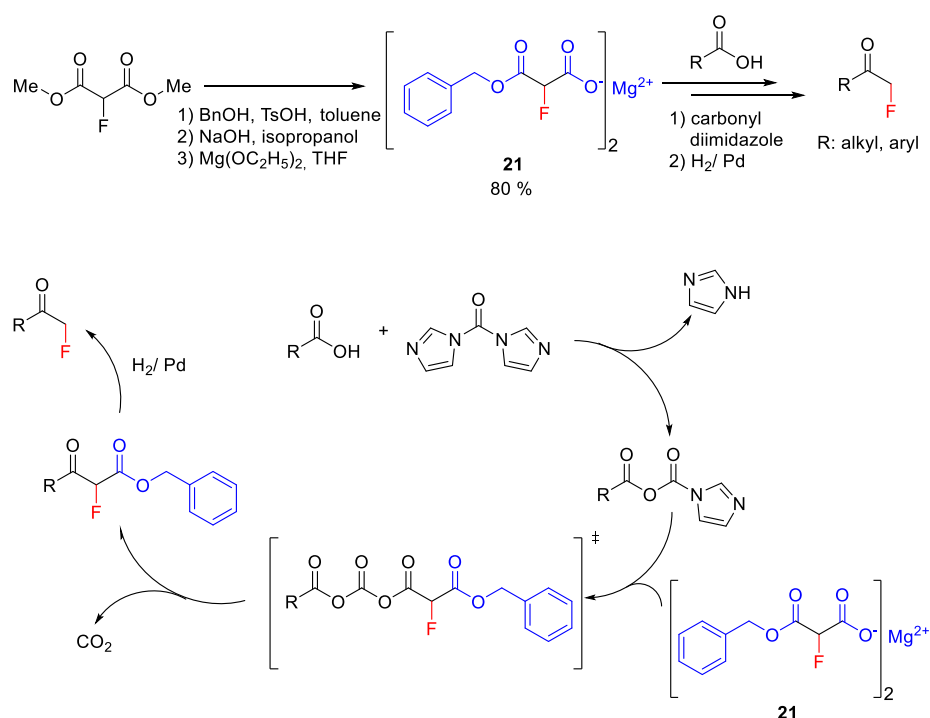
1.2.3 Indirect Monofluoromethylation

Due to the instability of organometallic fluoromethyl reagents such as fluoromethyl lithium, it is sometimes necessary to use precursor compounds containing a functionalized fluoromethyl group for some syntheses. After the transfer of the functionalized group to the substrate, the desired $-\text{CH}_2\text{F}$ moiety is generated during workup.

1.2.3.1 Nucleophilic Precursors

1.2.3.1.1 Fluoromalونات

In the 80s, the monofluoromethylation of organic compounds attracted increasing interest. Research in this area was focused in particular on the development of mild fluoroalkylating reagents, complementing the traditional methods based on fluoromethyl halides. *Palmer* reported an effective alternative reagent for the fluoromethylation of carboxylic acids, namely the magnesium salt **21** (Scheme 13).^[7a, 54]



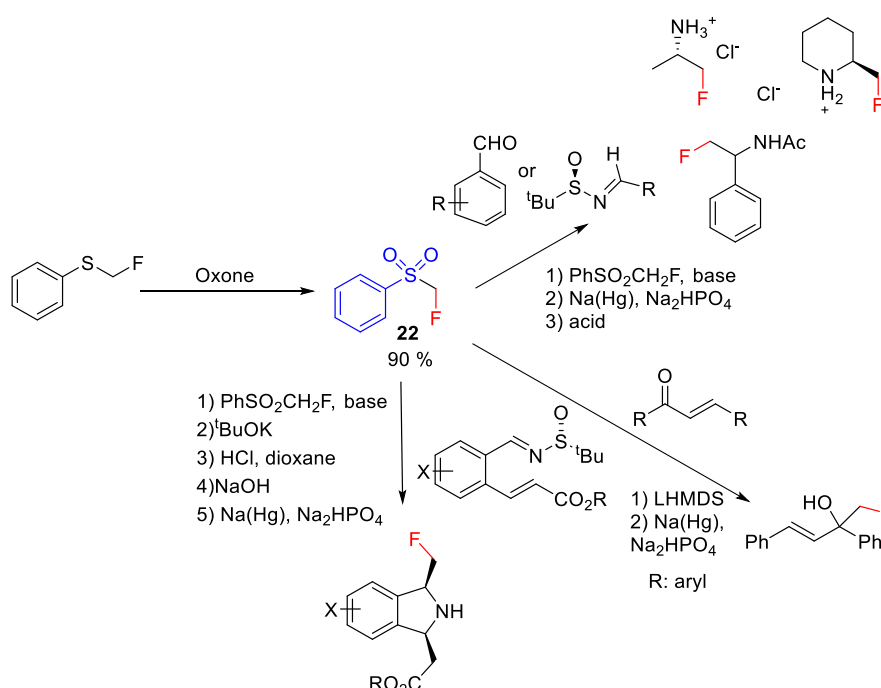
Scheme 13: Synthesis of fluoromethyl ketones using magnesium fluoromalonate **21**.

The key step involves the nucleophilic attack of an intermediately generated fluoromethyl carbanion to the imidazolide of the carboxylic acid. Thus, reagent **21** may be viewed as being a synthon of the unstable CH_2F^- anion. The resulting β -keto α -fluoroesters form the corresponding fluoromethyl ketones on hydrogenation in good yields. The starting fluoromalonnate ester is readily prepared^[54-55] and is nowadays commercially available.

Fluoromalonate methyl^[55a] and ethyl^[55b] ester have also been directly used in fluoromethylation reactions. The formation of **21** (colorless solid) is straightforward, although it comprises three steps. Furthermore, despite intensive studies, this substrate was not able to produce enantioselective compounds.^[7a]

1.2.3.1.2 Fluoromethylphenylsulfone and Related Compounds

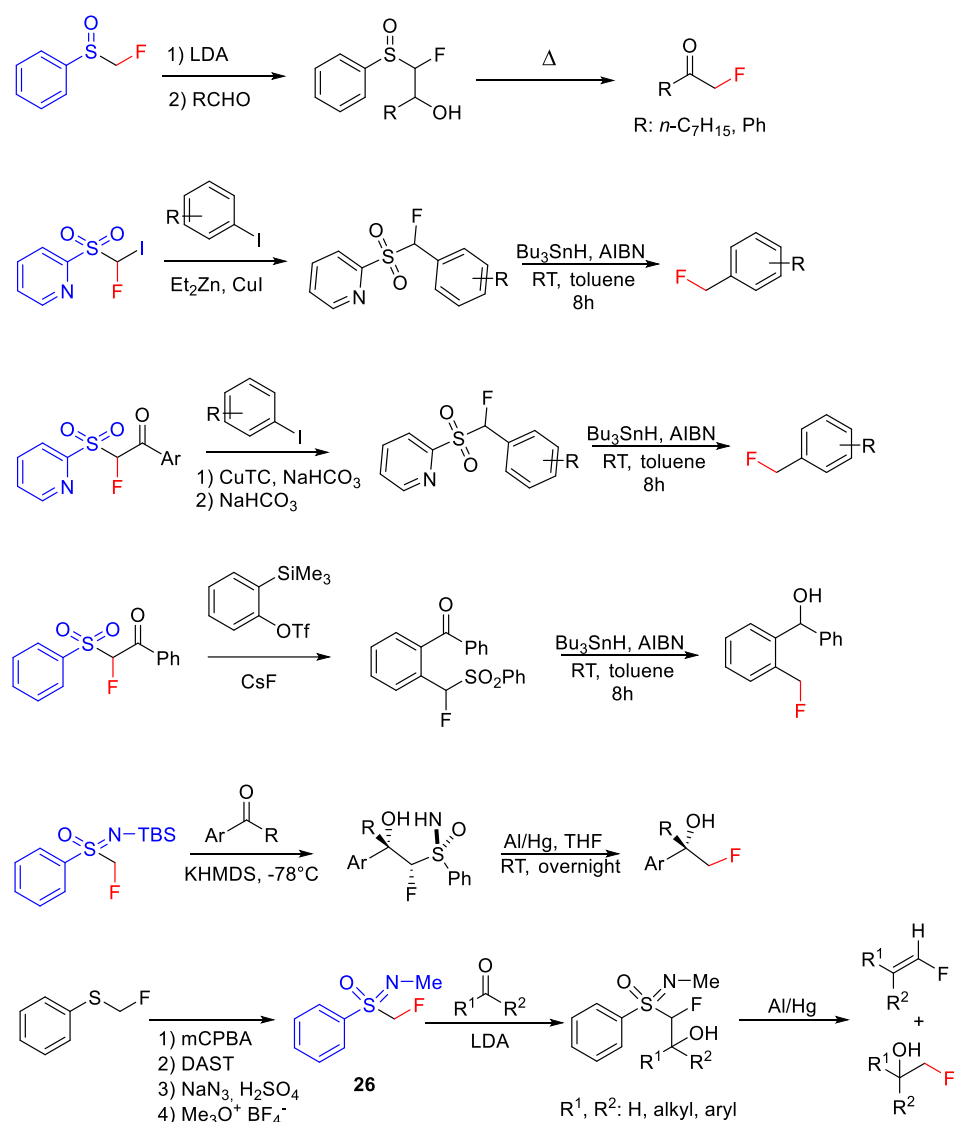
Fluoromethylphenylsulfone **22**, is a colorless solid which was reported as far back as 1985 to form the corresponding fluoromethylidene ylide, and has been used to prepare fluoroolefines in a Wittig analogous reaction.^[56] Later, in 2006, *Hu* and co-workers extended this methodology to formally transfer the CH₂F moiety, which is reformed after cleavage of the sulfonyl group (Scheme 14).^[57] Thus starting from (*R*)-(*tert*-butylsulfinyl)imines, primary α -fluoromethyl amines and cyclic secondary α -fluoromethyl amines become readily accessible with high stereoselectivity using this reagent. The method was further extended by *Fustero* et al. to include the synthesis of chiral fluoromethyl isoindolines^[58] and isoquinolines.^[59] *Hu* et al. further successfully utilized **22** for the stereoselective synthesis of a vicinal fluoromethyl ethylene diamine.^[60] Monofluoromethyl containing amides can also be prepared using **22** via a *Ritter* reaction.^[61] The reaction of sulfone **22** with 2-cyclohexanone and acyclic α,β -unsaturated ketones gives both addition to the carbonyl group as well as Michael addition, and yields the corresponding fluoromethyl derivatives after reductive cleavage of the sulfonyl group, as reported by *Hu* et al..^[7a, 58-59, 62]



Scheme 14: Fluoromethylation with fluoromethylphenylsulfone **22**.

A carbanion having a fluorine atom directly bonded to carbon can also be stabilized by a sulfoxide group. Deprotonation of fluoromethyl phenyl sulfoxide at the methylene group by LDA at -78 °C results in the formation of a carbanion, moderately stable at low temperatures. Reaction with aldehydes followed by pyrolysis generates the corresponding fluoromethyl

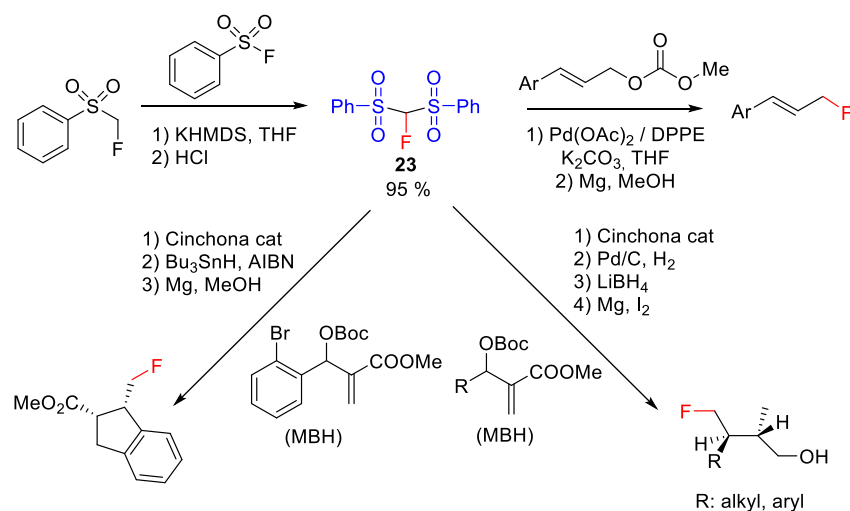
ketones in moderate yields (Scheme 15).^[63] An aromatic fluoromethylation with an α -fluoro- β -keto phenyl sulfone, acting as a soft nucleophile, has been reported by *Hu et. al.*^[62] The three step synthesis involves the addition to a benzyne generated *in situ*, followed by the reduction of the keto group and by the reductive cleavage (Na(Hg)) of the sulfonyl function.^[62] In addition to the frequently used fluoromethylphenyl sulfone **22**, derivatives of **22** -described by *Hu* and co-workers 2012/13/14 - with substituents at the fluoromethyl carbon atom or the analogous fluoromethyl TBS-sulfoximine have also been used to prepare corresponding fluoromethyl products (Scheme 15).^[15, 27f, 64] Some of the syntheses involve transition metal mediated C-C coupling reactions.^[15, 27f, 64a,b] *Finch* and co-workers described 1988 the sulfoximine **26** as a nucleophilic source for the fluoromethyl group. Reaction with aldehydes and ketones in the presence of a base proceeds with addition to the C=O bond yielding the corresponding β -fluorosulfonyl alcohols. The reductive cleavage of the sulfonyl substituent with aluminium amalgam produces the respective fluoroolefines together with the fluoromethyl alcohols. In the case of $R^1 = H$ and $R^2 = 4\text{-MeOC}_6\text{H}_4$, the fluoromethyl alcohol is obtained in 57 % yield, if aluminium amalgam is used (Scheme 15).^[65]



Scheme 15: Fluoromethylation with fluoromethyl phenyl sulfoxide and fluoromethyl phenyl sulfone derivatives.

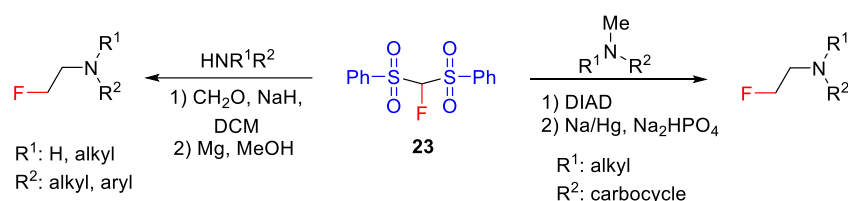
1.2.3.1.3 Fluorobis(phenylsulfonyl)methane

Since the discovery of fluorobis(phenylsulfonyl)methane (FBSM) **23** in 2006 by *Hu / Shibata* and co-workers and its ability to formally act as a fluoromethylating agent, a number of fluoromethylation reactions, including transition metal mediated cross couplings, have been performed.^[17, 28i, 66] The synthesis of **23** has also been improved. A convenient method of preparation of **23** is the reaction of fluoromethylphenylsulfone **22** with phenylsulfonyl fluoride.^[5c] *Hu* and *Prakash* reported that FBSM acts as a nucleophilic fluoromethylating reagent and undergoes addition reactions with epoxides,^[66a] aziridines,^[62] α,β -unsaturated ketones,^[62, 67] alkynyl ketones^[62] and benzynes.^[62] *Shibata* and *Prakash* found **22** to be an effective reagent in the palladium catalysed enantioselective fluoromethylation of allylic acetates, imines and α,β -unsaturated ketones and esters.^[5b, 67] Further, the fluoromethylation of alcohols, alkyl halides and α,β -unsaturated ketones with **23** (using a cinchona alkaloid derived catalyst) has been reported.^[7a, 67b] Using the *in situ* formation of an iminium compound as the catalyst, *Wang* et al. reported an enantioselective addition of **23** to enals.^[68] In the last 10 years, some research groups have described the reaction of FBSM with aliphatic aldehydes resulting in enantioselective fluoromethylation in the β -position,^[69] as well as the addition of FBSM to MBH carbonates or acetates yielding the products of an enantioselective asymmetric allylic alkylation (Scheme 16).^[70] *Gouverneur* and *You* showed that the palladium catalyzed reaction of **23** with Morita-Baylis-Hillmann (MBH) carbonates (allyl carbonates) and the iridium catalyzed allylic alkylation of **23** proceed with high regioselectivity.^[71] Also the addition to alkyl- and benzyl halides proceeds with high yields, as shown by *Olah* et al.^[72] The fluoromethyl group is finally formed after reductive cleavage of the sulfonyl substituents with Mg in MeOH (Scheme 16).^[70c, 71-73] Instead of the palladium catalyst, the combination of a cinchona alkaloid and FeCl₂ or a cinchona catalyzed Mannich type reaction can be used for enantioselective monofluoromethylation (*Shibata* et. al.).^[74] Furthermore, the addition of **23** to carbonyl compounds,^[69a] α,β -unsaturated carbonyl compounds^[75] and to functionalized alkynes^[76] as well as the enantioselective synthesis of tertiary allylic fluorides by the iridium catalyzed allylic fluoromethylation with **23** have been described by *Hu*, *Vesely* and *Hartwig*.^[77]



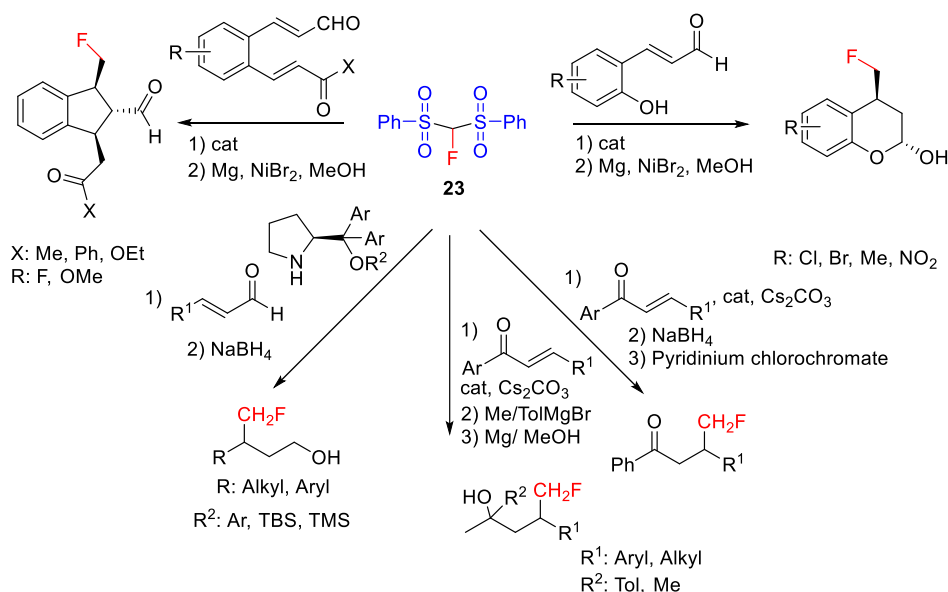
Scheme 16: Reactions of FBSM (**23**) with MBH carbonates.

Reductive cleavage of the sulfonyl substituents to yield the corresponding fluoromethyl derivatives, as in the other examples discussed above, was not reported. Reaction of **23** with MBH carbonates (*Toru* and *Tan*) proceeds with high enantio- and diastereoselectivity and yields alcohols with a fluoromethyl group in γ -position to the OH group after workup.^[74, 78] The introduction of a fluoromethyl group in Ibuprofen using **23** in place of the methyl group results in an increase of its inhibitory activity.^[79] The reaction of secondary amines with formaldehyde in the presence of FBSM (*Prakash* et al. 2013) opens up a general and straightforward synthetic route to β -fluoro ethylamines.^[80] *Hu* et al. reported in the same year, that starting from tertiary amines, further β -fluoro ethylamines can be prepared by *C,C*-coupling using **23** and diisopropyl azodicarboxylate (DIAD) as the coupling reagent (Scheme 17).^[77b]



Scheme 17: Synthesis of β -fluoro ethylamines using **23**.

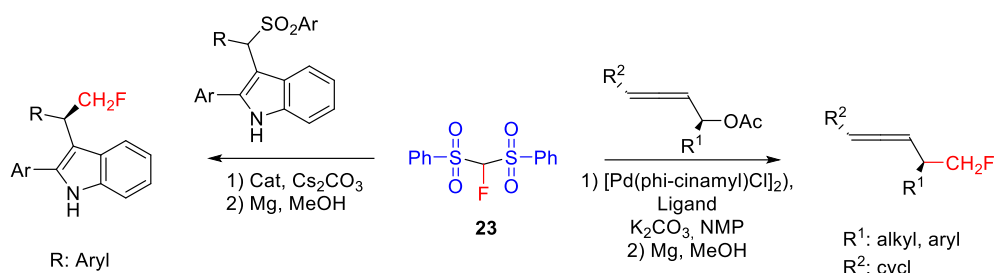
In 2014, *Ramos* and *Yang* extended the addition reaction of FBSM to enals, providing an enantioselective synthesis for fluoroindane and fluorochromanol derivatives (Scheme 18).^[81]



Scheme 18: Reaction of FBSM (**23**) with enals and enones.

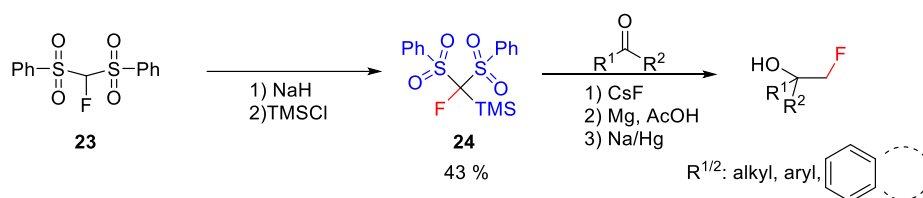
Shibata et al. reported an efficient method of preparing C2-arylindoles with a fluoromethyl group at the alkyl side chain starting from the corresponding aryl sulfonyl derivatives and replacing the SO_2Ar substituent by CH_2F utilizing **23** in the presence of a chiral phase transfer catalyst.^[82] Furthermore, the acetate group of allenyl acetates has been replaced by the CH_2F group by employing **23** (*Ma* and *Haiming*), yielding the corresponding fluoromethyl allenes (Scheme 19).^[83] FBSM is also the key reagent of a highly selective two step synthesis of functionalized monofluoromethylated allenes, reported by *Shibata* et. al.^[84] In the first step 2-bromo-1,3-dienes react with FBSM in a palladium catalyzed nucleophilic substitution which

selectively introduces the fluorobis(phenylsulfonyl)methyl group directly bonded to the allene skeleton. The following reductive desulfonation (Mg, MeOH) gives the fluoromethyl allenes in excellent (81-83 %) yields.^[84]



Scheme 19: Synthesis of fluoromethyl containing arylindoles and allenes with **23**.

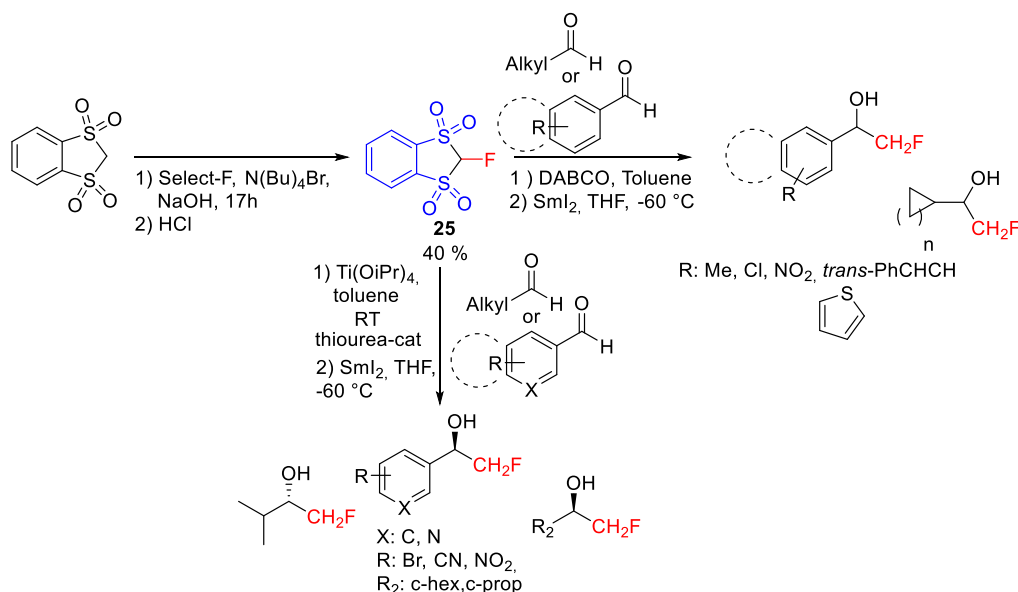
An efficient synthesis of α -fluoromethyl alcohols has been reported by *Prakash* and *Olah* in 2012, using the related trimethylsilyl derivative **24**. This reagent contains a SiMe₃ group in place of the hydrogen atom of FBSM and is readily prepared starting from **23** by deprotonation with NaH and subsequent silylation with Me₃SiCl (Scheme 20).^[85]



Scheme 20: Synthesis of **24** and its use for preparation of α -fluoromethyl alcohols.

1.2.3.1.4 2-Fluoro-1,3-benzothiole-1,1,3,3-tetraoxide

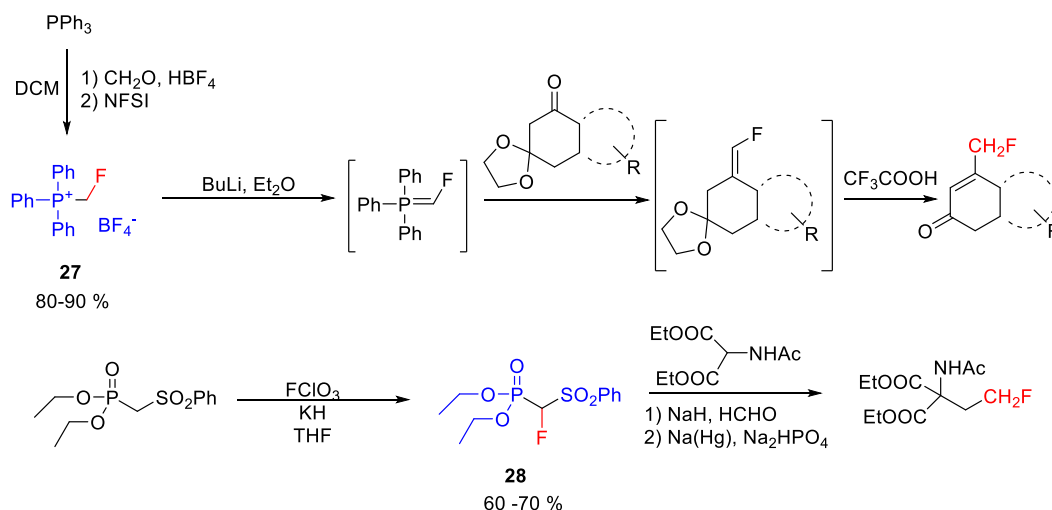
A cyclic version (FBDT) **25** of FBSM has been reported 2010 by *Shibata* et al.^[86] Reagent **25** is prepared starting from the corresponding methylene bridged derivative by fluorination with Select-FTM and forms as a colorless solid. FBDT adds efficiently to the C=O group in a variety of aldehydes yielding the corresponding α -fluoromethyl alcohols after workup. The addition is complete within 24 h. In the case of α,β -unsaturated aldehydes, 1,2-addition competes with 1,4-addition, and is strongly dependent on the base used (DABCO or pyrrolidone).^[86] In the presence of bifunctional cinchona alkaloid derived thiourea titanium complexes, the reaction of **25** with aldehydes becomes enantioselective (32-96 % ee) and yields the fluoromethyl alcohols in 73-91 % yield (Scheme 21).^[87]



Scheme 21: Synthesis of **25** and its reaction with aldehydes.

1.2.3.2 Phosphorus Containing Fluoromethylating Reagents

Fluoromethyl triphenylphosphonium tetrafluoroborate **27** has been utilized as a precursor to generate the corresponding fluoromethylidene phosphonium ylide, which has been employed in *Wittig* type reactions for the synthesis of fluoroalkenes. In the case of a special ketone (Scheme 22) subsequent proton shift catalyzed by trifluoroacetic acid results in the formation of a fluoromethyl derivative (Bohlmann et al. 1995).^[9c, 88] The structure of the fluoromethyl triphenylphosphonium salt in the solid state as its iodide salt has been determined by single crystal X-ray diffraction.^[8]



Scheme 22: Fluoromethylation reactions with the phosphorus reagents **27** and **28**.

The α -fluoromethyl phosphonate **28** displays increased acidity for the proton in α -position, supported by the electron withdrawing sulfonyl group. Its reaction with formaldehyde (Takeuchi et al., 1987) results in the formation of the corresponding sulfonyl substituted fluoroalkene, which can be converted with the anion of diethyl acetamido malonate to the

corresponding fluoromethyl derivative after reductive elimination of the sulfonyl group (Scheme 22).^[89]

1.2.4 Conclusion

The unique properties of organic molecules containing a fluoromethyl (CH₂F) group and their use in various fields of pharmacy and medicine has resulted in a high demand for reagents which are capable of selectively introducing a CH₂F group. In recent decades, great efforts have been made in the development of fluoromethylating reagents and several new reagents have been prepared and used. Most of the reagents are based on fluorohalomethanes, and, more specifically, fluorochloromethane, or derivatives thereof. The main synthetic strategies are the introduction of a suitable leaving group in place of the halogen (Cl, Br, I), or the introduction of electron withdrawing substituents at the carbon atom bonded to fluorine. In the former case, the CH₂F group is transferred as the electrophile. The alkylation strength of the reagents differs and can be fine-tuned by the nature of the respective leaving group. In the latter case, electron withdrawing substituents (SO₂Ar, PhCH₂OC(O), PhS(O)NTBS) stabilize a negative charge at the carbon atom bonded to fluorine and introduce CH₂F as a nucleophile, thus being a synthon for the unstable and very sensitive FCH₂Li. In the last decade, particular attention has been paid to reagents which are able to transfer the CH₂F group by a radical pathway. The strategy behind this approach was again the introduction of suitable substituents at the carbon atom bonded to fluorine, which favour radical formation. Despite the great progress which has been made, most of the reagents are effective in transferring CH₂F only to heteroatoms (nitrogen, oxygen, sulfur). The transfer of CH₂F with concurrent C-C bond formation is less effective, and the development of readily available fluoromethylating reagents capable of achieving this goal still remains a challenge for organofluorine chemists.

1.2.5 Acknowledgement

Ludwig-Maximilian-University of Munich (LMU) is gratefully acknowledged for financial support of this work. The authors thank Prof. T. M. Klapötke (LMU) for his continuous support of their work and Dr. M.-J. Crawford for her great help with the manuscript.

1.2.6 References

- [1] K. K. J. Chan, D. O'Hagan, *Methods Enzymol.* **2012**, *516*, 219–235.
- [2] a) D. O'Hagan, H. Deng, *Chem. Rev. (Washington, DC, U. S.)* **2015**, *115*, 634–649; b) X. Feng, D. Bello, P. T. Lowe, J. Clark, D. O'Hagan, *Chem. Sci.* **2019**, *10*, 9501–9505.
- [3] a) D. O'Hagan, R. Perry, J. M. Lock, J. J. M. Meyer, L. Dasaradhi, J. T. G. Hamilton, D. B. Harper, *Phytochemistry* **1993**, *33*, 1043–1045; b) A. T. Proudfoot, S. M. Bradberry, J. A. Vale, *Toxicol. Rev.* **2006**, *25*, 213–219.
- [4] K. Mueller, C. Faeh, F. Diederich, *Science (Washington, DC, U. S.)* **2007**, *317*, 1881–1886.
- [5] a) D. O'Hagan, *Chem. Soc. Rev.* **2008**, *37*, 308–319; b) T. Liang, C. N. Neumann, T. Ritter, *Angew. Chem., Int. Ed.* **2013**, *52*, 8214–8264; c) G. K. S. Prakash, N. Shao, F. Wang, C. Ni, *Org. Synth.* **2013**, *90*, 130–144.

- [6] a) N. A. Meanwell, *J. Med. Chem.* **2018**, *61*, 5822–5880; b) G. A. Showell, J. S. Mills, *Drug Discovery Today* **2003**, *8*, 551–556; c) N. A. Meanwell, *J. Med. Chem.* **2011**, *54*, 2529–2591.
- [7] a) J. Hu, W. Zhang, F. Wang, *Chem. Commun. (Cambridge, U. K.)* **2009**, 7465–7478; b) Y. Zhou, J. Wang, Z. Gu, S. Wang, W. Zhu, J. L. Acena, V. A. Soloshonok, K. Izawa, H. Liu, *Chem. Rev. (Washington, DC, U. S.)* **2016**, *116*, 422–518.
- [8] M. Reichel, J. Martens, E. Woellner, L. Huber, A. Kornath, K. Karaghiosoff, *Eur. J. Inorg. Chem.* **2019**, *2019*, 2530–2534.
- [9] a) C. Walsh, *Tetrahedron* **1982**, *38*, 871–909; b) T. Tsushima, K. Kawada, *Tetrahedron Lett.* **1985**, *26*, 2445–2448; c) R. Bohlmann, D. Bittler, M. Gottwald, P. Muhn, Y. Nishino, B. Schoenecker, G. Hobe, DE 4330237A1, Germany . **1995**.
- [10] a) Y. Qiu, Z. Wu, Y. Liu, S. Chen, H. Zhang (Amphastar Pharmaceuticals, Inc.), WO-2016054280A1, USA **2016**; b) D. Punde, C. Bohara, K. Pokharkar, M. K. Gadakar, V. Gore (Mylan Laboratories Ltd.), IN-2012CH03689A, India **2014**; c) W. Xu, H. Li, Zhejiang (Lantian Environmental Protection Hi-Tech Co., Ltd.), WO-2010022645A1, China **2010**; d) A. M. Acharya, IN-2007MU00917A, India **2009**.
- [11] a) EU, 1005/2009/EG, **2009**; b) M. M. Hurwitz, E. L. Fleming, P. A. Newman, F. Li, E. Mlawer, K. Cady-Pereira, R. Bailey, *Geophys. Res. Lett.* **2015**, *42*, 8686–8692.
- [12] K. L. Brocklesby, J. S. Waby, C. Cawthorne, G. Smith, *Tetrahedron Lett.* **2018**, *59*, 1635–1637.
- [13] a) N. Noto, T. Koike, M. Akita, *ACS Catal.* **2019**, *9*, 4382–4387; b) Y. Kita, S. Shigetani, K. Kamata, M. Hara, *Mol. Catal.* **2019**, *475*, 110463–110471.
- [14] J. Hu, C. Ni, *Vol. 2*, Georg Thieme Verlag, **2014**, 409–457.
- [15] C. Ni, L. Zhu, J. Hu, *Huaxue Xuebao* **2015**, *73*, 90–115.
- [16] C. Ni, M. Hu, J. Hu, *Chem. Rev. (Washington, DC, U. S.)* **2015**, *115*, 765–825.
- [17] N. Shibata, *Bull. Chem. Soc. Jpn.* **2016**, *89*, 1307–1320.
- [18] G. Olah, A. Pavlath, *Acta Chim. Acad. Sci. Hung.* **1953**, *3*, 203–207.
- [19] a) X. Chen (Zhenjiang Shengan Pharmaceutical Co., Ltd.), CN103724198A, China . **2014**; b) M. A. Kim, B. B. Lee, J. S. Oh, Y. S. Hong (LG Chem, Ltd.), KR2013047801A, S. Korea . **2013**.
- [20] M. Reichel, J. Martens, C. C. Unger, K. Karaghiosoff, *Phosphorus, Sulfur Silicon Relat. Elem.* **2019**, *194*, 467–468.
- [21] a) K. Uneyama, *Organofluorine Chemistry*, Wiley, **2008**; b) M. Reichel, B. Krumm, K. Karaghiosoff, *J. Fluorine Chem.* **2019**, *226*, 109351–109355; c) P. Kirsch, *Modern Fluoroorganic Chemistry: Synthesis, Reactivity, Applications*, Wiley, **2006**.
- [22] W. Zhang, L. Zhu, J. Hu, *Tetrahedron* **2007**, *63*, 10569–10575.
- [23] M. Reichel, B. Krumm, Y. V. Vishnevskiy, S. Blomeyer, J. Schwabedissen, H.-G. Stammer, K. Karaghiosoff, N. W. Mitzel, *Angew. Chem. Int. Ed.* **2019**, *58*, 18557–18561.
- [24] J. C. Orr, J. Edwards, A. Bowers (Syntex Corp.), US-3080395, USA **1963**.
- [25] D. Lesuisse, J. F. Gourvest, C. Hartmann, B. Tric, O. Benslimane, D. Philibert, J. P. Vever, *J. Med. Chem.* **1992**, *35*, 1588–1597.
- [26] U. Rheude, W. Sundermeyer, *Chem. Ber.* **1985**, *118*, 2208–2219.

- [27] a) H. Yin, J. Sheng, K.-F. Zhang, Z.-Q. Zhang, K.-J. Bian, X.-S. Wang, *Chem. Commun. (Cambridge, U. K.)* **2019**, 55, 7635–7638; b) L. An, Y.-L. Xiao, Q.-Q. Min, X. Zhang, *Angew. Chem., Int. Ed.* **2015**, 54, 9079–9083; c) J. Hu, B. Gao, L. Li, C. Ni, J. Hu, *Org. Lett.* **2015**, 17, 3086–3089; d) T. Ding, L. Jiang, J. Yang, Y. Xu, G. Wang, W. Yi, *Org. Lett.* **2019**, 21, 6025–6028; e) N.-Y. Wu, X.-H. Xu, F.-L. Qing, *ACS Catal.* **2019**, 9, 5726–5731; f) Y.-M. Su, G.-S. Feng, Z.-Y. Wang, Q. Lan, X.-S. Wang, *Angew. Chem., Int. Ed.* **2015**, 54, 6003–6007; g) J. Sheng, H.-Q. Ni, H.-R. Zhang, K.-F. Zhang, Y.-N. Wang, X.-S. Wang, *Angew. Chem., Int. Ed.* **2018**, 57, 7634–7639; h) X. Sun, S. Yu, *Org. Lett.* **2014**, 16, 2938–2941; i) H. Doi, I. Ban, A. Nonoyama, K. Sumi, C. Kuang, T. Hosoya, H. Tsukada, M. Suzuki, *Chem. - Eur. J.* **2009**, 15, 4165–4171; j) R. R. Merchant, J. T. Edwards, T. Qin, M. M. Kruszyk, C. Bi, G. Che, D.-H. Bao, W. Qiao, L. Sun, M. R. Collins, O. O. Fadeyi, G. M. Gallego, J. J. Mousseau, P. Nuhant, P. S. Baran, *Science (Washington, DC, U. S.)* **2018**, 360, 75–80; k) S. Han, Q. Wu, L. Mele, L. Ding, J. Li, D. Zou, Y. Wu, Y. Wu, *Tetrahedron Lett.* **2019**, Ahead of Print; l) Z.-Y. Li, L. Li, Q.-L. Li, K. Jing, H. Xu, G.-W. Wang, *Chem. - Eur. J.* **2017**, 23, 3285–3290; m) Z. Ruan, S.-K. Zhang, C. Zhu, P. N. Ruth, D. Stalke, L. Ackermann, *Angew. Chem., Int. Ed.* **2017**, 56, 2045–2049.
- [28] a) F. Liu, L. Jiang, H. Qiu, W. Yi, *Org. Lett.* **2018**, 20, 6270–6273; b) G. K. S. Prakash, I. Ledneczki, S. Chacko, G. A. Olah, *Org. Lett.* **2008**, 10, 557–560; c) X.-J. Tang, W. R. Dolbier, Jr., *Angew. Chem., Int. Ed.* **2015**, 54, 4246–4249; d) Y. Liu, L. Lu, Q. Shen, *Angew. Chem., Int. Ed.* **2017**, 56, 9930–9934; e) X. Shen, M. Zhou, C. Ni, W. Zhang, J. Hu, *Chem. Sci.* **2014**, 5, 117–122; f) V. Reutrakul, M. Pohmakotr, *Fluoromethyl phenyl sulfon*, John Wiley & Sons, Ltd., **2001**; g) N. Shibata, T. Furukawa, *1,1'-(Fluoromethylene)-bis(sulfonyl)]bis Benzene*, John Wiley & Sons, Ltd., **2010**; h) Y. Tamura, Y. Hinata, E. Kojima, H. Ozasa, (Shionogi & Co., Ltd.), WO-2016031842A1, Japan **2016**; i) T. Fukuzumi, N. Shibata, M. Sugiura, H. Yasui, S. Nakamura, T. Toru, *Angew. Chem., Int. Ed.* **2006**, 45, 4973–4977; j) X.-J. Tang, C. S. Thomason, W. R. Dolbier, Jr., *Org. Lett.* **2014**, 16, 4594–4597; k) T. Leitao, C. R. Turner (Hovione Inter Limited), WO 2011151624A1, Switz, **2011**; l) H. Wen, S. Wang, Q. Wang, *Shenyang Yaoke Daxue Xuebao* **2001**, 18, 411–413.
- [29] a) E. O. Aboagye, E. G. Robins, G. Smith, S. Luthra, (GE Healthcare Limited, Medi-Physics, Inc.), WO-2012040151A2, UK **2012**; b) H. Doi, M. Goto, M. Suzuki, *Bull. Chem. Soc. Jpn.* **2012**, 85, 1233–1238.
- [30] S. Cherkez (Chemagis Ltd.), IL-109656A, Israel **1998**.
- [31] S. Monticelli, V. Pace, *Aust. J. Chem.* **2018**, 71, 473–475.
- [32] C. Guo, X. Yue, F.-L. Qing, *Synthesis* **2010**, 1837–1844.
- [33] C. Yuan, L. Zhu, R. Zeng, Y. Lan, Y. Zhao, *Angew. Chem., Int. Ed.* **2018**, 57, 1277–1281.
- [34] P. O. Gitel, T. G. Spiridonova, A. Y. Yakubovich, *Zh. Obshch. Khim.* **1966**, 36, 871–874.
- [35] a) J. L. Barkin, M. D. Faust, Jr., W. C. Trenkle, *Org. Lett.* **2003**, 5, 3333–3335; b) W. J. Middleton, *J. Org. Chem.* **1984**, 49, 4541–4543.
- [36] S. Voltrova, J. Filgas, P. Slavicek, P. Beier, *Org. Chem. Front.* **2020**, 7, 10–13.

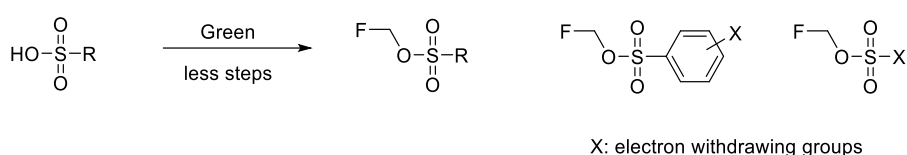
- [37] A. Ali, M. M.-C. Lo, Y.-H. Lim, A. Stamford, R. Kuang, P. Tempest, Y. Yu, X. Huang, T. J. Henderson, J.-H. Kim, C. Boyce, P. Ting, J. Zheng, E. Metzger, N. Zorn, D. Xiao, G. V. Gallo, W. Won, H. Wu (Merck Sharp & Dohme Corp.), WO-2014105666A1, **2014**; b) Y. Suzuki, T. Motoki, T. Kaneko, M. Takaishi, T. Ishida, K. Takeda, Y. Kita, N. Yamamoto, A. Khan, P. Dimopoulos (Eisai R & D Management Co., Ltd.), WO-2009091016A1, USA **2009**.
- [38] R. Iwata, C. Pascali, A. Bogni, S. Furumoto, K. Terasaki, K. Yanai, *Appl. Radiat. Isot.* **2002**, *57*, 347–352.
- [39] a) P. Li, L. P. Wennogle, J. Zhao, H. Zheng (Intra-Cellular Therapies Inc.), WO-2011043816A1, USA **2011**; b) R. Iwata, S. Furumoto, C. Pascali, A. Bogni, K. Ishiwata, *J. Labelled Compd. Radiopharm.* **2003**, *46*, 555–566; c) G. Smith, Y. Zhao, J. Leyton, B. Shan, Q.-d. Nguyen, M. Perumal, D. Turton, E. Arstad, S. K. Luthra, E. G. Robins, E. O. Aboagye, *Nucl. Med. Biol.* **2011**, *38*, 39–51.
- [40] D. Block, H. H. Coenen, G. Stoecklin, *J. Labelled Compd. Radiopharm.* **1987**, *24*, 1029–1042.
- [41] T. R. Neal, S. Apana, M. S. Berridge, *J. Labelled Compd. Radiopharm.* **2005**, *48*, 557–568.
- [42] a) A. Ali, M. M.-C. Lo, Y.-H. Lim, A. Stamford, R. Kuang, P. Tempest, Y. Yu, X. Huang, T. J. Henderson, J.-H. Kim, C. Boyce, P. Ting, J. Zheng, E. Metzger, N. Zorn, D. Xiao, G. V. Gallo, W. Won, H. Wu (Merck Sharp & Dohme Corp.), WO-2014105666A1, USA **2014**; b) Y. Suzuki, T. Motoki, T. Kaneko, M. Takaishi, T. Ishida, K. Takeda, Y. Kita, N. Yamamoto, A. Khan, P. Dimopoulos (Eisai R & D Management Co., Ltd.), WO-2009091016A1, Japan **2009**; c) K. Nakahara, K. Fuchino, K. Komano, N. Asada, G. Tadano, T. Hasegawa, T. Yamamoto, Y. Sako, M. Ogawa, C. Unemura, M. Hosono, H. Ito, G. Sakaguchi, S. Ando, S. Ohnishi, Y. Kido, T. Fukushima, D. Dhuyvetter, H. Borghys, H. J. M. Gijzen, Y. Yamano, Y. Iso, K.-i. Kusakabe, *J. Med. Chem.* **2018**, *61*, 5525–5546; d) H. Naito, Y. Kagoshima, H. Funami, A. Nakamura, M. Asano, M. Haruta, T. Suzuki, J. Watanabe, R. Kanada, S. Higuchi, K. Ito, A. Egami, K. Kobayashi (Daiichi Sankyo Company, Limited), WO-2018235966A1, Japan **2018**; e) K. Fuchino, Y. Mitsuoka, M. Masui, N. Kurose, S. Yoshida, K. Komano, T. Yamamoto, M. Ogawa, C. Unemura, M. Hosono, H. Ito, G. Sakaguchi, S. Ando, S. Ohnishi, Y. Kido, T. Fukushima, H. Miyajima, S. Hiroyama, K. Koyabu, D. Dhuyvetter, H. Borghys, H. J. M. Gijzen, Y. Yamano, Y. Iso, K.-i. Kusakabe, *J. Med. Chem.* **2018**, *61*, 5122–5137.
- [43] Y. Nomura, E. Tokunaga, N. Shibata, *Angew. Chem., Int. Ed.* **2011**, *50*, 1885–1889.
- [44] V. Reutrakul, M. Pohmakotr, e-EROS Encycl. Reagents Org. Synth., *Fluoromethyl phenyl sulfide*, John Wiley & Sons, Ltd., **2001**;
- [45] Y.-D. Yang, X. Lu, G. Liu, E. Tokunaga, S. Tsuzuki, N. Shibata, *ChemistryOpen* **2012**, *1*, 221–226.
- [46] G. Parisi, M. Colella, S. Monticelli, G. Romanazzi, W. Holzer, T. Langer, L. Degennaro, V. Pace, R. Luisi, *J. Am. Chem. Soc.* **2017**, *139*, 13648–13651.
- [47] X. Shen, W. Zhang, L. Zhang, T. Luo, X. Wan, Y. Gu, J. Hu, *Angew. Chem., Int. Ed.* **2012**, *51*, 6966–6970.

- [48] Y. Fujiwara, J. A. Dixon, F. O'Hara, E. D. Funder, D. D. Dixon, R. A. Rodriguez, R. D. Baxter, B. Herle, N. Sach, M. R. Collins, Y. Ishihara, P. S. Baran, *Nature (London, U. K.)* **2012**, *492*, 95–99.
- [49] Z. He, P. Tan, C. Ni, J. Hu, *Org. Lett.* **2015**, *17*, 1838–1841.
- [50] a) Y. Zhao, F. Liu, *Tetrahedron Lett.* **2018**, *59*, 180–187; b) J. Fang, W.-G. Shen, G.-Z. Ao, F. Liu, *Org. Chem. Front.* **2017**, *4*, 2049–2053.
- [51] W. Fu, Y. Sun, X. Li, *Synth. Commun.* **2019**, Ahead of Print.
- [52] J. Rong, L. Deng, P. Tan, C. Ni, Y. Gu, J. Hu, *Angew. Chem., Int. Ed.* **2016**, *55*, 2743–2747.
- [53] T. Koike, M. Akita, *Org. Biomol. Chem.* **2019**, *17*, 5413–5419.
- [54] J. T. Palmer (Prototek, Inc.), EP-442754A2, USA **1991**;
- [55] a) J.-J. Cao, X. Wang, S.-Y. Wang, S.-J. Ji, *Chem. Commun. (Cambridge, U. K.)* **2014**, *50*, 12892–12895; b) A. Harsanyi, G. Sandford, D. S. Yufit, J. A. K. Howard, *Beilstein J. Org. Chem.* **2014**, *10*, 1213–1219.
- [56] M. Inbasekaran, N. P. Peet, J. R. McCarthy, M. E. LeTourneau, *J. Chem. Soc., Chem. Commun.* **1985**, 678–679.
- [57] Y. Li, C. Ni, J. Liu, L. Zhang, J. Zheng, L. Zhu, J. Hu, *Org. Lett.* **2006**, *8*, 1693–1696.
- [58] S. Fustero, J. Moscardo, M. Sanchez-Rosello, E. Rodriguez, P. Barrio, *Org. Lett.* **2010**, *12*, 5494–5497.
- [59] S. Fustero, I. Ibanez, P. Barrio, M. A. Maestro, S. Catalan, *Org. Lett.* **2013**, *15*, 832–835.
- [60] J. Liu, Y. Li, J. Hu, *J. Org. Chem.* **2007**, *72*, 3119–3121.
- [61] J. Liu, C. Ni, Y. Li, L. Zhang, G. Wang, J. Hu, *Tetrahedron Lett.* **2006**, *47*, 6753–6756.
- [62] C. Ni, L. Zhang, J. Hu, *J. Org. Chem.* **2008**, *73*, 5699–5713.
- [63] V. Reutrakul, V. Rukachaisirikul, *Tetrahedron Lett.* **1983**, *24*, 725–728.
- [64] a) Y. Zhao, B. Gao, C. Ni, J. Hu, *Org. Lett.* **2012**, *14*, 6080–6083; b) Y. Zhao, C. Ni, F. Jiang, B. Gao, X. Shen, J. Hu, *ACS Catal.* **2013**, *3*, 631–634; c) X. Shen, W. Miao, C. Ni, J. Hu, *Angew. Chem., Int. Ed.* **2014**, *53*, 775–779.
- [65] M. L. Boys, E. W. Collington, H. Finch, S. Swanson, J. F. Whitehead, *Tetrahedron Lett.* **1988**, *29*, 3365–3368.
- [66] a) C. Ni, Y. Li, J. Hu, *J. Org. Chem.* **2006**, *71*, 6829–6833; b) Z. Zhang, A. Puente, F. Wang, M. Rahm, Y. Mei, H. Mayr, G. K. S. Prakash, *Angew. Chem., Int. Ed.* **2016**, *55*, 12845–12849; c) G. K. S. Prakash, F. Wang, N. Shao, T. Mathew, G. Rasul, R. Haiges, T. Stewart, G. A. Olah, *Angew. Chem., Int. Ed.* **2009**, *48*, 5358–5362; d) A. Tarui, S. Kondo, K. Sato, M. Omote, H. Minami, Y. Miwa, A. Ando, *Tetrahedron* **2013**, *69*, 1559–1565.
- [67] a) G. K. S. Prakash, X. Zhao, S. Chacko, F. Wang, H. Vaghoo, G. A. Olah, *Beilstein J. Org. Chem.* **2008**, *4*, 17; b) T. Furukawa, N. Shibata, S. Mizuta, S. Nakamura, T. Toru, M. Shiro, *Angew. Chem., Int. Ed.* **2008**, *47*, 8051–8054.
- [68] S. Zhang, Y. Zhang, Y. Ji, H. Li, W. Wang, *Chem. Commun. (Cambridge, U. K.)* **2009**, 4886–4888.
- [69] a) X. Shen, L. Zhang, Y. Zhao, L. Zhu, G. Li, J. Hu, *Angew. Chem., Int. Ed.* **2011**, *50*, 2588–2592; b) S.-L. Zhang, H.-X. Xie, J. Zhu, H. Li, X.-S. Zhang, J. Li, W. Wang, *Nat. Commun.* **2011**, *2*, 1214–1217.

- [70] a) X. Companyo, G. Valero, V. Ceban, T. Calvet, M. Font-Bardia, A. Moyano, R. Rios, *Org. Biomol. Chem.* **2011**, *9*, 7986–7989; b) L.-y. Mei, Z.-l. Yuan, M. Shi, *Organometallics* **2011**, *30*, 6466–6475; c) X. Zhao, D. Liu, S. Zheng, N. Gao, *Tetrahedron Lett.* **2011**, *52*, 665–667.
- [71] C. Hollingworth, A. Hazari, M. N. Hopkinson, M. Tredwell, E. Benedetto, M. Huiban, A. D. Gee, J. M. Brown, V. Gouverneur, *Angew. Chem., Int. Ed.* **2011**, *50*, 2613–2617.
- [72] G. K. S. Prakash, S. Chacko, H. Vaghoo, N. Shao, L. Gurung, T. Mathew, G. A. Olah, *Org. Lett.* **2009**, *11*, 1127–1130.
- [73] W.-B. Liu, S.-C. Zheng, H. He, X.-M. Zhao, L.-X. Dai, S.-L. You, *Chem. Commun. (Cambridge, U. K.)* **2009**, 6604–6606.
- [74] a) T. Furukawa, J. Kawazoe, W. Zhang, T. Nishimine, E. Tokunaga, T. Matsumoto, M. Shiro, N. Shibata, *Angew. Chem., Int. Ed.* **2011**, *50*, 9684–9688; b) S. Mizuta, N. Shibata, Y. Goto, T. Furukawa, S. Nakamura, T. Toru, *J. Am. Chem. Soc.* **2007**, *129*, 6394–6395.
- [75] X. Shen, C. Ni, J. Hu, *Helv. Chim. Acta* **2012**, *95*, 2043–2051.
- [76] a) M. Kamlar, P. Putaj, J. Vesely, *Tetrahedron Lett.* **2013**, *54*, 2097–2100; b) C. Ni, J. Hu, *Tetrahedron Lett.* **2009**, *50*, 7252–7255.
- [77] a) T. W. Butcher, J. F. Hartwig, *Angew. Chem., Int. Ed.* **2018**, *57*, 13125–13129; b) W. Huang, C. Ni, Y. Zhao, J. Hu, *New J. Chem.* **2013**, *37*, 1684–1687.
- [78] W. Yang, X. Wei, Y. Pan, R. Lee, B. Zhu, H. Liu, L. Yan, K.-W. Huang, Z. Jiang, C.-H. Tan, *Chem. - Eur. J.* **2011**, *17*, 8066–8070.
- [79] H. Su, Y. Xie, W.-B. Liu, S.-L. You, *Bioorg. Med. Chem. Lett.* **2011**, *21*, 3578–3582.
- [80] G. K. S. Prakash, L. Gurung, P. V. Jog, S. Tanaka, T. E. Thomas, N. Ganesh, R. Haiges, T. Mathew, G. A. Olah, *Chem. - Eur. J.* **2013**, *19*, 3579–3583.
- [81] Y. S. Kim, S. M. Kim, B. Wang, X. Companyo, J. Li, A. Moyano, S. Im, Z. Tosner, J. W. Yang, R. Rios, *Adv. Synth. Catal.* **2014**, *356*, 437–446.
- [82] K. Matsuzaki, T. Furukawa, E. Tokunaga, T. Matsumoto, M. Shiro, N. Shibata, *Org. Lett.* **2013**, *15*, 3282–3285.
- [83] a) J. Dai, X. Duan, J. Zhou, C. Fu, S. Ma, *Chin. J. Chem.* **2018**, *36*, 387–391; b) W.-Z. Zhang, H. Li, Y. Zeng, X. Tao, X. Lu, *Chin. J. Chem.* **2018**, *36*, 112–118.
- [84] M. Ogasawara, H. Murakami, T. Furukawa, T. Takahashi, N. Shibata, *Chem. Commun. (Cambridge, U. K.)* **2009**, 7366–7368.
- [85] G. K. S. Prakash, N. Shao, Z. Zhang, C. Ni, F. Wang, R. Haiges, G. A. Olah, *J. Fluorine Chem.* **2012**, *133*, 27–32.
- [86] T. Furukawa, Y. Goto, J. Kawazoe, E. Tokunaga, S. Nakamura, Y. Yang, H. Du, A. Kakehi, M. Shiro, N. Shibata, *Angew. Chem., Int. Ed.* **2010**, *49*, 1642–1647.
- [87] H. Ma, K. Matsuzaki, Y.-D. Yang, E. Tokunaga, D. Nakane, T. Ozawa, H. Masuda, N. Shibata, *Chem. Commun. (Cambridge, U. K.)* **2013**, *49*, 11206–11208.
- [88] a) S. Opekar, R. Pohl, P. Beran, L. Rulisek, P. Beier, *Chem. - Eur. J.* **2014**, *20*, 1453–1458; b) S. Opekar, R. Pohl, V. Eigner, P. Beier, *J. Org. Chem.* **2013**, *78*, 4573–4579; c) Y. L. Yagupolskii, N. V. Pavlenko, S. V. Shelyazhenko, A. A. Filatov, M. M. Kremlev, A. I. Mushta, I. I. Gerus, S. Peng, V. A. Petrov, M. Nappa, *J. Fluorine Chem.* **2015**, *179*, 134–141.
- [89] T. Koizumi, T. Hagi, Y. Horie, Y. Takeuchi, *Chem. Pharm. Bull.* **1987**, *35*, 3959–3962.

1.3 Objectives

At a time when climate change becomes dramatic and ecological issues are becoming increasingly important for industry, it is necessary and essential to find good replacements for the increasingly regulated and problematic CH_2FCl and CH_2FBr fluorocarbons. It is the task and duty of chemists to use their knowledge and offer acceptable solutions. Since the demand for pharmaceuticals containing the fluoromethyl group remains constantly high but the phasing out process of fluoromethylating agents has already initiated, research to find alternatives must be driven forward rapidly. The main purpose of this thesis is to develop various new sulfonic acid fluoromethyl esters as possible strong electrophilic monofluoromethylating agents for use in laboratory and industry (Scheme 1).



Scheme 1: Sulfonic acid ester based fluoromethylating agents.

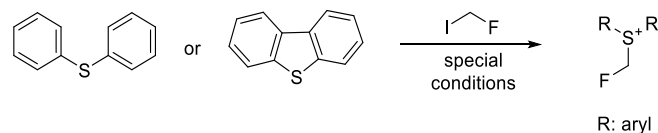
The concept of this work is based on the general experience with sulfonic acid alkyl esters as alkylating agents. The synthesis of the new reagents should be straight forward, comprise a minimum number of steps, make use of environmentally friendly chemicals, consider the possibility of recycling and be as cheap as possible. The properties of the new reagents are a second important issue. Solid stable reagents or liquid reagents of low volatility have the advantage of easy handling and might be preferred for laboratory and industry, although volatile reagents facilitate workup and might also be of interest for industrial purposes. The solid reagents should have good crystallizing properties, thus making the identification of possible by-products, formed during the fluoromethylation reaction.

The fluoromethylation ability of the most promising reagents should be tested by reaction with various nucleophiles. Important issues are the required reaction conditions, yields, tolerance of functional groups and selectivity, in particular when polyfunctional substrates are used, as well as the formation of (hazardous!) by-products.

The present thesis is intended to include applied research as well as fundamental research, thus showing, that these two ways to view and make chemistry belong intrinsically together. In this context the new reagents should also be used to experimentally enter and extend the exciting family of fluoromethyl pseudohalides. In addition to fundamental questions on the influence of fluorine on physical and chemical properties of the resulting new fluorine containing small molecules also their possible application as new reagents in preparative organoelement chemistry is of great interest.

A general objective (and the desire of every chemist) is to test the limits, which are in this thesis the maximal fluoromethylating power, e.g. using CH_2FI as source for CH_2F , in combination with suitable supporting reagents. A challenging question is the development of proper

conditions making fluoromethylation of very weak nucleophiles like special thioethers possible (Scheme 2). In this special case the resulting sulfonium cation should itself act as a strong fluoromethylating agent.



Scheme 2: Synthesis of fluoromethyl sulfonium salts under special conditions.

The fluoromethyl group (CH_2F) is bioisosteric to the hydroxymethyl function (CH_2OH). A central question connected with this analogy is the influence of fluorine on the toxicity or other possible biological activities of selected types of compounds. The comparison of fluoromethyl phosphonium salts with analogous hydroxymethyl phosphonium salts regarding their toxicity is another important objective in this thesis. This work is done in cooperation with the group of Dr. Roidl in our Department.

2 Summary and Conclusion

Fluoromethylating Agents - A Challenge for Organofluorine Chemists

The introduction of the fluoromethyl group in organic molecules has been an objective for competitive research in the field of organofluorine chemistry since several decades. The search for new exciting molecules, deeper understanding of the influence of the exciting element fluorine on the properties of organofluorine compounds and a great number of industrial applications have motivated and pushed investigations in this field worldwide.

The story starts 1953 with the first documented use of fluoromethanol, FCH_2OH - an intriguing molecule - as a fluoromethylating agent and extends to 2017, when the unstable fluoromethyl lithium - a real highlight - has been employed to transfer the CH_2F group (Figure 1). In between a series of in part quite complicated and sophisticated fluoromethylating reagents have been developed, operating under different reaction conditions and through different reaction mechanisms; none of them combines a simple and cheap synthesis, easy handling and general applicability, however, thus successfully replacing the classical fluoromethyl halides CH_2FCl , CH_2FBr and CH_2FI as fluoromethylating reagents.

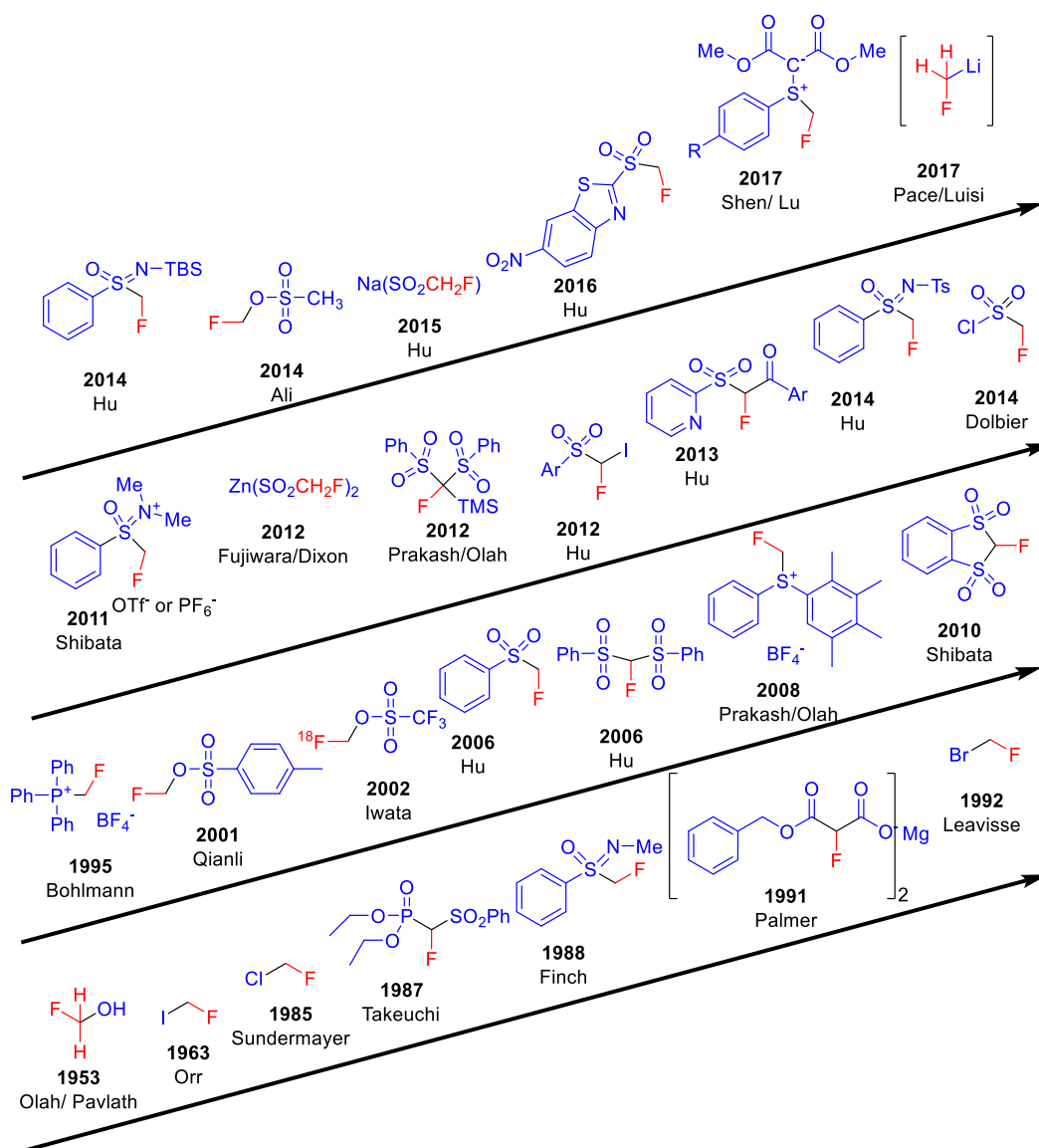


Figure 1: Timetable of new developed monofluoromethylating agents.

The Story Continues - *New Application of a General Concept*

The present thesis is intended to write the next page of the fluoromethylation story. It is based on an old, perhaps forgotten, but intuitively often applied concept: increasing the alkylation power of a reagent by optimizing the leaving group. Following this concept and using a variety of good leaving groups a series of new reagents have been prepared, most of which proved to transfer the CH_2F group to organic substrates (Figure 2).

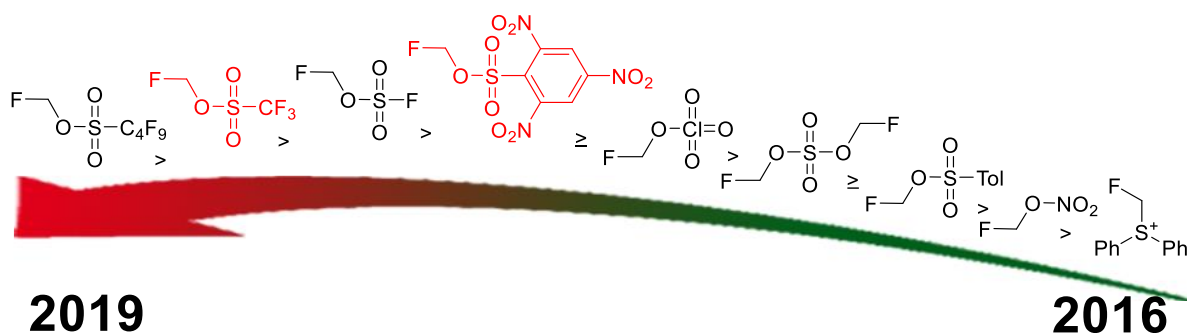
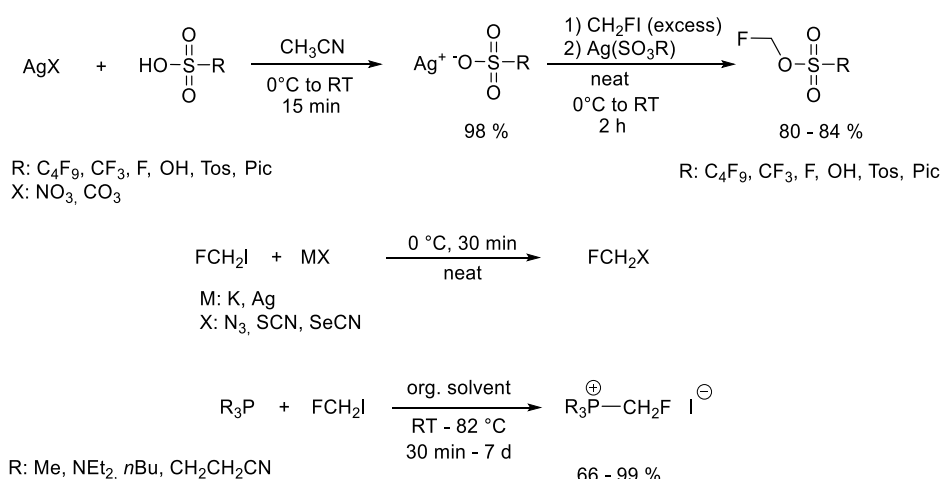


Figure 2: Newly synthesized and developed monofluoromethylating agents within this work (2016-2019).

The alkylating power of the new fluoromethylation reagents is anticipated to parallel the one of the corresponding methylating agents and is expected to increase to the left. For several cases it could be confirmed experimentally within the investigations in this thesis. All reagents are liquids except fluoromethyl-2,4,6-trinitrophenylsulfonate and fluoromethyl diphenylsulfonium tetrafluoroborate, which are solids. Some of the reagents, like fluoromethyl perchlorate or fluoromethyl nitrate are energetic. The compounds, which according to our experience are best suited for small scale application in the laboratory and large scale application in industry are fluoromethyl triflate and fluoromethyl-2,4,6-trinitrophenylsulfonate. They have been prepared several times on multi gram scale.

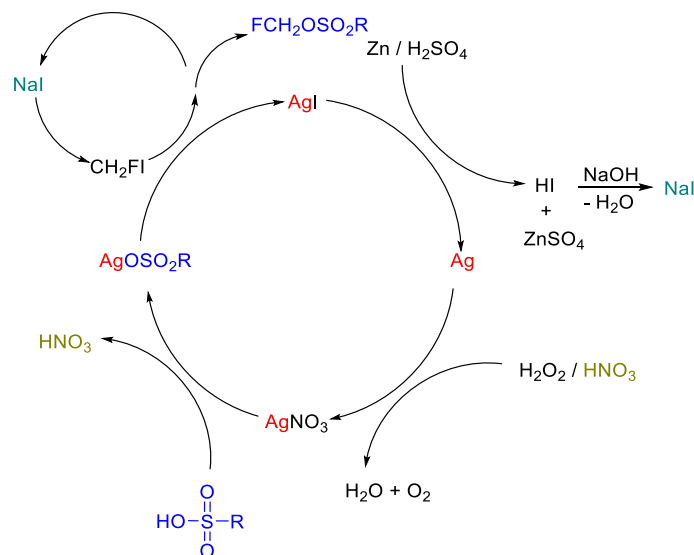
Straight Forward and Simple Syntheses - Thanks to Fluoroiodomethane

All reagents have been prepared using fluoroiodomethane (CH_2FI), as the source for the fluoromethyl group. Thus, CH_2IF , which is meanwhile readily available and environmentally unproblematic, is still essential and the main source of CH_2F . For fluoromethyl tosylate the synthesis was improved considerably, for fluoromethyl triflate a new synthesis was developed based on CH_2FI . All syntheses are easily performed, straight forward and simple. The reagents are obtained in very good yields (Scheme 1).



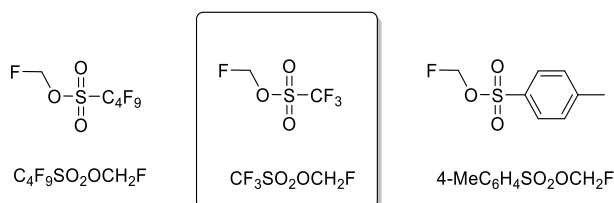
Scheme 1: Fluoroiodomethane based syntheses of fluoromethyl compounds.

In all syntheses the moderately reactive fluoriodomethane is activated by Ag^+ ions, either using the corresponding silver salt or, as in the case of $\text{Ph}_2\text{S}(\text{CH}_2\text{F})^+\text{BF}_4^-$, adding a suitable source of silver cations. This synthetic procedure might look very expensive, however the silver can be recovered within a cyclic process and reused (Scheme 2). The cyclic process shown in Scheme 2 was experimentally performed several times and consists of known steps, which have been combined in a proper manner.



Scheme 2: Recycling process for silver.

Fluoromethyl Triflate - *Simply the Best*



The new fluoromethyl sulfonates $\text{C}_4\text{F}_9\text{SO}_2\text{OCH}_2\text{F}$, $\text{CF}_3\text{SO}_2\text{OCH}_2\text{F}$ and $4\text{-MeC}_6\text{H}_4\text{SO}_2\text{OCH}_2\text{F}$ are promising fluoromethylating reagents. They are all colorless moisture sensitive liquids, which can be stored at ambient temperature under inert gas atmosphere for months.

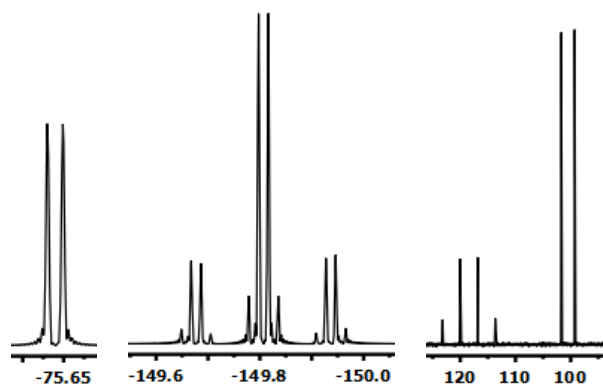


Figure 3: ^{19}F NMR spectrum (left, middle) and ^{13}C NMR spectrum (right) of $\text{CF}_3\text{SO}_2\text{OCH}_2\text{F}$.

By far the best reagent is fluoromethyl triflate. It is readily prepared starting from commercially available materials and obtained in very good yield. Batches of 25 mL each were prepared several times during this work. Fluoromethyl triflate shows a boiling point of about 90 °C, the other fluorosulfonates boil at higher temperatures.

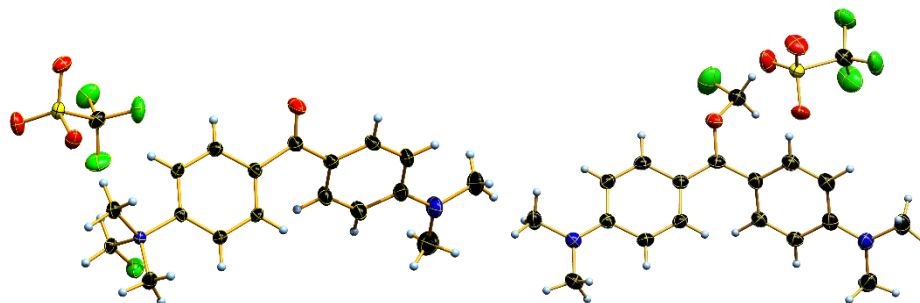
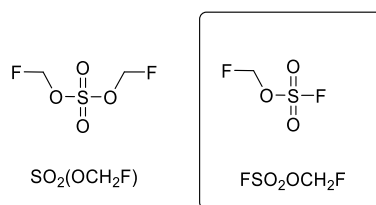


Figure 4: Fluoromethylated *Michler's Ketone*.

Fluoromethyl triflate is easy to handle and can be applied to our experience to a broad range of sulfur, oxygen, nitrogen and phosphorus nucleophiles. Triphenylphosphine oxide as well as diphenyl thioether and related thioethers can be readily fluoromethylated with fluoromethyl triflate. Noteworthy is the reaction with Michler's ketone, where fluoromethylation occurs at both nitrogen or oxygen (Figure 4). Both products could be isolated and characterized via single crystal X-ray diffraction.

Magic Fluoromethyl - the "Younger Brother"



Fluoromethyl fluorosulfonate, FSO₂OCH₂F (*Magic Fluoromethyl*) has been prepared together with bis(fluoromethyl) sulfate SO₂(OCH₂F)₂ for the first time. These reagents correspond to the well known methyl fluorosulfonate (*Magic Methyl*) and dimethylsulfate. Both are colorless liquids. While fluoromethyl fluorosulfonate is stable and can be stored at ambient temperature under inert gas atmosphere for a prolonged period of time, bis(fluoromethyl) sulfate is thermally much less stable and converts slowly at ambient temperature (faster on heating) to FSO₂OCH₂F releasing formaldehyde. *Magic Fluoromethyl* is a promising fluoromethylating reagent (Figure 5). Its alkylating power and the range of possible applications are one of the topics of a follow up project.

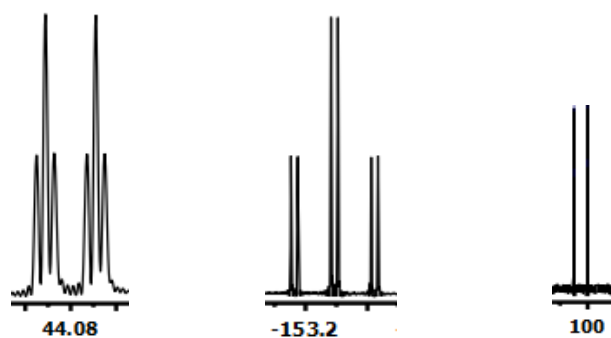


Figure 5: ^{19}F NMR spectrum (left) and ^{13}C NMR spectrum (right) of $\text{FSO}_2\text{OCH}_2\text{F}$.

Fluoromethyl Trinitrophenylsulfonate - *Solid, Selective, Easy to Use*

If a solid fluoromethylating reagent is needed, fluoromethyl 2,4,6-trinitrophenylsulfonate is in most cases definitely the reagent of choice. The compound is readily prepared with excellent yield and is isolated as a colorless microcrystalline solid (Figure 6). Several 20 g batches were prepared during this work. Fluoromethyl 2,4,6-trinitrophenylsulfonate is stable and can be stored at ambient temperature under inert gas atmosphere for several months.

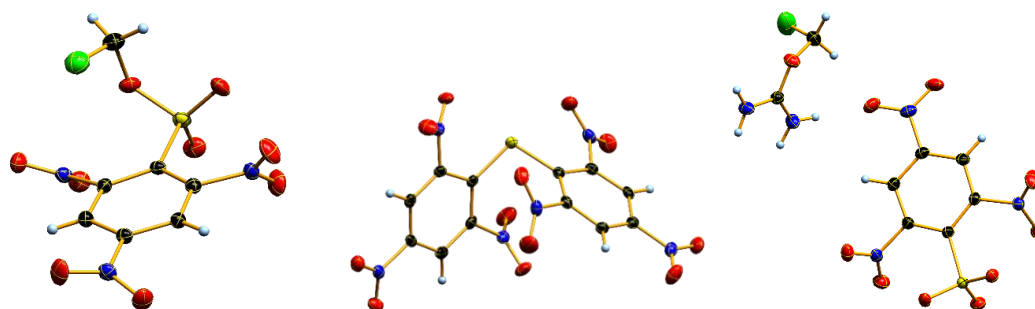


Figure 6: Molecular structure of fluoromethyl 2,4,6-trinitrophenylsulfonate (left), the di(2,4,6-trinitrophenyl)thioether (middle) and fluoromethyluronium 2,4,6-trinitrophenylsulfonate in the crystal.

Fluoromethyl 2,4,6-trinitrophenylsulfonate is a weaker fluoromethylating agent than fluoromethyl triflate. It does not react with triphenylphosphine oxide. With strong or protic nucleophiles attack of the nucleophile at the *ipso* carbon atom of the phenyl ring occurs, either blocking or cleaving the reagent. Thus reaction with triphenylphosphine sulfide in the presence of traces of water yields bis(2,4,6-trinitrophenyl) thioether - so absolutely dry solvents are necessary.

However, fluoromethyl 2,4,6-trinitrophenylsulfonate is an excellent reagent for the fluoromethylation of tertiary amines, pyridine derivatives, as well as urea and dialkylamides. It is particularly useful in cases, when crystalline products are preferred. Its use also facilitates the identification of by-products, which readily crystallize and can be characterized by single crystal X-ray diffraction. Fluoromethyl 2,4,6-trinitrophenylsulfonate is more selective than fluoromethyl triflate. With Michler's fluoromethylation occurs only at nitrogen.

Fluoromethyl Perchlorate - *Probing the Limits*

Fluoromethyl perchlorate has been prepared for the first time within this thesis. It represents a further member of the small family of alkyl perchlorates, which are characterized by excellent alkylating properties and at the same time by excellent explosive properties. Introduction of fluorine in the molecule to our experience increases the energetic properties of the compound. Fluoromethyl perchlorate is isolated as a colorless liquid, which is extremely sensitive towards external mechanical stimuli and displays the characteristic properties of a primary explosive. The ^{19}F NMR spectrum is remarkable, showing well separated signals for the ^{35}Cl and the ^{37}Cl isotopomers.

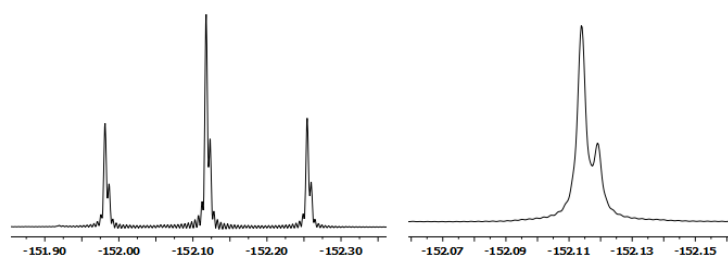


Figure 7: ^{19}F NMR spectrum of $\text{FCH}_2\text{OClO}_3$ (^1H coupled left, ^1H decoupled right) showing the signals of the ^{35}Cl and the ^{37}Cl isotopomers.

Fluoromethyl Nitrate - *a Small Exciting Molecule*

Fluoromethyl nitrate FCH_2ONO_2 - the fluoromethyl ester of nitric acid - has been prepared for the first time and its properties have been compared to those of the well known methyl nitrate. The study allows to detect the effect of fluorine on the properties of this small molecule. Fluoromethyl nitrate is a colorless highly volatile liquid, which causes headache when inhaled. Its sensitivity resembles that of nitroglycerine. As compared to methyl nitrate, the introduction of fluorine increases the energetic properties of the compound. Single crystals of fluoromethyl nitrate were obtained by low temperature crystallization and its structure in the solid state was determined by single crystal X-ray diffraction and compared to that of methyl nitrate (in cooperation with the group of Prof. Mitzel, Bielefeld). Remarkably, in the ^{17}O NMR spectrum separate signals for the dicoordinated and singly coordinated oxygen atoms can be observed.

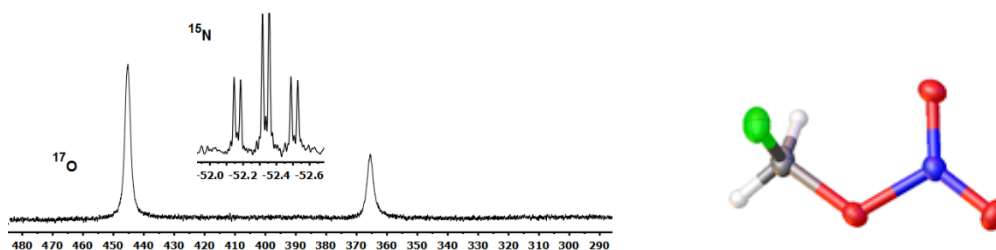


Figure 8: ^{17}O NMR Spectra (left, bottom), ^{15}N NMR Spectra (left, top) and molecular structure of FCH_2ONO_2 in the crystal (right).

Fluoromethyl Sulfonium Salts - *At the Limits of Stability*

Fluoromethyl sulfonium salts are anticipated to be good fluoromethylating reagents, due to the presence of the thioether motif as a good leaving group. The new fluoromethyl sulfonium salts prepared during this work displayed only limited stability, however. The compounds are isolated as microcrystalline colorless solids, which unfortunately tend to decompose when stored at ambient temperature under inert gas atmosphere over some weeks.

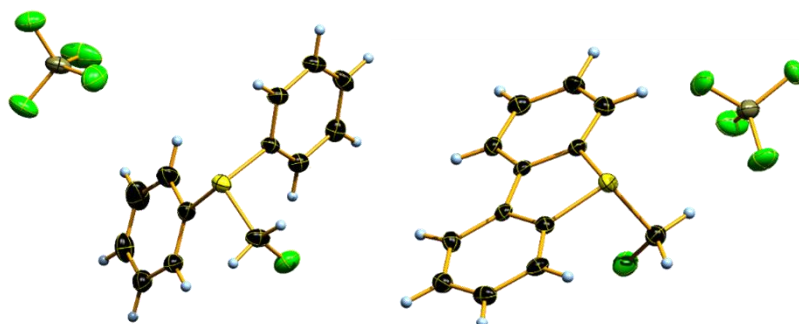


Figure 9: Crystal structures of fluoromethyl sulfonium salts.

Fluoromethyl Pseudohalides - *Fascinating Fluorine Containing Small Molecules*

The new fluoromethyl pseudohalides FCH_2N_3 , FCH_2SCN and FCH_2SeCN were prepared for the first time and characterized by multinuclear NMR spectroscopy. Fluoromethyl azide is a colorless highly volatile liquid, while fluoromethyl thiocyanate and fluoromethyl selenocyanate are isolated as colorless solids. Remarkably these two compounds are bench stable. A comparison of the physical properties of these new fluoromethyl pseudohalides with those of the well known methyl derivatives shows, that fluorine behaves like a huge hydrogen atom, showing no increased intermolecular interactions. The main effect is that of the higher mass of fluorine compared to hydrogen, which is reflected by the higher boiling points of the compounds as compared to the methyl analogues.

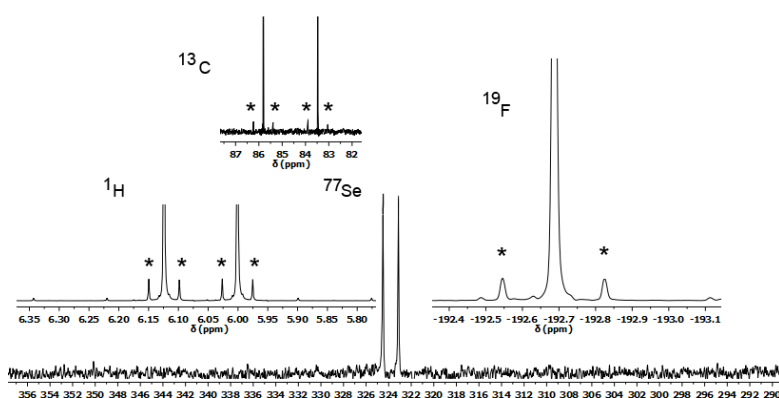


Figure 10: NMR spectra of FCH_2SeCN with ^{77}Se satellites (marked with *).

Fluoromethyl Phosphonium Salts - *Fluorine is NOT OH*

A series of fluoromethyl phosphonium salts were prepared and their structures in the crystal thoroughly investigated by single crystal X-ray diffraction. The study gives a first systematic insight into the structural behavior of the fluoromethyl group in intermolecular weak

interactions in the solid state and yields for the first time precious structural data for the CH₂F group bonded to phosphorus. In many fields the CH₂F group is considered bioisosteric to the CH₂OH group, assuming not only a similar space demand but also similar weak interactions with the environment. Our results show, that fluorine in CH₂F displays only weak interactions with the surrounding environment, mostly in form of weak hydrogen bonds acting as a H-acceptor. In contrast, OH groups form much stronger hydrogen bonding acting as H-acceptor as well as H-donor and influence much strongly the detailed arrangement of the molecules in the crystal. In contrast to P-OCH₂OH compounds, the investigated fluoromethyl phosphonium salt fluoromethyl trimethyl phosphonium iodide showed no biocidal activity towards *vibrio fisheri* and *e coli* bacteria.

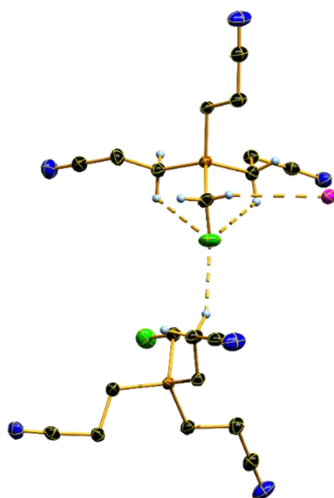
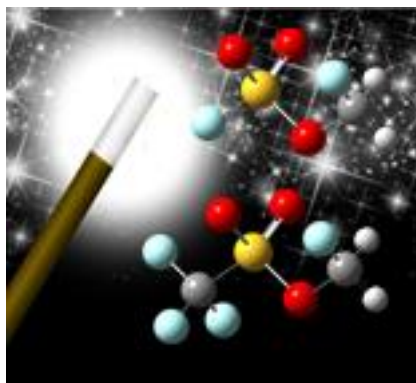


Figure 11: Molecular structure of fluoromethyl triscyanoethylphosphonium iodide in the crystal showing hydrogen bonding.

3 Fluoromethyltriflate: Magic Fluoromethyls Little Brother

Marco Reichel, Philipp Schmidt, Andreas Kornath, Konstantin Karaghiosoff

To be Submitted



Abstract: The hitherto unknown fluoromethyl fluorosulfonate $\text{FSO}_3\text{CH}_2\text{F}$ and – its “little brother” – fluoromethyl triflate $\text{CF}_3\text{SO}_3\text{CH}_2\text{F}$ have been prepared by a simple synthetic procedure in high yields. Both compounds are liquids and were characterized by vibrational and NMR spectroscopy. $\text{FSO}_3\text{CH}_2\text{F}$ was also obtained from the thermal decomposition of bis(fluoromethyl) sulfate $(\text{FCH}_2)_2\text{SO}_4$. Fluoromethyl triflate is a strong fluoromethylating agent and according to preliminary studies it represents a good alternative to replace the currently used ozone-depleting reagents CH_2FCl and CH_2FBr . Reactions of fluoromethyl triflate with different *N*, *O*, and *S* nucleophiles indicate its general applicability for the transfer of the CH_2F group to organic substrates. All fluoromethylated organic products were isolated as the pure compounds and characterised by vibrational- and NMR spectroscopy as well as by single crystal X-ray diffraction.

3.1 Introduction

Only five naturally occurring organofluorine compounds have been discovered until now.^[1] In spite of the low incidence of fluorinated products in nature, they play an extremely important role in fields of agrochemical and pharmaceutical industry.^[2] Since the introduction of fluoroalkyl groups in drug design became a routine practice, the high demand of these building blocks motivated the development of a series of fluoroalkylating agents.^[3] A CH_2F group is bioisosteric to various functional groups such as CH_2OH , CH_2NH_2 or CH_2SH and has the great advantage of high metabolic stability and lipophilicity. For these reasons CH_2F is of special interest as functional group in drugs.^[4] However, there is only a small number of suitable direct electrophilic monofluoromethylating agents described in the literature.^[3, 5] The fluoromethyl halides CH_2FBr and CH_2FCl have been used to fluoromethylate a series of oxygen, sulfur, nitrogen and carbon nucleophiles; unfortunately they are ozone-depleting gases and their use is going to be limited according to the Montreal protocol and EU regulations.^[5-6] However, due to their good fluoromethylating properties and their volatility, which makes industrial work-up easy, they are still used for industrial syntheses, e.g. for pharmaceuticals.^[7] Some research groups have described new, strong and efficient sulfonium derivatives as fluoromethylating

agents (Figure 1); nevertheless the starting materials of their syntheses are usually the environmentally problematic CH_2FBr or CH_2FCl .^[3, 8]

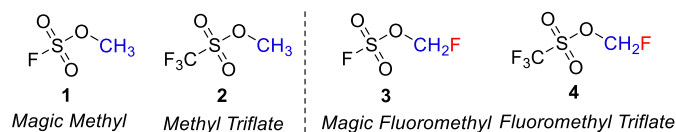
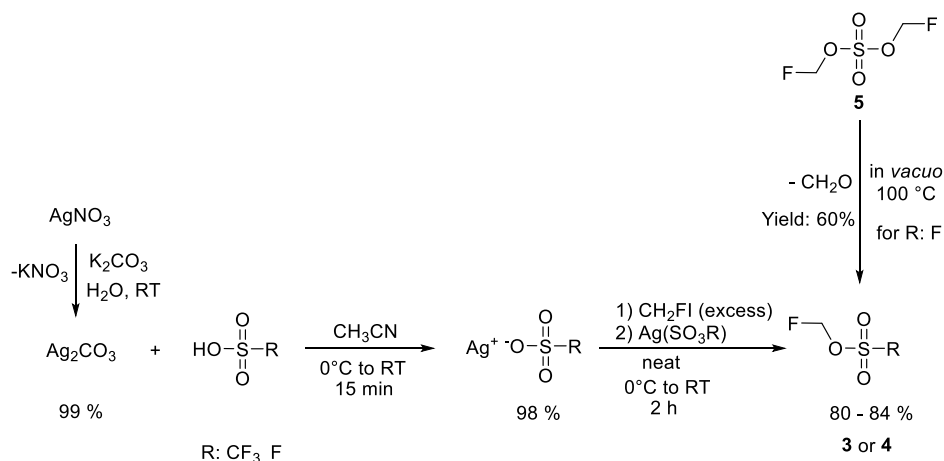


Figure 2: Fluoromethyl derivatives of *Magic Methyl*.

Fluoromethyl fluorosulfonate $\text{FSO}_3\text{CH}_2\text{F}$ (*Magic Fluoromethyl*) is not described in the literature. *Magic Methyl* is an extremely toxic compound and a similar toxicity can be expected also for the fluorine derivative **3**.^[10] Following the chemical properties of the methyl derivatives, fluoromethyl triflate **4** should be less toxic and at the same time a more powerful electrophilic fluoromethylating reagent than *Magic Fluoromethyl* **3**.^[9] In fact, in one Japanese patent fluoromethyl triflate **4** has been claimed to transfer the CH_2F group to a series of alkylaminopyridines.^[11] Further the ^{18}F labelled isotopomere of **4** was used for the synthesis of reagents^[5] suitable for PET imaging.^[12] The synthesis of ^{18}F labelled **4** is expensive and time consuming and requires a special equipments and quite harsh reaction conditions.^[3] Here we describe a straight forward and environmentally green synthesis of the new *Magic Fluoromethyl* **3** and of fluoromethyl triflate **4**, which provides the two compounds in good yields and opens the doors to systematic investigations of their chemical properties. The fluoromethylating properties of fluoromethyl triflate **4** are demonstrated by the reaction with a series of *O*, *N* and *S* nucleophiles.

3.2 Results and Discussion

Our strategy for the synthesis of **3** and **4** relies on our experience of introducing the CH_2F group with fluoroiodomethane CH_2FI in the presence of Ag^+ cations.^[13] The fluoromethylation of the silver sulfonate in different solvents at different temperatures turned out to be quite challenging. However: problems were a slow reaction rate and, depending on the temperature used, decomposition of CH_2FI and formation of several byproducts, which were hard to separate, overall resulting in low yields. The problems were solved omitting the solvent completely. When freshly prepared (synthesis adapted from ref.^[14]) or commercially available and dried silver fluorosulfonate or silver triflate is added to an excess of fluoroiodomethane at $0\text{ }^\circ\text{C}$ and allowed to react with stirring for 2 h at room temperature, the sulfonic ester (**3** or **4**) is formed. The excess of fluoroiodomethane acts as the solvent. The precipitate of AgI is filtered off, and the procedure is repeated with the filtrate to produce more of the sulfonic ester. As the sulfonic esters **3** and **4** are also liquids, they take over the function of the solvent when the reaction is progressing and the procedure is repeated until the complete consumption of CH_2FI . Repeating the reaction steps for 3-4 times amounts of 10 mL of the pure esters **3** and **4** can be obtained (80-84 % yield after purification) (Scheme 1).



Scheme 1: Synthesis of *Magic Fluoromethyl* **3** and fluoromethyl triflate **4**.

Interestingly *Magic Fluoromethyl* is also formed on heating of bis(fluoromethyl) sulfate (**5**) *in vacuo* with release of formaldehyde (Scheme 1). In fact, *Magic Fluoromethyl* (**3**) was obtained (60 %) by the attempted distillation of **5** at elevated temperatures. The formation of formaldehyde was confirmed by ¹H NMR spectroscopy. *Magic Fluoromethyl* **3** is a colorless liquid with a boiling point of 91 °C and a melting point of about -85 °C. Fluoromethyl triflate (**4**) is also a colorless liquid; it boils at 90 °C and solidifies at -62 °C. The two fluoromethyl sulfonates **3** and **4** complement and complete the series of fluoromethylating agents developed in our laboratory. Their ability to transfer a fluoromethyl group can be anticipated based on the analogous series of methylating agents^[9, 15] and is shown in Figure 3. In some cases, as for the pair CF₃CO₃CH₂F (**4**) / 2,4,6-trinitrophenylsulfonyl fluoromethyl ester (see Chapter 2) the order has been experimentally confirmed

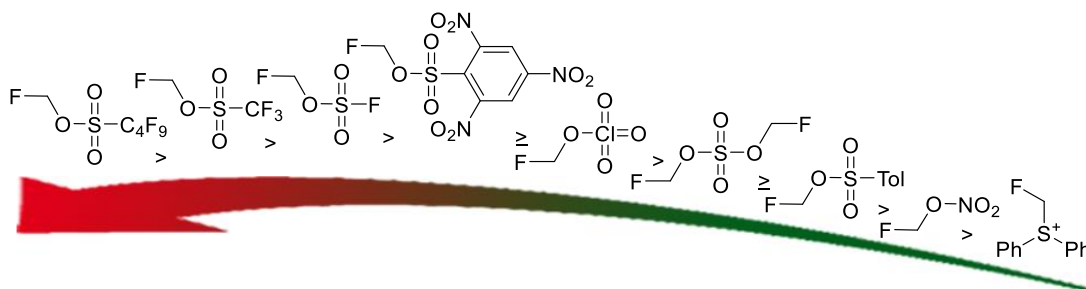


Figure 3: Anticipated CH₂F transfer ability of new fluoromethylating reagents (see chapters 2, 5, 9 and 10). The order is based on the analogous ranking of methylating agents.^[9, 15]

The triflate **4** which according to Figure 3 should be a stronger fluoromethylating reagent and at the same time less toxic than *Magic Fluoromethyl*,^[16] was used to investigate the ability of CH₂F transfer. Long term stability tests showed that the reagent, stored under argon at ambient temperature resulted unchanged after at least 6 months.

For *N*-fluoromethylation reactions with **4**, pyridine, *Steglich's* base, dipyridyl ketone and *Michlers ketone* were used. The starting organic compound was dissolved in dry DCM or diethylether and fluoromethyl triflate **4** was added at -30 °C with stirring. In THF a cationic polymerization of the solvent is induced by the ester **4**. After the reaction mixture was stirred over night the solvent was removed to give the *N*-fluoromethylated products **7** in yields between

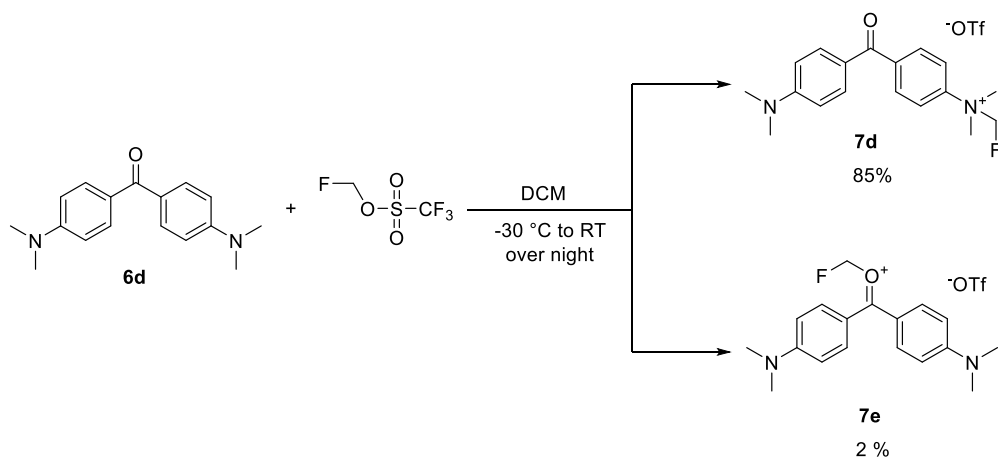
83 - 97 % (Table 1). The pyridinium salt **7a** is an ionic liquid, compounds **7b-d** were obtained as crystalline materials and characterized also by single crystal X-ray diffraction. The reaction with *Steglich's* base yielded the fluoromethyl pyridinium salt **7b** in better yield (97 %) as compared to the reported fluoromethylation with CH₂FBr (82 %).^[17]

Table 1: *N*-fluoromethylation reactions with triflate **4**.

entry	starting material	product	yield (%)
1	 6a	 7a	93
2	 6b	 7b	97
3	 6c	 7c	83

Figure 4: Molecular structure of **7b** in the crystal, DIAMOND representation, ellipsoids are drawn at 50 % probability level. Symmetry code: *i*: x, 1.5-y, z; *ii*: x, 0.5-y, z. Selected bond length [Å] and angles [°]: F3-C5: 1.385(3), C5-N2: 1.448(3), C5-H5: 0.96(2); F3-C5-N2: 107.5(2), F3-C5-H5: 107(2).

In the case of **6c** and **6d** two sites for attaching the fluoromethyl group are available (the pyridinic nitrogen and the oxygen of the carbonyl group) and we were interested in the selectivity of the triflate **4**. For **6c** only the *N*-fluoromethylated product **7c** was obtained (Table 1)



Scheme 2: Reaction of **6d** with fluoromethyltriflate.

In contrast, in the case of **6d** fluoromethylation at both the oxygen and the nitrogen atom was observed (Scheme 2). This is in accordance with the product distribution reported when *Michler's ketone* is methylated with methyltriflate **2**.^[18] The identity of both fluoromethylation products **7d** and **7e** was confirmed by the result of crystal X-ray diffraction studies (Figure 6).

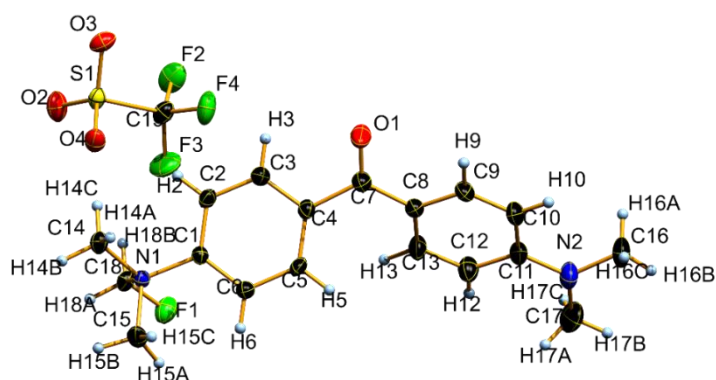


Figure 5: Molecular structure of **7d** in the crystal, DIAMOND representation, ellipsoids are drawn at 50 % probability level. Selected bond length [Å] and angles [°]: F1-C18: 1.353(4), C18-N1: 1.517(4), C18-H18A: 0.97(3), C18-H18B: 0.97(3); F1-C18-N1: 106.9(2), F1-C18-H18A: 110.3(1); F1-C18-N1-C1: 54.5(4).

Due to the electronegative character of fluorine, electrophilic fluoromethylation with **4** is expected to be slower as compared to methylation with the analogous reagent **2**. In fact fluoromethylation of acetamide (**8a**) and urea (**8b**) with **4** requires a reaction time of 12 h at ambient temperature, while the corresponding methylation with **2** is complete within 2 h.^[19] In both cases the yields of the alkylated products are comparable (Table 2). Fluoromethylation of thiourea (**8c**) with **4** is fast and is complete within 5 min at ambient temperature.

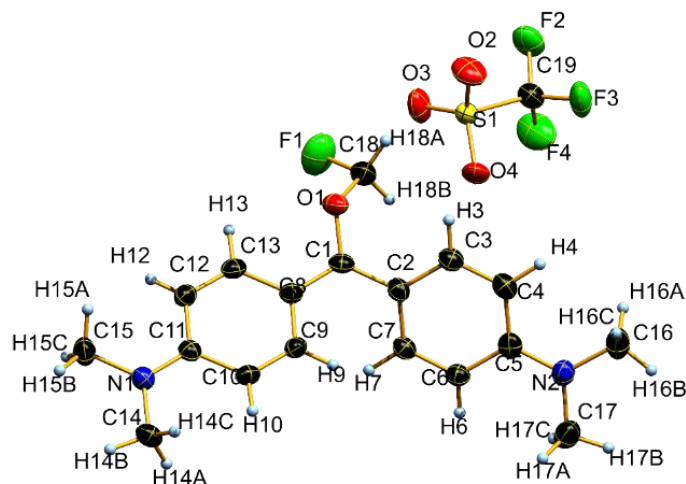


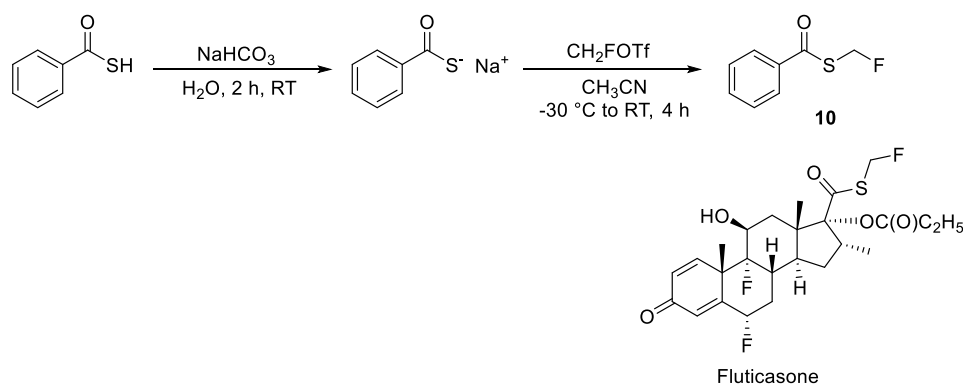
Figure 6: Molecular structure of **7e** in the crystal, DIAMOND representation, ellipsoids are shown at 50 % probability level. Selected bond lengths [Å] and angles [°]: F1-C18: 1.370(3), C18-O1: 1.414(3), C18-H18A: 0.96(2), C18-H18B: 0.96(2), O1-C1: 1.355(3); F1-C18-O1: 105.2(2), F1-C18-H18A: 110.7(2), C18-O1-C1: 121.6(2); F1-C18-O1-C1: 113.4(3).

Table 2: Fluoromethylation of selected amides with triflate **4**.

$$\text{8 a-c} + \text{F-CH}_2\text{-O-SO}_2\text{-CF}_3 \xrightarrow[\text{over night}]{\text{Et}_2\text{O or CH}_3\text{CN, RT}} \text{9 a-c}$$

entry	starting material	product	yield (%)
1	 8a	 9a ·OTf	74
2	 8b	 9b ·OTf	92
3	 8c	 9c ·OTf	86

The reaction is performed in acetonitrile or diethylether and the products **9a-c** are isolated in good yields (Table 2). As expected, **9a** and **9b** form colorless ionic liquids, while **9c** is isolated as a colorless solid. Unfortunately, no single crystals could be obtained for **9c**; its identity is confirmed by NMR spectroscopy, however. Fluticasone - a widely used drug – is mainly produced by the reaction of ozone-depleting CH_2FCl or CH_2FBr gases with the anion of a cyclopentane carbothioic acid glucocorticoid derivative.^[2, 20] In order to probe the suitability of fluoromethyl triflate ester **4** to act as a substitute for CH_2FCl or CH_2FBr we investigated its reactivity towards the anion of benzene carbothioic acid, which contains the same functionality.^[21]



Scheme 3: Synthesis of fluoromethylated benzenecarbothioic acid as a simulant for the synthesis of Fluticasone.

Benzene carbothioic acid was first converted to its sodium salt according to a literature known procedure^[22] and then was allowed to react with **4** in acetonitrile at $-30\text{ }^{\circ}\text{C}$. After workup pure fluoromethyl thioester **10** was obtained as a brownish liquid (Scheme 3). In order to further characterize the reactivity of fluoromethyl triflate **4** and to obtain deeper insight into its fluoromethylating ability the fluoromethylation of the triphenyl phosphine chalcogenides **11a-c** with **4** was attempted (Table 3).

Table 3: Fluoromethylation of phosphine chalcogenides **11** with **4**. (*NMR yield)

entry	starting material	product	yield (%)
1*	 11a	 12a	99
2	 11b	 12b	96
3	 11c	 12c	83

Fluoromethylation of phosphine chalcogenides **11a-c** with **4** requires elevated temperatures and a reaction time of three days to give complete conversion to the salts **12a-c**. Compounds **12b** and **12c** were isolated as colorless solids and both are stable when stored under argon at ambient temperature. The selenium derivative **12c** is very sensitive towards moisture and air and decomposes forming elemental selenium. The sulfur derivative is by far less sensitive and its molecular structure could be confirmed by single crystal X-ray diffraction (Figure 7). Although the oxygen compound **12a** formed in solution quantitatively and was characterized by multinuclear (^1H , ^{13}C , ^{31}P , ^{19}F) NMR spectroscopy, it could not be isolated. It decomposed on drying *in vacuo* during work up. As decomposition product the fluorophosphonium triflate **13** was identified by NMR spectroscopy.

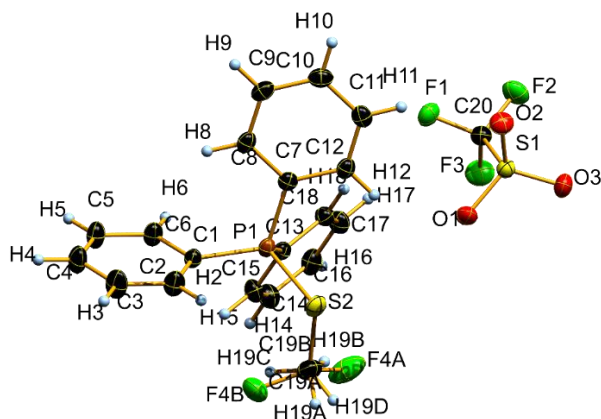
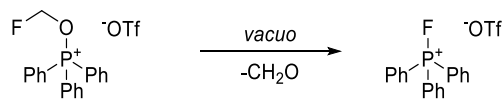


Figure 7: Molecular structure of **12b** in the crystal, DIAMOND representation, ellipsoids are drawn at 50 % probability level. Selected bond length [Å] and angles [°]: F4B-C19B: 1.357(4), C19B-S2: 1.810(2); F4B-C19B-S2: 114.2(2); F4B-C19B-S2-P1: -61.6(2).

The structure of **13** was also confirmed by the result of single crystal X-ray diffraction studies (Figure 8). The formation of **13** is most probably due to the loss of formaldehyde from the primary fluoromethylation product **12a** (Scheme 4). The instability of the OCH₂F group in **12a** compares well to that in bis(fluoromethyl)sulfate (FCH₂O)₂SO₂ and in fluoromethanol FCH₂OH^[23].



Scheme 4: Decomposition of **12a** on heating *in vacuo*.

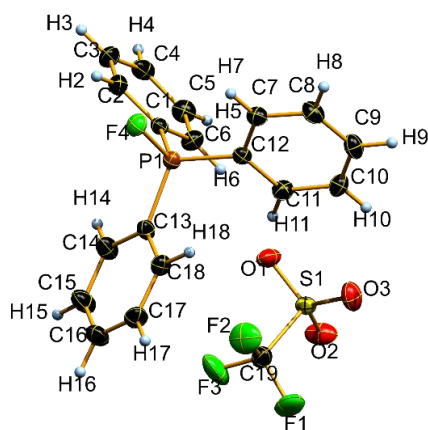


Figure 8: Molecular structure of fluorotriphenylphosphonium triflate **13** in the crystal, DIAMOND representation, ellipsoids are drawn at 50 % probability level.

In the case of **12c** the presence of the ⁷⁷Se isotopomer (⁷⁷Se: nat. abundance 7.58 %, I = 1/2) causes the appearance of ⁷⁷Se satellites in the ¹H, ¹⁹F (Figure 9), ¹³C and ³¹P NMR spectra. The ¹J_{Se,P} coupling constant of 426.9 Hz is characteristic for a dicoordinate selenium atom directly bonded to phosphorus. The bonding of the CH₂F group to selenium is indicated by the characteristic values of ¹J_{Se,C} (94.2 Hz), ²J_{Se,H} (20.1 Hz) and ²J_{Se,F} 100.7 Hz). ²J_{P,C} to the carbon atom of the CH₂F group is small and decreases in the order **12a** (9.1 Hz) > **12b** (5.0 Hz) > **12c**

(3.6 Hz). It is known, that triflic acid or triflic acid anhydride can be used as a starter for the cationic polymerization of THF.^[24]

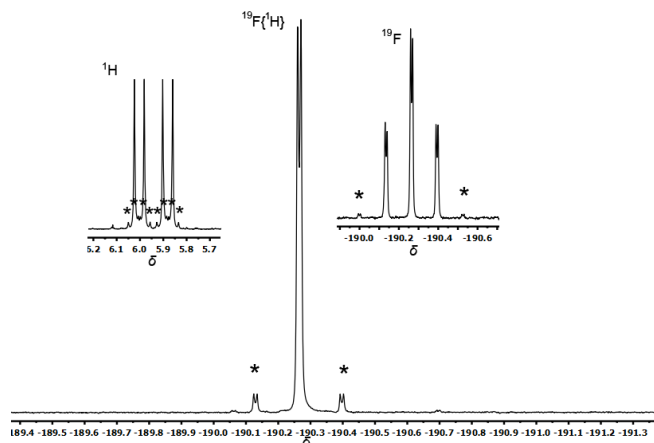


Figure 9: ^{19}F and ^1H NMR spectra of **12c**; ^{77}Se satellites are marked with an asterix.

An analogous behavior was observed also for fluoromethyl triflate **4**. Addition of **4** (1 mmol) to THF and stirring overnight resulted in the formation of a solid colorless polymer (Scheme 3, eq. 1). When **4** was added to acetonitrile, no reaction was observed by NMR spectroscopy within 20 days. However, leaving the reaction solution for 3 months at ambient temperature a small amount of colorless crystals was obtained. Analysis of the crystals by single crystal X-ray diffraction showed the formation of *N,N'*-methylene bis(acetamidium) triflate **14** (Figure 10).

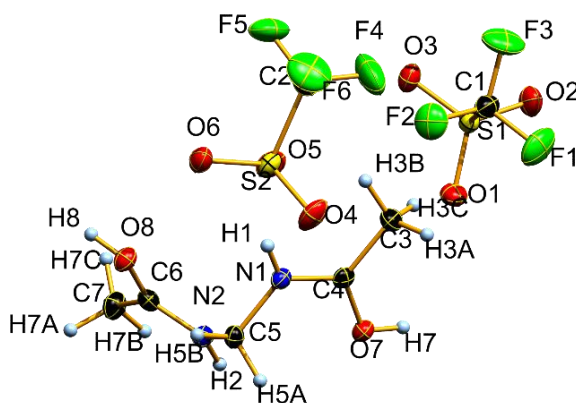
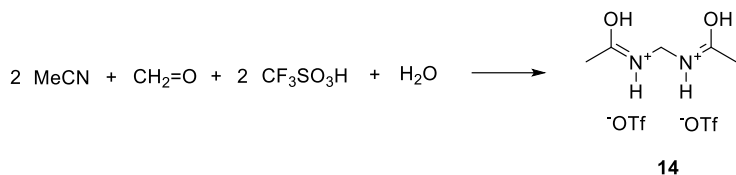
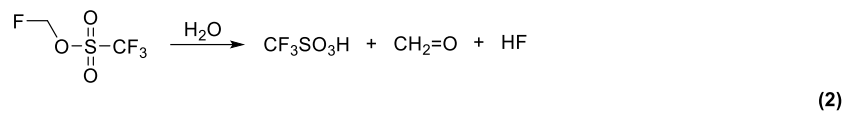
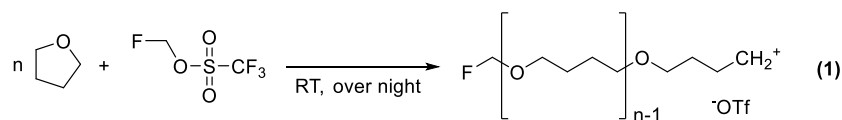


Figure 10: Molecular structure of **14** in the crystal; DIAMOND representation. Ellipsoids are drawn at the 50 % probability level.

A possible mechanism for the formation of **14** is proposed in Scheme 3, eq. 2. Slow hydrolysis of **4** generates trifluoromethyl sulfonic acid and fluoromethanol, which is known to decompose to HF and formaldehyde. The formaldehyde thus formed reacts with acetonitrile, trifluoromethyl sulfonic acid and water to give the bis(triflate) **14**. The analogous formation of *N,N'*-methylene bis(acetamide) from acetonitrile, and aqueous formaldehyde in the presence of a strong acid like HCl has been reported^[25] and supports the proposed mechanism.



Scheme 3: Cationic polymerization of THF initiated by **4** (1) and proposed mechanism for the formation of **14** from acetonitrile (2).

3.3 Conclusion

Efficient and straight forward syntheses for new fluorosulfonic acid fluoromethyl ester $\text{FSO}_3\text{CH}_2\text{F}$ – *Magic Fluoromethyl* – and fluoromethyl triflate $\text{CF}_3\text{SO}_3\text{CH}_2\text{F}$ have been developed. Both compounds have been characterized by multinuclear NMR spectroscopy and are strong fluoromethylating agents. Fluoromethyl triflate has been used to transfer the CH_2F group to different *N*, *O* and *S* nucleophiles and revealed to be a promising easy to handle fluoromethylating agent.

3.4 Acknowledgement

Financial support by Ludwig-Maximilian University (LMU) is grateful acknowledged. We are thankful to F-Select GmbH for a generous donation of fluoroiodomethane. We thank Prof. Dr. T. M. Klapötke (LMU) for the generous allocation of diffractometer time.

3.5 Experimental Section

3.5.1 General Procedure

All compounds were handled using *Schlenk* techniques under dry argon. Chemicals were purchased from VWR and used as received. Fluoroiodomethane was distilled under inert conditions before use. The samples for infrared spectroscopy were placed under ambient conditions onto a Smith DuraSAMPLIR II ATR device and measurements were performed with a Perkin Elmer BX II FR-IR System spectrophotometer. The samples for NMR spectroscopy were prepared under inert atmosphere using argon as protective gas. The solvents used were dried using 3 Å molecular sieve and stored under argon atmosphere. Spectra were recorded with a Bruker Avance III spectrometer operating at 400.1 MHz (^1H), 376.4 MHz (^{19}F), 162.0 MHz (^{31}P), 100.6 MHz (^{13}C), 76.3 MHz (^{77}Se), 40.6 MHz (^{15}N) and 28.9 MHz (^{14}N). Chemical shifts are referred to TMS (^1H , ^{13}C), CFCl_3 (^{19}F), H_3PO_4 (^{31}P), H_3SeO_4 (^{77}Se) and MeNO_2

($^{14}\text{N}/^{15}\text{N}$). All spectra were recorded at 299.15 K. Mass spectrometric investigations were performed on a Thermo Trace 1300 gas chromatograph with a Q Executive Injector.

3.5.2 Preparation

Fluorosulfonic acid fluoromethyl ester - *Magic Fluoromethyl* - (3)

Fluorosulfonic acid (2.5 mL, 45.9 mmol) was added dropwise with stirring to a cooled (0 °C) suspension of freshly prepared silvercarbonate^[14a] (7.00 g, 25.4 mmol) in acetonitrile (20 mL). The reaction mixture was allowed to warm up to ambient temperature and stirring was continued for 15 min. The excess of silvercarbonate was removed by filtration. From the filtrate the solvent was removed *in vacuo* and the resulting solid was dried overnight *in vacuo* to yield silver fluorosulfonate (98 %). Silver fluorosulfonate (1.00 g, 6.16 mmol) was added during 5 min with stirring to fluoroiodomethane (1.25 mL, 18.5 mmol), cooled with an ice bath at 0 °C. The reaction mixture was allowed to warm up to room temperature and stirring was continued for 1.5 h. The precipitated silver iodide was filtered off and to the cooled filtrate (0 °C) again silverfluorosulfonate (2.83 g, 12.3 mmol) was added with stirring. The reaction mixture was again allowed to warm up to ambient temperature and stirring was continued for 30 min. The precipitated silveriodide was filtered off, leaving analytically pure *Magic Fluoromethyl*, which was obtained as colorless liquid in 80 % yield. Mp. -82 °C; Bp. 91 °C; ^1H NMR (400 MHz, CDCl_3): δ =5.88 ppm (dd, $^2J_{\text{H,F}}$ =48.8, $^4J_{\text{H,F}}$ =1.5 Hz, 2H; CH_2F); $^{13}\text{C}\{^1\text{H}\}$ NMR (101 MHz, CDCl_3): δ =101.3 ppm (dd, $^1J_{\text{C,F}}$ =244.3, $^3J_{\text{C,F}}$ =0.7 Hz; CH_2F); $^{19}\text{F}\{^1\text{H}\}$ NMR (376 MHz, CDCl_3): δ =-152.8 (d, $^4J_{\text{F,F}}$ =8.3 Hz; CH_2F), 44.6 ppm (d, $^4J_{\text{F,F}}$ =8.3 Hz; FSO_3); ^{19}F NMR (376 MHz, CDCl_3): δ =44.6 (td, $^4J_{\text{F,H}}$ =8.3, $^4J_{\text{F,F}}$ =1.5 Hz; FSO_3), -152.8 ppm (td, $^2J_{\text{F,H}}$ =48.8, $^4J_{\text{F,F}}$ =8.3 Hz; CH_2F); ^{17}O NMR (54.2 MHz, CDCl_3): δ =150 (s; SO_2), 162 ppm (s; OCH_2F); IR (ATR): ν = 1443 (s), 1225 (s), 1149 (w), 1088 (m), 963 (s), 834 (s), 786 (s), 608 (w), 555 (s), 524 (s) cm^{-1} ; Raman (1074 mW): ν = 3071 (w), 3017 (s), 2957 (w), 2826 (w), 1490 (w), 1459 (w), 1274 (w), 1232 (s), 1152 (w), 1099 (w), 983 (w), 797 (s), 563 (w), 532 (w), 476 (w), 397 (w), 330 (w), 265 (w) cm^{-1} ; HRMS (GC/EI): m/z [M-H] calcd for $\text{CHF}_2\text{O}_3\text{S}$: 130.9614, found: 130.9608.

Fluoromethyl triflate (4)

Trifluoromethyl sulfonic acid (4.00 mL, 45.3 mmol) was added dropwise with stirring to a cooled (0 °C) suspension of freshly prepared silver carbonate^[14a] (8.00 g, 29.1 mmol) in acetonitrile (30 mL). The mixture was allowed to warm up to room temperature and stirring was continued for 15 min. The excess of silver carbonate was removed by filtration. The solvent from the filtrate was removed *in vacuo* and the remaining solid was dried overnight *in vacuo* to give silver triflate with a yield of 98 %. Silver triflate thus obtained (1.00 g, 3.89 mmol) was added within 5 min with stirring to fluoroiodomethane (1.00 mL, 14.8 mmol) while cooling with an ice bath (0 °C). The reaction mixture was allowed to warm up to room temperature and stirring was continued for 1.5 h. The precipitated silver iodide was filtered off and to the cooled (0 °C) filtrate silver triflate (2.80 g, 10.9 mmol) was added. The reaction mixture was again allowed to warm up to ambient temperature and stirring was continued for 30 min. The precipitated silver iodide was filtered off leaving analytically pure fluoromethyl triflate as

colorless liquid with a yield of 84 %. Mp. -62 °C; Bp.: 90 °C; ^1H NMR (400.1 MHz, CDCl_3): $\delta=5.87$ ppm (d, $^2J_{\text{H,F}}=48.8$ Hz, 2H; CH_2F); $^{13}\text{C}\{^1\text{H}\}$ NMR (101 MHz, CDCl_3): $\delta=118.4$ (qd, $^1J_{\text{C,F}}=319.3$, $^4J_{\text{C,F}}=1.7$ Hz; CF_3), 100.5 ppm (d, $^1J_{\text{C,F}}=242.7$ Hz; CH_2F); $^{19}\text{F}\{^1\text{H}\}$ NMR (376.4 MHz, CDCl_3): $\delta=-75.6$ (d, $^5J_{\text{F,F}}=7.0$ Hz; CF_3), -149.8 ppm (q, $^5J_{\text{F,F}}=7.0$ Hz; CH_2F); ^{19}F (376 MHz, CDCl_3): $\delta=-75.6$ (d, $^5J_{\text{F,F}}=7.0$ Hz; CF_3), -149.8 ppm (td, $^2J_{\text{F,H}}=48.8$, $^5J_{\text{F,F}}=7.0$ Hz; CH_2F); IR (ATR): $\nu = 1415$ (m), 1206 (s), 1133 (s), 975 (s), 802 (s), 758 (m), 613 (s), 565 (w), 508 (w) cm^{-1} ; Raman (1074 mW): $\nu = 3067$ (w), 3015 (m), 2951 (w), 2827 (w), 1488 (w), 1422 (w), 1251 (m), 1138 (m), 1095 (w), 957 (w), 811 (w), 761 (s), 625 (w), 565 (w), 502 (w), 408 (w), 329 (m), 297 (m), 204 (w), 178 (w) cm^{-1} ; HRMS (GC/ED): m/z [M+H] calcd for $\text{C}_2\text{H}_3\text{F}_4\text{O}_3\text{S}$: 182.9734, found: 182.9731.

1-(Fluoromethyl)pyridin-1-ium triflate (7a)

Pyridine (0.12 mL, 1.49 mmol) was dissolved in diethyl ether (5 mL) and the solution was cooled to -30 °C. To this solution fluoromethyl triflate **4** (0.17 mL, 1.49 mmol) was added dropwise within 20 min with stirring. The reaction mixture was allowed to warm up to room temperature and stirring was continued overnight. The solvent was removed *in vacuo* leaving a brownish liquid, which was washed with diethyl ether (2 \times 2 mL) and dried *in vacuo*. The triflate **7a** was obtained as a colorless liquid with 93 % yield. ^1H NMR (400.1 MHz, D_2O): $\delta=9.15$ (d, $J=5.8$ Hz, 2H; *o*-CH), 8.82 (t, $J=7.8$ Hz, 1H; *p*-CH), 8.33 - 8.24 (m, 2H; *m*-CH), 6.59 ppm (d, $^2J_{\text{H,F}}=46.8$ Hz, 2H; CH_2F); $^{13}\text{C}\{^1\text{H}\}$ NMR (100.6 MHz, D_2O): $\delta=149.1$ (s; *o*-CH), 144.2 (s; *p*-CH), 128.5 (s; *m*-CH), 119.6 (q, $^1J_{\text{C,F}}=317.0$ Hz; CF_3), 95.1 ppm (d, $^1J_{\text{C,F}} = 215.0$ Hz, CH_2F); $^{19}\text{F}\{^1\text{H}\}$ NMR (376.4 MHz, D_2O): $\delta=-79.3$ (s; CF_3), -174.5 ppm (s; CH_2F); ^{19}F NMR (376.4 MHz, D_2O): $\delta=-79.3$ (s; CF_3), -174.5 ppm (t, $^2J_{\text{F,H}}=46.8$ Hz; CH_2F); ^{14}N (28.9 MHz, CDCl_3): $\delta= -173$ ppm (s; Ar-N); IR (ATR): $\nu = 3146$ (w), 3080 (w), 3056 (w), 1624 (m), 1587 (w), 1489 (m), 1411 (m), 1250 (s), 1227 (s), 1152 (s), 1066 (m), 1047 (m), 1023 (s), 964 (w), 828 (m), 794 (m), 757 (w), 678 (s), 635 (s), 604 (w) cm^{-1} ; Raman (1074 mW): $\nu = 3102$ (m), 3002 (w), 1641 (w), 1584 (w), 1507 (w), 1474 (w), 1228 (w), 1190 (w), 1028 (s), 831 (w), 759 (m), 648 (m), 605 (w), 575 (w), 520 (w), 480 (w), 350 (m), 315 (m), 157 (m) cm^{-1} . Elemental analysis calcd for $\text{C}_7\text{H}_7\text{F}_4\text{NO}_3\text{S}$: C 32.19, H 2.70, N 5.36, S 12.27, found: C 32.23, H 2.55, N 5.94, S 12.53.

4-(Dimethylamino)-1-(fluoromethyl)pyridin-1-ium triflate (7b)

4-Dimethylaminopyridine (182 mg, 1.49 mmol) were dissolved in diethyl ether (10 mL) and the solution was cooled to -30 °C. Fluoromethyl triflate **4** (0.17 mL, 1.49 mmol), dissolved in diethylether (5 mL) was added dropwise within 15 min with stirring. The mixture was allowed to warm up to room temperature and stirring was continued for 15 min. The precipitate formed was filtered off and washed with diethyl ether (3 \times 5 mL). The product was dried *in vacuo* to give **7b** as a colorless crystalline powder with a yield of 97 %. ^1H NMR (400.1 MHz, CD_3CN): $\delta=8.09$ (m, 2H; 2,6-CH), 6.92 (m, 2H; 3,5-CH), 5.96 (d, $^2J_{\text{H,F}}=50.3$ Hz, 2H; CH_2F), 3.24 ppm (d, $J=0.9$ Hz, 6H; CH_3); ^{13}C NMR (100.6 MHz, CD_3CN): $\delta=158.5$ (s; C-4), 142.6 (d, $^3J_{\text{C,F}}=1.4$ Hz; C-2,6), 122.2 (q, $^1J_{\text{C,F}}=320.8$ Hz; CF_3), 108.9 (s; C-3,5), 93.8 (d, $^1J_{\text{C,F}}=205.2$ Hz; CH_2F), 41.1 ppm (s; CH_3); $^{19}\text{F}\{^1\text{H}\}$ NMR (376.4 MHz, CD_3CN): $\delta=-79.8$ (s; CF_3), -168.1 ppm (s; CH_2F); ^{19}F NMR (376.4 MHz, CD_3CN): $\delta=-79.8$ (s; CF_3), -168.1 ppm (t, $^2J_{\text{F,H}}=57.9$ Hz;

CH₂F); ¹H, ¹⁵N-HMBC: ¹⁵N NMR (40.6 MHz, CD₃CN): δ = -296.6 (s; NMe), -231.2 ppm (s; Ar-N); IR (ATR): ν = 3101 (w), 1650 (s), 1584 (m), 1531 (m), 1406 (w), 1395 (w), 1384 (m) 1263 (s), 1245 (s), 1209 (s), 1182 (s), 1146 (s), 1066 (w), 1028 (s), 994 (s), 943 (w), 832 (m), 814 (m), 756 (w), 733 (m), 712 (w), 661 (w), 535 (s), 572 (m), 557 (s), 517 (s), 502 (m), 451 (w); Raman (1074 mW): ν = 3111 (m), 3007 (m), 3946 (m), 1654 (m), 1593 (s), 1475 (w), 1416 (m), 1253 (w), 1255 (w), 1036 (s), 1003 (m), 945 (m), 835 (m), 756 (m), 735 (m), 661 (w), 574 (w), 348 (m), 312 (m) cm⁻¹; HRMS (GC/EI): *m/z* [M]⁺ calcd for C₈H₁₂FN₂⁺: 155.0979, found: 155.0983. Elemental analysis calcd for C₉H₁₂F₄N₂O₃S: C 35.53, H 3.98, N 9.21, S 10.54, found: C 35.63, H 3.92, N 9.29, S 10.81.

1-(fluoromethyl)-2-picolinoylpyridin-1-ium triflate (7c)

Dimethylaminopyridine (274 mg, 1.49 mmol), was dissolved in dichloromethane (20 mL) and fluoromethyltriflate (0.17 mL, 1.49 mmol) was added with stirring. The reaction mixture was stirred at room temperature for 72 h. The solvent was removed *in vacuo* to give **7c** as a brownish glasslike solid with 83 % yield. Mp.: 69.8 °C, Dec.p. 162.8 °C; ¹H NMR (400.1 MHz, CD₃CN): δ = 9.04 (d, *J* = 6.3 Hz, 1H; Ar-H), 8.82 (td, *J* = 7.9, 1.3 Hz, 1H; Ar-H), 8.68 (ddd, *J* = 4.8, 1.7, 1.0 Hz, 1H; Ar-H), 8.37 (ddd, *J* = 7.9, 1.3, 1.0 Hz, 1H; Ar-H), 8.33 (d, *J* = 7.9 Hz, 1H; Ar-H), 8.31 (ddd, *J* = 7.9, 6.3, 1.3 Hz, 1H; Ar-H), 8.15 (ddd, *J* = 7.9, 7.7, 1.6 Hz, 1H; Ar-H), 7.76 (ddd, *J* = 7.7, 4.9, 1.3 Hz, 1H; Ar-H), 6.49 ppm (d, ²*J*_{H,F} = 46.0 Hz, 2H, CH₂F); ¹³C {¹H} NMR (100.6 MHz, CD₃CN): δ = 187.5 (d, ⁴*J*_{C,F} = 0.6 Hz; CO), 151.5 (d, *J*_{C,F} = 0.7 Hz), 150.8 (s), 150.5 (s), 150.2 (d, *J*_{C,F} = 0.9 Hz), 147.3 (d, *J* = 2.4 Hz), 139.4 (s), 131.0 (s), 130.7 (s), 130.4 (s), 126.0 (s), 121.9 (q, ¹*J*_{C,F} = 320.7 Hz; CF₃), 94.9 ppm (d, ¹*J*_{C,F} = 214.7 Hz; CH₂F); ¹⁹F {¹H} NMR (376.4 MHz, CD₃CN): δ = -79.8 (s; CF₃), -174.8 ppm (s; CH₂F); ¹⁹F NMR (376.4 MHz, CD₃CN): δ = -79.8 (s; CF₃), -174.8 ppm (t, ²*J*_{F,H} = 46.0 Hz; CH₂F); IR (ATR): ν = 3115 (w), 1676 (m), 1540 (m), 1507 (m), 1422 (m), 1396 (m), 1378 (m), 1282 (s), 1187 (w), 1131 (m), 1086 (m), 970 (s), 856 (w), 765 (s), 734 (s), 680 (s), 563 (s), 626 (w) cm⁻¹; Raman (1074 mW): ν = 3078 (m), 3008 (w), 1686 (s), 1616 (m), 1583 (vs), 1570 (vs), 1441 (w), 1197 (m), 1172 (w), 1063 (m), 1045 (m), 1032 (s), 996 (m), 753 (m), 730 (w), 618 (w), 575 (w), 350 (s), 315 (s) cm⁻¹; HRMS (EI): *m/z* [M]⁺ calcd for C₁₂H₁₀FN₂O⁺: 217.0772, found: 217.0771. Elemental analysis calcd for C₁₃H₁₀F₄N₂O₄S: C 42.63, H 2.75, N 7.65, S 8.75, found: C 42.70, H 2.94, N 7.65, S 8.83.

4-(4-(dimethylamino)benzoyl)-N-(fluoromethyl)-N,N-dimethylbenzenaminium triflate (7d)

Michlers Keton (399 mg, 1.49 mmol) was dissolved in dichloromethane (20 mL) and the solution cooled to -30 °C. Fluoromethyl triflate (0.17 mL, 1.49 mmol) was added within 10 min with stirring. The reaction solution was allowed to warm up to ambient temperature and stirring was continued over night. The solvent was removed *in vacuo* leaving a lightly gray solid. A portion of this solid was dissolved in acetonitrile (0.5 mL) for crystallization using diethyl ether as the counter solvent. The remaining solid was dissolved in dichloromethane (10 mL) and extracted with water (30 mL). From the aqueous solution the solvent was removed *in vacuo* yielding **7d** as a green solid with 85 % yield. Mp. 142,3 °C; Dec.p. 155.4 °C; ¹H NMR (400.1 MHz, CD₃CN): δ = 7.93-7.86 (m, 4H; Ar-H), 7.75 (A-part of AA'XX', *N* = 8.9 Hz, 2H; Ar-H),

6.98 (X-part of AA'XX', $N=8.7$ Hz, 2H, Ar-H), 5.70 (d, $^2J_{H,F}=44.8$ Hz, 2H; CH₂F), 3.67 (d, $^4J_{H,F}=1.8$ Hz, 6H; CH₃), 3.03 ppm (s, 6H, CH₃); ¹³C {¹H} NMR (100.6 MHz, CD₃CN): $\delta=192.9$ (s; CO), 144.6 (s), 142.5 (s), 133.3 (s), 132.7 (s), 131.9 (s), 131.8 (s), 122.5 (d, $^4J_{C,F}=1.2$ Hz), 122.0 (q, $^1J_{CF}=320.5$ Hz; CF₃), 114.0 (s), 99.9 (d, $^1J_{C,F}=225.9$ Hz; CH₂F), 52.0 (d, $^3J_{C,F}=1.8$ Hz; CH₃) 41.9 ppm (s; CH₃); ¹⁹F {¹H} NMR (376.4 MHz, CD₃CN): $\delta=-79.8$ (s; CF₃), -188.3 ppm (s; CH₂F); ¹⁹F (376.4 MHz, CD₃CN): $\delta=-79.8$ (s; CF₃), -188.3 ppm (t, $^2J_{F,H}=44.8$ Hz; CH₂F); ¹H, ¹⁵N-HMBC: ¹⁵N NMR (40.6 MHz, CD₃CN): $\delta=-294.9$ (s; NMe₂), -281.1 ppm (s; NMe₂CH₂F); IR (ATR): $\nu = 3054$ (w), 2748 (w), 1672 (m), 1606 (m), 1471 (m), 1417 (w), 1255 (s), 1222 (s), 1192 (s), 1155 (s), 1127 (s), 1101 (m), 1079 (m), 1024 (s), 990 (m), 936 (m), 912 (m), 862 (m), 767 (m), 759 (m), 737 (w), 683 (m), 634 (s), 627 (vs), 573 (m), 516 (s) cm⁻¹; Raman (1074 mW): $\nu = 3082$ (m), 3052 (m), 2972 (m), 1672 (m), 1636 (m), 1606 (s), 1584 (s), 1228 (w), 1148 (m), 1121 (m), 1034 (s), 775 (m), 759 (w), 574 (w), 421 (w), 350 (m), 318 (m); HRMS (ESI): m/z [M⁺] calcd for C₁₈H₂₂FN₂O⁺: 301.17107, found: 301.17083.

O-Fluoromethyl-dimethylformamidium triflate (9a)

Dimethylformamide (0.11 mL, 1.49 mmol) was dissolved in diethyl ether (1 mL) and fluoromethyl triflate 4 (0.17 mL, 1.49 mmol) was added dropwise at 0 °C (ice bath) with stirring. The reaction solution was allowed to warm up to room temperature and stirring was continued overnight. The solvent was removed *in vacuo* and the crude product was washed with diethyl ether (2 × 2 mL) to give **9a** as a colorless oil with 74 % yield. ¹H NMR (400.1 MHz, CD₃CN): $\delta=8.66$ (sept, $^4J_{H,H}=1.5$ Hz, 1H; CH), 5.98 (d, $^2J_{H,F}=49.2$ Hz, 2H; CH₂F), 3.42 (d, $^4J_{H,H}=1.5$ Hz, 3H; NCH₃), 3.26 ppm (d, $^4J_{H,H}=1.5$ Hz, 3H; NCH₃); ¹³C {¹H} NMR (100.6 MHz, CD₃CN): $\delta=166.2$ (s; CH), 122.0 (q, $^1J_{C,F}=320.2$ Hz; CF₃), 104.6 (d, $^1J_{C,F}=234.5$ Hz; CH₂F), 43.1 (s; CH₃), 38.1 ppm (s; CH₃); ¹⁹F {¹H} NMR (376.4 MHz, CD₃CN): $\delta=-79.9$ (s, CF₃), -153.2 ppm (s; CH₂F); ¹⁹F (376.4 MHz, CD₃CN): $\delta=-79.9$ (s, CF₃), -153.2 ppm (t, $^2J_{F,H}=49.2$ Hz; CH₂F); ¹⁴N NMR (28.9 MHz, CD₃CN): $\delta=-229$ ppm (s; NCH₃); IR (ATR): $\nu = 3021$ (w), 1721 (m), 1457 (w), 1319 (w), 1241 (s), 1225 (s), 1150 (s), 1057 (m), 1028 (s), 990 (s), 847 (m), 757 (w), 635 (s), 574 (m), 517 (m) cm⁻¹; Raman (1074 mW): $\nu = 3025$ (m), 2968 (s), 2834 (w), 1723 (w), 1475 (w), 1430 (w), 1228 (w), 1163 (w), 1095 (w), 1035 (s), 995 (w), 851 (w), 795 (m), 629 (w), 576 (w), 520 (w), 433 (w), 351 (m), 316 (w), 201 (w) cm⁻¹; HRMS (DEI): m/z [M] calcd for C₄H₉FNO: 106.0663, found: 106.0664.

2-(Fluoromethyl)uronium triflate (9b)

Urea (98.5 mg, 1.49 mmol) was dissolved in acetonitrile (25 mL) and fluoromethyl triflate 4 (0.17 mL, 1.49 mmol) was added dropwise with stirring. The reaction mixture was stirred overnight and the solvent was removed *in vacuo* to give **9b** (92 %) as a colorless liquid. Dec.p. 143 °C; ¹H NMR (400.1 MHz, CD₃CN): $\delta=7.76$ (broad s, 2H; NH₂), 7.36 (broad s, 2H; NH₂) 5.81 ppm (d, $^2J_{H,F}=50.1$ Hz, 2H; CH₂F); ¹³C {¹H} NMR (100.6 MHz, CD₃CN): $\delta=162.3$ (s; CNH₂), 121.6 (q, $^1J_{C,F}=319.2$ Hz; CF₃), 99.9 ppm (d, $^1J_{C,F}=229.1$ Hz; CH₂F); ¹⁹F {¹H} NMR (376.4 MHz, CD₃CN): $\delta=-79.5$ (s; CF₃), -156.0 ppm (s; CH₂F); ¹⁹F (376.4 MHz, CD₃CN): $\delta=-79.5$ (s; CF₃), -156.0 ppm (t, $^2J_{F,H}=50.1$ Hz; CH₂F); ¹H, ¹⁵N-NMBC: ¹⁵N NMR (40.6 MHz, CD₃CN): $\delta=-292.7$ ppm (s; NH₂); IR (ATR): $\nu = 3357$ (m), 3164 (m), 1705 (s), 1542 (m), 1490 (w), 1405 (w), 1239 (s), 1225 (s), 1158 (s), 1092(m), 1022 (s), 892 (m), 763 (m), 532 (s), 575

(s), 513 (s) cm^{-1} ; Raman (1074 mW): $\nu = 3348$ (w), 3230 (w), 3064 (w), 3012 (w), 2942 (w), 1539 (w), 1493 (w), 1407 (w), 1277 (w), 1229 (w), 1095 (w), 1032 (s), 894 (m), 765 (s), 578 (w), 521 (w), 432 (w), 351 (m), 319 (m) cm^{-1} ; HRMS (ESI): m/z [$2\text{M}^+ + \text{M}^-$] calcd for $\text{C}_5\text{H}_{12}\text{F}_5\text{N}_4\text{O}_5\text{S}^+$: 335.04431, found: 335.04394.

2-(Fluoromethyl)thiuronium triflate (9c)

Thiourea (113 mg, 1.49 mmol) was dissolved in acetonitrile (30 mL) and fluoromethyltriflate (0.17 mL, 1.49 mmol) was added dropwise with stirring. The reaction mixture was stirred overnight and the solvent was removed *in vacuo* to give **9c** (86 %) as a colorless solid. Mp.: 46.3 °C; Dec.p. 181.4 °C; ^1H NMR (400.1 MHz, CD_3CN): $\delta = 8.28$ (s, 2H; NH_2), 7.85 (s, 2H; NH_2), 5.96 ppm (d, $^2J_{\text{H,F}} = 50.2$ Hz, 2H; CH_2F); ^{13}C { ^1H } NMR (100.6 MHz, CD_3CN): $\delta = 170.7$ (d, $^3J_{\text{C,F}} = 2.2$ Hz; CNH_2), 121.4 (q, $^1J_{\text{C,F}} = 318.9$ Hz; CF_3), 83.9 ppm (d, $^1J_{\text{C,F}} = 219.6$ Hz; CH_2F); ^{19}F { ^1H } NMR (376.4 MHz, CD_3CN): $\delta = -79.6$ (s; CF_3), -190.4 ppm (s; CH_2F); ^{19}F NMR (376.4 MHz, CD_3CN): $\delta = -79.6$ (s; CF_3), -190.4 ppm (t, $^2J_{\text{F,H}} = 50.2$ Hz; CH_2F); ^1H , ^{15}N -HMBC: ^{15}N NMR (40.6 MHz, CD_3CN): $\delta = -292.7$ ppm (s; NH_2); IR (ATR): $\nu = 3334$ (m), 3231 (m), 3176 (m), 1667 (s), 1572 (w), 1445 (m), 1325 (w), 1276 (s), 1224 (vs), 1183 (s), 1159 (s), 1067 (m), 1028 (s), 992 (s), 943 (m), 763 (m), 726 (s), 624 (s), 574 (s), 515 (s), 477 (s), 461 (s) cm^{-1} ; Raman (1074 mW): $\nu = 3253$ (w), 3037 (w), 2977 (w), 1433 (w), 1287 (w), 1228 (w), 1224 (m), 1072 (w), 1038 (s), 997 (w), 1095 (w), 765 (m), 728 (w), 698 (m), 579 (w), 478 (m), 463 (w), 350 (s), 316 (s); HRMS (ESI): m/z [M^+] calcd for $\text{C}_2\text{H}_6\text{FN}_2\text{S}^+$: 109.02302, found: 109.02308; Elemental analysis calcd for $\text{C}_3\text{H}_6\text{F}_4\text{N}_2\text{O}_3\text{S}_2$: C 13.96, H 2.34, N 10.85, S 24.83, found: C 14.24, H 2.66, N 11.02, S 24.72.

S-(Fluoromethyl) benzothioate (10)

Following a literature known synthesis^[22] benzenecarbothioic acid (0.34 mL, 2.88 mmol) was allowed to react with NaHCO_3 (241 mg, 2.88 mmol) in water (12 mL) and the reaction solution was stirred for 2 h at room temperature. The water was removed *in vacuo* to give yellowish sodium salt of benzenecarbothioic acid. The sodium salt thus prepared was dissolved in acetonitrile (10 mL) and fluoromethyl triflate (0.34 mL, 2.98 mmol) was added to the cooled solution (-30 °C) within 10 min with stirring. The reaction mixture was allowed to warm up to room temperature and stirring was continued for 4 h. The solvent was removed *in vacuo*. The crude product was dissolved in water (10 mL) and extracted with dichloromethane (3×10 mL). The combined organic layers were dried over sodium sulfate. The solvent was removed *in vacuo* to give **10** as brownish liquid with 78 % yield. Mp.: -10 °C; Bp.: 144 °C; Dec.p. 182.4 °C; ^1H NMR (400.1 MHz, CDCl_3): $\delta = 7.99$ (m, 2H; *o*-CH), 7.63 (m, 1H; *p*-CH), 7.49 (m, 2H; *m*-CH), 5.99 ppm (d, $^2J_{\text{H,F}} = 50.2$ Hz, 2H; CH_2F); ^{13}C { ^1H } NMR (100.6 MHz, CDCl_3): $\delta = 188.1$ (d, $^3J_{\text{C,F}} = 1.8$ Hz; CO), 136.1 (s; C-*i*), 134.4 (s; C-*o*), 129.0 (s; C-*m*), 127.9 (s; C-*p*), 80.8 ppm (d, $^1J_{\text{C,F}} = 215.2$ Hz; CH_2F); ^{19}F { ^1H } NMR (376.4 MHz, CDCl_3): $\delta = -192.6$ ppm (s; CH_2F); ^{19}F NMR (376.4 MHz, CDCl_3): $\delta = -192.6$ ppm (t, $^2J_{\text{F,H}} = 50.2$ Hz; CH_2F); IR (ATR): $\nu = 1744$ (w), 1678 (s), 1596 (w), 1582 (w), 1449 (m), 1421 (w), 1320 (w), 1208 (s), 1176 (m), 1099 (w), 984 (s), 934 (m), 892 (s), 772 (s), 734 (s), 682 (s), 646 (s), 616 (m), 561 (w), 539 (w) cm^{-1} ; Raman (1074 mW): $\nu = 3069$ (s), 2955 (w), 1682 (m), 1597 (s), 1450 (w), 1422 (w), 1321 (w), 1243 (w), 1211 (m), 1178 (w), 1162 (w), 1027 (w), 1002 (s), 737 (w), 686 (m), 617 (w), 540 (w),

299 (w), 259 (w), 179 (w) cm^{-1} ; HRMS (EI): m/z $[\text{M}]^+$ calcd for $\text{C}_8\text{H}_7\text{FOS}$: 170.0202, found: 170.0193; Elemental analysis calcd for $\text{C}_8\text{H}_7\text{FOS}$: C 56.46, H 4.15, S 18.84, found: C 56.85, H 4.30, S 18.78.

(Fluoromethyl)(triphenyl- λ^5 -phosphaneylidene)oxonium triflate (12a)

Triphenylphosphineoxide (414 mg, 1.49 mmol) was dissolved in CDCl_3 (3 mL) and fluoromethyl triflate (0.17 mL, 1.49 mmol) was added in one portion with stirring. The reaction solution was heated up to 50 $^\circ\text{C}$ for 72 h to give **12a** (99 %, determined *via* NMR). ^1H NMR (400.1 MHz, CDCl_3): δ =7.86 – 7.80 (m, 3H; *p*-CH), 7.79 – 7.72 (m, 6H; *o*-CH), 7.71 – 7.65 (m, 6H; *m*-CH), 5.83 ppm (dd, $^2J_{\text{H,F}}=49.9$, $^3J_{\text{H,P}}=17.1$ Hz, 2H; CH_2F); ^{13}C $\{^1\text{H}\}$ NMR (100.6 MHz, CDCl_3): δ =136.7 (d, $J=3.0$ Hz; C-*p*), 133.6 (d, $J=12.2$ Hz; C-*o*), 130.4 (d, $J=13.9$ Hz; C-*m*), 120.7 (q, $^1J_{\text{C,F}}=320.9$ Hz; CF_3), 117.6 (d, $^1J_{\text{C,P}}=106.5$ Hz; C-*i*), 100.3 ppm (dd, $^1J_{\text{C,F}}=233.9$, $^2J_{\text{C,P}}=9.1$ Hz; CH_2F); ^{19}F $\{^1\text{H}\}$ NMR (376.4 MHz, CDCl_3): δ =-78.8 (s; CF_3), -146.5 ppm (d, $^3J_{\text{F,P}}=1.4$ Hz; CH_2F); ^{19}F (376.4 MHz, CDCl_3): δ =-78.8 (s; CF_3), -146.5 ppm (td, $^2J_{\text{F,H}}=49.9$, $^4J_{\text{F,P}}=1.4$ Hz; CH_2F); ^{31}P $\{^1\text{H}\}$ NMR (162.0 MHz, CDCl_3): δ =67.5 ppm (d, $^3J_{\text{P,F}}=1.4$ Hz); IR (ATR): ν = 1590 (w), 1440 (m), 1299 (m), 1165 (m), 1123 (m), 1030 (m), 996 (m), 916 (m), 883 (w), 1724 (s), 688 (s), 634 (s), 560 (m), 533 (s), 514 (s), 490 (m) cm^{-1} ; HRMS (ESI): m/z $[\text{M}]^+$ calcd for $\text{C}_{19}\text{H}_{17}\text{FOP}^+$: 311.09956, found: 311.09956.

(Fluoromethyl)(triphenyl- λ^5 -phosphaneylidene)sulfonium triflate (12b)

Triphenylphosphinesulfide (438 mg, 1.49 mmol) was dissolved in dichloromethane (20 mL) and fluoromethyl triflate (0.17 mL, 1.49 mmol) was added in one portion with stirring. The reaction solution was heated to 50 $^\circ\text{C}$ and stirring was continued for 72 h. The solvent was removed, the crude product was washed with diethyl ether (3×10 mL) and dried in *vacuo* to give **12b** as a colorless powder in 96 % yield. Mp. 83.3 $^\circ\text{C}$; Dec.p.. 140.2 $^\circ\text{C}$; ^1H NMR (400.1 MHz, CD_3CN): δ =7.96 – 7.92 (m, 3H; *p*-CH), 7.89 – 7.75 (m, 12H; *o,m*-CH), 5.83 ppm (dd, $^2J_{\text{H,F}}=49.0$, $^3J_{\text{H,P}}=20.3$ Hz, 2H; CH_2F); ^{13}C $\{^1\text{H}\}$ NMR (100.6 MHz, CD_3CN): δ =138.1 (d, $J=3.2$ Hz; C-*p*), 135.9 (d, $J=11.5$ Hz; C-*o*), 132.4 (d, $J=13.8$ Hz; C-*m*), 123.0 (q, $^1J_{\text{C,F}}=321.7$ Hz; CF_3), 119.8 (d, $^1J_{\text{C,P}}=85.0$ Hz; C-*i*), 85.3 ppm (dd, $^1J_{\text{C,F}}=238.4$, $^2J_{\text{C,P}}=5.0$ Hz; CH_2F); ^{19}F $\{^1\text{H}\}$ NMR (376.4 MHz, CD_3CN): δ =-79.8 (s; CF_3), -186.5 ppm (d, $^3J_{\text{F,P}}=5.1$ Hz; CH_2F); ^{19}F NMR (376.4 MHz, CD_3CN): δ =-79.8 (s; CF_3), -186.5 ppm (td, $^2J_{\text{F,H}}=49.0$, $^3J_{\text{F,P}}=5.1$ Hz; CH_2F); ^{31}P $\{^1\text{H}\}$ NMR (162.0 MHz, CD_3CN): δ =46.9 (d, $^3J_{\text{P,F}}=5.1$ Hz; PF); IR (ATR): ν = 3071 (w), 1585 (w), 1483 (w), 1442 (m), 1320 (w), 1268 (s), 1224 (s), 1191 (w), 1164 (m), 1144 (s), 1106 (s), 1029 (s), 1010 (s), 995 (s), 750 (m), 725 (s), 686 (s), 634 (s), 567 (s), 516 (s), 502 (s), 443 (m); Raman (1074 mW): ν = 3069 (m), 1586 (m), 1096 (w), 1029 (m), 999 (s); HRMS (EI): m/z $[\text{M}]^+$ calcd for $\text{C}_{19}\text{H}_{17}\text{FPS}^+$: 327.07671, found: 327.07654; Elemental analysis calcd for $\text{C}_{20}\text{H}_{17}\text{F}_4\text{O}_3\text{PS}_2$: C 50.42, H 3.60, S 13.46 found: C 50.19, H 3.73, S 13.69.

(Fluoromethyl)(triphenyl- λ^5 -phosphaneylidene)selenonium triflate (12c)

Triphenylphosphineselenide (508 mg, 1.49 mmol) was dissolved in dichloromethane (20 mL) and fluoromethyl triflate (0.17 mL, 1.49 mmol) was added in one portion with stirring. The

reaction solution was heated up to 50 °C and stirring was continued for 72 h. The solvent was removed *in vacuo* and the crude product was washed with diethyl ether (3 × 10 mL) and dried *in vacuo* to give **12c** as a colorless powder in 96 % yield. Mp. 83.7 °C; Dec.p.. 120.3 °C; ¹H NMR (400.1 MHz, CD₃CN): δ=7.86 – 7.79 (m, 3H; *p*-CH), 7.85 – 7.72 (m, 12H; *o,m*-CH), 5.95 ppm (dd, ²J_{H,F}=48.7, ³J_{H,P}=17.0 Hz, ⁷⁷Se-sats: ²J_{H,Se}=20.1 Hz; CH₂F); ¹³C {¹H} NMR (100.6 MHz, CD₃CN): δ=136.9 (d, *J*=3.4 Hz; C-*p*), 135.1 (d, *J*=11.3 Hz; C-*o*), 131.6 (d, *J*=13.7 Hz; C-*m*), 122.2 (q, ¹J_{C,F}=320.9 Hz; CF₃), 119.7 (d, *J*=78.3 Hz; C-*i*), 83.3 ppm (dd, ¹J_{C,F}=283.3, ²J_{C,P}=3.6 Hz; ⁷⁷Se-sats: ¹J_{C,Se}=94.2 Hz; CH₂F); ¹⁹F {¹H} NMR (376.4 MHz, CD₃CN): δ=-79.8 (s; CF₃), -190.3 ppm (d, ³J_{F,P}=3.8 Hz, ⁷⁷Se-sats: ²J_{F,Se}=100.7 Hz; CH₂F); ¹⁹F (376.4 MHz, CD₃CN): δ=-79.8 (s; CF₃), -190.3 ppm (td, ²J_{F,H}=48.7, ³J_{F,P}=3.8 Hz, ⁷⁷Se-sats: ²J_{F,Se}=100.7 Hz; CH₂F); ³¹P {¹H} NMR (162.0 MHz, CD₃CN): δ=37.9 ppm (d, ³J_{P,F}=3.8 Hz, ⁷⁷Se-sats: ¹J_{P,Se}=426.9 Hz); ⁷⁷Se (76.3 MHz, CD₃CN): δ= 294.4 ppm (dd, ¹J_{Se,P}=426.9, ²J_{Se,F}=100.7 Hz); IR (ATR): ν = 3064 (w), 1586 (w), 1483 (w), 1441 (m), 1249 (s), 1221 (s), 1189 (m), 1152 (s), 1100 (s), 1025 (s), 1011 (s), 996 (s), 852 (w), 751 (m), 721 (m), 689 (s), 634 (s), 593 (m), 572 (m), 536 (s), 512 (s), 504 (s) cm⁻¹; Raman (1074 mW): ν = 3063 (w), 1587 (w), 1587 (w), 1097 (w), 1026 (m), 999 (m), 597 (w), 590 (m), 238 (s) cm⁻¹; HRMS (EI): *m/z* [M]⁺ calcd for C₁₉H₁₇FPSe⁺: 375.021116, found: 375.02105; Elemental analysis calcd for C₂₀H₁₇F₄O₃PSSe: C 45.90, H 3.27, S 6.13 found: C 46.14, H 3.38, S 6.34.

Fluorotriphenylphosphonium triflate (13)

From compound **12a**, the solvent was removed *in vacuo*. The remaining solid was crystallized using dichloromethane as solvent and diethylether as conter solvent. Crystals of the decomposition compound were obtained. The compound was identified by single X-Ray diffraction and ¹⁹F/ ³¹P NMR spectroscopy. ¹⁹F NMR (376.4 MHz, CD₃CN): δ=-79.8 (s; CF₃) -129.1 ppm (d, ¹J_{F,P}=988.5 Hz; PF); ¹⁹F (376 MHz, CD₃CN): δ=-79.8 (s; CF₃) -129.1 ppm (d, ¹J_{F,P}=988.5 Hz; PF); ³¹P NMR (162.0 MHz, CDCl₃): δ=96.1 ppm (d, ¹J_{P,F}=988.5 Hz; PF).

Polytetrahydrofuran

To tetrahydrofuran (15 mL, 185 mmol), fluoromethyl triflate (0.2 mL, 1 mmol) was added in one portion with stirring. The reaction solution was stirred for 24 h and polytetrahydrofuran was obtained as a colorless solid.

N-ethylidene-1-fluoromethaniminium triflate

To acetonitrile (15 mL, 285 mmol), fluoromethyl triflate (0.3 mL, 2.85 mmol) was added in one portion with stirring. The reaction solution was stirred for 24 h. *In situ* ¹⁹F NMR investigations showed, that no reaction occurred.

3.6 References

- [1] a) J. Chan, D. O'Hagan *Methods Enzymol.* **2012**, *516*, 219–235; b) D. O'Hagan, H. Deng *Chem. Rev. (Washington, DC, U. S.)* **2015**, *115*, 634–649.
- [2] M. Reichel, J. Martens, E. Woellner, L. Huber, A. Kornath, K. Karaghiosoff *Eur. J. Inorg. Chem.* **2019**, *2019*, 2530–2534.
- [3] Y. Liu, L. Lu, Q. Shen *Angew. Chem., Int. Ed.* **2017**, *56*, 9930–9934.

- [4] a) N. A. Meanwell *J. Med. Chem.* **2018**, *61*, 5822–5880; b) G. A. Showell, J. S. Mills *Drug Discovery Today* **2003**, *8*, 551–556; c) N. A. Meanwell *J. Med. Chem.* **2011**, *54*, 2529–2591; d) S. Zhang, Y. Zhang, Y. Ji, H. Li, W. Wang *Chem. Commun. (Cambridge, U. K.)* **2009**, 4886–4888; e) Y. Zhou, J. Wang, Z. Gu, S. Wang, W. Zhu, J. L. Acena, V. A. Soloshonok, K. Izawa, H. Liu *Chem. Rev. (Washington, DC, U. S.)* **2016**, *116*, 422–518.
- [5] J. Hu, W. Zhang, F. Wang *Chem. Commun. (Cambridge, U. K.)* **2009**, *48*, 7465–7478.
- [6] a) EU, 1005/2009/EG, **2009**; b) M. M. Hurwitz, E. L. Fleming, P. A. Newman, F. Li, E. Mlawer, K. Cady-Pereira, R. Bailey *Geophys. Res. Lett.* **2015**, *42*, 8686–8692.
- [7] a) Y. Qiu, Z. Wu, Y. Liu, S. Chen, H. Zhang (Amphastar Pharmaceuticals, Inc.), WO2016054280A1, **2016**; b) D. Punde, C. Bohara, K. Pokharkar, M. K. Gadakar, V. Gore (Mylan Laboratories Ltd.), IN2012CH03689A, **2014**; c) W. Xu, H. Li (Zhejiang Lantian Environmental Protection Hi-Tech Co., Ltd.), WO2010022645A1, **2010**; d) A. M. Acharya, IN2007MU00917A, **2009**.
- [8] a) G. K. S. Prakash, I. Ledneczeki, S. Chacko, G. A. Olah *Org. Lett.* **2008**, *10*, 557–560; b) T. Furukawa, J. Kawazoe, W. Zhang, T. Nishimine, E. Tokunaga, T. Matsumoto, M. Shiro, N. Shibata *Angew. Chem., Int. Ed.* **2011**, *50*, 9684–9688; c) Y.-D. Yang, X. Lu, G. Liu, E. Tokunaga, S. Tsuzuki, N. Shibata *Chemistry Open* **2012**, *1*, 221–226; d) Y. Nomura, E. Tokunaga, N. Shibata *Angew. Chem., Int. Ed.* **2011**, *50*, 1885–1889.
- [9] P. J. Stang, M. Hanack, L. R. Subramanian, *Synthesis* **1982**, 85–126.
- [10] a) J. Meyer, G. Schramm *Z. Anorg. Allg. Chem.* **1932**, *206*, 24–30; b) M. Hite, W. Rinehart, W. Braun, H. Peck *Am. Ind. Hyg. Assoc. J.* **1979**, *40*, 600–603.
- [11] M. Ando, H. Ito, M. Kameda, H. Kawamoto, K. Kobayashi, H. Miyazoe, C. Nakama, N. Sato, T. Tsujino (Banyu Pharmaceutical Co., Ltd.), WO2009110510A1, **2009**.
- [12] a) P. J. Klein, A. Metaxas, A. D. Windhorst, J. A. M. Christiaans, B. N. M. Van Berckel, (Stichting VU-VUmc), WO2012165956A1, **2014**; b) P. Li, L. P. Wennogle, J. Zhao, H. Zheng (Intra-Cellular Therapies, Inc.), US8858911B2, **2014**; c) S. Keiding, P. Ott, M. Sorensen, K. Frisch, A. Hofmann (Aarhus Universitet, Den.), WO2013113680A1, **2015**; d) D. Peters, D. B. Timmermann, E. O. Nielsen (Danpet AB), US8986654B2, **2015**; e) M. Cantore, M. Benadiba, P. H. Elsinga, C. Kwizera, R. A. J. O. Dierckx, N. A. Colabufo, G. Luurtsema, *ChemMedChem* **2016**, *11*, 108–118; f) S. Keiding, P. Ott, M. Soerensen, K. Frisch, A. Hofmann (Aarhus Universitet, Den.), WO2013113680A1, **2013**; g) P. J. Klein, A. Metaxas, A. D. Windhorst, J. A. M. Christiaans, B. N. M. Van Berckel (Stichting VU-VUmc); WO2012165956A1; **2012**; h) D. Peters, D. B. Timmermann, E. O. Nielsen, (NeuroSearch A/S, Den.), WO2012139925A1, **2012**; i) P. Li, L. P. Wennogle, J. Zhao, H. Zheng (Intra-Cellular Therapies, Inc.), WO2011043816A1, **2011**; j) M. Takashima, M. Shukuri, M. Goto, H. Doi, H. Onoe, M. Suzuki, Y. Watanabe (Riken Corp.), WO2011016376A1, **2011**; k) Q.-H. Zheng, M. Gao, B. H. Mock, S. Wang, T. Hara, R. Nazih, M. A. Miller, T. J. Receveur, J. C. Lopshire, W. J. Groh, D. P. Zipes, G. D. Hutchins, T. R. DeGrado *Bioorg. Med. Chem. Lett.* **2007**, *17*, 2220–2224; l) M. Gao, M. A. Miller, T. R. DeGrado, B. H. Mock, J. C. Lopshire, J. G. Rosenberger, C. Dusa, M. K. Das, W. J. Groh, D. P. Zipes, G. D. Hutchins, Q.-H. Zheng *Bioorg. Med. Chem.* **2007**, *15*, 1289–1297; m) P. Kaufmann, B.

- Weber, A. Buck (Schering A.-G.), WO2006082108A2, **2006**; n) F. Gasparini, Y. Auberson, L. Kessler, S. M. Ametamey (Novartis A.-G.), WO2005030723A1, **2005**. o) M. Schou, C. Halldin, J. Sovago, V. W. Pike, H. Hall, B. Gulyas, P. D. Mozley, D. Dobson, E. Shchukin, R. B. Innis, L. Farde *Synapse (N. Y., NY, U. S.)* **2004**, 53, 57–67; p) R. Iwata, S. Furumoto, C. Pascali, A. Bogni, K. Ishiwata *J. Labelled Compd. Radiopharm.* **2003**, 46, 555–566; q) R. Iwata, C. Pascali, A. Bogni, S. Furumoto, K. Terasaki, K. Yanai *Appl. Radiat. Isot.* **2002**, 57, 347–352.
- [13] a) M. Reichel, B. Krumm, K. Karaghiosoff *J. Fluorine Chem.* **2019**, 226, 109351–109355; b) A. Haas, K. Schinkel *Chem. Ber.* **1990**, 123, 685–689.
- [14] a) G. Brauer *Handbuch der präparativen anorganischen Chemie*, F. Enke, **1975**; b) J. Sniekers, N. R. Brooks, S. Schaltin, L. Van Meervelt, J. Fransaer, K. Binnemans *Dalton Trans.* **2014**, 43, 1589–1598.
- [15] a) A. Kutt, T. Rodima, J. Saame, E. Raamat, V. Maemets, I. Kaljurand, I. A. Koppel, R. Y. Garlyauskayte, Y. L. Yagupolskii, L. M. Yagupolskii, E. Bernhardt, H. Willner, I. Leito *J. Org. Chem.* **2011**, 76, 391–395; b) M. B. Smith, u. J. March *Advanced Organic Chemistry, Vol. 6. Auflage*, Wiley and Sons, Inc., Canada, **2007**.
- [16] R. W. Alder, J. G. E. Phillips, L. Huang, X. Huang *Methyl Trifluoromethansulfonate*, John Wiley & Sons, Ltd., **2001**.
- [17] L. An, Y.-L. Xiao, Q.-Q. Min, X. Zhang *Angew. Chem., Int. Ed.* **2015**, 54, 9079–9083.
- [18] H. Emde, A. Goetz, K. Hofmann, G. Simchen *Liebigs Ann. Chem.* **1981**, 1643–1657.
- [19] a) G. Li, Z. Xue, B. Cao, C. Yan, T. Mu *ACS Sustainable Chem. Eng.* **2016**, 4, 6258–6262; b) B. Cao, J. Du, Z. Cao, H. Sun, X. Sun, H. Fu *RSC Adv.* **2017**, 7, 11259–11270.
- [20] M. K. Singh, D. P. Patel, K. Solanki, D. J. Patel, T. C. Shah, R. Z. Bavadia (Cadila Healthcare Limited), IN2012CH03689A, **2013**;
- [21] S.-H. Guo, M.-Y. Wang, G.-F. Pan, X.-Q. Zhu, Y.-R. Gao, Y.-Q. Wang *Adv. Synth. Catal.* **2018**, 360, 1861–1869.
- [22] F. G. Baddour, A. S. Hyre, J. L. Guillet, D. Pascual, J. M. Lopez-de-Luzuriaga, T. M. Alam, J. W. Bacon, L. H. Doerrer *Inorg. Chem.* **2017**, 56, 452–469.
- [23] G. Olah, A. Pavlath *Acta Chim. Acad. Sci. Hung.* **1953**, 3, 203–207.
- [24] T. Hashimoto, K. Takeda, T. Kodaira *J. Macromol. Sci., Pure Appl. Chem.* **2000**, A37, 293–306.
- [25] J. Kleine, E. Heisenberg, R. Lotz (Vereinigte Glanzstoff-Fabriken A.-G.), US2742501, **1956**.

3.7 Supporting Information

Table 1: Structure refinement parameter of decomposed acetonitrile (left) and compound **7b** (right)

Empirical formula	C ₇ H ₁₂ F ₆ N ₂ O ₈ S ₂	C ₉ H ₁₂ F ₄ N ₂ O ₃ S
Formula weight	430.31	304.27
Temperature	143(2) K	143(2) K
Wavelength	0.71073 Å	0.71073 Å
Crystal system	Triclinic	Monoclinic
Space group	<i>P</i> -1	<i>P</i> 2 ₁ /m
Unit cell dimensions	a = 8.3960(6) Å b = 8.6410(7) Å c = 12.3290(14) Å α = 108.381(8)° β = 107.745(8)° γ = 95.777(6)°	a = 8.6407(9) Å b = 8.9695(7) Å c = 8.8193(9) Å α = 90° β = 115.812(13)° γ = 90°
Volume	789.06(13) Å ³	615.32(12) Å ³
Z	2	2
Density (calculated)	1.811 mg/m ³	1.642 mg/m ³
Absorption coefficient	0.446 mm ⁻¹	0.320 mm ⁻¹
F(000)	436	312
Crystal size	0.100 x 0.050 x 0.050 mm ³	0.100 x 0.050 x 0.050 mm ³
Theta range for data collection	4.742 - 28.279°	4.395 - 30.487°
Index ranges	-9 ≤ h ≤ 11, -11 ≤ k ≤ 11, -16 ≤ l ≤ 16	-12 ≤ h ≤ 12, -12 ≤ k ≤ 10, -12 ≤ l ≤ 12
Reflections collected	6993	6284
Independent reflections	3904 [R _{int} = 0.0313]	1979 [R _{int} = 0.0355]
Data / restraints / parameters	3904 / 0 / 244	1979 / 0 / 105
Goodness-of-fit on F ²	1.022	1.028
Final R indices [I > 2σ(I)]	R ₁ = 0.0426, wR ₂ = 0.0897	R ₁ = 0.0425, wR ₂ = 0.0989
R indices (all data)	R ₁ = 0.0660, wR ₂ = 0.1026	R ₁ = 0.0629, wR ₂ = 0.1113
Largest diff. peak and hole	0.395 and -0.417 e Å ⁻³	0.425 and -0.306 e Å ⁻³

Table 2: Structure refinement parameter of compound **7d** (left) and *O*-Fluoromethylated *Michler's* Ketone (right).

Empirical formula	C ₁₉ H ₂₂ F ₄ N ₂ O ₄ S	C ₁₉ H ₂₂ F ₄ N ₂ O ₄ S
Formula weight	450.44	450.44
Temperature	143(2) K	143(2) K
Wavelength	0.71073 Å	0.71073 Å
Crystal system	Monoclinic	Triclinic
Space group	<i>P</i> 2 ₁	<i>P</i> -1
Unit cell dimensions	a = 6.2114(3) Å b = 8.2897(3) Å c = 19.8827(7) Å α = 90° β = 90.483(4)° γ = 90°	a = 7.7552(4) Å b = 8.1229(8) Å c = 16.4467(11) Å α = 101.458(7)° β = 91.084(5)° γ = 93.752(6)°
Volume	1023.74(7) Å ³	1012.69(13) Å ³

Z	2	2
Density (calculated)	1.461 mg/m ³	1.477 mg/m ³
Absorption coefficient	0.223 mm ⁻¹	0.225 mm ⁻¹
F(000)	468	468
Crystal size	0.100 x 0.050 x 0.050 mm ³	0.100 x 0.050 x 0.050 mm ³
Theta range for data collection	4.219 - 28.278°	4.195 - 28.282°
Index ranges	-8 ≤ h ≤ 8, -11 ≤ k ≤ 11, -26 ≤ l ≤ 25	-10 ≤ h ≤ 9, -10 ≤ k ≤ 10, -21 ≤ l ≤ 21
Reflections collected	9152	8931
Independent reflections	4869 [R _{int} = 0.0365]	5022 [R _{int} = 0.0479]
Data / restraints / parameters	4869 / 1 / 288	5022 / 0 / 284
Goodness-of-fit on F2	1.002	1.003
Final R indices [I > 2σ(I)]	R ₁ = 0.0456, wR ₂ = 0.0924	R ₁ = 0.0635, wR ₂ = 0.1080
R indices (all data)	R ₁ = 0.0612, wR ₂ = 0.1012	R ₁ = 0.1241, wR ₂ = 0.1351
Largest diff. peak and hole	0.516 and -0.289 e Å ⁻³	0.324 and -0.294 e Å ⁻³

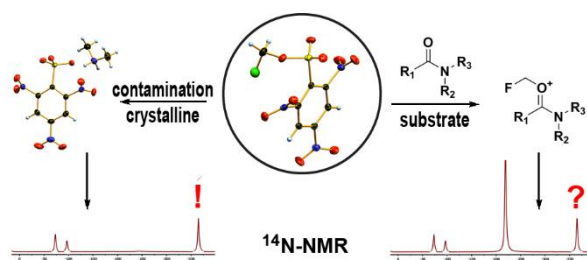
Table 3: Structure refinement parameter of compound **12b** (left) and compound **12a** (right).

Empirical formula	C ₂₀ H ₁₇ F ₄ O ₃ P S ₂	C ₁₉ H ₁₅ F ₄ O ₃ P S
Formula weight	476.42	430.34
Temperature	173(2) K	146(2) K
Wavelength	0.71073 Å	0.71073 Å
Crystal system	Monoclinic	Monoclinic
Space group	<i>P</i> 2 ₁ / <i>n</i>	<i>P</i> 2 ₁ / <i>n</i>
Unit cell dimensions	a = 10.9375(8) Å b = 8.3451(6) Å c = 23.7088(15) Å α = 90° β = 103.211(7)° γ = 90°	a = 11.1068(6) Å b = 8.6238(4) Å c = 19.8976(11) Å α = 90° β = 93.861(5)° γ = 90°
Volume	2106.7(3) Å ³	1901.52(17) Å ³
Z	4	4
Density (calculated)	1.502 mg/m ³	1.503 mg/m ³
Absorption coefficient	0.383 mm ⁻¹	0.310 mm ⁻¹
F(000)	976	880
Crystal size	0.150 x 0.050 x 0.050 mm ³	0.050 x 0.050 x 0.050 mm ³
Theta range for data collection	4.294 - 30.508°	4.206 - 28.281°
Index ranges	-15 ≤ h ≤ 15, -11 ≤ k ≤ 11, -31 ≤ l ≤ 33	-14 ≤ h ≤ 14, -9 ≤ k ≤ 11, -25 ≤ l ≤ 26
Reflections collected	21508	16263
Independent reflections	6397 [R _{int} = 0.0505]	4707 [R _{int} = 0.0461]
Data / restraints / parameters	6397 / 0 / 281	4707 / 0 / 268
Goodness-of-fit on F2	1.015	1.030
Final R indices [I > 2σ(I)]	R ₁ = 0.0447, wR ₂ = 0.0917	R ₁ = 0.0401, wR ₂ = 0.0846
R indices (all data)	R ₁ = 0.0781, wR ₂ = 0.1051	R ₁ = 0.0606, wR ₂ = 0.0940
Largest diff. peak and hole	0.439 and -0.344 e Å ⁻³	0.423 and -0.369 e Å ⁻³

4 Fluoromethyl 2,4,6 trinitrobenzenesulfonate: A New Electrophilic Monofluoromethylating Reagent

Marco Reichel, Andreas Kornath, Konstantin Karaghiosoff*

To be submitted



Abstract: Fluoromethyl 2,4,6-trinitrophenylsulfonate has been prepared for the first time and qualified as a potent and simply to use monofluoromethylating reagent. Its molecular structure in the solid state has been determined by single crystal X-ray diffraction studies. This reagent proves to be effective for the electrophilic introduction of a CH₂F group to amides or ketones. Monofluoromethyl derivatives of various bifunctional *N,O*-nucleophiles have been synthesized using fluoromethyl 2,4,6-trinitrophenylsulfonate. Due to the good crystallizing properties of the anion the fluoromethylated products as well as side products, difficult to identify by NMR spectroscopy, can readily be characterized by X-ray crystallography techniques.

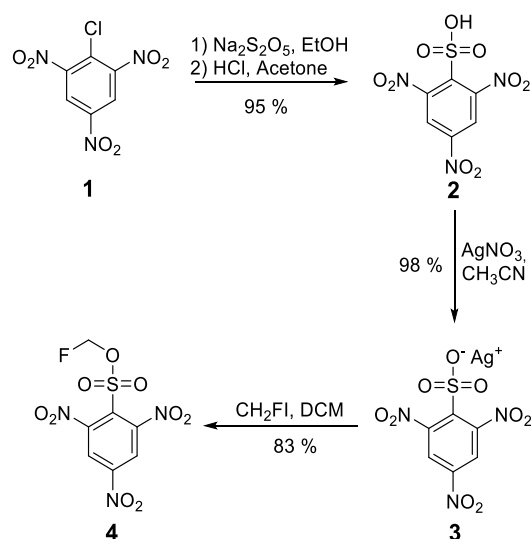
4.1 Introduction

Monofluoromethyl containing organic compounds are of great importance in pharmaceutical industry. The bioisosterism of the CH₂F group to essential functional groups occurring in living systems, combined with the enhanced metabolic stability, lipophilicity and membrane permeability induced by the fluorine substituent, allows an efficient drug design.^[1] The most prominent representative is Fluticasone, a widely used drug against inflammatory diseases and as analgesics for the treatment of certain types of cancer.^[2] Although a large number of biologically active monofluoromethyl containing substances have been described in literature, their synthesis by introduction of the CH₂F group as such is still a challenge and a series of new electrophilic fluoromethylation reagents have been developed in the last decade.^[3] In most of the cases, however, either ozone-depleting fluoromethyl halides, like CH₂FCl or CH₂FBr or reagents made by tedious multistep syntheses have been used. Among the CH₂F transferring reagents fluoromethyl sulfonates, e.g. fluoromethyl triflate, are mainly used today, usually for ¹⁸F labeling.^[3a,4] Their synthesis requires generally quite harsh conditions, however.

Pharmaceutical products often require Good Manufacturing Practices (GMP) certification, which certifies the high purity of the drug and the identification of all by-products occurring during its synthesis.^[5] The identification of by-products can often represent a difficult task, particularly when identification via multinuclear NMR spectroscopy is not unambiguous. X-ray crystallography is one method of elucidating by-products and identifying their structures

without any doubt. In the case of salts the formation of suitable single crystals strongly depends on the anion and in the case of triflates the salts are hard to crystallize.^[6] A fluoromethylation reagent, which is similarly strong in its alkylation power like fluoromethyl triflate but has good crystallization properties would be of particular importance for GMP processes with regard to the identification and structure elucidation of ionic impurities. Since protonation is generally similar to methylation, the pK_a values can be used to roughly estimate the alkylating power of a reagent. This is the case for triflic acid (pK_a 11.4) and trinitrobenzenesulfonic acid (pK_a 11.3). At the same time good crystallization properties can be anticipated for the trinitrobenzenesulfonate anion.^[7] Here we present the synthesis and first applications of fluoromethyl-2,4,6-trinitrobenzene sulfonate **4** - a new strong direct electrophilic fluoromethylating reagent (Scheme 1).

4.2 Results and Discussion



Scheme 1: Preparation of fluoromethyl-2,4,6-trinitrobenzene sulfonate (**4**).

Picryl chloride **1**, from which traces of picric acid were carefully removed by washing with acetone, was used as the starting material. Reaction with sodium metarsulfite followed by hydrolysis with aqueous HCl yields the sulfonic acid **2**, which was converted to the corresponding silver salt **3** by reaction with AgNO₃. These reactions were carried out following a literature procedure^[8], which was slightly modified. It is really important to completely remove traces of picric acid before starting the synthesis in order to prevent formation of explosive silver picrate. In contrast silver trinitrosulfonate does not show critical impact and friction sensitivity and can be handled safely. In the final step reaction of **3** with CH₂FI in DCM gives the fluoromethyl sulfonate **4** in very good yield. In our hands this final step worked only in dry DCM as solvent. Traces of moisture or solvents with lone pairs of electrons like acetonitrile, diethyl ether or THF will cause decomposition of **4**. A similar observation was reported also for other strong fluoromethylating reagents.^[9]

Fluoromethyl sulfonate **4** was obtained as colorless microcrystalline solid in good yield (Scheme 1). All intermediates in its synthesis were isolated and their identity proved by single crystal X-ray diffraction and further analyses (see Supporting Information). The reagent **4** is

stable at ambient temperature and can be stored under dry argon for several months without visible decomposition. Like strong fluoromethylating agents in general, **4** should be handled under dry protective gas in dry non nucleophilic solvents. It displays a melting point of 136.5 °C and a decomposition point of 138 °C. Single crystals of **4** were obtained by slow evaporation of a solution in DCM. The molecular structure of **4** in the crystal together with selected bond lengths and bond angles is shown in Figure 1.

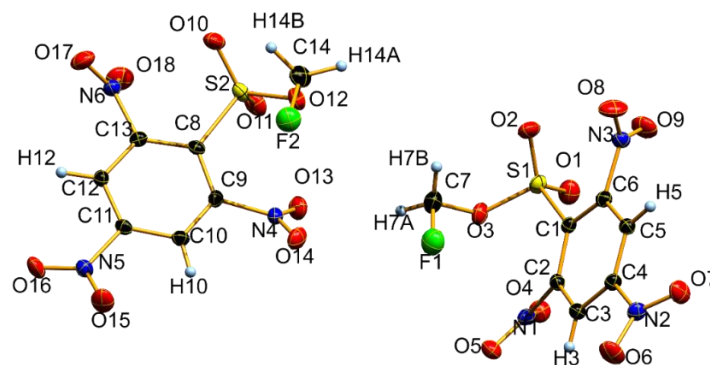
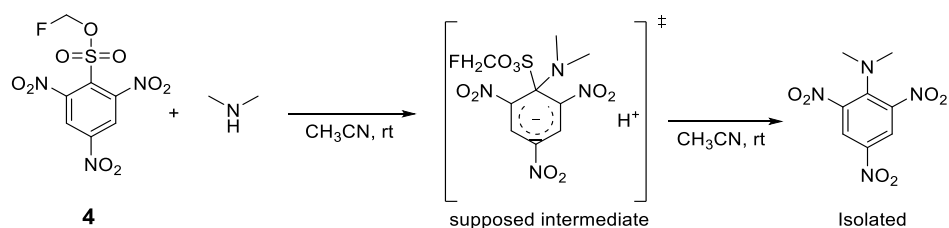


Figure 1: Molecular structure of **4** in the crystal, view of the asymmetric unit. DIAMOND representation, thermal ellipsoids are drawn at 50 % probability level. Selected bond lengths [Å] and angles [°]: F1-C7: 1.358(6), F2-C14: 1.362(5), O3-C7: 1.440(6), O12-C14: 1.433(6), O3-S1: 1.572(3), O12-S2: 1.573(3), F1-C7-O3: 107.6(3), F2-O12-C14: 107.3(3), C7-O3-S1: 120.3(3), C14-O12-S2: 120.3(3); F1-C7-O3-S1: -93.2(4), F2-C14-O12-S2: 95.8(4).

Fluoromethyl sulfonate **4** qualified to be the ideal reagent for the fluoromethylation of weak nucleophiles. In the case of strong nucleophiles like potassium *isopropanolate*, DBU, thiourea, *N,N,N',N'*-tetramethyl guanidine, pyridine, 4-DMAP, methylimidazole, dimethylamine and benzoxazole an intensely red colored solution was formed immediately after adding the reagent, from which no fluoromethylated product could be observed. In the case of dimethylamine 2,4,6-trinitroaniline was isolated and identified by single crystal X-ray diffraction (Figure 2). Most probably the colour change to red is due to the formation of a *Janovsky product*,^[10] whereby the nucleophile attacks the *ipso* position of the reagent and makes it inoperable (Scheme 2).^[11]



Scheme 2: Proposed mechanism for the reaction of **4** with dimethylamine, resulting in the formation of 2,4,6-trinitro-aniline.

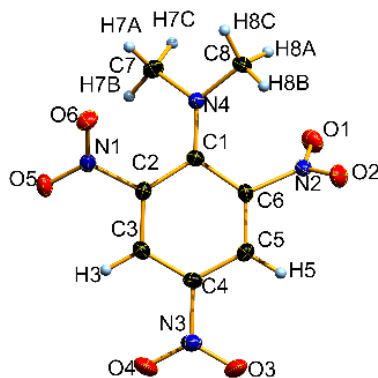
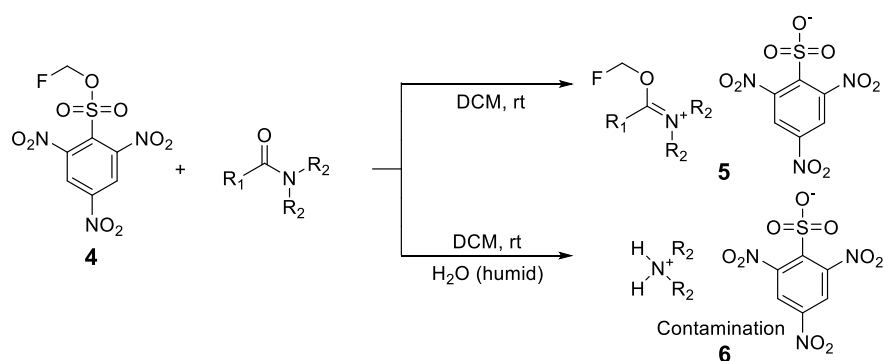


Figure 2: Molecular structure of 2,4,6-trinitroaniline in the crystal. DIAMOND representation, thermal ellipsoids are drawn at 50 % probability level. For bond length and angles see Supporting Information.

The fluoromethylation ability of the new reagent **4** towards weak nucleophiles was tested using a series of amides of carbonic acids (Table 1). The amides were selected based on our experience with the fluoromethylation by fluoromethyl triflate. In these cases the resulting triflate salts form ionic liquids and by-products were present in the reaction mixture.^[6] Mostly amides disubstituted at nitrogen yielded isolatable and stable monofluoromethyl products. The products resulting from the fluoromethylation of *N*-methyl acetamide or acetamide were too unstable and could not be isolated. All fluoromethylated amides were obtained as crystalline 2,4,6-trinitrophenyl-sulfonium salts and were characterized by multinuclear (¹H, ¹³C, ¹⁴N) NMR spectroscopy and by single crystal X-ray diffraction (Figures 3-5).

As main by-product (3-4 %) the ammonium salts **6** were identified by NMR spectroscopy and single crystal X-ray diffraction (Figure 6, Table 1). The formation of **6** indicates the possible presence of traces of water. To further elucidate the formation of **6** pure monofluoromethylated dimethylacetamide **5b** was allowed to react with D₂O. The ¹H NMR spectrum of the reaction solution indicated the formation of Me₂ND₂⁺, identified by the ¹H NMR signal of the methyl protons. A possible mechanism explaining the formation of **6b** is depicted in Scheme 3. The fate of the fluoromethyl substituent could not be determined with certainty, however.

Table 1: Fluoromethylation of amides with **4** to yield the salts **5**. Main by-product are the ammonium salts **6**.



entry	starting material	decomposition/product	yield (%)
1		 5a	80
2		 6a	3
3		 5b	78
4		 6b	4
5		 5c	82
6		 6b	3

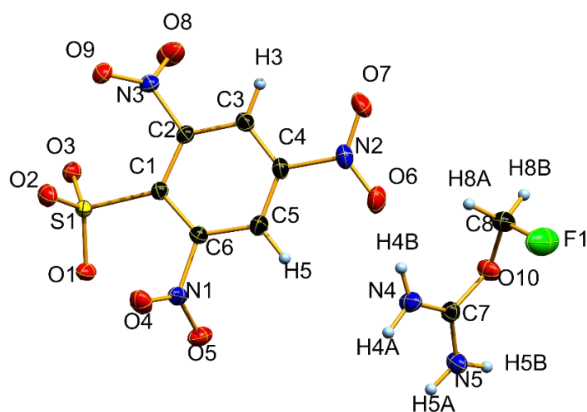


Figure 3: Molecular structure of **5a** in the crystal, view of the asymmetric unit. DIAMOND representation, thermal ellipsoids are drawn at 50 % probability level. Selected bond lengths [Å] and angles [°]: F1-C8: 1.354(2), O10-C8: 1.412(2), O10-C7: 1.330(2), F1-C8-O10: 108.0(2), F1-C8-O10-C7: 76.0(2).

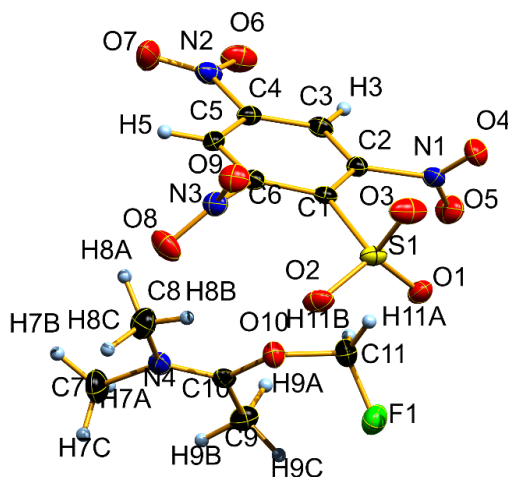


Figure 4: Molecular structure of **5b** in the crystal, view of the asymmetric unit. DIAMOND representation, thermal ellipsoids are drawn at 50 % probability level. Selected bond lengths [Å] and angles [°]: F1-C11: 1.367(2), C11-O10: 1.413(2), F1-C11-O10: 109.1(2), F1-C11-O10-C10: -80.6(2).

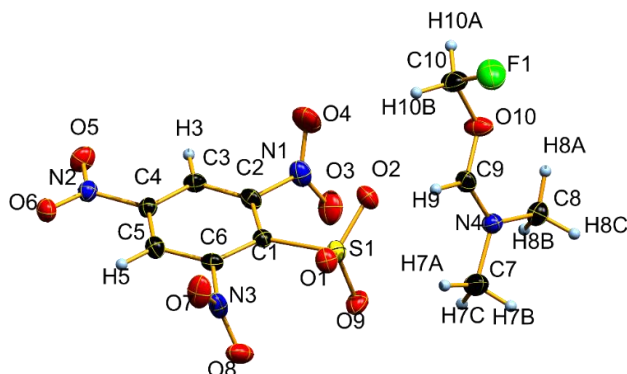


Figure 5: Molecular structure of **5c** in the crystal, view of the asymmetric unit. DIAMOND representation, thermal ellipsoids are drawn at 50 % probability level. Selected bond lengths [Å] and angles [°]: F1-C10: 1.349(4), C10-O10: 1.423(3), O10-C9: 1.318(3), F1-C10-O10: 107.2(3), C10-O10-C9: 116.3(2), F1-C10-O10-C9: 84.8(3).

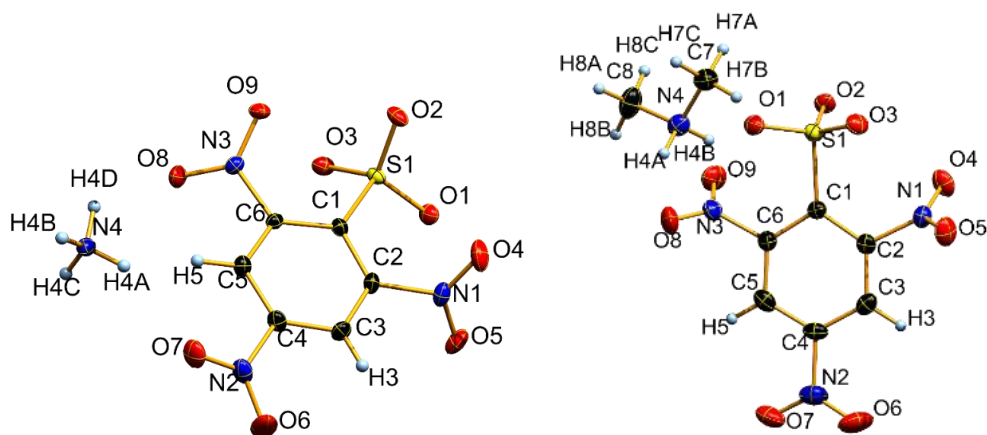
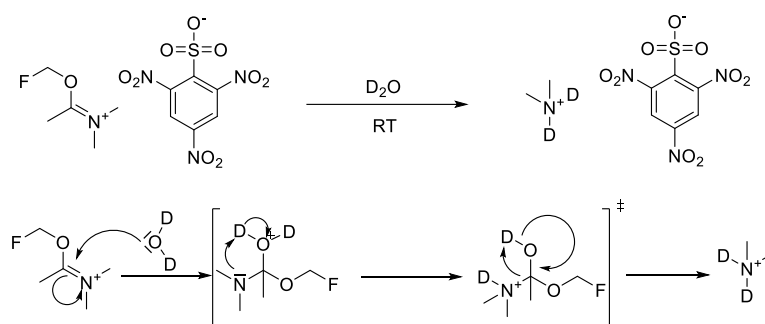


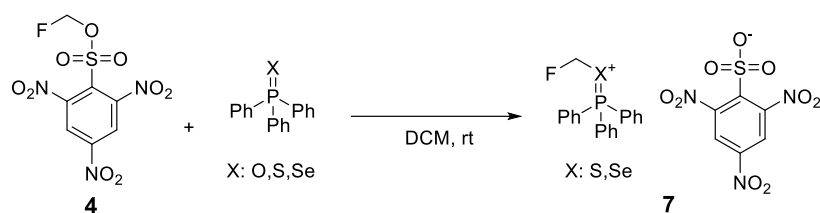
Figure 6: Molecular structure of **6a** and **6b** in the crystal, view of the asymmetric unit. DIAMOND representation, thermal ellipsoids are drawn at 50 % probability level. For bond lengths and angles see Supporting Information.



Scheme 3: Possible mechanism for the formation of **6b**.

To further explore the fluoromethylation potential of sulfonate **4** the transfer of the CH₂F group to the chalcogen atom of the triphenylphosphine chalcogenides Ph₃PX (X = O, S, Se) was investigated (Table 2). As can be seen from Table 2 the reaction of **4** with triphenyl-phosphine sulfide and selenide proceeds straight forward producing the fluoromethylated derivatives **7b,c** in good yields. The fluoromethylated selenide **7c** is highly sensitive to oxidation. The sulfide **7b**, on the other hand, is sufficiently stable and could be characterized by single crystal X-ray diffraction (Figure 7). No reaction was observed with triphenyl-phosphine oxide, in contrast to our experience with fluoromethyl triflate. Fluoromethylation of diphenylsulfide, butyrolactone, benzaldehyde and acetonitrile was also not possible with this reagent. In summary sulfonate **4** is a weaker fluoromethylating agent as compared to fluoromethyl triflate.

Table 2: Fluoromethylation of Ph₃PX (X = O, S, Se) with **4**.



entry	starting material	decomposition/product	yield (%)
1			0
2			78
3			66

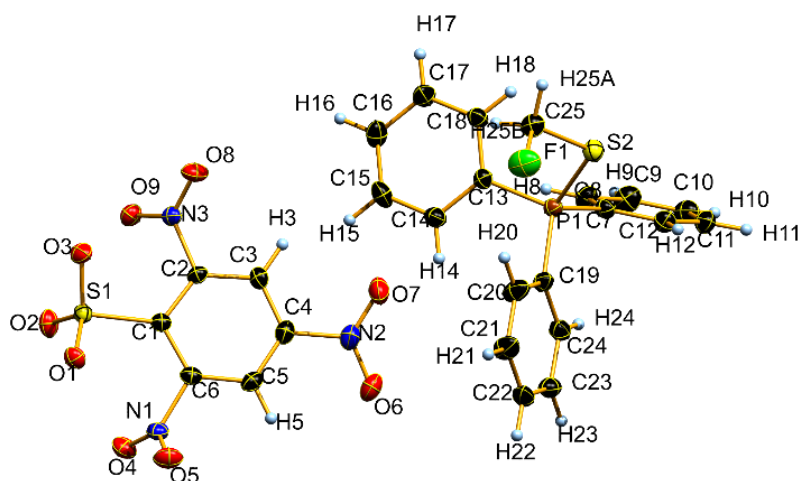
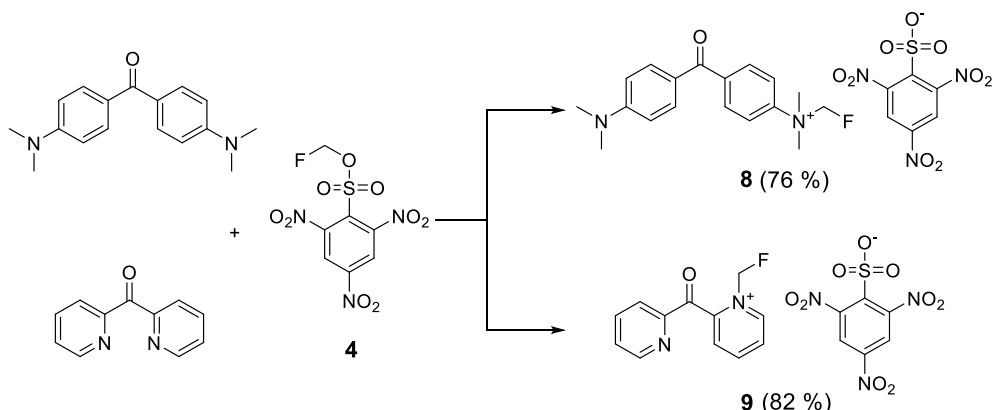


Figure 7: Molecular structure of **7b** in the crystal, view of the asymmetric unit. DIAMOND representation, thermal ellipsoids are drawn at 50 % probability level. Selected bond lengths [Å] and angles [°]: F1-C25: 1.379(2), C25-S2: 1.813(2), S2-P1: 2.076(1); F1-C25-S2: 111.2(2), C25-S2-P1: 104.5(1); F1-C25-S2-P1: 88.5(2).

Fluoromethylation of *Michler's* ketone and dipyrindyl ketone with sulfonate **4** occurs in both cases at nitrogen (Scheme 4). Interestingly with fluoromethyl triflate both *N*- and *O*-alkylation was observed in the reaction with *Michler's* ketone. This is in accordance with our overall

experience, that **4** is the weaker fluoromethylating reagent as compared to fluoro-methyl triflate.^[13]



Scheme 4: Fluoromethylation of *Michler's* ketone and dipyrindyl ketone with sulfonate **4**.

The salt **9** was isolated as a colorless microcrystalline solid. Single crystals of **9** were obtained from a dichloromethane solution by slow evaporation of the solvent. The molecular structure of **9** in the crystal was determined by single crystal X-ray diffraction and is shown in Figure 8 together with selected bond lengths and angles.

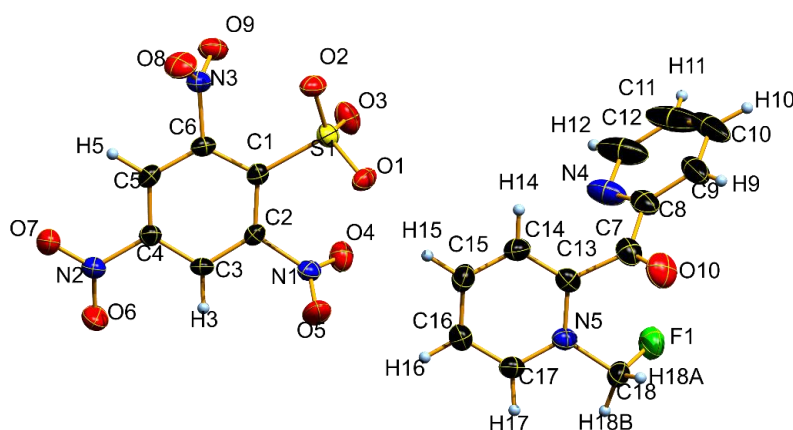


Figure 8: Molecular structure of **9** in the crystal, view of the asymmetric unit. DIAMOND representation, thermal ellipsoids are drawn at 50 % probability level. Selected bond lengths [Å] and angles [°]: F1-C18: 1.365(5), C18-N5: 1.481(5), F1-C18-N5: 107.1(3).

4.3 Conclusion

In conclusion we have prepared a new sulfonic acid fluoromethyl ester (**4**), which acts as a strong electrophilic direct monofluoromethylating reagent. With the new reagent the fluoromethyl group was successfully transferred to a series of carbonic acid amides, phosphorus chalcogenides and aromatic ketones. The fluoromethyl sulfonate **4** is a weaker fluoromethylating reagent compared to the related fluoromethyl triflate. The 2,4,6-trinitrophenylsulfonate anion qualified as strongly supporting crystallisation. By-products, which are formed during fluoromethylation, could readily be isolated and identified *via* single crystal X-ray diffraction.

4.4 Acknowledgement

Financial support by Ludwig–Maximilian University is gratefully acknowledged. We are thankful to F–Select GmbH for a generous donation of fluoroiodomethane.

4.5 Experimental Section

4.5.1 General Procedure

All compounds were handled using *Schlenk* techniques under dry Ar. Fluoroiodomethane (donation from F-Select GmbH) was distilled under inert conditions before use. Picrylchloride was solved in acetone and poured onto ice. The remaining solid was filtered off and the procedure was repeated until the solid was colorless. All other chemicals were purchased from VWR and Sigma Aldrich and were used without further purification. Melting and / or decomposition points were detected with a Linseis DSC-PT10 instrument and with a OZM DTA 552-Ex instrument under inert atmosphere and ambient conditions, respectively. The samples for infrared spectroscopy were placed under ambient conditions without further preparation onto a Smith DuraSampLIR II ATR device using a Perkin Elmer BX II FR-IR System spectrometer. Samples for Raman spectroscopy were sealed in glass tubes. The measurement was carried out on a Bruker MultiRam FT Raman device using a neodymium doped yttrium aluminum garnet (Nd:YAG) laser ($\lambda = 1064$ nm) with 1074 mW. The samples for NMR spectroscopy were prepared under inert atmosphere using Ar as protective gas. The solvents were dried using 3 Å mol sieve and stored under Ar atmosphere. Spectra were recorded on a Bruker Avance III spectrometer operating at 400.1 MHz (^1H), 376.4 MHz (^{19}F), 100.6 MHz (^{13}C), 161.9 MHz (^{31}P), 76.3 MHz (^{77}Se) and 28.9 MHz ($^{14/15}\text{N}$). Chemical shifts are referred to TMS ($^1\text{H}/^{13}\text{C}$), CFCl_3 (^{19}F), 85% H_3PO_4 (^{31}P) H_2SeO_3 (^{77}Se), MeNO_2 (^{14}N). All spectra were recorded at 299.15 K (26 °C). Elemental analyses were performed with an Elemental Vario EL Analyzer. The samples were prepared under N_2 atmosphere. High resolution mass spectral data were acquired using a Jeol MStation Sectorfield in ESI/ DEI mode. Single crystals, suitable for X-ray diffraction, were obtained by slow evaporation of a solution in acetonitrile or DCM. The crystals were introduced into perfluorinated oil and a suitable single crystal was carefully mounted on the top of a thin glass wire. Data collection was performed with an Oxford Xcalibur 3 diffractometer equipped with a Spellman generator (50 kV, 40 mA) and a Kappa CCD detector, operating with Mo- K_α radiation ($\lambda = 0.71073$ Å). Data collection and data reduction were performed with the CrysAlisPro software.^[1] Absorption correction using the multiscan method^[1] was applied. The structures were solved with SHELXS-97,^[2] refined with SHELXL-97^[3] and finally checked using PLATON.^[4] Details for data collection and structure refinement are summarized in the supplementary information.

4.5.2 Preparation

Caution! *Picrylchloride is a energetic material with sensitive behavior towards impact and friction. It must be washed free from picric acid residues before use to prevent the formation of highly shock and friction sensitive picrates such as silver picrate! Even if no accident*

has occurred, during the synthesis Kevlar gloves, and plastic spartulas should be used when synthesizing the Silversulfonate or working with the picrylchloride.

Picrylsulfonic acid (2)

The preparation of **1** was performed according to a modified literature known synthesis.^[5] Picric acid free washed picrylchloride (6.54 g, 26.4 mmol) was dissolved in ethanol (70 mL). To the vigorously stirred solution, subsequently within 30 min sodiummetabisulfite (6.54 g, 34.4 mmol) was added in small portions. The reaction mixture was heated under reflux for 4 h. The mixture was cooled to room temperature and the solid was filtered off. The filtercake was washed with cold ethanol (3 × 150 mL), till the filtrate was colorless. After the solid was dried at room temperature it was mixed with acetone (20 mL) and concentrated hydrochloric acid (6.5 mL) was dropped within 15 min to the solution. The precipitated sodium chloride was filtered off and the solvent was removed in high vacuum to give 7.33 g of colorless solid **2**. Yield: 95 %. T_{mp.}: 194 °C. T_{dec.}: 260 °C. ¹H NMR (CD₃CN): δ = 6.64 (bs, 1H), 8.59 (s, 1H) ppm. ¹³C NMR (CD₃CN): δ = 118.6, 137.1, 149.3, 150.6 ppm. ¹⁴N NMR (CD₃CN): δ = -21.4 (s, 1N), -14.7 (s, 2N) ppm. IR (ATR): $\tilde{\nu}$ = 3530 (m), 3447 (m), 3084 (m), 1724 (w), 1605 (w), 1539 (s), 1349 (s), 1268 (m), 1199 (m), 1128 (m), 1072 (s), 1032 (s), 924 (s), 733 (m), 718 (s), 626 (s), 552 (m), 445 (m). Raman: $\tilde{\nu}$ = 3085 (m), 1604 (s), 1552 (m), 1552 (m), 1374 (s), 1351 (s), 1272 (w), 1190 (w), 1077 (s), 1040 (w), 937 (w), 826 (w), 772 (s), 752 (w), 721 (w), 554 (w), 353 (m), 324 (m), 170 (s). HRMS (DEI): calculated for C₆H₃N₃O₉S. Expected: 292.9590 Observed: 292.9590 (0 ppm).

Silverpicryl sulfonate (3)

The preparation of **2** was performed according to a modified literature known synthesis.^[5] Picrylsulfonic acid (6.62 g, 22.6 mmol), solved in water (10 mL) and silvernitrate (5.10 g, 30.1 mmol), solved in water (10 mL) were heated to 50 °C under the exclusion of light. The silver nitrate solution was added while vigorously stirring, in one portion to the sulfonic acid. The mixture was stirred until the temperature was cooled down to roomtemperature and then cooled with an icebath. The solid was filtered off and washed with ethanol (2 × 25 mL) and diethylether (1 × 25 mL). The product was recrystallized in dry diethylether/ acetonitrile mixture (1:1, 60 mL), filtered off and dried in high vacuum, to obtain 8.85 g of white solid **3**. Yield: 98 %. T_{mp.}: 119 °C. T_{dec.}: 295 °C. ¹H NMR (CD₃CN): δ = 8.52 (s, CH) ppm. ¹³C NMR (CD₃CN): δ = 118.8, 137.6, 149.0, 150.6 ppm. ¹⁴N NMR (CD₃CN): δ = -18.4 (s, 1N), -11.4 (s, 2N) ppm. IR (ATR): $\tilde{\nu}$ = 2963 (m), 2917 (m), 2853 (w), 1576 (w), 1543 (w), 1260 (s), 1093 (s), 1020 (s), 863 (w), 798 (s). Raman: $\tilde{\nu}$ = 3088 (w), 1605 (m), 1557 (w), 1541 (w), 1370 (m), 1656 (s), 1188 (w), 1072 (m), 937 (w), 387 (m), 359 (w), 342 (w), 327 (m), 238 (w), 216 (w), 182 (w). Elemental analysis for C₆H₂AgN₃O₉S·2 H₂O. Expected: C, 16.53; H, 1.39; N, 9.64; S, 7.35. Observed: C, 16.56; H, 1.40; N, 9.43; S, 7.44. FS: > 360N. IS: > 40 J.

Fluoromethyl-2,4,6-trinitrobenzene sulfonate (**4**)

Silverpicrylsulfonate (3.60 g, 9.00 mmol) was suspended in dry dichloromethane (40 mL) under argon atmosphere. To the cooled suspension, fluoroiodomethane (0.7 mL, 10.0 mmol) was added dropwise over a period of 15 min. The mixture was stirred for 1 h and the precipitated silver iodide was filtered off and washed with dry acetonitrile (10 mL). The solvent was removed in high vacuum to give 2.44 g of colorless solid **4**. Yield: 95 %. $T_{\text{mp.}}$: 136 °C. $T_{\text{dec.}}$: 138 °C. $^1\text{H NMR}$ (d_6 -Acetone): δ = 6.11 (d, J = 49.1 Hz, 2H), 9.21 (s, 2H). $^{13}\text{C NMR}$ (d_6 -Acetone): δ = 102.2 (d, J = 236.9 Hz), 124.0, 128.6, 151.0, 152.7 ppm. $^{19}\text{F NMR}$ (d_6 -Acetone): δ = -151.1 (s) ppm. $^{19}\text{F NMR}$ (d_6 -Acetone): δ = -151.1 (t, J = 49.1 Hz) ppm. $^{14}\text{N NMR}$ (d_6 -Acetone): δ = -23.4 (s, 1N), -19.7 (s, 2N) ppm. IR (ATR): $\tilde{\nu}$ = 3086 (m), 2959 (w), 2927 (w), 1727 (w), 1608 (m), 1547 (s), 1453 (w), 1417 (w), 1393 (m), 1348 (s), 1300 (w), 1204 (w), 1189 (s), 1150 (m), 1120 (m), 1074 (s), 944 (s), 920 (s), 826 (w), 794 (m), 746 (s), 735 (s), 717 (s), 662 (w), 619 (s), 582 (w), 542 (m), 511 (m). Raman: $\tilde{\nu}$ = 3086 (m), 3019 (w), 2905 (w), 1603 (m), 1550 (m), 1369 (s), 1354 (s), 1191 (m), 1055 (m), 826 (m), 807 (m), 437 (m), 395 (m), 365 (m), 340 (m), 323 (m), 285 (m), 253 (m). HRMS (DEI): calculated for $\text{C}_7\text{H}_4\text{FN}_3\text{O}_9\text{S}$. Expected: 324.9652 Observed: 324.9647. Elemental analysis for $\text{C}_7\text{H}_4\text{FN}_3\text{O}_9\text{S}$. Expected: C, 25.86 ; H, 1.24; N, 12.92; S, 9.86. Observed: C, 26.01 ; H, 1.41; N, 12.82; S, 10.28.

2-(fluoromethyl)isouronium-2,4,6-trinitrobenzene sulfonate (**5a**)

The reagent **4** (100 mg, 309 μmol) was solved in acetonitrile (1.5 mL) and was added dropwise to a solution of urea (18.6 mg, 309 μmol) within acetonitrile (5 mL). The resulting solution was stirred over night and the solvent was removed in vacuum. The crude product was recrystallized in a dichloromethane/ acetonitrile mixture (5 mL/ 0.3 mL). The mixture was centrifuged and the solvent decanted off. The remaining solid was dried in high vacuum to give 95 mg of a white solid. Yield: 80 %. $T_{\text{mp.}}$: 180 °C. $T_{\text{dec.}}$: 200 °C. $^1\text{H NMR}$ (CD_3CN): δ = 5.80 (d, J = 50.2 Hz, 2H), 7.49 (d, J = 50.2 Hz, 4H), 8.57 (s, 2H). $^{13}\text{C NMR}$ (CD_3CN): δ = 99.9 (d, J = 229.0 Hz), 122.1, 137.8, 149.3, 150.8, 162.2 ppm. $^{19}\text{F NMR}$ (CD_3CN): δ = -156.5 (s) ppm. $^{19}\text{F NMR}$ (CD_3CN): δ = -156.5 (t, J = 50.2 Hz) ppm. $^{15}\text{N NMR}$ (d_6 -Acetone): δ = -298.3 (s, 1N), -22.6 (s, 1N), -15.6 (s, 2N) ppm. IR (ATR): $\tilde{\nu}$ = 3419 (m), 3393 (m), 3352 (m), 3247 (m), 3183 (m), 3162 (m), 3113 (m), 3085 (m), 1703 (s), 1643 (w), 1603 (w), 1556 (s), 1544 (s), 1531 (s), 1414 (w), 1349 (s), 1282 (w), 1235 (s), 1188 (w), 1168 (m), 1121 (m), 1095 (w), 1072 (m), 1026 (s), 934 (w), 926 (w), 912 (w), 892 (m), 826 (w), 749 (m), 731 (m), 719 (s), 637 (s), 564 (m), 547 (s), 526 (m), 483 (m), 451 (m), 441 (s). Raman: $\tilde{\nu}$ = 3084 (w), 1602 (m), 1567 (m), 1547 (m), 1377 (m), 1351 (s), 1187 (w), 1075 (m), 1030 (w), 893 (m), 826 (m), 529 (w), 454 (w), 442 (m), 352 (m), 318 (w), 276 (w), 238 (w), 207 (s), 172 (s). HRMS (ESI): calculated for $\text{C}_2\text{H}_6\text{FN}_2\text{O}^+$. Expected: 93.0459. Observed: 93.04589 (-0.1 ppm). Elemental analysis for $\text{C}_8\text{H}_8\text{FN}_5\text{O}_{10}\text{S}$. Expected: C, 24.94; H, 2.09; N, 18.18; S, 8.32. Observed: C, 24.94; H, 2.38; N, 18.34; S, 8.03.

Impurity detection: Ammonium-2,4,6-trinitrobenzenesulfonate (6a)

The decanted solution from **5a** was slowly removed from the solvent at reduced pressure, to give 3.5 mg of colorless crystals. Yield: 3 %. T_{dec} : 254.8 °C. $^1\text{H NMR}$ (CD_3CN): δ = 5.96 (t, J = 50.2 Hz, 4H), 8.54 (s, 2H) ppm. $^{13}\text{C NMR}$ (CD_3CN): δ = 121.8 ppm. $^{14}\text{N NMR}$ (CD_3CN): δ = -360.1 (s, 1N), -22.4 (s, 1N), -15.2 (s, 2N) ppm. IR (ATR): $\tilde{\nu}$ = 3462 (w), 3208 (s), 3072 (s), 2895 (w), 1842 (w), 1658 (w), 1600 (w), 1532 (s), 1415 (s), 1350 (s), 1249 (s), 1227 (s), 1120 (s), 1072 (s), 1032 (s), 983 (m), 936 (m), 918 (s), 827 (w), 749 (s), 733 (s), 714 (s), 663 (m), 633 (s), 559 (s), 520 (m), 479 (m), 454 (s), 435 (m). Raman: $\tilde{\nu}$ = 3078 (w), 1602 (m), 1558 (m), 1544 (m), 1371 (s), 1353 (s), 1078 (s), 827 (s), 770 (s), 561 (w), 523 (w), 455 (w), 436 (m), 356 (m), 321 (w), 275 (w), 240 (w), 215 (w), 177 (m), 128 (m). HRMS (ESI): calculated for $\text{C}_6\text{H}_{10}\text{N}_5\text{O}_9\text{S}^+$. Expected: 328.0194 Observed: 328.01902 (-1.1 ppm).

Dimethylacetamidinium fluoromethyl-2,4,6-trinitrobenzene sulfonat (5b)

The reagent **4** (126 mg, 387 μmol) was solved in acetonitrile (1.0 mL) and was added dropwise to a solution of dimethylacetamide (33.7 mg, 387 μmol) within acetonitrile (5 mL). The yellowish solution was stirred for 18 h at room temperature. After the solvent was removed in vacuum, the crude product was recrystallized in a dichloromethane/ acetonitrile mixture (10 mL/ 0.3 mL). The Mixture was centrifuged and the solvent decanted off. The remaining solid was dried in high vacuum to give 143 mg of a white solid. Yield: 78 %. $T_{\text{mp.}}$: 175 °C. T_{dec} : 185 °C. $^1\text{H NMR}$ (CD_3CN): δ = 2.55 (s, 3H), 3.30 (s, 3H), 3.39 (s, 3H), 5.95 (d, J = 49.7 Hz, 2H), 8.53 (s, 2H) ppm. $^{13}\text{C NMR}$ (CD_3CN): δ = 16.1, 40.8, 42.8, 100.8 (d, J = 231.3 Hz), 121.7, 139.4, 148.9, 150.6, 175.9 ppm. $^{19}\text{F NMR}$ (CD_3CN): δ = -154.7 (s) ppm. $^{19}\text{F NMR}$ (CD_3CN): δ = -154.7 (t, J = 49.7 Hz) ppm. $^{14}\text{N NMR}$ (CD_3CN): δ = -232.9 (s, 1N), -22.4 (s, 1N), -15.2 (s, 2N) ppm. IR (ATR): $\tilde{\nu}$ = 3090 (m), 1686 (m), 1606 (m), 1535 (s), 1448 (w), 1395 (w), 1352 (s), 1263 (s), 1247 (s), 1190 (m), 1151 (w), 1122 (m), 1068 (m), 1050 (m), 1035 (s), 1005 (s), 936 (w), 917 (w), 902 (m), 826 (w), 766 (w), 749 (s), 733 (s), 718 (s), 631 (s), 586 (m), 559 (s), 528 (w), 513 (w), 482 (m), 455 (m), 440 (s). Raman: $\tilde{\nu}$ = 3097 (m), 3029 (w), 2962 (m), 1601 (w), 1558 (m), 1544 (m), 1381 (m), 1353 (s), 1265 (w), 1188 (w), 1070 (m), 827 (m), 725 (w), 352 (w), 322 (m), 234 (w), 212 (w), 173 (m), 116 (m). HRMS (ESI): calculated for $\text{C}_5\text{H}_{11}\text{FNO}^+$. Expected: 120.0819 Observed: 120.08199 (0.7 ppm). Elemental analysis for $\text{C}_{11}\text{H}_{13}\text{FN}_4\text{O}_{10}\text{S}$. Expected: C, 32.04; H, 3.18 N, 13.59; S, 7.78 Observed: C, 31.83; H, 3.03 N, 13.40; S, 7.71.

Dimethylformamidinium fluoromethyl-2,4,6-trinitrobenzene sulfonat (5c)

The reagent **4** (358 mg, 1.10 mmol) was solved in dichloromethane (5 mL) and dimethylformamide (80.5 mg, 1.10 mmol) were added subsequently. The yellowish solution was stirred for 24 h at room temperature. After the precipitate was centrifuged, the solvent was decanted off and the crude product was washed with dichloromethane (3×5 mL). The remaining solid was dried in high vacuum to give 359 mg of a white solid. Yield: 82 %. $T_{\text{mp.}}$: 150 °C. $^1\text{H NMR}$ (CD_3CN): δ = 3.26 (s, 3H), 3.41 (s, 3H), 5.96 (d, J = 49.2 Hz, 2H), 8.54 (s, 2H), 8.58 (hep, J = 0.9 Hz, 1H) ppm. $^{13}\text{C NMR}$ (CD_3CN): δ = 38.1, 43.1,

104.6 (d, $J = 234.6$ Hz), 121.9, 138.9, 148.9, 150.8, 166.5 ppm. ^{19}F NMR (CD_3CN): $\delta = -153.1$ (s) ppm. ^{19}F NMR (CD_3CN): $\delta = -153.1$ (t, $J = 49.2$ Hz) ppm. ^{14}N NMR (CD_3CN): -230.9 (s, 1N), -22.7 (s, 1N), -14.9 (s, 2N) ppm. IR (ATR): $\tilde{\nu} = 3095$ (m), 3041 (w), 2997 (m), 2904 (w), 1723 (m), 1607 (m), 1542 (s), 1443 (w), 1403 (w), 1353 (s), 1314 (m), 1269 (s), 1236 (s), 1187 (w), 1164 (w), 1120 (m), 1056 (m), 1035 (m), 1004 (m), 991 (s), 937 (w), 924 (w), 912 (w), 902 (w), 844 (m), 825 (w), 749 (s), 732 (m), 718 (s), 632 (s). Raman: $\tilde{\nu} = 3095$ (w), 3039 (w), 3025 (w), 3972 (m), 1722 (w), 1602 (m), 1554 (w), 1431 (w), 1381 (m), 1358 (s), 1071 (m), 827 (m), 349 (w), 319 (w), 268 (m), 231 (m), 168 (w), 151 (m). Elemental analysis for $\text{C}_{10}\text{H}_{11}\text{FN}_4\text{O}_{10}\text{S}$. Expected: C, 30.16; H, 2.78; N, 14.07; S, 8.05 Observed: C, 30.01; H, 2.93 N, 14.23; S, 7.82.

Impurity detection: Dimethylammonium-2,4,6-trinitrobenzenesulfonate (6b)

The decanted solution from **5b** or **5c** was slowly removed from the solvent (seperately) at reduced pressure, to give 2 mg and 13 mg of colorless crystals. Yield: 3 %. T_{dec} : 189 °C. ^1H NMR (CD_3CN): $\delta = 2.65$ (t, $J = 5.7$ Hz, 6H), 6.62 (t, $J = 50.7$ Hz, 2H), 8.57 (s, 2H) ppm. ^{13}C NMR (CD_3CN): $\delta = 36.1$, 121.9, 138.6, 149.1, 150.8 ppm. ^{14}N NMR (CD_3CN): $\delta = -358.9$ (s, 1N), -22.9 (s, 1N), -15.5 (s, 2N) ppm. IR (ATR): $\tilde{\nu} = 3159$ (m), 3099 (m), 1665 (w), 1607 (m), 1541 (s), 1467 (m), 1354 (s), 1275 (m), 1223 (s), 1153 (m), 1122 (m), 1071 (m), 1034 (m), 984 (w), 926 (w), 911 (m), 901 (m), 883 (w), 823 (w), 749 (s), 732 (m), 719 (s). Raman: $\tilde{\nu} = 3097$ (w), 3051 (w), 2980 (m), 1604 (m), 1549 (m), 1533 (w), 1469 (w), 1370 (s), 1355 (s), 1189 (w), 1074 (s), 883 (w), 824 (m), 450 (w), 354 (m), 322 (m), 271 (m), 234 (s), 181 (s). HRMS (ESI): calculated for $\text{C}_{10}\text{H}_{18}\text{N}_5\text{O}_9\text{S}^+$. Expected: 384.0820 Observed: 384.08194 (-0.1 ppm).

Impurity detection: Dimethylammonium- d_2 -2,4,6-trinitrobenzene sulfonate

The decomposition of dimethylacetamidiniumfluoromethyl-2,4,6-trinitrobenzenesulfonat was tracked by ^1H -NMR spectroscopy. Dimethylacetamidiniumfluoromethyl-2,4,6-trinitrobenzenesulfonat (5 mg, 0.01 mmol) placed in an NMR tube under argon was dissolved in deuteriumoxide (0.6 mL) and an ^1H -NMR was measured after 5 min. ^1H NMR (D_2O): $\delta = 2.74$ (p, $J = 0.7$ Hz, 6H), 8.93 (s, 2H) ppm.

Dimethyl-2,4,6-trinitroaniline

Dimethylamine (500 mg, 11.1 mmol) was solved in acetonitrile (10 mL) and a solution of **4** (3.61 g, 11.1 mmol) solved in acetonitrile (10 mL) were added subsequently under virgously stirring. The deep red solution was stirred for 30 min at roomtemperature and the solid was filtrated off. The solvent of the filtrate solwly removed in vacuum to obtain 2.10 g of yellowish crystals. Yield: 73 %. T_{mp} : 138 °C. T_{dec} : 250 °C. ^1H NMR (CD_3CN): $\delta = 2.90$ (s, 6H), 8.69 (s, 2H). ppm. ^{13}C NMR (CD_3CN): $\delta = 43.1$, 126.8, 137.4, 142.9, 144.1 ppm. ^{14}N NMR (CD_3CN): $\delta = -20.1$ (s, 1N), -14.2 (s, 2N) ppm. IR (ATR): $\tilde{\nu} = 3062$ (m), 2956 (w), 2924 (w), 2875 (w), 2819 (w), 1857 (w), 1603 (m), 1575 (s), 1530 (s), 1505 (s), 1473 (s), 1456 (s), 1428 (m), 1411 (m), 1376 (m), 1359 (m), 1325 (m), 1302 (s), 1235 (s), 1179 (m), 1170 (m), 1131 (w), 1086 (m), 1063 (m), 953 (m), 930 (s), 821 (m), 760 (m), 748

(s), 732 (s), 708 (m), 662 (w), 624 (w), 545 (m), 517 (m), 430 (w). Raman: $\tilde{\nu}$ = 2956 (w), 1607 (w), 1542 (w), 1476 (w), 1447 (w), 1422 (w), 1343 (m), 1328 (s), 1180 (w), 1088 (w), 934 (w), 823 (w), 761 (w), 667 (w), 331 (w), 195 (w). HRMS (DEI): calculated for C₈H₈N₄O₆. Expected: 256.0444 Observed: 256.0444 (0 ppm). Elemental analysis for C₈H₈N₄O₆. Expected: C, 37.51; H, 3.15; N, 21.87 Observed: C, 37.41; H, 3.26; N, 21.89.

Fluoromethyl triphenylphosphansulfonium-2,4,6-trinitrobenzene sulfonate (7b)

The reagent **4** (54.0 mg, 166 μ mol) was dissolved in dichloromethane (2 mL) and triphenylphosphinesulfide (49.0 mg, 166 μ mol) was added in one portion. The mixture was reacted for 5 days at 40 °C under exclusion of light. The solvent was removed in high vacuum and solved in dichloromethane (0.5 mL) again. Diethylether (5 mL) was added dropwise under vigorously stirring over a period of 15 min. The precipitate was centrifuged and the solvent decanted. This procedure was repeated three times to obtain 80 mg of white product. Yield: 78 %. T_{dec}: 164 °C. ¹H NMR (CD₃CN): δ = 5.72 (dd, J = 49.0 Hz, J = 20.3 Hz, 2H), 7.75-7.81 (m, 8H), 7.83-7.87 (m, 4H), 7.92-7.97 (m, 3H), 8.52 (s, 2H) ppm. ¹³C NMR (CD₃CN): δ = 84.5 (dd, J = 228.3 Hz, J = 5.1 Hz), 118.9 (dd, J = 85.1 Hz, J = 0.8 Hz), 121.6, 131.6 (d, J = 13.9 Hz), 135.2 (dd, J = 11.6 Hz, J = 0.8 Hz), 137.3 (d, J = 3.3 Hz), 137.8, 148.7, 150.9 ppm. ¹⁹F NMR (CD₃CN): δ = -186.5 (d, J = 4.6 Hz) ppm. ¹⁹F NMR (CD₃CN): δ = -186.5 (td, J = 49.0 Hz, J = 4.6 Hz) ppm. ³¹P NMR (CD₃CN): δ = 46.9 (d, J = 4.5 Hz) ppm. ³¹P NMR (CD₃CN): δ = 46.9 (m) ppm. IR (ATR): $\tilde{\nu}$ = 3109 (w), 3056 (w), 3015 (w), 2951 (w), 1607 (w), 1539 (s), 1485 (w), 1439 (m), 1398 (w), 1353 (m), 1244 (m), 1188 (w), 1107 (m), 1068 (m), 1024 (m), 996 (m), 926 (w), 899 (w), 825 (w), 747 (m), 721 (m), 686 (s), 630 (m), 569 (m), 507 (s), 449 (w). Elemental analysis for C₂₅H₁₉FN₃O₉PS₂. Expected: C, 48.47; H, 3.09; N, 6.78; S, 10.35 Observed: C, 47.17; H, 3.29; N, 6.54; S, 10.33 (EA interference with P, phosphorus carbide formation!)

Fluoromethyl triphenylphosphanselenium-2,4,6-trinitrobenzene sulfonate (7c)

The reagent **4** (125 mg, 0.384 mmol) and triphenylphosphineselenide (131 mg, 0.384 mmol) were solved in degassed dichloromethane (5 mL) and reacted for one day at 50 °C. The solvent was slowly removed in vacuum, until a precipitate was formed. The remaining solvent was decanted off and the solid dried in high vacuum. The crude brownish product was three times slurried with diethylether (4 mL), centrifuged and decanted off until 169 mg of a beige solid was formed. Yield: 66 %. T_{dec}: 147 °C. ¹H NMR (CD₃CN): δ = 5.94 (dd, J = 48.7 Hz, J = 17.1 Hz, 2H, ⁷⁷Se-sats: ²J_{H,Se}=20.4 Hz; CH₂F), 7.65-7.83 (m, 12H), 7.86-7.95 (m, 3H), 8.52 (s, 2H) ppm. ¹³C NMR (CD₃CN): δ = 83.2 (dd, J = 228.3 Hz, J = 5.5 Hz), 119.3 (dd, J = 87.7 Hz, J = 1.0 Hz), 121.7, 131.6 (d, J = 13.8 Hz), 135.4 (dd, J = 11.7 Hz, J = 0.8 Hz), 136.9 (d, J = 3.3 Hz), 148.8, 150.8 ppm. ¹⁹F NMR (CD₃CN): δ = -190.2 (d, J = 4.6 Hz, ⁷⁷Se-sats: ²J_{F,Se}=100.9 Hz; CH₂F) ppm. ¹⁹F NMR (CD₃CN): δ = -190.2 (td, J = 48.7 Hz, J = 4.6 Hz, ⁷⁷Se-sats: ²J_{F,Se}=100.9 Hz; CH₂F) ppm. ³¹P NMR (CD₃CN): δ = 37.9 (d, J = 4.5 Hz, ⁷⁷Se-sats: ¹J_{P,Se}=426.6 Hz) ppm. ³¹P NMR (CD₃CN): δ = 37.9 (m, ⁷⁷Se-sats: ¹J_{P,Se}=426.6 Hz) ppm. ⁷⁷Se NMR (CD₃CN): δ = 293.5 (dd, J = 100.9 Hz, J = 426.6 Hz) ppm. IR (ATR): $\tilde{\nu}$ = 3104 (w), 1604 (w), 1539 (w), 1439 (w), 1399 (w), 1399 (w), 1341

(w), 1241 (w), 1104 (w), 1068 (w), 1033 (w), 829 (w), 899 (w), 824 (w), 747 (w), 719 (w), 688 (w), 630 (w), 535 (w), 502 (w), 445 (w). Raman: $\tilde{\nu}$ = 3059 (w), 1599 (w), 1548 (w), 1353 (m), 1185 (w), 1094 (w), 1068 (w), 1027 (w), 999 (w), 935 (w), 826 (w). Due to the high oxidation and hydrolysis sensitivity no HRMS and EA could be measured.

4-(4-(dimethylamino) benzoyl) -N-(fluoromethyl) - N,N – dimethyl benzen aminium - 2,4,6-trinitrobenzene sulfonate (8)

Michler's ketone was recrystallized (2 ×) in dichloromethane and purified by column chromatography (2 ×) before use. The reagent 4 (105 mg, 0.323 mmol) was dissolved in a mixture of acetonitrile/dichloromethane (1:1, 5 mL) and the purified ketone (87.0 mg, 0.323 mmol), dissolved in a mixture of acetonitrile/ dichloromethane (1:1, 5 mL), was added in one portion. The mixture was heated to reflux under exclusion of light for 16 h. A third of the solvent was removed in high vacuum, until a green solid precipitated. The precipitate was filtered off and washed with chloroform (3 × 5 mL). The product was dried in high vacuum until 145 mg of a green solid was formed. Yield: 76 %. T_{dec}: 218 °C. ¹H NMR (CD₃CN): δ = 3.08 (s, 6H), 3.65 (d, J = 2.1 Hz, 6H), 5.65 (d, J = 44.8 Hz, 2H), 6.82 (A-part of AA'XX', N = 9.0 Hz, 2H), 7.71 (X-part of AA'XX', N = 9.0 Hz, 2H, Ar-H), 7.87 (s, 4H), 8.52 (s, 2H) ppm. ¹³C NMR (CD₃CN): δ = 40.4, 51.9 (d, J = 1.7 Hz), 99.8 (d, J = 225.9 Hz), 111.9, 122.1, 122.3 (d, J = 1.4 Hz), 123.8 (d, J = 0.9 Hz), 131.8, 133.7, 138.2, 142.8, 144.5, 149.1, 150.7, 155.2, 194.1 ppm. ¹⁹F NMR (CD₃CN): δ = -188.3 (s) ppm. ¹⁹F NMR (CD₃CN): δ = -188.3 (t, J = 44.8 Hz) ppm. ¹H, ¹⁵N-HMBC: ¹⁵N NMR (CD₃CN): δ = -323.6 (s, 1N), -311.8 (s, 1N), -22.3 (s, 2N), -15.1 (s, 1N) ppm. IR (ATR): $\tilde{\nu}$ = 3135 (w), 1643 (w), 1596 (s), 1550 (s), 1503 (s), 1475 (w), 1445 (w), 1351 (s), 1327 (s), 1290 (m), 1246 (s), 1192 (m), 1152 (m), 1117 (m), 1091 (m), 1067 (m), 1032 (m), 1001 (m), 978 (w), 930 (m), 907 (m), 849-813 (m), 769 (s), 748 (s), 721 (s), 688 (m), 631 (m), 593 (s), 559 (s), 513 (m). Raman: $\tilde{\nu}$ = 3086 (w), 1641 (m), 1589 (s), 1555 (w), 1544 (w), 1371 (m), 1351 (m), 1154 (m), 1068 (m), 825 (m), 774 (w), 724 (w), 645 (w), 625 (w), 569 (w), 355 (w), 325 (w), 231 (w), 173 (w). HRMS (ESI): calculated for C₁₈H₂₂FN₂O⁺. Expected: 301.1711 Observed: 301.17089 (0.7 ppm). Elemental analysis for C₂₄H₂₄FN₅O₁₀S. Expected: C, 48.57; H, 4.08; N, 11.80; S, 5.40 Observed: C, 48.30; H, 4.36; N, 11.62; S, 5.49.

1-(fluoromethyl)-2-picolinoylpyridin-1-ium-2,4,6-trinitrobenzene sulfonate (9)

The reagent 4 (178 mg, 0.547 mmol) was dissolved in dichloromethane (12 mL) and bipyridylketone (101 mg, 0.547 mmol), dissolved in dichloromethane (3 mL) was added in one portion. The mixture was reacted for 24 h under exclusion of light at room temperature. The precipitate was filtered off, washed with a mixture of acetonitrile/ dichloromethane (10:1, 5 × 3 mL) and dried in high vacuum, to obtain 217 mg of a white product. Yield: 82 %. T_{mp}: 184 °C. T_{dec}: 202 °C. ¹H NMR (CD₃CN): δ = 6.52 (d, J = 46.0 Hz, 2H), 7.70-7.79 (m, 1H), 8.81-8.82 (m, 1H), 8.25-8.41 (m, 3H), 8.52 (s, 2H), 8.67 (m, 1H), 8.83 (t, J = 7.9 Hz, 1H), 9.10 (d, J = 6.1 Hz, 1H) ppm. ¹³C NMR (CD₃CN): δ = 94.8 (d, J = 215.0 Hz), 121.7, 125.9, 130.5, 130.7, 130.9, 139.4, 147.2, 150.1 (d, J = 1.2 Hz, 1H), 150.8, 151.6 (d, J = 0.8 Hz, 1H), 187.4 ppm. ¹⁹F NMR (CD₃CN): δ = -174.7 (s) ppm. ¹⁹F NMR (CD₃CN): δ = -174.7 (t, J = 46.8 Hz) ppm. ¹H, ¹⁵N-HMBC: ¹⁵N NMR (CD₃CN): δ = -22.4 (s, 2N), -15.2 (s, 1N) ppm. IR (ATR): $\tilde{\nu}$ = 3108 (m), 3086 (s), 1700 (s), 1622-1605 (w), 1557 (s), 1534

(s), 1480 (s), 1443 (m), 1354 (s), 1333-1289 (w), 1241 (s), 1179 (m), 1126 (m), 1095 (s), 1068 (s), 1034 (s), 995 (w), 946 (m), 834 (m), 814 (m), 785 (m), 752-702 (s), 656 (m), 633 (s), 614 (s), 559 (s), 527 (s), 479 (w), 442, 405 (w). Raman: $\tilde{\nu} = 3106$ (w), 3057 (w), 1700 (m), 1603 (m), 1584 (m), 1570 (m), 1387 (m), 1349 (s), 1197 (w), 1071 (m), 1046 (m), 995 (m), 826 (m), 350 (m), 319 (w), 266 (w), 228 (w), 170 (m), 152 (m). HRMS (DEI): calculated for $C_{12}H_{10}FN_2O^+$. Expected: 217.0772 Observed: 217.0781 (4 ppm). Elemental analysis for $C_{18}H_{12}FN_5O_{10}S$. Expected: C, 42.44; H, 2.37; N, 13.75; S, 6.29 Observed: C, 42.11; H, 2.40; N, 13.75; S, 6.16.

4.6 References

- [1] a) J. Hu, W. Zhang, F. Wang, *Chem. Commun. (Cambridge, U. K.)* **2009**, 7465–7478; b) Y. Zhou, J. Wang, Z. Gu, S. Wang, W. Zhu, J. L. Acena, V. A. Soloshonok, K. Izawa, H. Liu, *Chem. Rev. (Washington, DC, U. S.)* **2016**, *116*, 422–518.
- [2] M. Reichel, J. Martens, E. Woellner, L. Huber, A. Kornath, K. Karaghiosoff, *Eur. J. Inorg. Chem.* **2019**, *2019*, 2530–2534.
- [3] a) G. K. S. Prakash, I. Ledneczki, S. Chacko, G. A. Olah, *Org. Lett.* **2008**, *10*, 557–560; b) Y. Liu, L. Lu, Q. Shen, *Angew. Chem., Int. Ed.* **2017**, *56*, 9930–9934; c) Y. Nomura, E. Tokunaga, N. Shibata, *Angew. Chem., Int. Ed.* **2011**, *50*, 1885–1889.
- [4] a) W. Zhang, L. Zhu, J. Hu, *Tetrahedron* **2007**, *63*, 10569–10575; b) Y. Li, C. Ni, J. Liu, L. Zhang, J. Zheng, L. Zhu, J. Hu, *Org. Lett.* **2006**, *8*, 1693–1696; c) Y. Zhao, B. Gao, C. Ni, J. Hu, *Org. Lett.* **2012**, *14*, 6080–6083; d) T. W. Butcher, J. F. Hartwig, *Angew. Chem., Int. Ed.* **2018**, *57*, 13125–13129; e) T. Furukawa, Y. Goto, J. Kawazoe, E. Tokunaga, S. Nakamura, Y. Yang, H. Du, A. Kakehi, M. Shiro, N. Shibata, *Angew. Chem., Int. Ed.* **2010**, *49*, 1642–1647.
- [5] J. D. Nally, *Good Manufacturing Practices for Pharmaceuticals*, CRC Press, **2016**.
- [6] G. Li, Z. Xue, B. Cao, C. Yan, T. Mu, *ACS Sustainable Chem. Eng.* **2016**, *4*, 6258–6262.
- [7] A. Kutt, T. Rodima, J. Saame, E. Raamat, V. Maemets, I. Kaljurand, I. A. Koppel, R. Y. Garlyauskayte, Y. L. Yagupolskii, L. M. Yagupolskii, E. Bernhardt, H. Willner, I. Leito, *J. Org. Chem.* **2011**, *76*, 391–395.
- [8] D. J. Pettitt, G. K. Helmkamp, *J. Org. Chem.* **1964**, *29*, 2702–2706.
- [9] G. K. S. Prakash, C. Weber, S. Chacko, G. A. Olah, *Org. Lett.* **2007**, *9*, 1863–1866.
- [10] Z. Wang, *Comprehensive Organic Name Reactions and Reagents, Vol. 3*, John Wiley & Sons, New Jersey, **2009**.
- [11] J. Meisenheimer, *LIEBIG'S Ann.* **1902**, *323*, 205–246.
- [12] a) R. G. Salomon, S. R. Raychaudhuri, *J. Org. Chem.* **1984**, *49*, 3659–3660; b) W. Kantlehner, H. D. Gutbrod, *Liebigs Ann. Chem.* **1980**, 1677–1688.
- [13] H. Emde, A. Goetz, K. Hofmann, G. Simchen, *Liebigs Ann. Chem.* **1981**, 1643–1657.

4.7 Supporting Information

Table 1: Structure refinement parameter of compound **2** (left) and compound **3** (right).

Empirical formula	C ₂₀ H ₁₇ F ₄ O ₃ P S ₂	C ₆ H ₆ Ag N ₃ O ₁₁ S
Formula weight	476.42	436.07
Temperature	173(2) K	143(2) K
Wavelength	0.71073 Å	0.71073 Å
Crystal system	Monoclinic	Triclinic
Space group	<i>P</i> 2 ₁ / <i>n</i>	<i>P</i> -1
Unit cell dimensions	a = 10.9375(8) Å b = 8.3451(6) Å c = 23.7088(15) Å α = 90° β = 103.211(7)° γ = 90°	a = 8.0870(7) Å b = 8.1600(6) Å c = 10.4590(7) Å α = 75.109(6)° β = 75.218(7)° γ = 67.201(7)°
Volume	2106.7(3) Å ³	605.45(8) Å ³
Z	4	2
Density (calculated)	1.502 mg/m ³	2.392 mg/m ³
Absorption coefficient	0.383 mm ⁻¹	1.910 mm ⁻¹
F(000)	976	428
Crystal size	0.150 x 0.150 x 0.100 mm ³	0.25 x 0.15 x 0.04 mm ³
Theta range for data collection	4.294 - 30.508°	4.27 - 25.34°
Index ranges	-15 ≤ h ≤ 15, -11 ≤ k ≤ 11, -31 ≤ l ≤ 33	-7 ≤ h ≤ 9, -9 ≤ k ≤ 9, -12 ≤ l ≤ 12
Reflections collected	21508	4272
Independent reflections	6397 [R _{int} = 0.0505]	2200 [R _{int} = 0.0225]
Data / restraints / parameters	6397 / 0 / 281	2200 / 6 / 215
Goodness-of-fit on F ²	1.015	1.063
Final R indices [I > 2σ(I)]	R ₁ = 0.0447, wR ₂ = 0.0917	R ₁ = 0.0281, wR ₂ = 0.0566
R indices (all data)	R ₁ = 0.0781, wR ₂ = 0.1051	R ₁ = 0.0321, wR ₂ = 0.0596
Largest diff. peak and hole	0.439 and -0.344 e Å ⁻³	1.348 and -0.877 e Å ⁻³

Table 2: Structure refinement parameter of compound **4** (left) and dimethyltrinitroaniline (right).

Empirical formula	C ₇ H ₄ F N ₃ O ₉ S	C ₈ H ₈ N ₄ O ₆
Formula weight	325.19	256.18
Temperature	143(2) K	143(2) K
Wavelength	0.71073 Å	0.71073 Å
Crystal system	Orthorhombic	Monoclinic
Space group	<i>P</i> ca2 ₁	<i>P</i> 2 ₁ / <i>c</i>
Unit cell dimensions	a = 10.4441(3) Å b = 7.0497(2) Å c = 31.5597(10) Å α = 90° β = 90° γ = 90°	a = 8.5350(4) Å b = 16.4220(5) Å c = 8.3440(4) Å α = 90° β = 118.618(7)° γ = 90°
Volume	2323.67(12) Å ³	1026.63(10) Å ³

Z	8	4
Density (calculated)	1.859 mg/m ³	1.657 mg/m ³
Absorption coefficient	0.350 mm ⁻¹	0.144 mm ⁻¹
F(000)	1312	528
Crystal size	0.150 x 0.050 x 0.050 mm ³	0.5 x 0.4 x 0.3 mm ³
Theta range for data collection	4.340 - 30.507°	4.61 - 25.35°
Index ranges	-14 ≤ h ≤ 14, -10 ≤ k ≤ 9, -45 ≤ l ≤ 44	-10 ≤ h ≤ 10, -19 ≤ k ≤ 17, -10 ≤ l ≤ 10
Reflections collected	23116	7232
Independent reflections	6869 [R _{int} = 0.0406]	1863 [R _{int} = 0.0152]
Data / restraints / parameters	6869 / 1 / 412	1863 / 0 / 165
Goodness-of-fit on F2	1.050	1.042
Final R indices [I > 2σ(I)]	R ₁ = 0.0394, wR ₂ = 0.0862	R ₁ = 0.0276, wR ₂ = 0.0727
R indices (all data)	R ₁ = 0.0505, wR ₂ = 0.0938	R ₁ = 0.0299, wR ₂ = 0.0745
Largest diff. peak and hole	0.587 and -0.407 e Å ⁻³	0.216 and -0.226 e Å ⁻³

Table 3: Structure refinement parameter of compound **5a** (left) and compound **6a** (right).

Empirical formula	C ₈ H ₈ F N ₅ O ₁₀ S	C ₆ H ₆ N ₄ O ₉ S
Formula weight	385.25	310.21
Temperature	143(2) K	143(2) K
Wavelength	0.71073 Å	0.71073 Å
Crystal system	Monoclinic	Orthorhombic
Space group	<i>P</i> 2 ₁ / <i>n</i>	<i>P</i> bca
Unit cell dimensions	a = 7.3512(2) Å b = 9.4110(2) Å c = 20.6030(5) Å α = 90° β = 98.760(2)° γ = 90°	a = 8.4167(3) Å b = 9.3286(4) Å c = 28.5429(13) Å α = 90° β = 90° γ = 90°
Volume	1408.73(6) Å ³	2241.08(16) Å ³
Z	4	8
Density (calculated)	1.816 mg/m ³	1.839 mg/m ³
Absorption coefficient	0.313 mm ⁻¹	0.348 mm ⁻¹
F(000)	784	1264
Crystal size	0.100 x 0.050 x 0.050 mm ³	0.100 x 0.100 x 0.050 mm ³
Theta range for data collection	4.275 - 30.506°	4.284 - 28.280°
Index ranges	-10 ≤ h ≤ 10, -13 ≤ k ≤ 13, -29 ≤ l ≤ 29	-11 ≤ h ≤ 6, -12 ≤ k ≤ 11, -37 ≤ l ≤ 38
Reflections collected	27991	19358
Independent reflections	4285 [R _{int} = 0.0378]	2775 [R _{int} = 0.0609]
Data / restraints / parameters	4285 / 0 / 258	2775 / 0 / 205
Goodness-of-fit on F2	1.059	1.058
Final R indices [I > 2σ(I)]	R ₁ = 0.0332, wR ₂ = 0.0794	R ₁ = 0.0395, wR ₂ = 0.0843
R indices (all data)	R ₁ = 0.0432, wR ₂ = 0.0864	R ₁ = 0.0579, wR ₂ = 0.0939
Largest diff. peak and hole	0.371 and -0.404 e Å ⁻³	0.408 and -0.411 e Å ⁻³

Table 4: Structure refinement parameter of compound **6a** · H₂O (left) and compound **5b** (right).

Empirical formula	C ₆ H ₈ N ₄ O ₁₀ S	C ₁₁ H ₁₃ F N ₄ O ₁₀ S
Formula weight	328.22	412.31
Temperature	143(2) K	143(2) K
Wavelength	0.71073 Å	0.71073 Å
Crystal system	Triclinic	Monoclinic
Space group	<i>P</i> -1	<i>P</i> 2 ₁ / <i>n</i>
Unit cell dimensions	a = 7.8975(10) Å b = 8.2772(8) Å c = 10.1691(9) Å α = 73.685(8)° β = 80.191(9)° γ = 66.637(10)°	a = 8.5159(3) Å b = 23.1510(7) Å c = 8.7624(4) Å α = 90° β = 109.508(5)° γ = 90°
Volume	584.36(12) Å ³	1628.35(12) Å ³
Z	2	4
Density (calculated)	1.865 mg/m ³	1.682 mg/m ³
Absorption coefficient	0.345 mm ⁻¹	0.272 mm ⁻¹
F(000)	336	848
Crystal size	0.125 x 0.100 x 0.100 mm ³	0.150 x 0.050 x 0.050 mm ³
Theta range for data collection	4.186 - 30.504°	4.182 - 28.282°
Index ranges	-10 ≤ h ≤ 11, -11 ≤ k ≤ 11, -14 ≤ l ≤ 14	-11 ≤ h ≤ 11, -30 ≤ k ≤ 29, -11 ≤ l ≤ 11
Reflections collected	6040	14914
Independent reflections	3547 [R _{int} = 0.0370]	4023 [R _{int} = 0.0381]
Data / restraints / parameters	3547 / 0 / 222	4023 / 0 / 255
Goodness-of-fit on F ²	1.048	1.026
Final R indices [I > 2σ(I)]	R ₁ = 0.0459, wR ₂ = 0.0971	R ₁ = 0.0377, wR ₂ = 0.0863
R indices (all data)	R ₁ = 0.0633, wR ₂ = 0.1132	R ₁ = 0.0552, wR ₂ = 0.0960
Largest diff. peak and hole	0.479 and -0.599 e Å ⁻³	0.352 and -0.328 e Å ⁻³

Table 5: Structure refinement parameter of compound **5c** (left) and compound **6b** (right).

Empirical formula	C ₁₀ H ₁₁ F N ₄ O ₁₀ S	C ₈ H ₁₀ N ₄ O ₉ S
Formula weight	398.29	338.26
Temperature	143(2) K	143(2) K
Wavelength	0.71073 Å	0.71073 Å
Crystal system	Monoclinic	Monoclinic
Space group	<i>C</i> 2/ <i>c</i>	<i>P</i> 2 ₁ / <i>c</i>
Unit cell dimensions	a = 24.606(3) Å b = 8.2530(5) Å c = 16.5340(14) Å α = 90° β = 111.874(10)° γ = 90°	a = 11.0820(5) Å b = 13.3770(5) Å c = 9.1000(4) Å α = 90° β = 95.478(4)° γ = 90°
Volume	3115.9(5) Å ³	1342.86(10) Å ³
Z	8	4
Density (calculated)	1.698 mg/m ³	1.673 mg/m ³

Absorption coefficient	0.285 mm ⁻¹	0.298 mm ⁻¹
F(000)	1632	696
Crystal size	0.183 x 0.118 x 0.079 mm ³	0.25 x 0.15 x 0.1 mm ³
Theta range for data collection	4.20 - 25.35°	4.31 - 26.37°
Index ranges	-26 ≤ h ≤ 29, -9 ≤ k ≤ 9, -19 ≤ l ≤ 19	-13 ≤ h ≤ 13, -16 ≤ k ≤ 16, -9 ≤ l ≤ 11
Reflections collected	10780	10273
Independent reflections	2832 [R _{int} = 0.0658]	2731 [R _{int} = 0.0602]
Data / restraints / parameters	2832 / 0 / 244	2731 / 0 / 211
Goodness-of-fit on F ²	1.055	1.022
Final R indices [I > 2σ(I)]	R ₁ = 0.0440, wR ₂ = 0.0844	R ₁ = 0.0421, wR ₂ = 0.0793
R indices (all data)	R ₁ = 0.0777, wR ₂ = 0.0990	R ₁ = 0.0678, wR ₂ = 0.0906
Largest diff. peak and hole	0.260 and -0.305 e Å ⁻³	0.382 and -0.436 e Å ⁻³

Table 6: Structure refinement parameter of compound **7b** (left) and compound **9** (right).

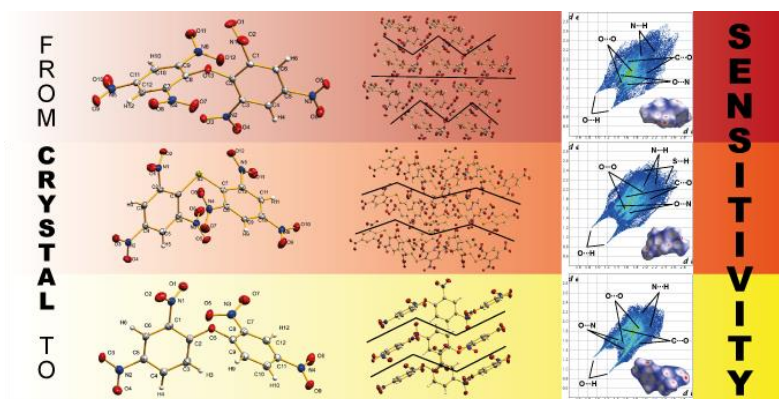
Empirical formula	C ₂₅ H ₁₉ F N ₃ O ₉ P S ₂	C ₁₈ H ₁₂ F N ₅ O ₁₀ S
Formula weight	619.52	509.39
Temperature	143(2) K	143(2) K
Wavelength	0.71073 Å	0.71073 Å
Crystal system	Monoclinic	Triclinic
Space group	<i>P</i> 2 ₁ / <i>c</i>	<i>P</i> -1
Unit cell dimensions	a = 8.1640(2) Å b = 24.0719(5) Å c = 13.6190(3) Å α = 90° β = 93.193(2)° γ = 90°	a = 5.5545(4) Å b = 10.7059(9) Å c = 18.2101(17) Å α = 81.755(7)° β = 83.317(7)° γ = 76.062(7)°
Volume	2672.29(10) Å ³	1036.35(15) Å ³
Z	4	2
Density (calculated)	1.540 mg/m ³	1.632 mg/m ³
Absorption coefficient	0.326 mm ⁻¹	0.236 mm ⁻¹
F(000)	1272	520
Crystal size	0.150 x 0.100 x 0.050 mm ³	0.100 x 0.050 x 0.050 mm ³
Theta range for data collection	3.307 - 30.508°	4.176 - 28.276°
Index ranges	-11 ≤ h ≤ 11, -34 ≤ k ≤ 28, -17 ≤ l ≤ 19	-7 ≤ h ≤ 7, -14 ≤ k ≤ 14, -24 ≤ l ≤ 24
Reflections collected	28986	9019
Independent reflections	8144 [R _{int} = 0.0549]	5135 [R _{int} = 0.0726]
Data / restraints / parameters	8144 / 0 / 370	5135 / 0 / 364
Goodness-of-fit on F ²	1.019	0.987
Final R indices [I > 2σ(I)]	R ₁ = 0.0478, wR ₂ = 0.1031	R ₁ = 0.0766, wR ₂ = 0.0934
R indices (all data)	R ₁ = 0.0787, wR ₂ = 0.1183	R ₁ = 0.1861, wR ₂ = 0.1284
Largest diff. peak and hole	0.455 and -0.427 e Å ⁻³	0.368 and -0.335 e Å ⁻³

5 The Correlation Between Structure and Energetic Properties of Three Nitroaromatic Compounds: Bis(2,4-dinitrophenyl) Ether, Bis(2,4,6-trinitrophenyl) Ether and Bis(2,4,6-trinitrophenyl) Thioether

Marco Reichel, Dominik Dosch, Thomas Klapötke, Konstantin Karaghiosoff

Published in *J. Am. Chem. Soc.* **2019**, *141*, 19911–19916.

DOI: 10.1021/jacs.9b11086



Abstract: Decades after the initial discovery of TNB ether derivatives, the first single-crystal X-ray structures for three members of this compound class could finally be shown and the analytical data could be completed. This group of molecules is an interesting example that illustrates why older predictive models for the sensitivity values of energetic materials like bond dissociation enthalpy and electrostatic potential sometimes give results that deviate significantly from the experimentally determined values. By applying newer models like Hirschfeld surface analysis and fingerprint plot analysis that utilize the crystal-structure of an energetic material, the experimentally found trend of sensitivities could be understood and the older models could be brought into a proper perspective. In the future the prediction of structure-property relationships for energetic molecules starting from a crystal structure can be achieved and should be pursued.

5.1 Introduction

About 150 years ago, Alfred Nobel recognized, that the industrialization of “new” synthetic explosives must be accompanied by their safe handling. The development of dynamite was the first step in this direction.^[1] Just a quarter of a century later, Dynamit Nobel AG focused on TNT, which replaced its predecessors due to its excellent handling safety and brisance.^[2] Although nitroaromatic compounds are no longer the centerpiece of modern explosive investigations,^[3] Alfred Nobel's fundamental aim of increased handling safety that was implemented with this group of materials continues to exist.^[4] The insensitivity to external stimuli is one of the most important requirements for the synthesis of new HEDMs, next to other characteristics such as higher environmental compatibility, high density, high thermal stability and higher detonation speed/pressure.^[3b, 5] The desired high performance of HEDMs can be achieved by using compounds with a high heat of formation, but these candidates tend

to be more sensitive towards external stimuli.^[4a] The contrary behavior of the desired parameters for HEDMs^[4a, 6] leads to the conclusion, that not only the molecular design, but also the crystallographic design has to be considered to find a balance between performance and safety for new energetic materials.^[7] A better visualization and understanding of the sensitizing properties can be achieved by combining older prediction models - such as the calculation of h_{50} values, ESP or E_{ES} values^[3b, 4a] - with newer methods like Hirschfeld surface analysis and Fingerprint plot analysis.^[8] After many years of uncertainty, a deeper insight into the energetic behavior of the title compounds Bis(2,4-dinitrophenyl) ether (**1**), Bis(2,4,6-trinitrophenyl) ether (**2**) and Bis(2,4,6-trinitrophenyl) thioether (**3**), could be gained. This was achieved by combining theoretical methods with structural investigations of the HEDMs to understand the trends that were found for the experimental sensitivity values.

5.2 Results and Discussion

5.2.1 Synthesis and Properties

All three compounds were prepared according to modified and optimized methods.^[9] Although some of these compounds have existed for almost a century and show some importance today, various fundamental analytical data such as NMR or vibrational spectroscopy are still missing.^[9a, 10] Therefore all three compounds were characterized through multinuclear NMR-, infrared-, Raman spectroscopy, elemental analysis, and single-crystal X-ray diffraction. The ¹H NMR chemical shifts of the proton in ortho position between the NO₂ groups (**1**: 8.9, **2**: 8.6; **3**: 9.1), correspond well with those of 1-substituted trinitro derivatives such as TNT (8.8 ppm) or picric acid (9.0 ppm).^[11] In the ¹³C NMR spectra, the corresponding chemical shifts are observed between 160 ppm and 120 ppm. In the ¹⁴N NMR of **1**, **2** and **3** the differently substituted NO₂ groups are not distinct, due to the signal width of 316 Hz, 280 Hz, and 520 Hz. Characteristic infrared and Raman vibration modes could be assigned according to the literature^[12] and are listed in Table 1.

Table 1: Characteristic vibration modes of **1**, **2** and **3**.

	1		2		3	
	IR	Raman	IR	Raman	IR	Raman
$\nu(\text{C-H})$	3090	3106	3103	3107	3093	3094
$\nu_{\text{as}}(\text{NO}_2)$	1530	1543	1536	1543	1530	1545
$\nu_{\text{s}}(\text{NO}_2)$	1342	1361	1339	1362	1332	1354
$\nu(\text{C-N})$	913	940	913	941	911	936
$\delta(\text{NO}_2)$	743	796	749	797	748	773

$\nu_{\text{as/s}}$ asymmetric/ symmetric vibration mode; δ : deformation vibration

The substitution of the sulfur in **3** by the more electronegative oxygen in **2** and **1** causes a shift to higher wavenumbers, which is observed for the $\nu(\text{C-N})$ vibration mode. This displacement can be regarded as a measure of the corresponding bond strength. The greater the shift to higher wavenumbers, the stronger the C-N bond. Thus, the bond strength correlates proportionally with the bond dissociation enthalpy (BDE), which – as many researchers have shown – is associated with the sensitivity of energetic materials.^[13] According to this model **3** is expected

to have the lowest BDE whereby **2** and **1** should be in a similar range. In this work, the BDEs were calculated from their crystal structure data using the B3LYP/6-311G+(d,p) method.

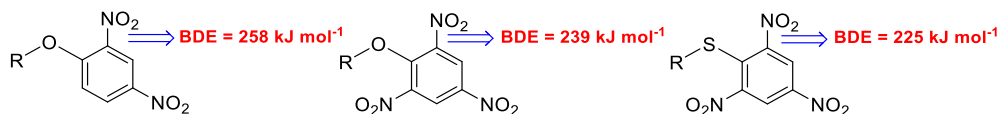


Figure 1: Calculated BDE values of the weakest bond in the molecule **1**, **2**, **3** considering all X-C bonds (X: C, O, N, S).

Since the values of the BDEs for the three compounds all range between RDX (161 kJ mol^{-1}) and TATB (355 kJ mol^{-1}), they can be categorized as sensitive.^[14] The calculated trend of decreasing BDEs from **1** to **3** is consistent with the trend of experimental observation of the shift to higher wavenumbers of the $\nu(\text{C-N})$ vibration mode. As numerous studies have shown, BDEs are considered the most important factor in pyrogenic decomposition for the possible trigger binding that breaks first and can therefore be used to assess the sensitivity of a material.^[7] Besides the calculation of h_{50} values or the determination of *volume-based sensitivities*, the electrostatic potential (ESP) is often used to understand changes of the sensitivities and to visualize the bond strength variation.^[3b]

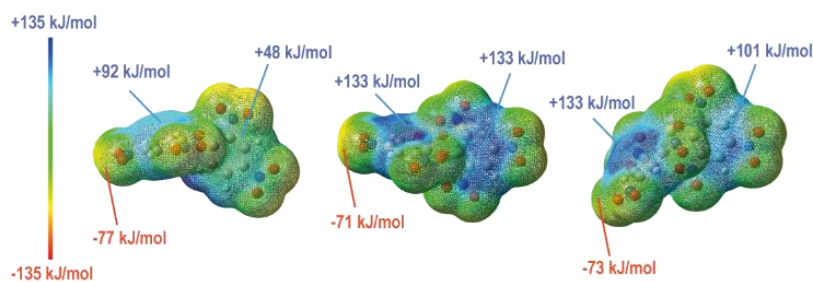


Figure 2: ESP of **1** (left), **2** (center), **3** (right), calculated on the $0.02 \text{ electron bohr}^{-3}$ hypersurface.

For all compounds, the positive range is larger than the negative range. All positive values are significantly stronger than the negative absolute values. In addition to the strongly positive center of the respective molecules, this is a general indication of their sensitive character.^[3b-d] According to the BDEs and the ESP, the sensitivity of the compounds should increase from **1** to **3**. However, a different trend is present in experimental observations ($\mathbf{1} < \mathbf{3} < \mathbf{2}$). Thus, these older prediction models are insufficient to explain the actual sensitivities values that were obtained in experiments. In order to explain this, more modern methods that use the crystal structure and packaging effects have to be applied to correctly assess the structure property relationships and therefore the sensitivities of this group of nitroaromatic compounds.

5.2.2 Structure Property Relationship

In the crystal an external mechanical stimulus like impact or friction can cause a displacement of the layers, which generates internal strains. If this strain energy is below the lowest BDE, the molecular integrity is not destroyed. If the strain energy is higher than the energy required to break the weakest bond the material is destroyed.^[8b] The strain caused by the sliding of the layers depends strongly on the stacking of the layers and other interactions in the crystal, such as hydrogen bridges.^[15]

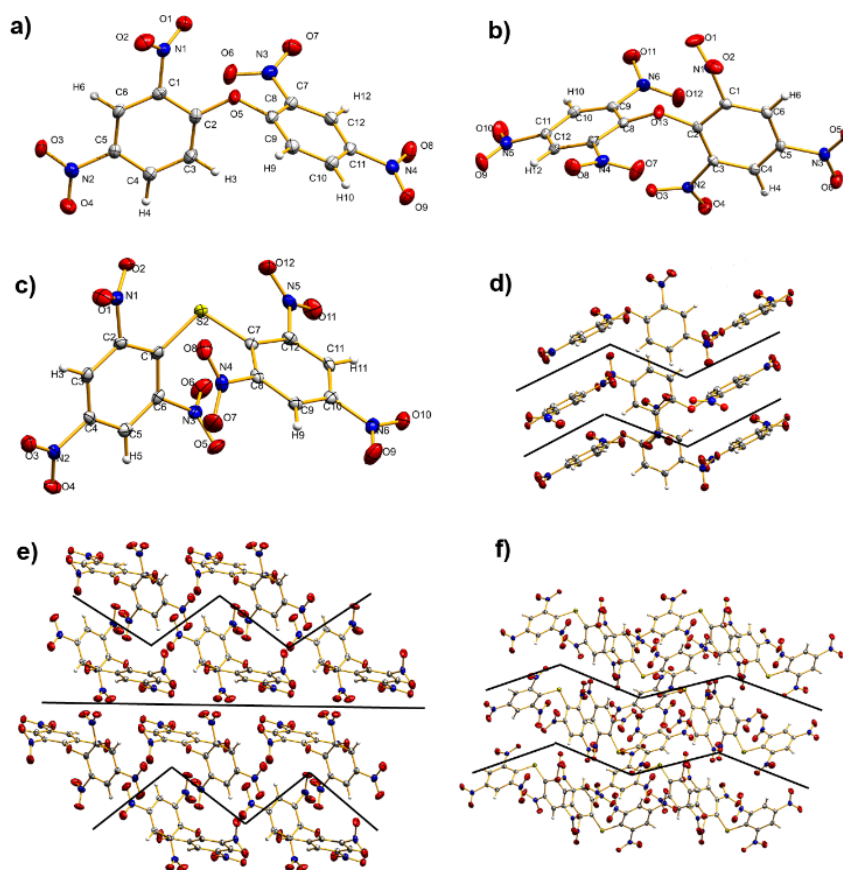


Figure 3: Single-crystal X-ray structure of **1** (a), **2** (b), **3** (c) and the crystal packing of **1** (d), **2** (e), **3** (f).

It can be seen from the monomers a, b and c, that the phenyl residues in the molecules are twisted against each other to different degrees (Figure 3). This results in a different packing behavior in the crystal (d, e, f). The strain energy resulting from a mechanical stimulus should be the greatest for **2**, since the gearing of the individual layers is the highest. The higher interlayer distance which is present in **3** facilitates an easier moving of the layers against each other. This effect can reduce the slip barrier to such an extent that it becomes smaller than the BDE.^[8b] In addition to the lower gearing of **3** versus **2**, this effect is another indication for the higher sensitivity of compound **2** when compared with compound **3**. In addition to crystal packing, intermolecular interactions contribute significantly to the height of the slide barrier and therefore to the sensitivity to external mechanical stimuli. A feature exhibited by insensitive molecules is, that the Hirschfeld surface on a plane has the most red dots representing close contacts.^[15] In the present case all compounds (**1**, **2** and **3**) have red dots which point out of a plane (Figure 4). The close contacts are not arranged in a slideable plane, which results in interlayer repulsion that can be significantly increased by shifting the plane.

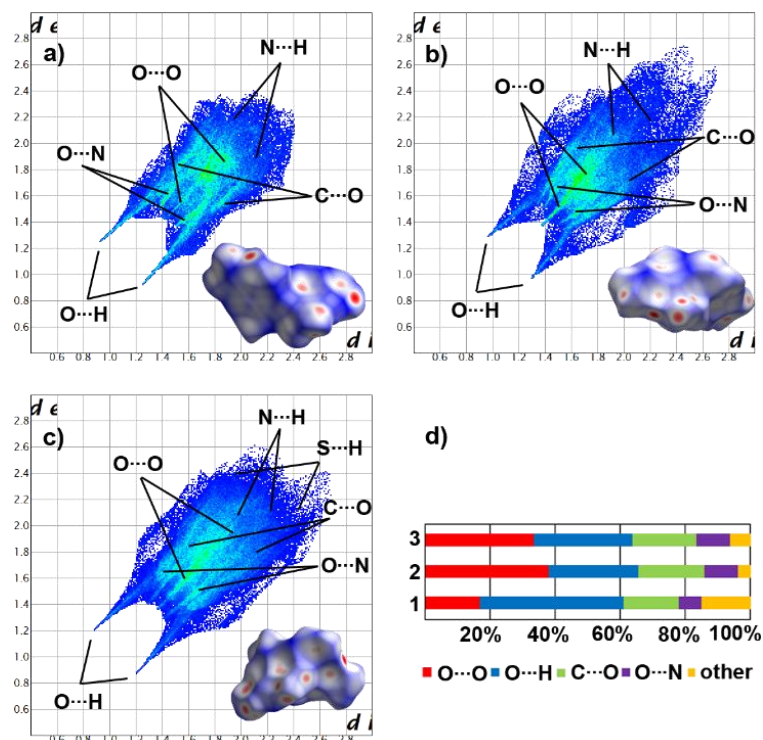


Figure 4: Two dimensional fingerprint plot in crystal stacking as well as the corresponding Hirschfeld surface (bottom right in 2D plot) of **1** (a), **2** (b) and **3** (c) (color coding: white, distance d equals VDW distance; blue, d exceeds VDW distance, red, d , smaller than VDW distance). Population of close contacts of **1**, **2**, and **3** in crystal stacking (d).

The $O \cdots O$ interaction is a very important close contact interaction. In most cases a high frequency of $O \cdots O$ contacts indicates a high sensitivity, because more nitro groups are exposed on the molecular surface and that increases the risk of explosion due to the exceeding repulsion via an interlayer sliding.^[7, 8b, 14a, 15] Thus, graph d clearly shows that **2** is the most sensitive compound. With 37.9 % of $O \cdots O$ contacts, **2** has the most of those contacts compared to **3** with 33.5 % and **1** with 16.6 %. This distribution can be retrieved from the 2D plot because the marked $O \cdots O$ interactions decrease from a via c to b in area and color intensity. Furthermore, $O \cdots H$ and $N \cdots H$ contacts, which generate an intermolecular 3D network, can make a compound more sensitive, since an interlayer slide strongly alters these stabilizing interactions. However, the replacement of hard $O \cdots O$ interactions with softer $N \cdots H$ or $O \cdots H$ interactions often leads to a better absorption of mechanical stimuli in a material.^[14a] Strong $O \cdots H$ and $N \cdots H$ interactions are often found in less sensitive compounds, because the interlayers are more rigid and can absorb energy better without a shifting of the planes, which would induce a repulsion between the layers.^[8b] The 2D fingerprint plot exhibits two distinctive spikes for strong $O \cdots H$ bonding.^[15] With respect to $d_i + d_e$ (d_i : distance from the Hirschfeld surface to the nearest atom interior; d_e : distance from the Hirschfeld surface to the nearest atom exterior) we can ascertain that for **1** with a total of 44.3 % the most and strongest hydrogen bonds are present. For **2** the 27.7 % of H-bridges are the fewest and weakest. With a total of 30.1 %, molecule **3** forms more H-bridges than compound **2** but less than molecule **1** while showing similar strong H-bridges than compound **1**. The interlayer contacts of $C \cdots O$ show weak interactions (distances above 3.5 Å) and therefore can be neglected. This also applies for the $N \cdots H$ and $N \cdots O$ contacts.^[15] According to this newer model the frequencies of $O \cdots O$ contacts and the strength and frequency of H-bridges are the most relevant indicator for the impact sensitivity of an explosive material

and therefore the order of decreasing sensitivity for the discussed compounds should be **2** > **3** > **1**.

5.2.3 Energetic Properties

Density plays an important role for the performance of energetic materials and is a direct result of the packing in the crystal. With respect to **1**, **2** and **3**, crystal densities are observed to be 1.73, 1.84 and 1.85 g cm⁻³ at 143 K and the extrapolated values at room temperature are 1.69, 1.80 and 1.81 g cm⁻³. These values deviate significantly from the older literature values 1.70 (**2**) and 1.61 g cm⁻³ (**3**).^[2] To gain accurate values for the heat of formation (HOF) it is important to use high precision theoretical methods, as experimental values are often inaccurate.^[7] Therefore, the heat of formation was computed by ab initio calculations using the optimized geometry of molecules starting from the X-ray diffraction experiment.

Table 2: Physical and calculated detonation parameter of compound **1**, **2**, **3** using EXPLO5 computer code.

	1	2	3
formula	C ₁₂ H ₆ N ₄ O ₉	C ₁₂ H ₄ N ₆ O ₁₃	C ₁₂ H ₄ N ₆ O ₁₂ S
M_r [g mol ⁻¹]	350.20	440.19	456.25
$IS^{[a]}$ [J]	>40	9	12.5
$FS^{[b]}$ [N]	>360	>360	>360
ESD [mJ]	50	50	50
N ^[c] [%]	16.00	19.09	18.42
N + O ^[d] [%]	57.12	66.34	60.50
$\Omega_{CO_2}^{[e]}$ [%]	-82.24	-47.25	-56.11
$T_{melt}^{[f]}$ [°C]	246.32	---	253
$T_{dec}^{[g]}$ [°C]	336.73	256	310
$\rho_{143K}^{[h]}$ [g cm ⁻³] (X-ray)	1.73	1.84	1.85
$\Delta H_f^{[i]}$ [kJ mol ⁻¹]	-168.1	-132.9	-20.3
EXPLO5 V 6.03			
$\Delta U_f^{[j]}$ [kJ kg ⁻¹]	-3934	-4850	-4689
$T_{C-J}^{[k]}$ [K]	2958	3695	2740
$P_{C-J}^{[l]}$ [GPa]	16.7	24.9	15.9
$V_{det}^{[m]}$ [ms ⁻¹]	6582	7634	6912
$V_o^{[n]}$ [dm ³ kg ⁻¹]	582.5	620.4	427.5
[a] Impact sensitivity ^[14d] [b] friction sensitivity ^[14e] [c] nitrogen content [d] combined nitrogen and oxygen content [e] absolute oxygen balance assuming the formation of CO or CO ₂ [f] melting point from DTA [g] decomposition from DTA [h] density determined by X-ray experiment at 100K [i] Heat of formation calculated at the CBS-4M level of theory for FMN, experimental determined for MN [j] detonation energy [k] detonation temperature [l] detonation pressure [m] detonation velocity [n] volume of detonation gases at standard temperature and pressure conditions			

According to *Trouton's Rule*, the HOF was calculated by subtracting the enthalpy of sublimation from the HOF of the corresponding gas-phase species.^[16] The values for the HOF of the gas phase species was obtained by subtraction of the atomization energies from the total enthalpy of the molecule.^[17] Calculations were performed using the CBS-4M level of theory in combination with the crystal structures. By using the specific densities and the EXPLO5 (V6.01) program, the detonation properties of **1**, **2** and **3** could be determined. They were calculated at the C-J point (*Chapman-Jouguet* point) with the help of the stationary detonation model using a modified *Becker-Kistiakowski-Wilson* state equation for the system. The C-J point was found by the Hugoniot curve of the system by its first derivative.^[18] Given a high density and heat of formation, it is not surprising that compound **2** exhibits a better performance than **1** and **3**. Although **1** has a higher heat of formation, the influence of the increased density

of **2** predominates so strongly that **2** has the best performance. As can be seen in Table 2, the oxygen balance for **1** is lowest due to the lower number of NO₂ groups. The substitution of the ether bridge in **2** by a sulfur atom deteriorates the oxygen balance from **2** to **3** as expected. With respect to the detonation velocity, the values of **2** and **3** exceed TNT (6881 m s⁻¹) were **1** falls below it.

5.3 Conclusion

Bis(2,4-dinitrophenyl) ether, bis(2,4,6-trinitrophenyl) ether, and bis(2,4,6-trinitrophenyl) thioether have been synthesized and characterized. The structures of these three compounds were determined by single-crystal X-ray diffraction. The results of the older prediction models (BDE, ESP) for the sensitivities were compared with results for newer prediction models based on the crystal structure (Hirschfeld Surface & Fingerprint Plot analysis). The inaccurate trend for the sensitivities that was observed for the older models (**3** > **2** > **1**) could be corrected. The trend for the sensitivities shown by the experimental values (decreasing **2** > **3** > **1**), could be verified by the newer predictive methods which are based on the crystal structure. The application of this newer methods could lead to a better understanding and assessment of sensitivity values without the necessity to synthesize large amounts of new energetic materials, which leads to an increase in safety. The performance of the compounds was calculated and it was found that it decreases from **2** to **3** to **1** with all three compounds showing similar values as TNT.

5.4 Acknowledgement

For financial support of this work by Ludwig–Maximilian University (LMU), the Office of Naval Research (ONR) under grant no. ONR.N00014-16-1-2062 and the Strategic Environmental Research and Development Program (SERDP) under contract no. WP19-1287 are gratefully acknowledged. The authors also thank Ms. Teresa Küblböck for help with the graphics and F–Select GmbH for the generous donation of fluoro-chemicals.

5.5 Experimental Section

5.5.1 General Procedure

Diphenylether, nitric acid, oleum, picryl chloride and sodium thiosulfate were commercially available. For NMR spectroscopy the solvent DMSO-d₆ was dried using 3 Å mole sieve. Spectra were recorded on a Bruker Avance III spectrometer operating at 400.1 MHz (¹H), 100.6 MHz (¹³C) and 28.9 MHz (¹⁴N). Chemical shifts are referred to TMS (¹H, ¹³C) and MeNO₂ (¹⁴N). Raman spectra were recorded with a Bruker MultiRam FT Raman spectrometer using a neodymium-doped yttrium aluminum garnet (Nd:YAG) laser (λ = 1064 nm) with 1074 mW. The samples for Infrared spectroscopy were placed under ambient conditions onto an ATR unit using a Perkin Elmer Spectrum BX II FT-IR System spectrometer. Melting and / or decomposition points were detected with a OZM DTA 552-Ex instrument. The scanning temperature range was set from 293 K to 673 K at a scanning rate of 5 K min⁻¹. Elemental analysis was done with a Vario EL instrument and a Metrohm 888 Titrando device. For X-ray measurements, Bis(2,4,6-trinitrophenyl) ether and Bis(2,4-dinitrophenyl) ether were solved in

ethylacetate and single crystals have been received after slow solvent evaporation. Single crystals of Bis(2,4,6-trinitrophenyl) thioether have been received of the decomposition of Fluoromethyl-(2,4,6)-trinitrobenzene sulfonate with triphenylphosphine sulfid in DCM after slow solvent evaporation. Data collection was performed with an Oxford Xcalibur3 diffractometer with a CCD area detector, equipped with a multilayer monochromator, a Photon 2 detector and a rotating-anode generator were employed for data collection using Mo-K α radiation ($\lambda = 0.7107 \text{ \AA}$). Data collection and reduction were carried out using the CrysAlispro software.^[19] The structures were solved by direct methods (SIR-2014)^[20] and refined (SHELXLE)^[21] by full-matrix least-squares on F2 (ShelxL)^[(22), (23)] and finally checked using the platon software^[24] integrated in the WinGX software suite.^[25] The non-hydrogen atoms were refined anisotropically and the hydrogen atoms were located and freely refined. All Diamond 3 plots are shown with thermal ellipsoids at the 50% probability level and hydrogen atoms are shown as small spheres of arbitrary radius.

5.5.2 Preparation

Caution! *All investigated compounds are explosives, which show partly increased sensitivities toward various stimuli (e.g. higher temperatures, impact, friction or electrostatic discharge). Therefore, proper safety precautions (safety glass, Kevlar gloves and earplugs) have to be applied while synthesizing and handling the described compounds.*

Bis(2,4-dinitrophenyl) ether (1)

Diphenylether (2.15 g, 12.65 mmol) was added at 0 °C to a mixed acid consisting of 1.15 mL sulfuric acid, 2.74 mL Oleum (65%) and white fuming nitric acid (2.7 mL, 63.26 mmol). The mixture was stirred for 45 min. After being warmed to room temperature, the solution was heated to 125 °C for 19 hours. The obtained reddish suspension was cooled to room temperature and poured into 750 mL of ice water. The solid was filtered off and washed with water (3 \times 100 mL). The filter cake was recrystallized from boiling ethyl acetate and the beige-red powder was dried under ambient conditions (1.4 g, yield: 32%). ¹H NMR (DMSO-*d*₆, 400 MHz): δ 7.67 (d, 2H, $J = 2.8$ Hz), 8.60 (dd, 2H, $J = 9.1, 2.8$ Hz), 8.98 (s, 2H, $J = 9.1$ Hz) ppm. ¹³C NMR (DMSO-*d*₆, 100 MHz): δ 151.7, 143.8, 140.3, 130.2, 122.4, 122.3 ppm. ¹⁴N (DMSO-*d*₆, 29 MHz): δ -20 (s, NO₂) ppm. FT-IR (ATR): $\tilde{\nu}$ 3365 (w), 3090 (w), 3076 (w), 2879 (w), 1592 (m), 1530 (s), 1483 (m), 1472 (m), 1422 (w), 1342 (s), 1265 (s), 1155 (w), 1136 (w), 1122 (w), 1067 (s), 972 (w), 928 (m), 913 (s), 867 (s), 834 (s), 787 (w), 762 (w), 743 (s), 721 (s), 687 (w), 661 (m), 639 (m), 603 (w), 521 (w), 499 (w), 458 (w), 435 (w). Raman (1064 nm, 300 mW): $\tilde{\nu}$ 3076 (w), 2263 (w), 2217 (w), 2202 (w), 2157 (w), 2137 (w), 2062 (w), 1951 (w), 1611 (m), 1597 (w), 1547 (w), 1352 (s), 1270 (w), 1213 (w), 1156 (w), 1137 (w), 1066 (w), 838 (m), 641 (w). EA calcd (%) for C₁₂H₆N₄O₉: C 41.16, H 1.73, N 16.00; found: C 41.09, H 1.82, N 15.82. DTA: 246 °C (melting), 336 °C (dec) IS: >40.0 J. FS: >360 N. ESD: 50 mJ.

Bis(2,4,6-trinitrophenyl) ether (2)

Diphenylether (1.00 g, 5.88 mmol) was added at 0 °C successively to a mixed acid consisting of 22 mL oleum (30 %) and white fuming nitric acid (4.4 mL, 106 mmol). The mixture was

stirred for 30 min. After being warmed to room temperature, the solution was heated to 150 °C for 4 d. The obtained white suspension was cooled to room temperature and poured into 750 mL of ice water. The solid was filtered off and washed with water (3 × 100 mL). The filter cake was recrystallized from boiling chloroform and the colorless powder was dried under ambient conditions (0.53 g, yield: 24%). ¹H NMR (DMSO-*d*₆, 400 MHz): δ 8.60 (s, 4H) ppm. ¹³C NMR (DMSO-*d*₆, 100 MHz): δ 160.6, 141.8, 125.2, 124.6 ppm. ¹⁴N (DMSO-*d*₆, 29 MHz): δ -11 (s, NO₂) ppm. FT-IR (ATR): ν̄ 3103 (m), 1612 (m), 1601 (m), 1536 (s), 1455 (m), 1415 (m), 1339 (s), 1268 (s), 1212 (m), 1191 (m), 1085 (m), 944 (m), 927 (m), 913 (m), 832 (m), 795 (m), 749 (m), 733 (m), 717 (s), 523 (m). Raman (1064 nm, 1074 mW): ν̄ 3107 (w), 1627 (m), 1559 (m), 1543 (m), 1362 (s), 1275 (w), 1214 (m), 1171 (w), 1083 (w), 941 (w), 829 (m), 797 (w), 329 (w), 270 (w), 202 (w). EA calcd (%) for C₁₂H₄N₆O₁₃: C 32.74, H 0.92, N 19.09; found: C 32.71, H 1.01, N 18.88. DTA: 256 °C (dec) IS: 9.0 J. FS: 360 N. ESD: 50 mJ.

Bis(2,4,6-trinitrophenyl) thioether (3)

Sodium thiosulfate (0.498 g, 3.15 mmol) was added successively to a reflux heated suspension of picryl chloride (1.00 g, 4.04 mmol) and magnesium carbonate (0.190 g, 2.26 mmol) in absolute ethanol (25 mL). The mixture was heated for 1 h. The mixture turned into a yellow suspension. After being cooled to room temperature the obtained suspension was filtered off and the filter cake washed with ethanol (3 × 15 mL), 1.0 M HCl (3 × 5 mL) and water (3 × 5 mL). The yellow powder was dried under a nitrogen stream (1.1 g, yield: 60%). ¹H NMR (DMSO-*d*₆, 400 MHz): δ 9.17 (s, 4H) ppm. ¹³C NMR (DMSO-*d*₆, 100 MHz): δ 151.6, 147.8, 125.6, 124.4 ppm. ¹⁴N (DMSO-*d*₆, 29 MHz): δ -19 (s, NO₂) ppm. FT-IR (ATR): ν̄ 3093 (m), 2917 (w), 2850 (w), 1598 (m), 1530 (s), 1392 (w), 1332 (s), 1169 (w), 1112 (w), 1047 (m), 931 (m), 911 (s), 822 (m), 748 (m), 726 (s), 718 (s), 687 (m). Raman (1064 nm, 1074 mW): ν̄ 3094 (w), 1601 (m), 1545 (m), 1354 (s), 1301 (w), 1180 (m), 1059 (m), 936 (m), 825 (w), 773 (m), 433 (w), 370 (w), 331 (w), 287 (w). EA calcd (%) for C₁₂H₄N₆O₁₂S: C 31.59, H 0.88, N 18.42, S 7.03; found: C 31.48, H 0.94, N 18.34, S 7.17. DTA: 253 °C (mp), 310 °C (dec) IS: 12.5 J. FS: 360 N. ESD: 50 mJ.

5.6 References

- [1] Nobel, A. Dynamit. United Kingdom, **1867**.
- [2] Köhler, J.; Meyer, R.; Homburg, A. *Explosivstoffe*, Wiley-VCH, **2008**.
- [3] a) Giles, J. Green explosives: collateral damage. *Nature* **2004**, *427*, 580-581; b) Klapötke, T. M. *Chemistry of High-Energy Materials*, De Gruyter, 5th edn., **2019** c) Reichel, M.; Krumm, B.; Vishnevskiy, Y.; Blomeyer, S.; Schwabedissen, J.; Stammler, H.-G.; Karaghiosoff, K.; Mitzel, N. W. *Angew. Chem. Int. Ed.* **2019**, *in Press* (DOI: 10.1002/anie.201911300); d) Reichel, M.; Krumm, B.; Karaghiosoff, K. Synthesis and investigation of highly energetic and shock-sensitive fluoromethyl perchlorate. *J. Fluorine Chem.* **2019**, *226*, 109351.
- [4] a) Zhi, C.-Y.; Cheng, X.-L.; Zhao, F. The Correlation between Electric Spark Sensitivity of Polynitroaromatic Compounds and Their Molecular Electronic Properties. *Propellants, Explos., Pyrotech.* **2010**, *35*, 555-560; b) Zeman, S.; Krupka, M. New aspects of impact reactivity of polynitro compounds, part III. Impact sensitivity as a

- function of the intermolecular interactions. *Propellants, Explos., Pyrotech.* **2003**, *28*, 301-307; c) Tan, B.; Li, H.; Huang, H.; Han, Y.; Li, J.; Li, M.; Long, X. Large π - π separation energies of some energetic compounds. *Chem. Phys.* **2019**, *520*, 81-87.
- [5] Gao, H.; Shreeve, J. Azole-Based Energetic Salts. *Chem. Rev. (Washington, DC, U. S.)* **2011**, *111*, 7377-7436.
- [6] Thottempudi, V.; Gao, H.; Shreeve, J. Trinitromethyl-substituted 5-nitro- or 3-azo-1,2,4-triazoles: synthesis, characterization, and energetic properties. *J. Am. Chem. Soc.* **2011**, *133*, 6464-6471.
- [7] Zhang, J.; Zhang, Q.; Vo, T. T.; Parrish, D. A.; Shreeve, J. Energetic Salts with π -Stacking and Hydrogen-Bonding Interactions Lead the Way to Future Energetic Materials. *Journal of the American Chemical Society* **2015**, *137*, 1697-1704.
- [8] a) Spackman, M. A.; Jayatilaka, D. Hirshfeld surface analysis. *CrystEngComm* **2009**, *11*, 19-32; b) Ma, Y.; Zhang, A.; Xue, X.; Jiang, D.; Zhu, Y.; Zhang, C. Crystal Packing of Impact-Sensitive High-Energy Explosives. *Cryst. Growth Des.* **2014**, *14*, 6101-6114.
- [9] a) Rath, C.; Rost, A.; Rittler, K. W. Hexanitrodiphenyl ether. *Chemische Fabrik von Heyden A.-G.* . **1936**; b) Sprengstoff-A.-G. Carbonit . **1912**.
- [10] a) Isanbor, C.; Emokpae, T. A. Anilinolysis of nitro-substituted diphenyl ethers in acetonitrile: The effect of some ortho-substituents on the mechanism of S_NAr reactions. *Int. J. Chem. Kinet.* **2009**, *42*, 37-49; b) Davydov, D. V.; Mikaya, A. I.; Zaikin, V. G. Mass-spectrometric study of substituted trinitrobenzenes. *Zh. Obshch. Khim.* **1983**, *53*, 455-462; c) Desvergnès, L. Some physical properties of nitro derivatives. *Monit. Sci. Doct. Quesneville* **1926**, *16*, 201-208; d) Zhou, J.; Zhang, C.; Wang, Y.; Zhang, M.; Li, Y.; Huang, F.; Hu, L.; Xi, W.; Wang, Q. 2,2',4,4',6,6'-hexanitrodiphenyl sulfide refining method. Modern Chemistry Research Institute, Peop. Rep. China . **2015**, p. 6pp.
- [11] a) Hussain, I.; Tariq, M. I.; Siddiqui, H. L. Structure elucidation of chromogen resulting from Jaffe's reaction. *J. Chem. Soc. Pak.* **2009**, *31*, 937-948; b) Soojhawon, I.; Lokhande, P. D.; Kodam, K. M.; Gawai, K. R. Biotransformation of nitroaromatics and their effects on mixed function oxidase system. *Enzyme Microb. Technol.* **2005**, *37*, 527-533.
- [12] Lewis, I. R.; Daniel, N. W.; Griffiths, P. R. Interpretation of Raman spectra of nitro-containing explosive materials. Part I: Group frequency and structural class membership. *Appl. Spectrosc.* **1997**, *51*, 1854-1867.
- [13] a) Li, J. Relationships for the Impact Sensitivities of Energetic C-Nitro Compounds Based on Bond Dissociation Energy. *J. Phys. Chem. B* **2010**, *114*, 2198-2202; b) Li, J. A quantitative relationship for the shock sensitivities of energetic compounds based on X-NO₂ (X = C, N, O) bond dissociation energy. *J. Hazard. Mater.* **2010**, *180*, 768-772.
- [14] a) Tang, Y.; Zhang, J.; Mitchell, L. A.; Parrish, D. A.; Shreeve, J. Taming of 3,4-Di(nitramino)furazan. *J. Am. Chem. Soc.* **2015**, *137*, 15984-15987; b) Test methods according to the UN Manual of Tests and Criteria, Recommendations on the Transport of Dangerous Goods, N. Y. United Nations Publication, Geneva, 4th revised ed., 2003: Impact: insensitive >40 J, less sensitive \geq 35 J, sensitive \geq 4 J, very sensitive \leq 3 J; friction: insensitive >360 N, less sensitive: 360 N, sensitive <360 N and >80 N, very sensitive \leq 80 N, extremely sensitive \leq 10 N; c) www.reichel-partner.com; d) NATO, Standardization Agreement 4489 (STANAG 4489), Explosives, Impact Sensitivity

- Tests. Brussels, Belgium 1999; e) NATO, Standardization Agreement 4487 (STANAG 4487), Explosives, Friction Sensitivity Tests. Brussels, Belgium 2002.
- [15] Zhang, C.; Xue, X.; Cao, Y.; Zhou, Y.; Li, H.; Zhou, J.; Gao, T. Intermolecular friction symbol derived from crystal information. *CrystEngComm* **2013**, *15*, 6837-6844.
- [16] Klapötke, T. M. *Chemie der hochenergetischen Materialien*, De Gruyter, 2009.
- [17] a) Curtiss, L. A.; Raghavachari, K.; Redfern, P. C.; Pople, J. A. Assessment of Gaussian-2 and density functional theories for the computation of enthalpies of formation. *J. Chem. Phys.* 1997, *106*, 1063–1079; b) Byrd, E.; Rice, B. M. Improved Prediction of Heats of Formation of Energetic Materials Using Quantum Mechanical Calculations. *J. Phys. Chem. A* 2006, *110*, 1005–1013.
- [18] a) Suceška, M. *EXPLO5 6.01 2013, Brodarski Institute: Zagreb, Croatia*; b) Klapoetke, T. M.; Krumm, B.; Steemann, F. X.; Umland, K.-D. Bis(1,3-dinitratoprop-2-yl) nitramine, a new sensitive explosive combining a nitrate ester with a nitramine. *Z. Anorg. Allg. Chem.* 2010, *636*, 2343-2346.
- [19] CrysAlisPRO (Version 171.33.41), 2009, Oxford Diffraction Ltd.
- [20] Burla, M. C.; Caliandro, R.; Carrozzini, B.; Cascarano, G. L.; Cuocci, C.; Giacovazzo, C.; Mallamo, M.; Mazzone, A.; Polidori, G., Crystal structure determination and refinement via SIR2014. *J. Appl. Crystallogr.* 2015, *48*, 306.
- [21] Hübschle, C.B., Sheldrick, G.M., Dittrich B. ShelXle: a Qt graphical user interface for SHELXL. *J. Appl. Cryst.* 2011, *44*, 1281
- [22] Sheldrick, G. M., SHELXL-97, Program for the Refinement of Crystal Structures., **1997** University of Göttingen, Germany.
- [23] Sheldrick, M. A short history of SHELX. *Acta Crystallogr. Sect. A* **2008**, 112.
- [24] Spek, A. L., PLATON, A Multipurpose Crystallographic Tool., **1991**, Utrecht University, The Netherlands.
- [25] Farrugia, L. J., WinGX and ORTEP for Windows: an update. *J. Appl. Cryst.* **2012**, 849.

5.7 Supporting Information

Table 1: Structure refinement data of compound **1**, **2**, **3**.

Empirical formula	C ₁₂ H ₆ N ₄ O ₉ (1)	C ₁₂ H ₄ N ₆ O ₁₃ (2)	C ₁₂ H ₄ N ₆ O ₁₂ S (3)
Formula weight	350.21	440.21	456.27
Temperature	150(2) K	143(2) K	298(2) K
Wavelength	0.71073 Å	0.71073 Å	0.71073 Å
Crystal system	Triclinic	Monoclinic	Monoclinic
Space group	<i>P</i> -1	<i>P</i> 2 ₁	<i>P</i> 2 ₁
Unit cell dimensions	a = 7.9044(12) Å b = 8.0845(11) Å c = 11.3617(15) Å α = 81.224(11)° β = 69.815(13)° γ = 84.647(12)°	a = 8.0043(3) Å b = 8.7613(3) Å c = 11.7424(5) Å α = 90° β = 105.700(4)° γ = 90°	a = 10.9756(5) Å b = 11.0066(4) Å c = 14.0260(5) Å α = 90° β = 104.829(4)° γ = 90°

Volume	672.83(17) Å ³	792.75(5) Å ³	1637.96(12) Å ³
Z	2	2	4
Density (calculated)	1.729 mg/m ³	1.844 mg/m ³	1.850 mg/m ³
Absorption coefficient	0.152 mm ⁻¹	0.172 mm ⁻¹	0.288 mm ⁻¹
F(000)	356	444	920
Crystal size	0.2 x 0.04 x 0.04 mm ³	0.4 x 0.2 x 0.05 mm ³	0.2 x 0.05 x 0.05 mm ³
Theta range for data collection	2.552 - 28.282°	3.521 - 30.504°	4.172 - 28.278°
Index ranges	-10 ≤ h ≤ 10, -10 ≤ k ≤ 10, -15 ≤ l ≤ 15	-11 ≤ h ≤ 11, -12 ≤ k ≤ 12, -16 ≤ l ≤ 16	-14 ≤ h ≤ 14, -14 ≤ k ≤ 14, -18 ≤ l ≤ 10
Reflections collected	6048	15900	15113
Independent reflections	3342 [R _{int} = 0.0464]	4833 [R _{int} = 0.0393]	7871 [R _{int} = 0.0404]
Data / restraints / parameters	3342 / 0 / 226	4833 / 1 / 280	7871 / 1 / 559
Goodness-of-fit on F ²	1.006	1.038	1.032
Final R indices [I > 2σ(I)]	R ₁ = 0.0644, wR ₂ = 0.1334	R ₁ = 0.0388, wR ₂ = 0.0779	R ₁ = 0.0424, wR ₂ = 0.0755
R indices (all data)	R ₁ = 0.1174, wR ₂ = 0.1603	R ₁ = 0.0498, wR ₂ = 0.0835	R ₁ = 0.0556, wR ₂ = 0.0817
Largest diff. peak and hole	0.387 and -0.313 e Å ⁻³	0.297 and -0.222 e Å ⁻³	0.388 and -0.264 e Å ⁻³

6 Preparation and Investigation of Fluoromethyl Azide and Chalcogenocyanates

Marco Reichel, Mara Egenhöfer, Burkhard Krumm and Konstantin Karaghiosoff*

Published in *Z. Anorg. Allg. Chem.* **2020**, *646*, 328–331.

DOI: 10.1002/zaac.202000055



Abstract: Fluoromethylating agents are a highly studied and controversially discussed class of compound. New fluoromethyl pseudohalides FCH₂N₃, FCH₂SCN and FCH₂SeCN have been prepared for the first time and their physical and spectroscopic properties investigated. Their synthesis is performed conveniently by fluoromethylation of the respective silver or potassium pseudohalogenides with fluoroiodomethane.

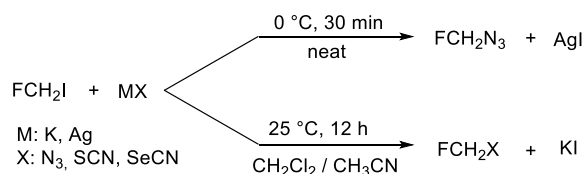
6.1 Introduction

The monofluoromethyl halides FCH₂Cl, FCH₂Br and FCH₂I are extensively investigated materials. However, due to the ozone-depleting effect of some representatives, they are under close observation and are already partially banned under Annex I of Regulation (EC) No 1005/2009.^[1] In addition to their use as coolants, they are mainly used as fluoromethylating agents.^[2] As one of the strategic fluorine-containing building blocks, the fluoromethyl group is used by the pharmaceutical industry in many drugs and drug candidates.^[3] The introduction of this building block unit often leads to dramatic changes in physical and chemical properties. Also the metabolic stability is often drastically increased.^[4] The change in chemical and physical parameters can be observed particularly well with small molecules. For small molecules additional intermolecular interactions are negligible and the effect of the fluoromethyl substituent can be studied without overlapping with other effects. This also would apply for fluoromethyl pseudohalides. But only a few examples carrying the fluoromethyl group such as the well known fluoroacetonitrile FCH₂CN^[5] and the rather unstable fluoromethyl isocyanate FCH₂NCO^[6] have been isolated and investigated until now. Theoretical investigations for FCH₂R (R = NCO, NCS, N₃ and CNO)^[7] further add to available information. Recently, our initial studies on the system fluoroiodomethane with selected silver salts enabled access to the corresponding fluoromethyl derivatives FCH₂OClO₃^[8] and FCH₂ONO₂^[9]. In this contribution we would like to study the reactivity of metal pseudohalides, i.e. azide and chalcogenocyanates, towards fluoroiodomethane.

6.2 Results and Discussion

Fluoromethyl azide

The reaction of freshly prepared dried silver azide with fluoroiodomethane in equimolar mixture resulted in the formation of pure fluoromethyl azide, which was obtained as a highly volatile colorless liquid (Scheme 1).



Scheme 1: Synthesis of fluoromethyl pseudohalides.

Similar to methyl azide, FCH₂N₃ is anticipated to be highly sensitive. The high vapor pressure can be demonstrated by the very fast evaporation on a cooled plate and is also reflected in an estimated boiling point of approx. 22 °C (method of *Siwoloboff*^[10]). With a boiling point of approx. 20 °C,^[11] methyl azide has a slightly lower boiling point than fluoromethyl azide. Final proof of the identity of the compound results from multinuclear NMR spectra (DMSO-D₆). In the ¹H NMR spectrum, the FCH₂ signal is observed at 5.46 ppm with a coupling constant of ²J_{F,H} = 51.5 Hz, the ¹³C{¹H} resonance at 91.6 ppm as a doublet with ¹J_{F,C} = 205.4 Hz. Both resonances of fluoromethyl azide are shifted to low field due to the deshielding character of the

fluorine substituent compared to CH_3N_3 (^1H NMR: 2.98 ppm; ^{13}C NMR: 37.9 ppm).^[12] The ^{19}F NMR resonance of FCH_2N_3 is detected at -170.1 ppm as a triplet. Since the azide substituent is less electronegative than a nitrate substituent, which with its electronegativity lies between the OCN/NCO cyanates, the resonance of fluoromethyl azide is shifted to lower frequency compared to fluoromethyl nitrate (-155.9 ppm).^[9,13] The ^{14}N NMR resonances for fluoromethyl azide are observed at -135(N_β), -166(N_γ) and -297(N_α) ppm. These are slightly shifted compared to those of CH_3N_3 , -129(N_β), -171(N_γ) and -321(N_α) ppm, in C_6F_6 (Table 1). The shielding of the N atoms by the substituent increases from $\text{N}_\alpha > \text{N}_\gamma > \text{N}_\beta$ where N_β and N_γ are in most cases close to each other. In addition, N_α and N_γ are considered most sensitive to inductive and conjugative effects of the substituent. Chemical shifts can usually be explained by the influence of the paramagnetic term:

$$\sigma_p \approx \langle r^{-3} \rangle_{2p} \Sigma Q (\Delta E)^{-1}$$

In the paramagnetic term (σ_p), the radial factor ($\langle r^{-3} \rangle_{2p}$), the asymmetry of the valence electrons (ΣQ) and the excitation energy between the frontier orbitals (ΔE) are included.

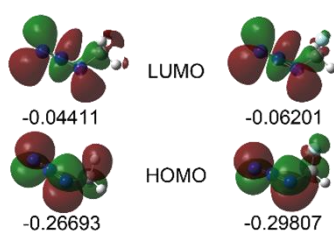


Figure 1: Molecular orbitals (HOMO/LUMO) and their energies in Hartree (below) of methyl azide (left) and fluoromethyl azide (right), calculated at the B3LYP/6-311G+(d,p) level of theory.

This term, which dominates the chemical shift, depends on a virtual excitation of the charge between the HOMO and the LUMO in the magnetic field. A higher energy difference causes a shift to lower frequencies of particularly the N_α but also the N_γ signal. For fluoromethyl azides such as FCH_2N_3 , as well as found for CF_3N_3 , the excitation energy is higher than in CH_3N_3 (Figure 1). However, the experimental finding is contrary for the $\text{N}_\alpha/\text{N}_\gamma$ NMR shifts, as also found for $\text{CH}_3/\text{CF}_3\text{-N}_3$.

Table 1: Nitrogen chemical shifts (^a C_6F_6 , ^bDMSO- D_6 , ^cneat).^{[14]*}

Compound	$\delta^{14/15}\text{N}_\alpha$	$\delta^{14/15}\text{N}_\beta$	$\delta^{14/15}\text{N}_\gamma$
CH_3N_3^a	-321.7	-130.2	-171.5
FCH_2N_3^b	-297	-135	-166
F_3CN_3^c	-286.2	-147.8	-144.7

*For F_2CHN_3 no ^{14}N NMR data are available.^[15]

The assignments of the vibration modes in the infrared spectrum of the compounds were based on literature data and were supported by quantum mechanical calculations using Gaussian 09 (Table 2).^[15]

Table 2: Selected vibration modes (IR) of CH₃N₃^[15a,b] (gas), CH₃SCN^[15e] and CH₃SeCN^[15d] (liquids) and fluoromethyl pseudohalides (liquids).

Vib.	CH ₃ N ₃	FCH ₂ N ₃	Vib.	CH ₃ SCN	FCH ₂ SCN	Vib.	CH ₃ SeCN	FCH ₂ SeCN
$\nu_{as}(\text{N}_3)^*$	2100(s)	2110(s)	$\nu(\text{CN})$	2173(s)	2167(s)	$\nu(\text{CN})$	2153(s)	2162(m)
$\delta(\text{CH}_2)$	1417(w)	1489(w)	$\delta(\text{CH}_2)$	1436(s)	1439(m)	$\delta(\text{CH}_2)$	1421(m)	1434(m)
$\nu(\text{CF})$	---	1034(s)	$\nu(\text{CF})$	---	1003(s)	$\nu(\text{CF})$	---	1011(s)
$\nu(\text{CN})$	910(m)	932(w)	$\nu(\text{CS})$	705(m)	813(w)	$\nu(\text{CSe})$	576(w)	606(s)
$\delta(\text{N}_3)$	---	610(w)	$\nu(\text{SC})$	674(m)	693(s)	$\nu(\text{SeC})$	519(m)	518(m)
$\delta(\text{N}_3)$	666(w)	680(w)	$\delta(\text{SCN})$	460(m)	474(m)	$\delta(\text{SeCN})$	393(w)	408(w)

* $\nu_s(\text{N}_3)$ 1270/1269 cm⁻¹. $\zeta(\text{FCN})$ --/462 cm⁻¹.

The vibrations at 2110 and 1269 cm⁻¹ correspond to the antisymmetric and symmetric stretching vibrations of the N₃ group. The deformation vibrations of the azide group perpendicular and parallel to the plane appear at 680 and 610 cm⁻¹. Due to the electronegative fluorine substituent compared to methyl azide, a shift to higher wave numbers of the mentioned vibration modes occurs.

The molecular ion peak of FCH₂N₃ in the mass spectrum is detected at 75.0228 m/z [M]⁺ and that of hydrogen abstraction at 74.0149 m/z [M-H]⁺. Further characteristic fragments are assigned to [FCH₂N₂]⁺ and [N₃]⁺ at 61.0284 m/z and 42.0085 m/z, respectively.

Fluoromethyl thiocyanate

Fluoromethyl thiocyanate was obtained from the reaction of KSCN with fluoroiodomethane in a solvent mixture of acetonitrile and dichloromethane (Scheme 1). In contrast to fluoromethyl azide, fluoromethyl thiocyanate is a slightly yellowish, air-stable liquid with an estimated melting point of -28 °C and a boiling point of 155 °C (DTA). Compared to the methyl analogue CH₃SCN, the melting and boiling points are increased.^[16] Since the pseudohalogens are close to iodine in terms of electronegativity (Table 3),^[17] the NMR chemical shifts and coupling constants are very similar to fluoroiodomethane and towards each other.^[18] Thus, similar to FCH₂I (5.63 ppm, ²J_{H,F} = 49.5 Hz), the ¹H NMR resonance of FCH₂SCN is observed at 5.90 ppm with a coupling constant ²J_{H,F} = 49.4 Hz. The ¹³C NMR resonance is observed as a doublet at 87.4 ppm with ¹J_{C,F} = 227.6 Hz. Another good proof of the electronegativity concept is very obvious in ¹⁹F NMR spectroscopy. Here, the resonance of FCH₂SCN is detected at -189.2 ppm (CD₃CN) in close proximity to that of fluoroiodomethane at -190.3 ppm (CD₃CN).

Table 3: Group electronegativities (χ_p) of selected pseudohalides, halogenides and functional groups (R) by decreasing EN.^[18]

R	χ_p	R	χ_p	R	χ_p	R	χ_p
F	4.00	CF ₃	3.16	N ₃	2.95	SCN	2.64
ClO ₄	3.40	OCN	3.07	NCS	2.78	SeCN	2.60
SO ₃ F	3.30	OH	3.03	CN	2.76	FCH ₂	2.56
Cl	3.16	NCO	2.98	I	2.66	CH ₃	2.40

In the IR spectrum of FCH₂SCN an opposite trend is observed regarding the SCN stretching vibration at 2167 cm⁻¹: a shift to lower wave numbers compared to the methyl analogue. The influence of the more electropositive and heavier pseudohalide SCN can be illustrated by the $\nu(\text{CF})$ stretching vibration and its shift towards lower wave numbers compared to fluoromethyl azide. The fluorine substituent, on the other hand, causes a shift to higher wave numbers of the C-SCN and S-CN stretching vibrations at 705 and 674 cm⁻¹ compared to methyl thiocyanate. In the mass spectrum, the molecular ion peak is detected at 90.9888 m/z [M]⁺, the [M-H]⁺ ion at 98.9810 m/z, and at 57.9781 m/z the [SCN]⁺ fragment.

Fluoromethyl selenocyanate

With similar conditions as above, the reaction of selenocyanate with fluoriodomethane results in the formation of fluoromethyl selenocyanate (Scheme 1). Compared to fluoromethyl thiocyanate with a more aromatic odor, the selenocyanate FCH₂SeCN has an unpleasant, disgusting odor (a drop was sufficient to refuse entry into a lab for several weeks). Due to its low volatility and a boiling point of +185 °C (DTA), the smell of the yellowish compound, which solidifies at approximately -32 °C, stays for a long time. Due to the almost identical electronegativities of thiocyanate and selenocyanate, the NMR chemical shifts differ more from those of the azide. Thus, in the ¹H NMR spectrum the FCH₂ group is observed at 6.20 ppm with a coupling constant of 49.3 Hz. The coupling to selenium ²J_{Se,H}, as determined from ⁷⁷Se satellites is 20.5 Hz. Similar, selenium satellites with a coupling constant of 84.9 Hz ¹J_{Se,C} are observed in the ¹³C NMR spectrum, in which the FCH₂ resonance occurs at 84.6 ppm. The 105.0 Hz ²J_{Se,F} coupling constant, as determined from the Se satellites in the ¹⁹F NMR spectrum, correspond to the coupling of the doublet at 323 ppm in ⁷⁷Se NMR. (Figure 2). The ¹⁴N NMR resonance of the selenocyanate unit is detected at -90 ppm, slightly low-field shifted to that of the thiocyanate, which was observed at -103 ppm.

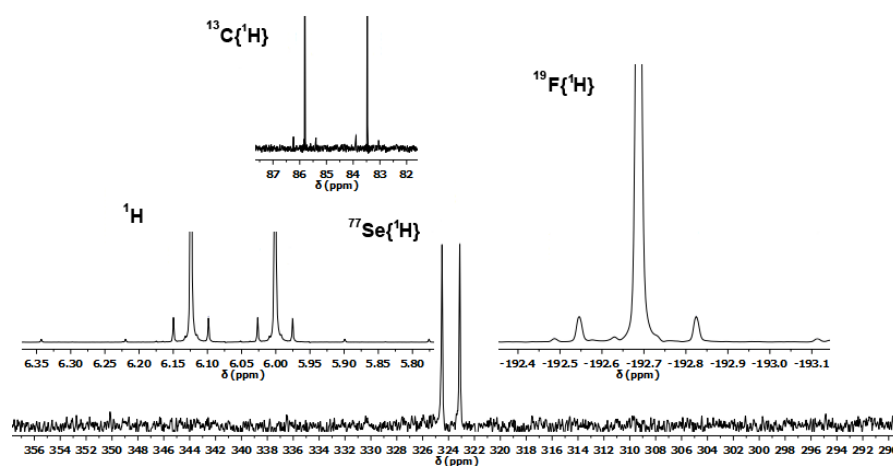


Figure 2: ¹H, ¹³C, ¹⁹F and ⁷⁷Se NMR spectra of fluoromethyl selenocyanate in CD₃CN (25 °C).

Isotope effects in nuclear shielding can well be determined for all three compounds. The ¹Δ¹⁹F(¹³/¹²C) absolute values increase steadily from fluoromethyl selenocyanate to fluoromethyl thiocyanate to fluoromethyl azide (Table 4) and correspond to the isotope effects of other fluoromethanes (CH₂F₂, -112 ppb; CHF₃, -127 ppb; CFCl₃, -194 ppb).^[19]

Table 4: Isotope effects in nuclear shielding in ppb.

	FCH ₂ N ₃	FCH ₂ SCN	FCH ₂ SeCN
¹ Δ ¹⁹ F(^{13/12} C)	-187.0	-122.2	-112.6

In the IR spectrum of fluoromethyl selenocyanate the vibration modes are shifted in comparison to methyl selenocyanate to higher wave numbers. The SeC≡N stretching vibration is detected at 2162 cm⁻¹, the C-SeCN stretching vibration at 606 cm⁻¹ and the Se-CN stretching vibration at 518 cm⁻¹. The CF stretching vibration compared to fluoromethyl azide is shifted to lower wave numbers, but due to the comparable electronegativities of SCN and SeCN in the same range as fluoromethyl thiocyanate. The low volatility of fluoromethyl selenocyanate can also be observed in mass spectra due to the low relative intensity of the molecule peak at 138.9330 m/z [M]⁺ and the peak at 105.9188 m/z assigned for the fragment [SeCN]⁺.

Attempts to fluoromethylate cyanate and tellurocyanate anions remained unsuccessful. Regarding the reaction of FCH₂I with KOCN, the starting materials were recovered without any sign of conversion. Interestingly, the corresponding methylation of cyanate with methyl iodide as well did not result in the formation of methyl cyanate. Based on literature, methyl cyanate can only be isolated starting from complicated precursor compounds by thermal decomposition.^[6,20] In the case of tellurocyanate TeCN⁻, which was generated according to a literature procedure,^[21] the formation of HF was observed, even if using dried solvents and working under inert atmosphere.

While this manuscript was in its final stage for submission, another report of the synthesis of fluoromethyl azide appeared in the recent press.^[22]

6.3 Conclusion

The fluoromethyl substituted pseudohalides, FCH₂N₃, FCH₂SCN, and FCH₂SeCN were synthesized conveniently from their silver and potassium salts with fluoroiodomethane. The compounds were investigated using spectroscopic methods and compared with their methyl derivatives. For fluoromethyl thiocyanate and fluoromethyl selenocyanate, and in contrast to fluoromethyl azide, the physical properties are changed towards higher boiling and melting points compared to their methyl analogues.

6.4 Acknowledgement

Financial support by Ludwig–Maximilian University is grateful acknowledged. We thank Prof. Dr. T. M. Klapötke for his continuous support of our work. We are also thankful to F–Select GmbH for a generous donation of fluoroiodomethane.

6.5 Experimental Section

6.5.1 General Procedure

All compounds were handled using *Schlenk* techniques under dry argon. Silver nitrate, potassium cyanate/thiocyanate/selenocyanate and sodium azide purchased from VWR, were dried *in vacuo* at room temperature for 30 min and fluoriodomethane (donation from F-Select GmbH) was distilled under inert conditions before use. Silver cyanate was freshly prepared from KOCN with silver nitrate. Potassium tellurocyanate was generated *in situ* according the literature.^[21] Boiling points were determined using the Siwoloboff method in a Büchi B-540 apparatus using a heating rate of 1 °C min⁻¹.^[10] The samples for infrared spectroscopy were placed under ambient conditions without further preparation onto an Smith DuraSampLIR II ATR device using a Perkin Elmer BX II FT-IR System spectrometer. Samples for Raman spectroscopy were sealed in glass tubes. The measurement was carried out on a Bruker MultiRam FT Raman device using a neodymium doped yttrium aluminum garnet (Nd:YAG) laser ($\lambda = 1064$ nm) with 1074 mW. The samples for NMR spectroscopy were prepared under inert atmosphere using argon as protective gas. The NMR solvents CD₃CN and DMSO-D₆ were dried using 3 Å molecular sieve and stored under argon atmosphere. NMR spectra were recorded with a Bruker Avance III spectrometer operating at 400.1 MHz (¹H), 376.4 MHz (¹⁹F), 100.6 MHz (¹³C), 28.9 MHz (¹⁴N) and 76.4 MHz (⁷⁷Se). Chemical shifts are referred to TMS (¹H/¹³C), CFC₃ (¹⁹F), MeNO₂ (¹⁴N) and Me₂Se (⁷⁷Se). All spectra were recorded at 298.15 K (25 °C). Elemental analysis of the azide was not performed due to the high volatility, as well as of the selenocyanate due to the obnoxious odor. High resolution mass spectra were recorded on a MStation JMS 700 JEOL instrument using a DEP/EI ionization mode.

6.5.2 Preparation

Caution! *Silver azide and fluoromethyl azide are energetic materials. AgN₃ is highly sensitive towards friction and impact. Sensitivity values were not determined for fluoromethyl azide, due to the high volatility, but the compound should be handled with care. Even if no accident has occurred during the synthesis and manipulation of these compounds, additional proper protective precautions like ear plugs, Kevlar gloves, face shield, shatterproof jacket and helmet, Kevlar arm guards and heavy armored blast shields should be used.*

Fluoromethyl azide

Silver azide AgN₃ (0.247 g, 1.65 mmol) was freshly prepared from AgNO₃ (0.28 g, 1.65 mmol) and NaN₃ (0.107 g, 1.65 mmol) and dried *in vacuo*. Subsequently it was placed in a tiny Schlenk tube until the tube was completely filled. Before filling the tube a needle, which serves to introduce the fluoriodomethane, was fixed such that the top was in the center of the Schlenk tube. Within 30 min the fluoriodomethane (0.11 mL, 1.65 mmol) was injected while cooling with an ice bath. The product was collected in a cooling trap (80 %). The boiling point was estimated by the method of *Siwoloboff* to be approximately +22 °C. ¹H NMR (400 MHz, DMSO-D₆, 25°C): $\delta = 5.46$ ppm (d, ²J_{H,F} = 51.5 Hz); ¹³C{¹H} NMR (101 MHz, DMSO-D₆, 25°C): $\delta = 91.6$ ppm (d, ¹J_{C,F} = 205.4 Hz); ¹⁹F NMR (376 MHz, DMSO-D₆, 25°C): $\delta = -170.1$

ppm (t, $^2J_{F,H} = 51.5$ Hz); ^{14}N NMR (29 MHz, DMSO- D_6 , 25°C): $\delta = -135$ (N_β), -166 (N_γ), -297 ppm (N_α). IR (ATR): 2110 (s) $\nu_{\text{as}}(\text{N}_3)$, 1489 (w) $\delta(\text{CH}_2)$, 1269 (m) $\nu_{\text{s}}(\text{N}_3)$, 1232 (m), 1060 (s), 1034 (s) $\nu(\text{CF})$, 956 (w), 932 (m), 754 (m), 680 (w) $\delta(\text{N}_3)$, 610 (w) $\delta(\text{N}_3)$, 462 (w) cm^{-1} $\zeta(\text{FCN})$. HRMS (EI) m/z [M] $^+$ calcd for CH_2FN_3 : 75.0233, found: 75.0228.

Fluoromethyl thiocyanate

Into a solution of KSCN (0.30 g, 3.13 mmol) in a mixture of dichloromethane (3 mL) and acetonitrile (3 mL) was added fluoriodomethane (0.21 mL, 3.13 mmol) dropwise at ambient temperature. The cloudy solution was stirred over night, and then the solvent was removed at reduced pressure. The product was extracted in pentane (10 mL) and separated from KI. Pentane was removed at reduced pressure and FCH_2SCN (95 %) was obtained pure according to NMR spectroscopy. $T_{\text{melt}} -28$ °C; $T_{\text{boil}} +155$ °C. ^1H NMR (400 MHz, CD_3CN , 25°C): $\delta = 5.90$ ppm (d, $^2J_{H,F} = 49.4$ Hz); $^{13}\text{C}\{^1\text{H}\}$ NMR (101 MHz, CD_3CN , 25°C): $\delta = 111.2$ (d, $^3J_{C,F} = 2.2$ Hz, SCN), 87.4 ppm (d, $^1J_{C,F} = 227.6$ Hz, FCH_2); ^{19}F NMR (376 MHz, CD_3CN , 25°C): $\delta = -189.2$ ppm (t, $^2J_{F,H} = 49.4$ Hz); ^{14}N NMR (29 MHz, CD_3CN , 25°C): $\delta = -103$ (SCN). IR (ATR): 3038 (w), 2967 (w), 2167 (m) $\nu(\text{CN})$, 1439 (m), 1326 (m) $\omega(\text{CH}_2)$, 1237 (w) $\tau(\text{CH}_2)$, 1003 (s) $\nu(\text{CF})$, 955 (m) $\rho(\text{CH}_2)$, 813 (w) $\nu(\text{CS})$, 693 (s) $\nu(\text{CS})$, 474 (m) $\delta(\text{SCN})$. Raman (1074 mW): 3032 (w), 2968 (m), 2254 (w), 2168 (s), 1440 (w), 1327 (w), 1239 (w), 1014 (w), 955 (w), 696 (m), 354 (w), 194 (w). HRMS (EI) m/z [M] $^+$ calcd for CH_2FSN : 90.9892, found: 90.9888.

Fluoromethyl selenocyanate

Into a solution of KSeCN (0.59 g, 4.09 mmol) in a mixture of dichloromethane (5 mL) and acetonitrile (5 mL) was added fluoriodomethane (0.28 mL, 4.09 mmol) dropwise at ambient temperature. The cloudy solution was stirred over night, and then the solvent was removed at reduced pressure. The product was extracted in pentane (10 mL) and separated from KI. Pentane was removed at reduced pressure and FCH_2SeCN (66 %) was obtained pure. $T_{\text{melt}} -32$ °C; $T_{\text{boil}} +185$ °C. ^1H NMR (400 MHz, CD_3CN , 25°C): $\delta = 6.20$ ppm (d, $^2J_{H,F} = 49.3$ Hz; ^{77}Se -sats: $^2J_{\text{Se,H}} = 20.5$ Hz); $^{13}\text{C}\{^1\text{H}\}$ NMR (101 MHz, CD_3CN , 25°C): $\delta = 102.3$ (d, $^3J_{C,F} = 2.3$ Hz, SeCN), 84.6 ppm (d, $^1J_{C,F} = 235.7$ Hz, FCH_2 ; ^{77}Se -sats: $^1J_{\text{Se,C}} = 84.9$ Hz); ^{19}F NMR (376 MHz, CD_3CN , 25°C): $\delta = -192.7$ ppm (t, $^2J_{F,H} = 49.3$ Hz); ^{14}N NMR (29 MHz, CD_3CN , 25°C): $\delta = -90$ ppm (SeCN); $^{77}\text{Se}\{^1\text{H}\}$ (76 MHz, CD_3CN , 25°C): $\delta = 323$ (d, $^2J_{\text{Se,F}} = 105.0$ Hz). IR (ATR): 2294 (w), 2253 (m), 2162 (m) $\nu(\text{CN})$, 1629 (w), 1434 (m), 1374 (m), 1236 (w), 1011 (s) $\nu(\text{CF})$, 919 (w), 895 (w), 751 (w), 606 (s) $\nu(\text{SeC})$, 518 (m) $\nu(\text{SeC})$, 408 (w) $\delta(\text{SeCN})$. Raman (1074 mW): 3042 (w), 2973 (m), 2942 (s), 2730 (w), 2293 (w), 2252 (s), 2161 (s), 1435 (w) $\zeta(\text{CH}_2)$, 1374 (w), 1295 (w), 920 (m), 608 (s), 519 (m), 380 (m), 299 (m), 170 (m). HRMS (EI) m/z [M] $^+$ calcd for CH_2FSeN : 138.9336, found: 138.9330.

Reaction of fluoroiodomethane with cyanate and tellurocyanate

a) Into a mixture of potassium cyanate (0.3 g, 3.70 mmol) in acetonitrile (10 mL) fluoroiodomethane (0.25 mL, 3.70 mmol) was added dropwise at ambient temperature and stirred over night. NMR spectroscopic investigations showed no indication of a reaction.

b) Into a freshly generated solution of potassium tellurocyanate (0.3 g, 1.56 mmol) in dimethylsulfoxide (10 mL) was added fluoroiodomethane (0.11 mL, 1.56 mmol) dropwise at ambient temperature and stirred over night. NMR spectroscopic investigations showed no indication of a formation of fluoromethyl tellurocyanate.

6.6 References

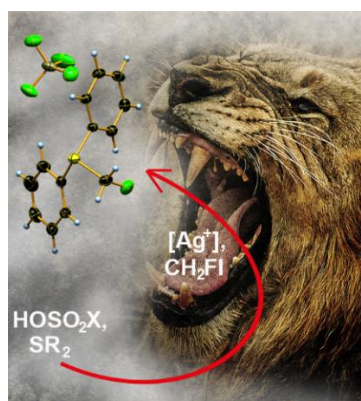
- [1] R. J. Cicerone, R. S. Stolarski, S. Walters, *Science* **1974**, *185*, 1165–1167.
- [2] a) T. Leitao, C. R. Turner (Hovione Inter Ltd.), US- 20130225844A1, **2011**; b) P. J. Joseph, W. D. Sherod (Smithkline Beecham Corp.), WO-2003013427A2, **2003**.
- [3] F. Liu, L. Jiang, H. Qiu, W. Yi, *Org. Lett.* **2018**, *20*, 6270–6273.
- [4] J. Wei, L. Wang, R. Wu, G. Cheng, X. Li, Y. Hu, J. Hu, R. Sheng, *Org. Chem. Front.* **2017**, *4*, 214–223.
- [5] F. Swarts, *Bull. Soc. Belg.* **1922**, *31*, 364–365.
- [6] W. J. Middleton, *J. Org. Chem.* **1984**, *49*, 4541–4543.
- [7] a) C. Glidewell, H. D. Holden, *J. Mol. Struct.: THEOCHEM* **1982**, *89*, 325–332; b) M. H. Palmer, A. D. Nelson, *J. Mol. Struct.* **2004**, *689*, 161–173.
- [8] M. Reichel, B. Krumm, K. Karaghiosoff, *J. Fluorine Chem.* **2019**, *226*, 109351.
- [9] M. Reichel, B. Krumm, Y. Vishnevskiy, S. Blomeyer, J. Schwabedissen, H.-G. Stammler, K. Karaghiosoff, N. W. Mitzel, *Angew. Chem. Int. Ed.* **2019**, *in press*.
- [10] a) Laborpraxis Band 2: Messmethoden, Springer International Publishing, 2016; b) A. Siwoloboff, Ueber die Siedepunktbestimmung kleiner Mengen Flüssigkeiten, *Ber. Dtsch. Chem. Ges.* **19** (1886) 795–796; c) https://static1.buchi.com/sites/default/files/shortnotes/Short_Note_0.pdf.
- [10] O. Dimroth, W. Wislicenus, *Ber. Dtsch. Chem. Ges.* **1905**, *38*, 1573–1576.
- [11] A. Hassner, M. Stern, H. E. Gottlieb, F. Frolow, *J. Org. Chem.* **1990**, *55*, 2304–2306.
- [12] J. E. Huheey, *J. Phys. Chem.* **1965**, *69*, 3284–3289.
- [13] G. Schatte, H. Willner, M. Willert–Porada, *Magn. Reson. Chem.* **1992**, *30*, 118–123.
- [14] a) S. Voltrova, I. Putovny, V. Matousek, B. Klepetarova, P. Beier, *Eur. J. Org. Chem.* **2018**, 5087–5090; b) H. Bock, R. Dammel, *Inorg. Chem.* **1985**, *24*, 4427–4429.
- [15] a) F. A. Miller, D. Bassi, *Spectrochim. Acta* **1963**, *19*, 565–573; b) J. Goubeau, E. Allenstein, A. Schmidt, *Chem. Ber.* **1964**, *97*, 884–890; c) GAUSSIAN 09, revision C.01, G. W. T. M. J. Frisch, H. B. Schlegel, G. E. Scuseria, M. A. Robb, J. R. Cheeseman, G. Scalmani, V. Barone, B. Mennucci, G. A. Petersson, H. Nakatsuji, M. Caricato, X. Li, H. P. Hratchian, A. F. Izmaylov, J. Bloino, G. Zheng, J. L. Sonnenberg, M. Hada, M. Ehara, K. Toyota, R. Fukuda, J. Hasegawa, M. Ishida, T. Nakajima, Y. Honda, O. Kitao, H. Nakai, T. Vreven, J. A. Montgomery, Jr., J. E. Peralta, F. Ogliaro, M. Bearpark, J. J. Heyd, E. Brothers, K. N. Kudin, V. N. Staroverov, R. Kobayashi, J.

- Normand, K. Raghavachari, A. Rendell, J. C. Burant, S. S. Iyengar, J. Tomasi, M. Cossi, N. Rega, J. M. Millam, M. Klene, J. E. Knox, J. B. Cross, V. Bakken, C. Adamo, J. Jaramillo, R. Gomperts, R. E. Stratmann, O. Yazyev, A. J. Austin, R. Cammi, C. Pomelli, J. W. Ochterski, R. L. Martin, K. Morokuma, V. G. Zakrzewski, G. A. Voth, P. Salvador, J. J. Dannenberg, S. Dapprich, A. D. Daniels, Ö. Farkas, J. B. Foresman, J. V. Ortiz, J. Cioslowski, D. J. Fox, Gaussian, Inc., Wallingford, CT, 2009 ; d) E. E. Aynsley, N. N. Greenwood, M. J. Sprague, *J. Chem. Soc.* **1965**, 2395–2402; e) G. A. Crowder, *J. Mol. Struct.* **1971**, 7, 147–153.
- [16] a) A. Y. Yakubovich, V. A. Ginsburg, *Zh. Obshch. Khim.* **1958**, 28, 1031–1035; b) J. Gillis, *Chem. Weekbl.* **1918**, 15, 48–78.
- [17] a) A. R. Cherkasov, V. Galkin, R. Cherkasov, *J. Mol. Struct.: THEOCHEM* **1999**, 489, 43–46; b) J. Liu, *Nitrate Esters Chemistry and Technology*, Springer, Singapore **2019**, p. 446.; c) H. Liu, Q. Wang, L. Liu, *J. Chem. Educ.* **1992**, 69, 783–784; d) S. Balters, E. Bernhardt, H. Willner, T. Berends, *Z. Anorg. Allg. Chem.* **2004**, 630, 257–267; e) M. S. Matheson, W. A. Mulac, J. L. Weeks, J. Rabani, *J. Phys. Chem.* **1966**, 70, 2092–2099; f) A. F. Clifford, *J. Phys. Chem.* **1959**, 63, 1227–1231; g) A. Haas, *Adv. Inorg. Chem. Radiochem.* **1984**, 28, 167–202.
- [18] R. Steudel, *Chemie der Nichtmetalle: Synthesen – Strukturen – Bindung – Verwendung*, De Gruyter, **2013**.
- [19] P. E. Hansen, *Prog. Nucl. Magn. Reson. Spectrosc.* **1988**, 20, 207–255.
- [20] a) C. Wentrup, B. Gerecht, D. Laqua, H. Briehl, H. W. Winter, H. P. Reisenauer, M. Winnewisser, *J. Org. Chem.* **1981**, 46, 1046–1048; b) R. Bunnenberg, J. C. Jochims, *Chem. Ber.* **1981**, 114, 2075–2086.
- [21] H. Spencer, M. Lakshmikantham, M. Cava, *J. Am. Chem. Soc.* **1977**, 99, 1470–1473.
- [22] S. Voltrova, J. Filgas, P. Slavicek, P. Beier, *Org. Chem. Front.* **2019**, DOI: 10.1039/C9QO01295H.

7 Releasing the “Beast”: Direct, Silver Catalyzed Electrophile Monofluoromethylation

Marco Reichel,^[a] Burkhard Krumm,^[a] Andreas Kornath,^[a] Konstantin Karaghiosoff*^[a]

To be submitted

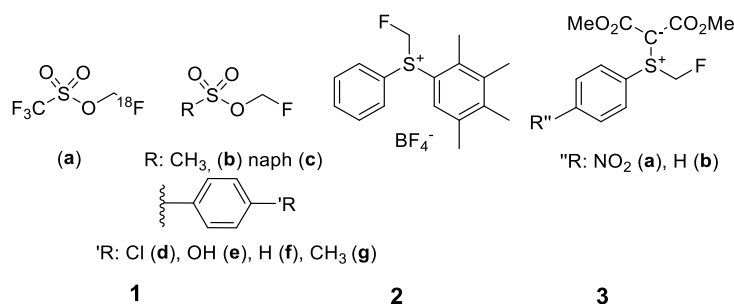


Abstract: Weak *O* and *S* nucleophiles have been monofluoromethylated using various silver salts in combination with fluoriodomethane. This combination has been shown to enable the

electrophilic introduction of the monofluoromethyl group to selected sulfonic acids and sulfones. The syntheses are performed under mild conditions and comprise a minimal number of steps. The resulting products are strong fluoromethylating agents themselves. The structures of two salts with fluoromethyl sulfonium cations have been determined.

7.1 Introduction

Fluorine - “a small atom with a big ego”^[1] - is since many years of great importance for the pharmaceutical and agrochemical industry.^[2] Due to the unique properties of fluorine containing organic molecules,^[3] such as a modified metabolic stability, some Australian and Brazilian plants have become deadly traps for living organisms.^[4] The pharmaceutical industry adopted this knowledge and combined it with Paracelsus' principle: the dose makes the poison.^[5] This resulted in a number of fluorinated drugs.^[3, 6] The monofluoromethyl unit is considered to be of particular importance because it is bioisosteric to a CH₂OH or CH₂NH₂ group. However, there is only a small number of reagents available, which are capable to transfer a CH₂F group to a nucleophile and which can be employed for the synthesis of fluorine containing drugs.^[1] Early studies concentrate on the use of the fluoromethyl halides CH₂FX (X = Cl, Br, I).^[3] CH₂FCl (FCM) and CH₂FBr (BFM) are used for pharmaceutical syntheses; in particular BFM is essential for the final step of the synthesis of Fluticasone.^[7] However these reagents show an ozone-depleting effect and according to the Montreal Protocol their use should be phased out successively;^[8] their future is therefore questionable. Fluoroiodomethane (FIM) is a good alternative: it does not show the ozone-depleting effect, it is less volatile than FCM and BFM and so easier to handle. However, a problem is represented by its limited stability: on storage, even at low temperatures, it slowly decomposes forming iodine. A general limitation of the fluoromethyl halides is also their weak alkylating power: weak nucleophiles like ethers, or anions like the perchlorate or sulfonate anion, cannot be fluoromethylated using CH₂FX (X = Cl, Br, I).^[9] Sulfonic acid derivatives (**1** Scheme 1) were developed as the first generation of strong and non ozone-depleting fluoromethylating reagents and were mainly used to synthesize ¹⁸F labeled radiopharmaceuticals.^[10] The fluoromethyl tosylate **1g** is able to fluoromethylate a large number of substrates^[11] and has been used to prepare L- and D-prolinamide derivatives as Ep300/CREBBP inhibitors^[11b] and OCH₂F containing BACE1 inhibitors.^[11] However, a special equipment and extremely harsh reaction conditions are required for the synthesis of **1** which makes their application limited, complicated and unattractive.^[1] Newer generations (e.g. **2** and **3**, Scheme 1) have a wider range of applications and have a stronger fluoromethylating power. Thus using the sulfonium salt **2**, **1d**, **e** and **f** can be prepared. *Prakash* et al. reported **2** as a suitable reagent for the synthesis of the drug Fluticasone and a series of sulfonic acid fluoromethyl esters as well as for the fluoromethylation of phosphines, amines and phenols.^[9] The *S*-Ylide **3** was used to prepare sulfonic acid fluoromethyl ester derivatives and fluoromethyl ethers and even the formation of C-CH₂F bond was possible with this reagent.^[1] However the sulfonium salt **2** and the *S*-ylides **3** are only available in multi-step syntheses^[1, 9, 12] and are therefore unattractive for industrial applications on a larger scale. Alternative syntheses of these fluoromethylating agents employing less steps and milder reaction conditions are desirable.

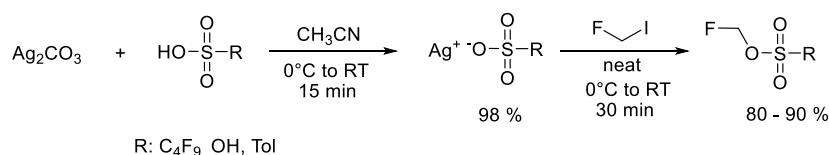


Scheme 1: Strong electrophilic monofluoromethylating agents with broad substrate scope and no ozone-depleting potential.

In the course of our systematic studies on the fluorine containing small molecules we observed, that FIM is activated by Ag^+ ions and under these conditions fluoromethylation of very weak nucleophiles like the perchlorate^[12] or nitrate^[13] anion is possible. Here we report on the combination of FIM and silver salts as a strong fluoromethylating agent operating under mild conditions, which is applicable to a broad range of substrates with different nucleophilicity. New fluoromethyl sulfonium salts as well as new sulfonic acid fluoromethyl esters become readily available using this protocol. The molecular and crystal structures of two fluoromethyl sulfonium cations are presented and offer first insight in weak interactions of *S*-bonded CH_2F groups in the solid state.

7.2 Results and Discussion

The synthesis of sulfonic acid fluoromethyl esters using Ag^+ /FIM is described in Scheme 2. The silver sulfonates are readily obtained from freshly prepared Ag_2CO_3 ^[15] and the respective acid. After drying in high vacuum they are added to an excess of fluoroiodomethane at 0 °C, and the reaction mixture is allowed to warm to ambient temperature.



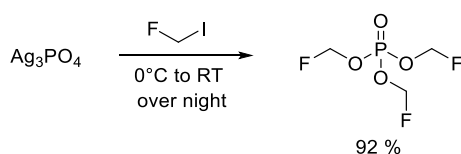
Scheme 2: Synthesis of sulfonic ester derivatives.

After removal of AgI by filtration and of the excess of FIM by distillation the fluoromethyl sulfonates are obtained analytically pure as colorless liquids in excellent yields (Table 1). The unreacted FIM is recovered and can be reused in further syntheses. As shown in Table 1, the conversion of the silver salts with fluoroiodomethane to the corresponding sulfonic acid fluoromethyl esters proceeds straight forward. In the same way silver phosphate yields on reaction with fluoroiodomethane the corresponding tris(fluoromethyl) ester (Scheme 3, entry 4).

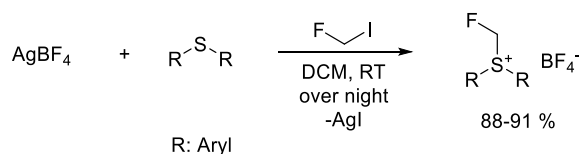
Table 1: Reaction of a corresponding silver salt with fluoroiodomethane.

entry	starting material	product	yield (%)
1			93
2			80
3			96
4			92

In the case of bis(trifluoromethylsulfon)amide, however, no definite product could be isolated. The reaction results in the formation of a precipitate, containing most probably among other compounds AgI, which was insoluble in common polar organic solvents.

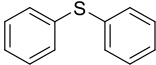
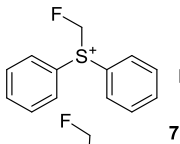
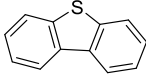
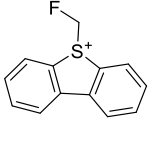
**Scheme 3:** Synthesis of tris(fluoromethyl) phosphate.

The system Ag^+/FIM can also be applied to synthesize fluoromethyl sulfonium salts (Table 2), starting from the corresponding diaryl thioether (Scheme 4). In this case freshly prepared AgBF_4 was used to activate fluoroiodomethane.

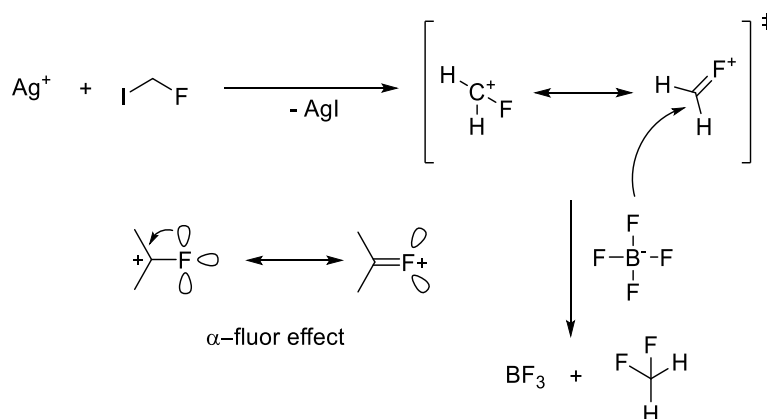
**Scheme 4:** Synthesis of fluoromethylated sulfonium salts.

The starting AgBF_4 must be completely free of acetonitrile residues, otherwise decomposition of the fluoromethyl sulfonium salt takes place.^[15] The reaction is performed in DCM over night. The product is precipitated as a colorless solid by addition of diethyl ether and is isolated in good yields (Table 2). The only reasonable solvent for the fluoromethyl sulfonium salts was found to be DCM. In acetonitrile, chloroform or acetone fast decomposition was observed.

Table 2: Reaction of selected aryloxyethers with fluoroiodomethane and AgBF₄ in a one pot synthesis.

entry	starting material	product	yield (%)
1			91
2			88

It was not possible to convert diphenyl ether to the corresponding fluoromethyl oxonium cation using the combination AgBF₄/CH₂FI. Although reaction with formation of a precipitate of AgI is clearly observed, formation of BF₃ and CH₂F₂ is shown by the ¹⁹F NMR spectrum. Obviously in this case fluoride from BF₄⁻ competes effectively for the CH₂F group, resulting in the formation of CH₂F₂. A possible pathway involving the CH₂F⁺ cation (isoelectronic to formaldehyde, stabilized through the α-fluorine effect^[16]) as a reactive intermediate is depicted in Scheme 5.

**Scheme 5:** Possible mechanism of the formation of BF₃ and CH₂F₂.

This mechanism is supported by the observation that reaction of AgBF₄ with CH₂FI in the absence of diphenyl ether also results in the formation of BF₃ and CH₂F₂. This anticipates the diphenyl fluoromethyl oxonium cation to be a very strong fluoromethylating reagent itself and to be stable only in combination with very weakly nucleophilic anions.

Single crystals of the sulfonium salts **7** and **8** were obtained by slow diffusion of Et₂O into a solution of the salt in DCM. The asymmetric units are shown in Figures 1 and 2. The salts **7** and **8** are the first crystallographically investigated sulfonium salts containing fluoromethyl sulfonium cations. In both cations the sulfur atom displays a pyramidal environment with the CSC angles smaller than the ideal tetrahedral angle (Figures 1 and 2). In the case of **7** the phenyl groups adopt a propeller like arrangement. The most interesting feature in the structure of both cations is the SCH₂F group. The S1-C13 bond length in **7** (1.813(3) Å) and **8** (1.841(4) Å) corresponds to a C_{sp3}-S(3) (1.804 Å) single bond and compares well to the S-CH₂F bond length

reported for the literature known fluoromethyl-phenylbis(carbomethoxy)methylide (**3b**) (1.818(2) Å). Thus, the presence of the methylide group seems not to affect this bond length.

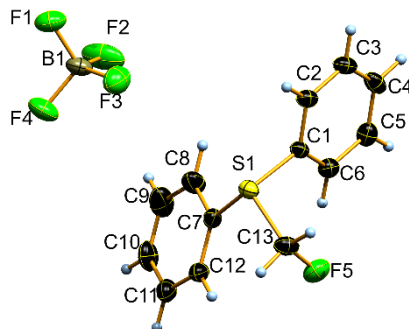


Figure 1: Asymmetric unit of (fluoromethyl)diphenylsulfonium tetrafluoroborate **4** in the solid state, DIAMOND representation, thermal ellipsoids shown at 50 % probability level.

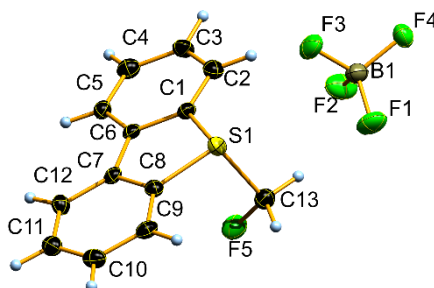


Figure 2: Asymmetric unit of (fluoromethyl)dibenzothiophenium tetrafluoroborate **5** in the solid state, DIAMOND representation, thermal ellipsoids shown at 50 % probability level.

A different behavior is observed for the C13-F5 bond length. While the length of this bond in **3b** (1.399(2) Å)^[11] compares well to the value of 1.399 Å (C_{sp^3} -F), reported in the literature for a typical C-F single bond,^[17] for **7** (1.356(3) Å) and **8** (1.365(4) Å) these distances are shortened. This can be viewed in terms of a negative hyperconjugation involving the lone pair at sulphur and the antibonding orbital of the C-F bond.^[18] This hyperconjugation is less pronounced in **4** and **5** as compared to **3b**.

In order to obtain information on weak interactions in the crystal structures of the salts **7** and **8** and in particular on the structural behavior of the SCH₂F unit, Hirshfeld analyses of the crystal structures have been performed. The related structure of **3b**^[11] has also been included in the analysis. For structures **7** and **8**, F \cdots H interactions represent the major part of all interactions (Figure 3).

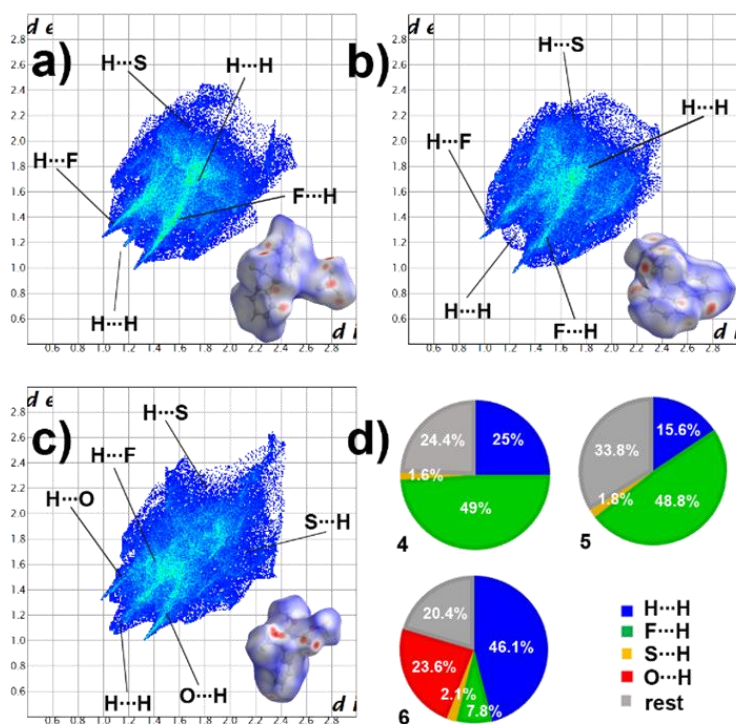


Figure 3: Two dimensional fingerprint plot as well as the corresponding Hirschfeld surface (bottom right in 2D plot) of **7** (a), **8** (b) and **3a** (c). Color coding: white, distance d equals VDW distance; blue, d exceeds VDW distance, red, d , smaller than VDW distance). Population of close contacts of **7**, **8** and **3a** in crystal stacking (d).

In the structure of ylide **3b**, F...H interactions account for only 7.8 %. In the structures of **4** and **5**, where two types of fluorine atoms are present, most of the F...H interactions involve the BF_4^- anion. The Hirschfeld surface of **7** and **8** indicates that only a small number of weak^[19] contacts are present around the fluorine atom of the CH_2F unit (less red dots). Most of the contacts result from the interaction of fluorine from BF_4^- with the protons of CH_2F and the protons of aryl groups (more red dots, Figure 3). The 2D fingerprint plot shows for stronger interactions two distinctive spikes. With respect to $d_i + d_e$ (d_i : distance from the Hirschfeld surface to the nearest atom interior; d_e : distance from the Hirschfeld surface to the nearest atom exterior), we can see that for **7**, more short H...F contacts are present than for **8**, although the sum of these interactions is in the same range for both compounds (49 % vs. 48.8 %). In the case of **3b**, however, which contains oxygen atoms, stronger O...H bridges are present (23.6 %). The shortest F...H contacts in the structures of **7** (2.331(2) Å) and **8** (2.33(4) Å) involve the protons of the CH_2F group and one fluorine atom of the BF_4^- anion. Weak hydrogen bonds involving the CH_2F protons were also observed in the structures of fluoromethyl phosphonium salts.^[2a] The intermolecular H...F interactions in compounds **7** and **8** (Table 3) similar strong than for those reported for compound **3a** (Table 3).^[1]

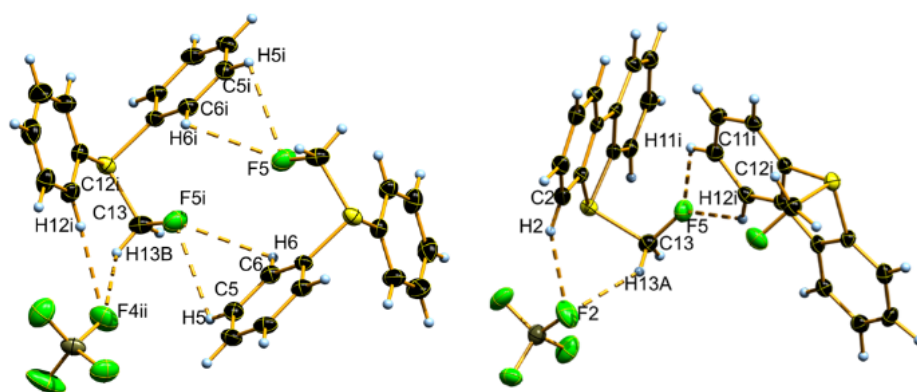


Figure 4: Hydrogen bonding in the crystal structure of compound **7** (left) and **8** (right), DIAMOND representation. Thermal ellipsoids are shown at 50 % probability level. Symmetry code left structure: *i*) -x, 1-y, 1-z; *ii*) -1+x, y, z. Symmetry code right structure: *i*) 2-x, 0,5+y, 1.5-z.

Table 3: Bond lengths [Å] and bond angles [°] of HF bridges in compound **3b**, **7** and **8**. Symmetry code for **3b**: *i*) 1+x, y, z. Symmetry code for **7**: *i*) -x, 1-y, 1-z; *ii*) -1+x, y, z. Symmetry code for **8**: *i*) 2-x, 0,5+y, 1.5-z.

Comp.	Bond	d(D-H)	d(H \cdots A)	d(D \cdots A)	< (D-H \cdots A)
3b	C13-F2 \cdots H1B ^{<i>ii</i>}	0.99	2.557(2)	3.348(3)	136.8(2)
4	C13-H13B \cdots F4 ^{<i>ii</i>}	0.99	2.330(2)	3.151(3)	139.7(2)
	C12 ^{<i>i</i>} -H12 ^{<i>i</i>} \cdots F4 ^{<i>ii</i>}	0.95	2.536(2)	3.475(4)	176.4(2)
	C5-H5 \cdots F5 ^{<i>i</i>}	0.95	2.880(2)	3.648(3)	105.3(2)
	C6-H6 \cdots F5 ^{<i>i</i>}	0.95	2.801(2)	3.203(4)	106.5(2)
	C5 ^{<i>i</i>} -H5 ^{<i>i</i>} \cdots F5	0.95	2.880(2)	3.261(4)	105.2(2)
5	C6 ^{<i>i</i>} -H6 ^{<i>i</i>} \cdots F5	0.95	2.800(2)	3.203(4)	106.5(2)
	C13-H13A \cdots F2	1.03(3)	2.33(4)	3.162(4)	137(2)
	C2-H2 \cdots F2	0.97(3)	2.43(3)	3.241(4)	142(2)
	C11 ^{<i>i</i>} -H11 ^{<i>i</i>} \cdots F2	0.96(3)	2.58(3)	3.21(4)	123(2)
	C12 ^{<i>i</i>} -H12 ^{<i>i</i>} \cdots F5	0.97(3)	2.49(2)	3.16(4)	127(2)

7.3 Conclusion

In summary, we have shown that the combination of a silver salt with fluoroiodomethane represents one of the strongest fluoromethylating agents known. Using this agent new sulfonic acid fluoromethyl esters have been prepared under mild conditions and with high yields. These esters are themselves strong monofluoromethylating agents. The methodology has been extended to the synthesis of new fluoromethyl sulfonium salts, which also are anticipated to act as fluoromethylating agents. For the first time molecular and crystal structures of fluoromethyl sulfonium cations have been determined and analyzed. A short C-F bond length is observed indicating that hyperconjugation involving the lone pair at sulfur is not effective in these cases. Hydrogen bonds account for most interactions in the crystal structures of the fluoromethyl sulfonium salts. These weak interactions involve the protons of the CH₂F moiety as well as some aryl protons and fluorine atoms of the BF₄⁻ anion.

7.4 Acknowledgement

Financial support by Ludwig–Maximilian University (LMU) is gratefully acknowledged. We are thankful to F–Select GmbH for a generous donation of fluoroiodomethane. The authors thank Prof. Dr. T. M. Klapötke, LMU, for the generous allocation of diffractometer time.

7.5 Experimental Section

7.5.1 General Procedure

All compounds were handled using *Schlenk* techniques under dry argon. Fluoroiodomethane (donation from F-Select GmbH) was distilled under inert conditions before use. All other chemicals were purchased from VWR and Sigma Aldrich and were used without further purification. Melting and / or decomposition points were measured with a Linseis DSC-PT10 instrument and with an OZM DTA 552-Ex instrument under inert atmosphere and ambient conditions, respectively. The samples for infrared spectroscopy were placed under ambient conditions without further preparation onto a Smith DuraSampLIR II ATR device and were measured with a Perkin Elmer BX II FR-IR System instrument. Samples for Raman spectroscopy were sealed in glass tubes. The measurement was carried out with a Bruker MultiRam FT Raman device using a neodymium doped yttrium aluminum garnet (Nd:YAG) laser ($\lambda = 1064$ nm) with 1074 mW. The samples for NMR spectroscopy were prepared under inert atmosphere using argon as protective gas. The solvents were dried using 3 Å mol sieve and stored under argon atmosphere. Spectra were recorded with a Bruker Avance III spectrometer operating at 400.1 MHz (^1H), 376.4 MHz (^{19}F), 100.6 MHz (^{13}C) and 161.9 MHz (^{31}P). Chemical shifts are referred to TMS ($^1\text{H}/^{13}\text{C}$), CFCl_3 (^{19}F) and 85% H_3PO_4 (^{31}P). All spectra were recorded at 299.15 K (26 °C). Elemental analyses were performed with an Elemental Vario EL Analyzer. The samples were prepared under N_2 atmosphere. High resolution MS data were acquired with a Jeol MStation Sectorfield in ESI / DEI mode. X-ray data were collected on single crystals with an Oxford Xcalibur 3 diffractometer equipped with a Spellman generator (50 kV, 40 mA) and a Kappa CCD detector, operating with $\text{Mo-K}\alpha$ radiation ($\lambda = 0.71073$ Å). Data collection and data reduction were performed with the CrysAlisPro software.^[20] Absorption correction using the multiscan method^[20] was applied. The structures were solved with SHELXS-97,^[21] refined with SHELXL-97^[22] and finally checked using PLATON.^[23] Details for data collection and structure refinement are contained in the supplementary information.

7.5.2 Preparation

Fluoromethyl-4-methylbenzene sulfonate (1g)

Freshly prepared silver carbonate^[15] (5.93 g, 21.5 mmol) was suspended in acetonitrile (15 mL). 4-Methylbenzene sulfonic acid (3.37 g, 19.6 mmol) was added dropwise at ambient temperature with stirring. The reaction mixture was stirred for 15 min when the evolution of CO_2 was complete. Remaining silver carbonate was filtrated off und the solvent was removed in *vacuo*. The silver salt thus obtained (5.35 g, 19.2 mmol) was added in small portions without further purification to cooled (0 °C) fluoroiodomethane (15 mL) while stirring. The reaction

mixture was allowed to warm up to room temperature and stirring was continued for 30 min. The precipitate of silver iodide was filtered off, the excess of fluoroiodomethane was distilled off yielding **1g** as a colorless liquid (3.64 g, 17.8 mmol). Yield 93 %; m.p. -8 °C; ¹H NMR (400.1 MHz, CDCl₃): δ=7.84 (A part of AA'BB', *N*=8.4 Hz, 2H; Ar-H), 7.36 (B part of AA'BB', *N*=8.4 Hz, 2H; Ar-H), 5.74 (d, ²*J*_{H,F}=51.0 Hz, 2H; CH₂F), 2.46 ppm (s, 3H; CH₃). ¹³C{¹H} NMR (100.6 MHz, CDCl₃): δ=145.7 (s; Ar), 134.0 (s; Ar), 130.1 (s; Ar), 128.1 (s; Ar), 98.3 (d, ¹*J*_{C,F}=231.0 Hz; CH₂F), 21.8 ppm (s, CH₃); ¹⁹F{¹H} NMR (376.4 MHz, CDCl₃): δ=-153.7 ppm (s; CH₂F); ¹⁹F NMR (376.4 MHz, CDCl₃): δ=-153.7 ppm (t, ²*J*_{F,H}=51.0 Hz; CH₂F); IR (ATR): ν=2998 (w), 1597 (m), 1494 (w), 1451 (w), 1368 (s), 1308 (w), 1294 (w), 1212 (w), 1192 (s), 1177 (s), 1146 (m), 1121 (w), 1095 (w), 1061 (m), 981 (s), 814 (m), 733 (s), 701 (m), 662 (s), 556 (s), 532 (s) cm⁻¹; Raman (1078 mW): ν=3072 (s), 3001 (m), 2929 (s), 1598 (m), 1483 (w), 1382 (w), 1310 (w), 1276 (w), 1194 (s), 1178 (w), 1147 (w), 1096 (w), 1067 (w), 818 (m), 747 (m), 702 (w), 666 (w), 635 (w), 560 (w), 440 (w), 382 (w), 287 (m) cm⁻¹; MS (70 eV): *m/z* (%): 204(40) [M]⁺, 155(80) [M-OCH₂F]⁺, 91(100) [M-SO₃CH₂F]⁺; HRMS (DEI): *m/z* (%) calcd for C₈H₉FO₃S: 204.0256 [M]⁺; found: 204.0244; elemental analysis calcd (%) for C₈H₉FO₃S: C 47.05, H 4.44, S 15.70; found: C 47.34, H 4.62, S 15.66.

Bis(fluoromethyl) sulfate (**4**)

Freshly prepared silver sulfate^[15] (3.00 g, 9.62 mmol) was added in small portions without further purification to cooled (0 °C) fluoroiodomethane (10 mL) with stirring. The reaction mixture was allowed to warm up to room temperature and stirring was continued for further 30 min. The precipitate of silver iodide was filtered off and the excess of fluoroiodomethane was removed *in vacuo*. Compound **4** was obtained as colorless liquid (1.25 g, 7.70 mmol). Yield 80 %; b.p. 32.5 °C (7.5·10⁻² mbar); The two fluorine atoms and the four hydrogen atoms form the A part and the X part of an [AX₂]₂ spin system. The two fluorine atoms and one carbon atom form the A part and the X part of an AA'X spin system. The spectra are shown in the supporting information. Only the large coupling constants have been estimated. ¹H NMR (400.1 MHz, CDCl₃): δ=5.79 ppm (d, ²*J*_{H,F}=49.8 Hz, 2H; CH₂F); ¹³C{¹H} NMR (100.6 MHz, CDCl₃): δ=100.1 ppm (d, ¹*J*_{C,F}=237.6 Hz; CH₂F); ¹⁹F{¹H} NMR (376.4 MHz, CDCl₃): δ=-154.4 ppm (s; CH₂F); ¹⁹F NMR (376.4 MHz, CDCl₃): δ=-154.4 ppm (t, ²*J*_{F,H}=49.8 Hz; CH₂F); IR (ATR): ν=3012 (w), 2950 (w), 1485 (w), 1429 (s), 1408 (s), 1276 (w), 1206 (s), 1150 (m), 1073 (s), 994 (s), 951 (s), 803 (s), 758 (s), 528 (w), 570 (m), 543 (s), 519 (m) cm⁻¹; Raman (1078 mW): ν=3067 (m), 3014 (s), 2950 (m), 2622 (w), 1488 (w), 1417 (w), 1276 (w), 1208 (s), 1150 (w), 1075 (w), 1003 (w), 765 (s), 577 (w), 548 (w), 453 (w), 408 (w), 371 (w), 316 (w) cm⁻¹; MS (70 eV): *m/z* (%): 161(10) [M]⁺, 113(100) [M-OCH₂F]⁺, 33(100) [CH₂F]⁺; HRMS (FAB⁺): *m/z* (%) calcd for C₂H₄F₂O₄S⁺: 161.9798 [M]⁺; found: 161.9826; elemental analysis calcd (%) for C₂H₄F₂O₄S: C 14.82, H 2.49, S 19.78; found: C 14.89, H 2.64, S 19.92.

Fluoromethyl-1,1,2,2,3,3,4,4,4-nonfluorobutane-1-sulfonate (**5**)

Freshly prepared silver carbonate^[15] (1.00 g, 3.63 mmol) was suspended in acetonitrile (15 mL). Nonfluorobutyl sulfonic acid (2.07 g, 6.89 mmol) was added dropwise with stirring. The reaction mixture was further stirred for 15 min when the evolution of CO₂ was complete. The remaining silver carbonate was filtrated off and the solvent was removed *in vacuo*. The silver salt thus prepared (1.45 g, 3.56 mmol) was added in small portions without further purification

to cooled (0 °C) fluoroiodomethane (5 mL) with stirring. The reaction mixture was allowed to warm to room temperature and stirred was continued for further 30 min. The precipitate of silver iodide was filtered off and the excess of fluoroiodomethane was distilled off yielding **5** as a colorless liquid (1.13 g, 3.41 mmol). Yield 96 %; m.p. -12 °C; b.p. 116 °C; $\rho(273\text{K})$ 1.69 g/cm³; ¹H NMR (400.1 MHz, CD₃CN): δ =6.00 ppm (d, ²J_{H,F}=48.5 Hz, 2H; CH₂F); ¹³C{¹H} NMR (100.6 MHz, CD₃CN): δ =117.6 (qtt, ¹J_{C,F}=288.4 Hz, ²J_{C,F}=32.8 Hz; ³J_{C,F}=1.5 Hz; CF₃), 114.9 (tt, ¹J_{C,F}=301.3 Hz, ²J_{C,F}=35.9 Hz; CF₂), 110.9 (tt, ¹J_{C,F}=296.1 Hz, ²J_{C,F}=32.2 Hz; CF₂), 109.5 (tqt, ¹J_{C,F}=271.1 Hz, ²J_{C,F}=39.8 Hz; ³J_{C,F}=1.8 Hz; CF₂CF₃), 103.4 ppm (d, ¹J_{C,F}=241.6 Hz; CH₂F); ¹⁹F{¹H} NMR (376.4 MHz, CDCl₃): δ =-81.5 (tt, ³J_{F,F}=9.9 Hz, ⁴J_{F,F}=2.3 Hz, 3F; CF₃), -111.6 (m, 2F; CF₂), -121.6 (m, 2F; CF₂), 126.4 (m, 2F, CF₂), -149.5 ppm (tt, ⁵J_{F,F}=8.7 Hz, ⁶J_{F,F}=1.5 Hz, 1F; CH₂F); ¹⁹F NMR (376.4 MHz, CDCl₃): δ =-80 (tt, ³J_{F,F}=9.9 Hz, ⁴J_{F,F}=2.3 Hz, 3F; CF₃), -111.6 (m, 2F; CF₂), -121.6 (m, 2F; CF₂), 126.4 (m, 2F, CF₂), -149.5 ppm (ttt, ²J_{F,H}=48.6 Hz, ⁵J_{F,F}=8.7 Hz, ⁶J_{F,F}=1.5 Hz, 1F; CH₂F); IR (ATR): ν =3080 (m), 2980 (m), 1642 (vw), 1589 (w), 1539 (vs), 1477 (s), 1459 (s), 1413 (m), 1393 (m), 1345 (s), 1292 (w), 1262 (m), 1245 (m), 1184 (s), 1102 (w), 1063 (m), 1034 (m), 998 (m), 909 (s), 821 (w), 786 (s), 716 (vs), 632 (m), 558 (w), 522 (w), 457 (w) cm⁻¹; Raman (1078 mW): ν =3079 (w), 2988 (m), 2942 (m), 2585 (w), 1592 (m), 1551 (m), 1459 (w), 1418 (w), 1370 (w), 1345 (s), 1295 (w), 1181 (w), 1106 (w), 1023 (m), 924.6 (w), 824.3 (w), 731.8 (w), 706.7 (w), 627.6 (w), 521.6 (w), 456.0 (m), 423.2 (m), 321.0 (m), 247.7 (w), 197.6 (s), 159.0 (m), 81.9 (m) cm⁻¹; elemental analysis calcd (%) for C₅H₂F₁₀O₃S: C 18.08, H 0.61, S 9.65; found: C 18.30, H 0.61, S 10.02.

Tris(fluoromethyl) phosphate (**6**)

Freshly prepared silver phosphate^[24] (2.39 g, 5.71 mmol) was added to cooled (0 °C) fluoroiodomethane (1.5 mL, 22.2 mmol) in one portion with stirring. The reaction mixture was warmed to room temperature and was stirred overnight. The precipitate of silver iodide was filtered off, washed with pentane (2 × 20 mL) and diethylether (2 × 20 mL) and from the combined filtrates the solvent and the excess of fluoroiodomethane was removed *in vacuo*. Compound **6** was obtained as a colorless liquid (1.02 g, 5.26 mmol). Yield 92 %; m.p. -81 °C; $\rho(273\text{K})$ 1.48 g/cm³; ¹H NMR (400.1 MHz, CD₃CN): δ =5.69 ppm (dd, ²J_{H,F}=50.3 Hz, ²J_{H,P}=16.9 Hz, 2H; CH₂F); ¹³C{¹H} NMR (100.6 MHz, CDCl₃): δ =97.9 ppm (dd, ¹J_{C,F}=228.2 Hz, ²J_{C,P}=5.9 Hz; CH₂F); ¹⁹F{¹H} NMR (376.4 MHz, CDCl₃): δ =-152.3 ppm (d; ³J_{F,P}=0.9 Hz; CH₂F); ¹⁹F NMR (376.4 MHz, CDCl₃): δ = -152.3 ppm (t, ²J_{F,H}=50.0 Hz, ³J_{F,P} not resolved; CH₂F); ³¹P{¹H} NMR (109.4 MHz, CDCl₃): δ =-4.9 ppm (s, ³J_{F,P} not resolved; POCH₂F); ³¹P NMR (109.4 MHz, CDCl₃): δ =-4.9 ppm (sept, ²J_{P,H}=16.9 Hz, ³J_{F,P} not resolved; POCH₂F); IR (ATR): ν =3018 (w), 2956 (w), 2923 (w), 2852 (w), 1729 (w), 1498 (w), 1432 (w), 1292 (s), 1159 (s), 1085 (s), 978 (s), 862 (s), 842 (s), 766 (m), 558 (m) cm⁻¹; Raman (1078 mW): ν =3056 (m), 3019 (s), 2957 (s), 2859 (m), 2836 (m), 2651 (w), 1499 (m), 1430 (w), 1279 (m), 1162 (w), 1121 (m), 1044 (m), 878.3 (w), 766.5 (m), 473.3 (w), 238.1 (w), 93.4 (m) cm⁻¹; MS (70 eV): *m/z* (%): 195(15) [M]⁺, 112(100) [M-OCH₂F-CH₂F]⁺; HRMS (DEI): *m/z* (%) calcd for C₃H₆F₃O₄P⁺: 193.9956 [M]⁺; found: 195.0043; elemental analysis calcd (%) for C₃H₆F₃O₄P: C 18.57, H 3.12; found: C 18.60, H 2.85.

(Fluoromethyl)diphenylsulfonium tetrafluoroborate (7)

Freshly prepared silver tetrafluoroborate^[15] (905 mg, 4.65 mmol) was dissolved in dichloromethane (3 mL) and diphenylsulfid (953 mg, 5.12 mmol) was added dropwise with stirring at ambient temperature. The black reaction solution was stirred at room temperature for 4 h and fluoroiodomethane (743 mg, 4.65 mmol) was added. The reaction mixture was refluxed overnight. The precipitate of silver iodide was filtrated off and washed with dichloromethane (2 × 5 mL) and the filtrate was triturated with diethylether (10 mL). The colorless crystals formed were filtrated off to give pure **7** (1.29, 4.23 mmol). Yield 91 %; m.p. 79 °C; ¹H NMR (400.1 MHz, CD₃CN): δ=7.88 (m, 4H; Ar-H), 7.81 (m, 2H; Ar-H), 7.72 (m, 4H; Ar-H), 6.57 ppm (d, ²J_{H,F}=46.5 Hz, 2H; CH₂F); ¹³C{¹H} NMR (100.6 MHz, CDCl₃): δ=135.1 (s; Ar), 131.7 (s; Ar), 131.68 (d; J_{C,F}=1.6 Hz; Ar), 121.0 (d, ³J_{C,F}=1.9 Hz; C_{ar}-S), 90.8 ppm (d, ¹J_{C,F}=243.6 Hz; CH₂F); ¹⁹F{¹H} NMR (376.4 MHz, CDCl₃): δ=-151.0 (s, 4F; BF₄); -208.2 ppm (s, 1F; CH₂F); ¹⁹F NMR (376.4 MHz, CDCl₃): δ=-151.0 (s, 4F; BF₄); -208.2 ppm (t, ²J_{F,H}=46.5 Hz, 1F; CH₂F); IR (ATR): ν=3103 (w), 3023 (w), 2965 (w), 1580 (w), 1479 (m), 1445 (m), 1311 (w), 1286 (w), 1229 (w), 1188 (w), 1166 (w), 1060 (s), 1021 (s), 992 (s), 946 (m), 847 (w), 756 (m), 746 (s), 700 (m), 680 (s), 652 (m), 611 (w), 520 (m), 508 (w) cm⁻¹; Raman (1078 mW): ν=3251 (w), 3077 (s), 3024 (w), 2963 (m), 1580 (m), 1455 (w), 1174 (w), 1080 (w), 1024 (m), 1001 (m), 766 (w), 654 (w), 613 (w), 389 (w), 281 (w), 217 (w), 124 (m) cm⁻¹; HRMS (FAB⁺): *m/z* (%) calcd for C₁₃H₁₂FS⁺: 219.0638 [M]⁺; found: 219.0663; elemental analysis calcd (%) for C₂H₄F₂O₄S: C 51.01, H 3.95; found: C 50.61, H 4.08.

(Fluoromethyl)dibenzothiophenium tetrafluoroborate (8)

To freshly prepared silver tetrafluoroborate^[15] (1.04 g, 5.35 mmol) dissolved in dichloromethane (20 mL) dibenzothiophene (0.987 g, 5.35 mmol) was added in one portion with stirring. After stirring the solution for 15 min, fluoroiodomethane (5.14 g, 32.1 mmol) was added dropwise within 30 min. The reaction mixture was stirred over night at room temperature, the precipitate was filtrated off and washed with dichloromethane (20 mL). The solvent of the filtrate was removed in vacuo until a solid started to precipitate. This mixture was poured onto diethylether (100 mL) and the colorless solid formed was filtered off, washed with diethylether (20 mL) and dried *in vacuo* to give pure **8** (1.43 g, 4.71 mmol). Yield 88 %; m.p. 78 °C; ¹H NMR (400.1 MHz, CD₃CN): δ=8.31 (d, ³J_{H,H}=8.0 Hz, 2H; Ar-H), 8.28 (d, ³J_{H,H}=8.0 Hz, 2H; Ar-H), 7.95 (t, ³J_{H,H}=8.0 Hz, 2H; Ar-H), 7.79 (t, ³J_{H,H}=8.0 Hz, 2H; Ar-H), 6.32 ppm (d, ²J_{H,F}=45.2 Hz, 2H; CH₂F); ¹³C{¹H} NMR (100.6 MHz, CD₃CN): δ=141.7 (s; Ar), 135.4 (s; Ar), 132.1 (s; Ar), 129.3 (s; Ar), 125.1 (s; Ar), 125.0 (d, ³J_{C,F}=2.8 Hz; Ar), 92.4 ppm (d, ¹J_{C,F}=246.0 Hz; CH₂F); ¹⁹F{¹H} NMR (376.4 MHz, CD₃CN): δ=-150.5 (s, 4F; BF₄), -280.3 ppm (s, 1F; CH₂F); ¹⁹F NMR (376.4 MHz, CD₃CN): δ=-150.5 (s, 4F; BF₄), -280.3 ppm (t, ²J_{F,H}=45.2 Hz, 1F; CH₂F); IR (ATR): ν=3098 (w), 3038 (w), 2967 (w), 1577 (w), 1450 (m), 1295 (w), 1232 (w), 1166 (w), 1028 (s), 884 (m), 757 (s), 705 (m), 634 (m), 519 (s), 460 (m), 425 (s) cm⁻¹; Raman (1078 mW): ν=3088 (w), 2966 (w), 1595 (m), 1485 (w), 1343 (w), 1311 (w), 1237 (w), 1168 (w), 1128 (w), 1028 (w), 765 (w), 699 (w), 636 (w), 498 (w), 462 (w), 402 (w), 295 (w), 240 (w), 202 (w), 125 (w) cm⁻¹; HRMS (ESI): *m/z* (%) calcd for C₁₃H₁₀FS⁺: 217.0482 [M]⁺; found: 217.04812; elemental analysis calcd (%) for C₂H₄F₂O₄S: C 51.35, H 3.31; found: C 51.06, H 3.51.

7.6 References

- [1] Y. Liu, L. Lu, Q. Shen, *Angew. Chem., Int. Ed.* **2017**, *56*, 9930–9934.
- [2] M. Reichel, J. Martens, E. Woellner, L. Huber, A. Kornath, K. Karaghiosoff, *Eur. J. Inorg. Chem.* **2019**, *2019*, 2530–2534.
- [3] J. Hu, W. Zhang, F. Wang, *Chem. Commun. (Cambridge, U. K.)* **2009**, 7465–7478.
- [4] a) D. O'Hagan, R. Perry, J. M. Lock, J. J. M. Meyer, L. Dasaradhi, J. T. G. Hamilton, D. B. Harper, *Phytochemistry* **1993**, *33*, 1043–1045; b) A. T. Proudfoot, S. M. Bradberry, J. A. Vale, *Toxicol. Rev.* **2006**, *25*, 213–219.
- [5] Paracelsus, *Das Buch Paragranum-Septem Defensiones*, Vol. 2, Holzinger, Darmstadt, **1965**.
- [6] a) N. A. Emokpare, *Dermatol Monatsschr* **1975**, *161*, 1019–1021; b) N. A. Meanwell, *J. Med. Chem.* **2018**, *61*, 5822–5880.
- [7] a) S. Cherkez, Chemagis Ltd., IL109656A, Israel, **1998**; b) Y. Qiu, Z. Wu, Y. Liu, S. Chen, H. Zhang, Amphastar Pharmaceuticals, Inc., WO2016054280A1, USA . **2016**.
- [8] R. J. Cicerone, R. S. Stolarski, S. Walters, *Science* **1974**, *185*, 1165–1167.
- [9] G. K. S. Prakash, I. Ledneczki, S. Chacko, G. A. Olah, *Org. Lett.* **2008**, *10*, 557–560.
- [10] a) P. Li, L. P. Wennogle, J. Zhao, H. Zheng, Intra-Cellular Therapies, Inc., WO2011043816A1, USA . **2011**; b) R. Iwata, S. Furumoto, C. Pascali, A. Bogni, K. Ishiwata, *J. Labelled Compd. Radiopharm.* **2003**, *46*, 555–566; c) G. Smith, Y. Zhao, J. Leyton, B. Shan, Q.-d. Nguyen, M. Perumal, D. Turton, E. Arstad, S. K. Luthra, E. G. Robins, E. O. Aboagye, *Nucl. Med. Biol.* **2011**, *38*, 39–51.
- [11] a) K. Nakahara, K. Fuchino, K. Komano, N. Asada, G. Tadano, T. Hasegawa, T. Yamamoto, Y. Sako, M. Ogawa, C. Unemura, M. Hosono, H. Ito, G. Sakaguchi, S. Ando, S. Ohnishi, Y. Kido, T. Fukushima, D. Dhuyvetter, H. Borghys, H. J. M. Gijzen, Y. Yamano, Y. Iso, K.-i. Kusakabe, *J. Med. Chem.* **2018**, *61*, 5525–5546; b) H. Naito, Y. Kagoshima, H. Funami, A. Nakamura, M. Asano, M. Haruta, T. Suzuki, J. Watanabe, R. Kanada, S. Higuchi, K. Ito, A. Egami, K. Kobayashi, Daiichi Sankyo Company, Limited, WO2018235966A1, Japan . **2018**.
- [12] M. Reichel, B. Krumm, K. Karaghiosoff, *J. Fluorine. Chem.* **2019**, *226*, 109351.
- [13] M. Reichel, B. Krumm, Y. Vishnevskiy, S. Blomeyer, J. Schwabedissen, H. Stammeler, K. Karaghiosoff, N. Mitzel, *Angew. Chem. Int. Ed.* **2019**, 18557–18561.
- [14] Y. Nomura, E. Tokunaga, N. Shibata, *Angew. Chem., Int. Ed.* **2011**, *50*, 1885–1889, S1885/1881-S1885/1140.
- [15] G. Brauer, *Handbuch der präparativen anorganischen Chemie*, F. Enke, **1975**.
- [16] P. Kirsch, *Modern Fluoroorganic Chemistry: Synthesis, Reactivity, Applications*, Wiley, **2006**.
- [17] O. K. Frank H. Allen, David G. Watson, Lee Brammer, A. Guy Orpen and Robin Taylor, *J. Chem. Soc., Perkin Trans. 2* **1987**, 1–19.
- [18] K. Uneyama, *Organofluorine Chemistry*, Wiley, **2008**.
- [19] T. Steiner, *Angew. Chem., Int. Ed.* **2002**, *41*, 48–76.
- [20] Program package CrysAlisPro 1.171.38.46 Rigaku OD, **2015**.
- [21] G. M. Sheldrick, SHELXS-97: Program for Crystal Structure Solution, University of Göttingen, Germany, **1997**.

- [22] G. M. Sheldrick, SHELXL-97: Program for the Refinement of Crystal Structures, University of Göttingen, Germany, **1997**.
- [23] A. L. Spek, PLATON: A Multipurpose Crystallographic Tool, Utrecht University, Utrecht, The Netherlands, **1999**.
- [24] T. L. Brown, B. E. Bursten, H. E. LeMay, *Chemie: Studieren kompakt*, Pearson, Higher Education, **2011**.

7.7 Supporting Information

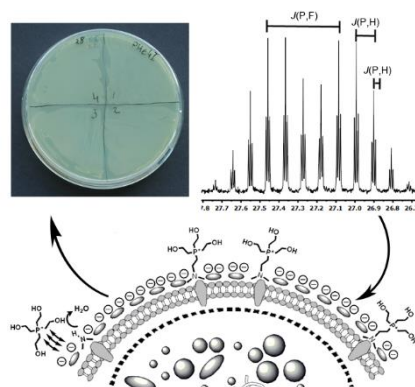
Table 1: Structure refinement data of compound **4** (left) and compound **5** (right).

Empirical formula	C ₁₃ H ₁₂ B F ₅ S	C ₁₃ H ₁₀ B F ₅ S
Formula weight	306.10	304.08
Temperature	123(2) K	146(2) K
Wavelength	0.71073 Å	0.71073 Å
Crystal system	Monoclinic	Monoclinic
Space group	<i>P</i> 2 ₁ / <i>n</i>	<i>P</i> 2 ₁ / <i>c</i>
Unit cell dimensions	a = 11.4241(11) Å b = 7.8553(5) Å c = 15.2360(11) Å α = 90° β = 106.105(9)° γ = 90°	a = 9.4454(8) Å b = 11.3178(7) Å c = 12.1478(10) Å α = 90° β = 107.778(9)° γ = 90°
Volume	1313.62(19) Å ³	1236.60(18) Å ³
Z	4	4
Density (calculated)	1.548 mg/m ³	1.633 mg/m ³
Absorption coefficient	0.290 mm ⁻¹	0.308 mm ⁻¹
F(000)	624	616
Crystal size	0.100 x 0.100 x 0.100 mm ³	0.100 x 0.100 x 0.100 mm ³
Theta range for data collection	4.427 - 28.277°	3.523 - 26.372°
Index ranges	-14 ≤ h ≤ 5, -9 ≤ k ≤ 10, -20 ≤ l ≤ 20	-11 ≤ h ≤ 11, -13 ≤ k ≤ 14, -15 ≤ l ≤ 13
Reflections collected	11642	7958
Independent reflections	3255	2525
Goodness-of-fit on F ²	1.036	0.996
Final R indices [I > 2σ(I)]	R ₁ = 0.0573, wR ₂ = 0.0961	R ₁ = 0.0557, wR ₂ = 0.0790
R indices (all data)	R ₁ = 0.1086, wR ₂ = 0.1185	R ₁ = 0.1111, wR ₂ = 0.0984
Largest diff. peak and hole	0.372 and -0.325 e Å ⁻³	0.372 and -0.325 e Å ⁻³

8 Synthesis and Investigation of Quarternary Phosphonium Salts Containing the Bioisoster -CH₂F Moiety

Marco Reichel, Cornelia Unger, Sviatlana Dubovnik, Andreas Roidl, Andreas Kornath and Konstantin Karaghiosoff*

Submitted to *Chem. – Eur. J.*



Abstract: Tertiary alkyl, aryl or amino phosphines PR₃ (R = Me, *n*Bu, C₂H₄CN, NEt₂) and the bis(phosphine) POP were allowed to react with fluoroiodomethane to produce fluoromethyl phosphonium salts in yields between 60 - 99 %. The compounds were characterized by vibrational and NMR spectroscopy and in most cases also by single crystal X-ray diffraction. Diphenyl(fluoromethyl) phosphine was synthesized as a mixed aryl-alkyl-phosphine and the TEP value (Tolman electronic parameter) was determined in order to explain its low reactivity. The molecular and crystal structures of the new fluoromethyl phosphonium salts [R₃PCH₂F]I with R = Me, C₂H₄CN and NEt₂ as well as of the salt resulting from the fluoromethylation of POP provided additional information on the structural behavior of the bioisoster CH₂F group bonded to phosphorus. Hydrogen bonding in the crystal is compared with that observed in the crystal structure of PPh₃CH₂FI. The toxicity of the sufficiently water soluble salt [Me₃PCH₂F]I was investigated and the toxicological effect of the CH₂F group was compared to that of the bioisoster CH₂OH group in THPS.

8.1 Introduction

Phosphonium salts are a long known class of compounds and widely used by chemists, e. g. as starting materials for *Wittig* reactions.^[1] Fluoromethyl phosphonium salts have been described to serve as precursors for the synthesis of fluoroolefines,^[2] and have also been employed to simple transfer the fluoromethyl group to other substrates.^[3] This property of fluoromethyl phosphonium salts is particularly interesting for the preparation of biological active compounds, due to the bioisosteric properties of the CH₂F group.^[3b,4] In the course of our recent systematic investigations on fluoromethylating agents we experienced that very little is known on the structural properties of CH₂F bonded to phosphorus.^[3a] This prompted us to investigate some more phosphonium salts, containing the PCH₂F structural motive. In addition to the fluoromethylating ability and the use for the synthesis of fluoroolefines the biological activity

and in particular the toxicity of fluoromethyl phosphonium salts is of interest.^[5] It is known that phosphonium salts containing the bioisosteric CH₂OH group can have a biocidal effect on biofilms and in particular tetrakis(hydroxymethyl) phosphonium sulfate (THPS) is widely used as biocide in oil pipelines and/or oil fields as well as in the paper producing industry against gram negative bacteria.^[6] Considering the opposite charges of phosphonium cations and gram negative bacteria, it is not surprising that the mechanism of interaction is based on a strong electrostatic interaction. The mode of action can be described in such a way, that the proteins of the membrane wall of the bacteria will react with the CH₂OH groups of THPS to form CH₂NR₂ with cleavage of water. This event damages the structure of the bacteria and as consequence nonspecific increase of cell permeability or abnormal morphology cause lysis (Figure 1).^[7]

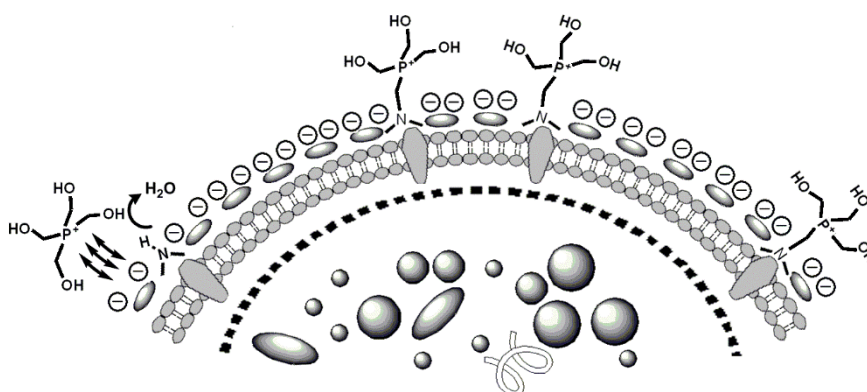


Figure 1: Mechanism of interaction and mode of action of THPS with the cell wall of gram negative bacteria.

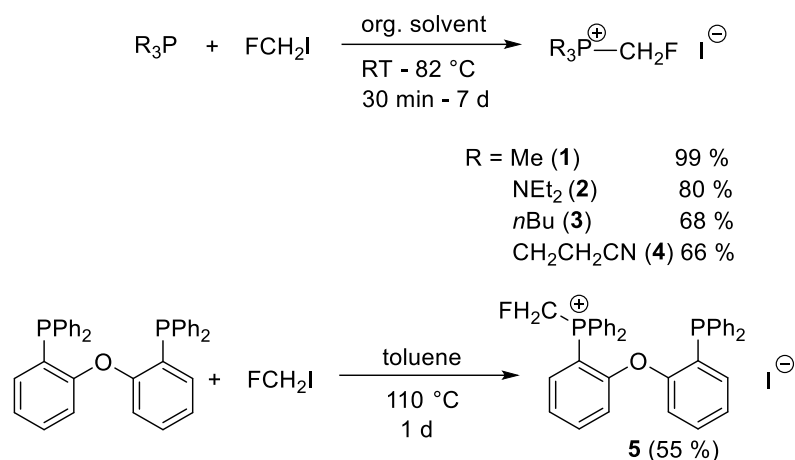
It is already known from warfare agents of the G series (Sarin, Cyclosarin, Soman) that also strong element fluorine bonds can be cleaved by organisms under formation of HF.^[8] This prompted us to investigate, the toxicity of the most water soluble phosphonium salt, [Me₃PCH₂F]I, in particular regarding a possible cleavage of the C-F bond on hydrolysis under biological conditions with formation of toxic HF.

8.2 Results and Discussion

The new trifluoromethyl phosphonium salts **1-5** were prepared by reaction of the respective phosphines with CH₂FI (Scheme 1). The phosphonium salts **1-5** are isolated as colorless crystalline air stable solids. Except **1** they are quite poorly soluble in water and readily soluble in polar aprotic solvents like MeCN, DCM or THF.

The challenge of phosphine fluoromethylation with CH₂FI is represented by the reaction rate, which is in part quite slow, and by the choice of proper reaction conditions. In fact, already small deviation from the selected reaction conditions leads to the formation of byproducts, which are difficult to separate. In general fluoromethylation with CH₂FI is more difficult than methylation with CH₃I.^[9] Reaction time, necessary for complete reaction, strongly depends on the substituents at phosphorus. Fluoromethylation is fast (30 min/-78 °C) in the case of Me₃P and much slower in the case of *n*Bu₃P (32 h/35 °C) or bis(phosphine) POP (24 h/110 °C). Thus the electron donor ability of the phosphine seems to play an important role. Considering the

long reaction time needed for the fluoromethylation of triphenyl phosphine the reaction of the new alkyl / aryl substituted fluoromethyldiphenylphosphine **6** with CH₂FI was investigated.



Scheme 1: Synthesis of fluoromethylphosphonium iodides **1** – **5**.

Phosphine **6** is readily prepared starting from diphenylphosphine by lithiation and subsequent fluoromethylation with CH₂FI (Scheme 2). Unfortunately, further reaction of **6** with CH₂FI under different conditions did not yield the corresponding bis(fluoromethyl) phosphonium salt. Either no reaction or the formation of several unidentified phosphorus containing products at elevated temperatures was observed.

In order to characterize phosphine **6** with respect to its donor ability its *Tolman* electronic parameter (TEP) was determined (Figure 2).^[10] In the series of phosphines the donor properties for **6** are similar to those for Ph₂PMe and Ph₃P, which explains its low tendency to form the phosphonium salt.

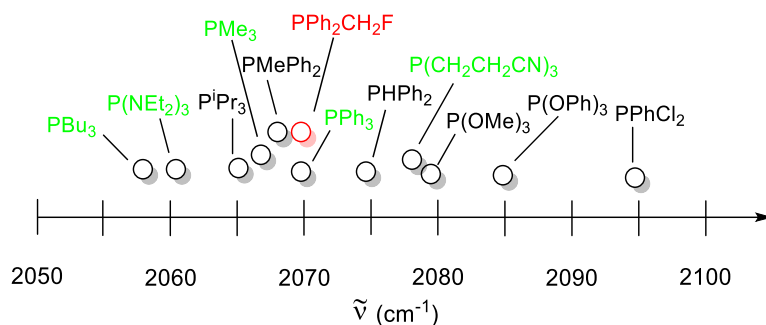


Figure 2: TEP value of PPh₂CH₂F compared to the used and common phosphines.

The fluoromethyl phosphonium salts **1-5** have lower melting points and lower decomposition points as compared to the corresponding methyl derivatives.^[11] The same trend has been reported for [Ph₃PCH₂F]BF₄ as compared to [Ph₃PCH₃]BF₄.^[12]

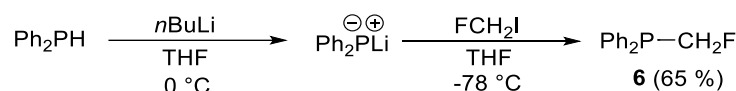
While the ³¹P chemical shifts of the phosphonium salts **1-5** reflect also the influence of the other three substituents at phosphorus the P-bonded CH₂F group displays characteristic ¹H, ¹³C and ¹⁹F chemical shifts and coupling constants (Table 1). The ¹H, ¹³C and ¹⁹F NMR signals of P-CH₂F in **1-5** are typically found in the quite narrow ranges of 5 – 6 ppm, 76 – 78 ppm and -240 – -250 ppm, respectively. Also for the coupling constants ¹J_{CF} (180 – 190 Hz), ²J_{PF} (50 – 60 Hz) and ²J_{FH} (44 – 46 Hz) characteristic ranges are observed. The coupling of phosphorus to

the proton of CH₂F is very small (< 1 Hz), in contrast to ²J_{PH} to the protons of the other alkyl substituents at phosphorus in **3** and **4**.

Table 1: Chemical shifts and coupling constants for the CH₂F group in the fluoromethyl phosphonium salts **1-5**.

	Chemical shift			Coupling constant		
	¹ H	¹³ C	¹⁹ F	¹ J(C,F)	² J(P,F)	² J(F,H)
1	5.44	77.1	-242	183.8	60.3	45.3
2	5.77	78.2	-241	182.6	59.9	45.9
3	5.92	76.1	-247	190.4	51.6	45.9
4	5.85	76.8	-249	188.3	56.8	44.8
5	6.28	---	-240	---	62.2	46.0
6	5.28	84.6	-230	199.9	114.0	49.0

Only in the case of **1** a ²J_{PH} coupling of 1.6 Hz to the CH₂ protons of CH₂F was clearly observed. This effect is obviously due to the fluorine atom, as impressively shown by the ³¹P NMR spectrum of **1** (Figure 3, top). Coupling of phosphorus to the methyl protons (15.0 Hz) is much larger than ²J_{PH} to the methylene protons (1.6 Hz); both are smaller than ²J_{PF} of 45.3 Hz. These couplings cause splitting of the ³¹P NMR signal of **1** to the well resolved multiplet shown in Figure 3 (top). In the ¹⁹F NMR spectrum of **1** a doublet of triplets due to coupling of ¹⁹F with ³¹P and with ¹H of the CH₂F group is observed. Each of the resulting six lines is further splitted by long range coupling of ¹⁹F to ¹H of the methyl groups over four bonds (Figure 3 bottom). The NMR data of the CH₂F group fit well to those reported for [Ph₃PCH₂F]BF₄.^[13]



Scheme 2: Synthesis of fluoromethyldiphenylphosphine **6**.

Single crystals, suitable for X-ray diffraction studies were obtained for compound **1**, **2**, **4** and **5**. Compound **1** crystallizes in the orthorhombic space group *Pnma* with one formula unit in the unit cell. The asymmetric unit is shown in Figure 4. The fluoromethyl group is disordered almost equally over two positions. The phosphorus displays a tetrahedral surrounding. The P,C distance to the CH₂F group (1.792(2) Å) compares well to that in the tetramethyl phosphonium cation (1.783(2) Å).^[14] and seems to be somewhat shorter as compared to the corresponding distance in [Ph₃PCH₂F]I (1.810(4) Å)^[3a] and to the P,C distance in P(CH₂OH)₄⁺ (1.809(6) Å)^[15]. The C,F bond length (1.369(5) Å) is in the expected range.^[3a, 14a] In the crystal weak interactions involving the iodide anion and the fluorine atom are observed (Figure 5). A weak hydrogen bond F⋯H (2.489(4) Å)^[16] between the fluorine atom and one of the methyl hydrogen atoms of a second phosphonium cation leads to the formation of chains. Similar interactions have been reported also for the crystal structure of Ph₃PCH₂FI.^[3a]

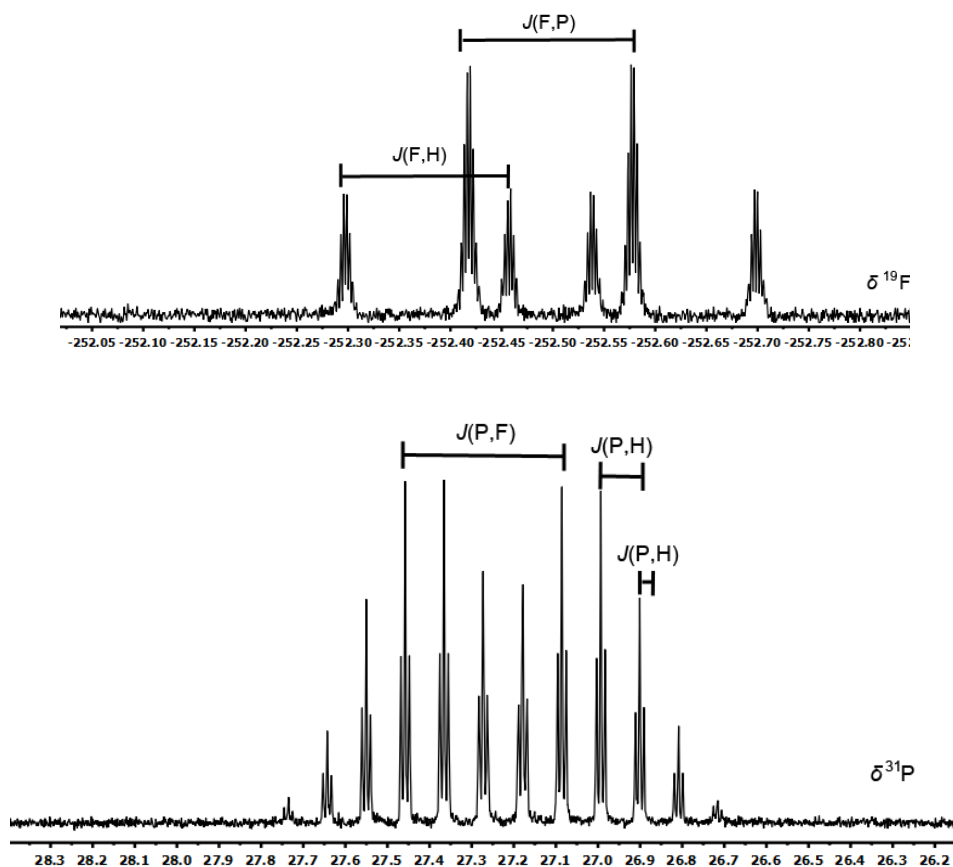


Figure 3: ^{31}P NMR spectrum (top) and ^{19}F NMR spectrum (bottom) of **1** in CDCl_3 .

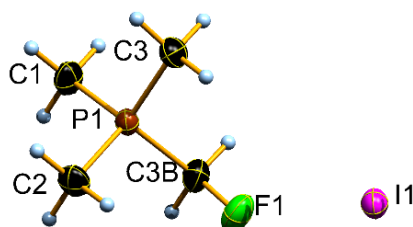


Figure 4: Molecular structure of compound **1** in the crystal; DIAMOND representation, thermal ellipsoids shown at 50 % probability level. The CH_2F group is disordered over two positions; only one of the positions is shown.

The iodide anions are located between the chains and display weak $\text{I}\cdots\text{H}$ interactions ($3.14(2)$ Å)^[17] to hydrogen atoms of the CH_2F group (Figure 5). Compound **2** crystallizes in the triclinic space group $P\bar{1}$ with two formula units in the asymmetric unit (Figure 6). The phosphorus atom shows in both cases a distorted tetrahedral surrounding, similar to that observed in the $\text{P}(\text{NEt}_2)_3\text{CH}_3^+$ cation.^[18] The ethyl units are twisted with respect to each other.

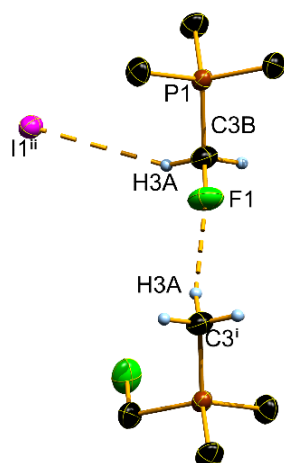


Figure 5: Hydrogen bonding in the crystal structure of compound **1**. Only one of the two positions of the CH₂F group and only the relevant hydrogen atoms are shown. DIAMOND representation, thermal ellipsoids shown at 50 % probability level. Symmetry code: *i*: 1-x, 1-y, 1-z; *ii*: -0.5+x, 0.5-y, 0.5-z.

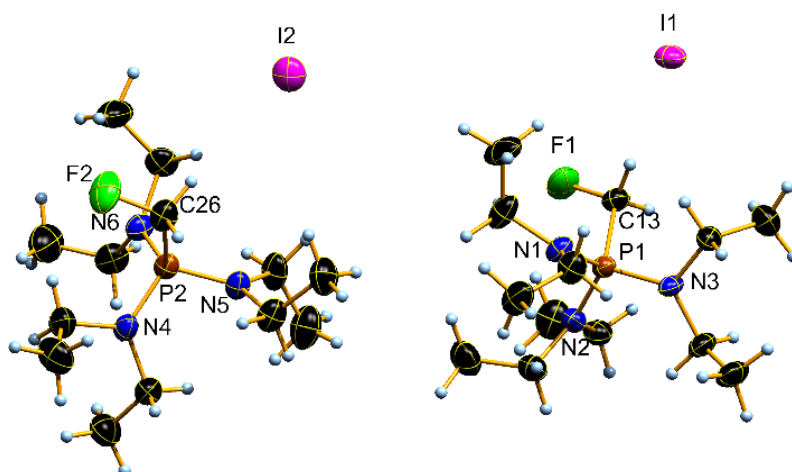


Figure 6: Molecular structure of compound **2** in the crystal, DIAMOND representation, thermal ellipsoids shown at 50 % probability level.

While the C13-F1 (1.378(4) Å) and C26-F2 (1.393(4) Å) distances are in the expected range, the P1-C13 (1.824(3) Å) and P2-C26 (1.813(4) Å) distances are elongated as compared to those in the P(NEt₂)₃CH₃⁺ cation (1.783(3) Å)^[18] and in **1**. Similar to **1**, compound **2** also shows weak intermolecular CH...F and CH...I interactions (Table 2), as already reported for [PPh₃CH₂F]I.^[3a, 16] The CH...F interactions (Figure 7) favor an arrangement of the cations in the crystal to form chains, which are interconnected by the iodide anions through CH...I hydrogen bonds. Compound **4** crystallizes in the monoclinic space group *P21/c*. The asymmetric unit is shown in Figure 8. Atom distances and bond angles of phosphonium salt **4** are as expected. The C1-F1 distance (1.384(2) Å) compares well to those found for the fluoromethyl phosphonium salts **1** and **2** and seems to stay unaffected by the other substituents at phosphorus.

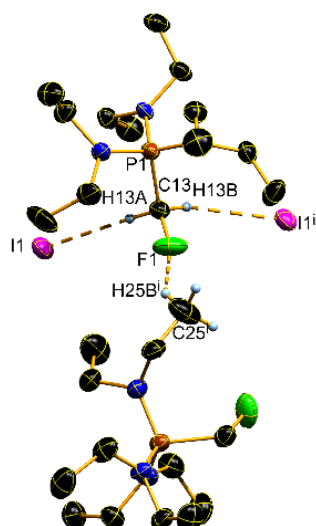


Figure 7: Hydrogen bonding in the crystal structure of compound 2. Only the relevant hydrogen atoms are shown. DIAMOND representation, thermal ellipsoids shown at 50 % probability level. Symmetry code: *i*: 1-x, 1-y, -z; *ii*: 1-x, 1-y, 1-z.

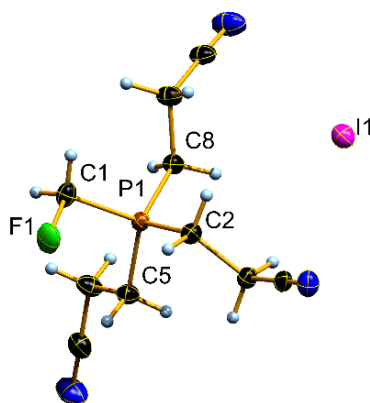


Figure 8: Molecular structure of compound 4 in the crystal; DIAMOND representation; thermal ellipsoids drawn at 50 % probability level.

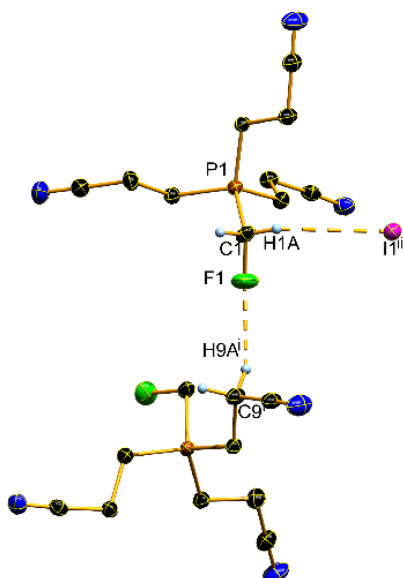


Figure 9: Hydrogen bonding in the crystal structure of compound 4. Only the relevant hydrogen atoms are shown. DIAMOND representation, thermal ellipsoids shown at 50 % probability level. Symmetry code: *i*: 1-x, -0.5+y, 1.5-z; *ii*: 1-x, 1-y, 1-z.

In the crystal weak intermolecular CH \cdots F interactions between the cations involving the CH₂CN hydrogen atoms and CH \cdots I interactions between the cations and the iodide anions involving the hydrogen atoms of the CH₂F group are observed (Figure 9). They result in a similar arrangement of cations and anions as found for phosphonium salts **1** and **2**.

Phosphonium salt **5** crystallizes in the triclinic space group *P*-1. The asymmetric unit, shown in Figure 10 contains one molecule of water.

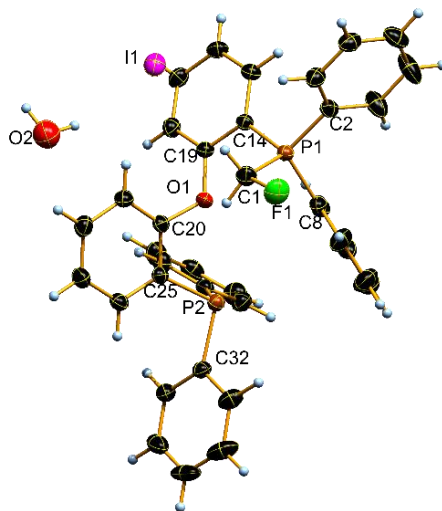


Figure 10: Molecular structure of compound **5** in the solid state, DIAMOND representation, thermal ellipsoids shown at 50 % probability level.

The phosphorus atom P1 in the cation of **5** carrying the CH₂F group displays a distorted tetrahedral environment, while the arrangement around P2 is pyramidal (sum of CPC angles 304.3°). As expected, CPC angles at P2 (100.6(2)-102.3(2)°) are smaller as compared to CPC angles at P1 (108.6(2)-111.4(2)°). The aryl substituents at both phosphorus atoms are rotated around the PC-axis to adopt a propeller-like arrangement. Atom distances and bond angles of the P-CH₂F unit fit well to those found for the fluoromethyl phosphonium salts **1**, **2** and **4**. In the crystal the arrangement of cations and anions is governed by weak OH \cdots I, CH \cdots I and CH \cdots F hydrogen bonds (Figure 11, Table 2). Weak CH \cdots F interactions favor the formation of dimers and involve one hydrogen atom of each CH₂F group. The second hydrogen atom undergoes CH \cdots I hydrogen bonding to one iodide anion. The resulting aggregates are interconnected by OH \cdots I hydrogen bonds to form chains with the water molecules acting as bridges.

In order to obtain a more precise analysis of the intermolecular interactions in the crystal of the fluoromethyl phosphonium salts, fingerprint plots and Hirshfeld surfaces were created for compounds **2**, **4** and **5**. Phosphonium salt **1** has been omitted due to the disorder in the crystal. The red dots on the Hirshfeld surfaces indicate contacts between layers (Figure 12).

The sum $d_i + d_e$ (d_i : distance from the Hirshfeld surface to the nearest atom interior; d_e : distance from the Hirshfeld surface to the nearest atom exterior) indicates that all H \cdots I interactions in the structures of **2**, **4** and **5** are weak. As can be seen from the width of the flanks in plots a) - c) (Figure 12) the number of hydrogen bonds to I decrease in the order **4** > **2** > **5**. The more pronounced spikes for H \cdots F contacts in the case of **4** (plot b), Figure 12) indicates for this compound the greatest number of hydrogen bonds involving fluorine. The absence of

such spikes in the case of **5** (plot c), Figure 12) is representative for less H...F interactions in the crystal, which is in accord with the formation of isolated dimers. The sum of $d_i + d_e$ also shows, that the H...F interactions are weak.

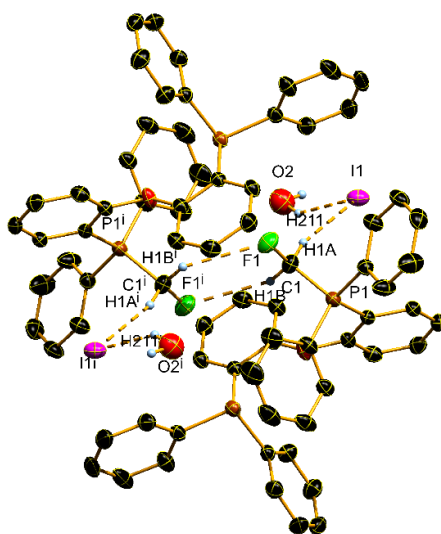


Figure 11: Hydrogen bonding in the crystal structure of compound **5**. Only the relevant hydrogen atoms are shown. DIAMOND representation, thermal ellipsoids shown at 50 % probability level. Symmetry code: $i -x, 1-y, 1-z$.

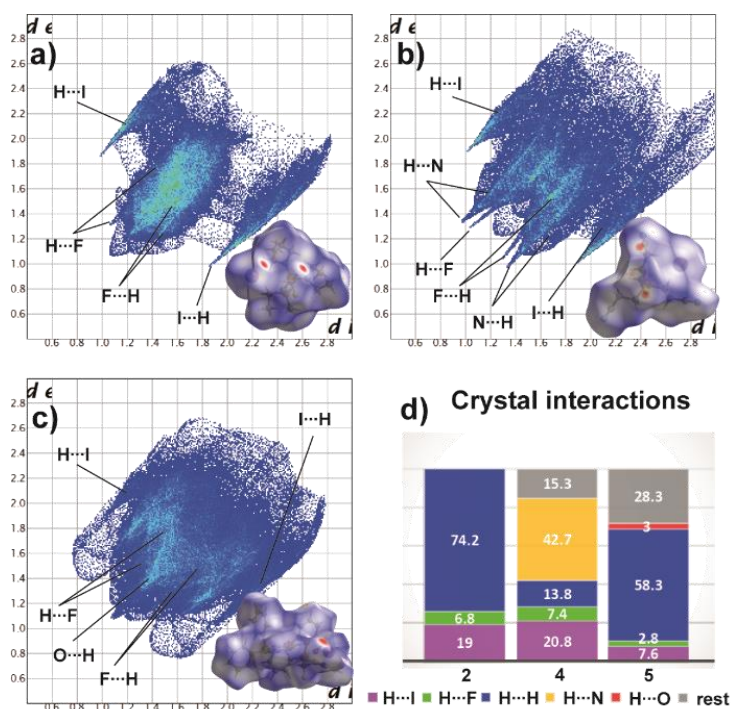


Figure 12: Two dimensional fingerprint plot and the corresponding Hirshfeld surface (bottom right in 2D plot) for **2** (a), **4** (b) and **5** (c). Color coding: white, distance d equals VdW distance; blue, d exceeds VdW distance, red, d , smaller than VdW distance). Population of close contacts of **2**, **4** and **5** in crystal is shown in plot d).

Single crystals of (fluoromethyl)diphenyl phosphine oxide (**6**) was collected from an NMR tube originally containing the phosphine dissolved in CDCl_3 . The compound crystallizes in the space group $P-1$ with four crystallographically independent molecules in the asymmetric unit (Figure 13).

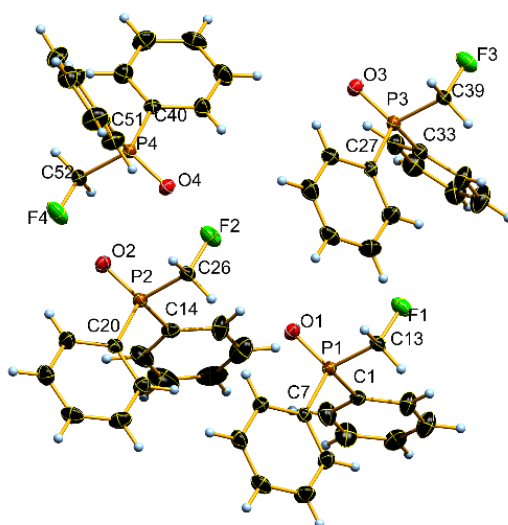


Figure 13: Molecular structure of (fluoromethyl)diphenyl phosphine oxide in the crystal. DIAMOND representation, thermal ellipsoids shown at 50 % probability level.

The phosphorus atom shows in all four molecules a distorted tetrahedral arrangement of the substituents. The phenyl groups are slightly twisted against each other. The P-CH₂F distances (P1-C13: 1.815(2) Å; P2-C26: 1.817(2) Å; P3-C39: 1.813(2) Å; P4-C52: 1.817(2) Å) are slightly elongated as compared to that in diphenylmethyl phosphine oxide (1.790(3) Å)^[19] and similar to that reported for diphenyl hydroxymethyl phosphine oxide (1.816(2) Å)^[20]. The C-F bonds (C13-F1: 1.398(2) Å; C26-F2: 1.393(2) Å; C39-F3: 1.390(2) Å; C52-F4: 1.383(3) Å) fit well to those observed for the phosphonium salts **1**, **2** and **4** and are obviously not influenced by phosphorus coordination. In the crystal one intramolecular and two weak intermolecular H···F contacts to aromatic CH hydrogen atoms are observed (Figure 14, Table 2).

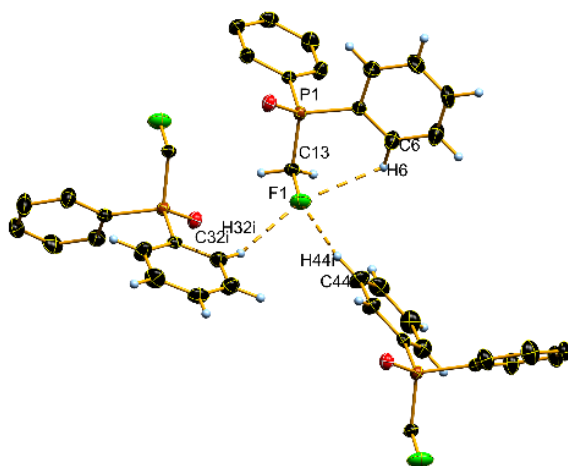


Figure 14: Hydrogen bonding in the crystal structure of fluoromethyl diphenyl phosphine oxide. For a better overview, H atoms were partially omitted. DIAMOND representation, thermal ellipsoids shown at 50 % probability level. Symmetry code: $i - x, 1 - y, 1 - z$.

However, the intermolecular F \cdots H interactions, which according to a Hirshfeld analysis represent 12,4 % of all intermolecular interactions in the crystal of **6**, are more numerous than observed for **2**, **4** or **5** (Figure 12d).

Table 2: Structural parameters of the hydrogen bonds in the crystals of compounds **1**, **2**, **4** and **5**; bond lengths in Å, bond angles in °.

Compound	Bond	d(D-H)	d(H \cdots A)	d(D \cdots A)	\angle (D-H \cdots A)
1	C3B-H3A \cdots I1 ⁱⁱ	0.99(2)	3.14(2)	4.026(3)	149.7(2)
	C3 ⁱ -H3A ⁱ \cdots F1	0.98(3)	2.48(4)	3.436(4)	162.6(2)
2	C13-H13A \cdots I1	0.99(2)	2.92(2)	3.901(4)	178(2)
	C13-H13B \cdots I1 ⁱ	0.99(2)	3.13(2)	4.084(4)	164(1)
	C25 ⁱⁱ -H25 ⁱⁱ \cdots F1	0.98(2)	2.47(3)	3.324(6)	144.4(4)
4	C1-H1A \cdots I1 ⁱⁱ	0.92(2)	3.13(9)	3.841(2)	91.6(7)
	C9 ⁱ -H9A ⁱ \cdots F1	0.96(2)	2.46(1)	3.348(3)	153.4(8)
5	C1-H1B \cdots F1 ⁱ	0.94(2)	2.68(2)	3.482(2)	143(1)
	C1-H1A \cdots I1	0.94(2)	2.95(2)	3.863(3)	165(1)
6	O2-H211 \cdots I1	0.88(2)	2.7(2)	3.45(2)	146(2)
	C32 ⁱ -H32 ⁱ \cdots F1	0.95(2)	2.60(2)	3.465(4)	152(2)
	C44 ⁱ -H44 ⁱ \cdots F1	0.96(3)	2.42(2)	3.181(3)	137(2)
	C6-H6 \cdots F1	0.97(3)	2.75(3)	3.250(3)	113(2)

Symmetry code: **1**) *i*: 1-x, 1-y, 1-z; *ii*: -0.5+x, 0.5-y, 0.5-z; **2**) *i*: 1-x, 1-y, -z; *ii*: 1-x, 1-y, 1-z; **4**) *i*: 1-x, -0.5+y, 1.5-z; *ii*: 1-x, 1-y, 1-z; **5**) *i*: -x, 1-y, 1-z; **6**) *i*: -x, 1-y, 1-z.

In order to find out whether the phosphorus bonded CH₂F unit can react with the membrane proteins in analogy to the bioisosteric P-CH₂OH group (Figure 1), it was first necessary to choose a suitable phosphonium salt. Solubility tests showed that only compound **1** is sufficiently soluble in water to perform such tests. Sodium iodide (EC₅₀: 289.61) was measured to rule out that a possible toxicity was caused by the iodide anion. Tetramethyl phosphonium iodide was also included in the investigations to determine whether the phosphonium cation itself already has a toxic effect on bacteria. The aqueous toxicity,^[21] which was determined by inhibition of the bioluminescence of gram negative *vibrio fisheri* bacteria, shows clear differences for the toxicity of **1**, [PMe₄]I and THPS ([P(CH₂OH)₄]SO₄) (Figure 15). According to the directives,^[21] **1** and [PMe₄]I are considered as non-toxic ([PMe₄]I being at the limit of non-toxic), whereas THPS is considered as very toxic. Furthermore, the assessment of bactericidal activity on E-coli was determined on the basis of the number of colonies formed on a culture medium at four different concentrations of the substrates.^[22] Due to the low EC₅₀ values for THPS, lower substrate concentrations during the breeding of colonies on the plates were used. As already indicated by the EC₅₀ values, sodium iodide showed no effect on the bacteria within this experiment. Compared with the control sample a), only [P(CH₂OH)₄]SO₄ for the concentrations **2**, **3** and **4** shows lower colony numbers (Figure 16). This confirms the results obtained in Figure 15, that only THPS is to be classified as toxic. In Figure 16 subsection e), the result of additional growth inhibition studies is shown. The results indicate that THPS also inhibits bacterial growth. All other substances used do not inhibit bacterial growth. Based on these investigations it can be concluded that the C-F bond in **1** remains stable despite the stronger enthalpy of HF formation compared to H₂O. This illustrates once more the high metabolic stability of the CH₂F group as compared to the bioisosteric CH₂OH group.^[3b]

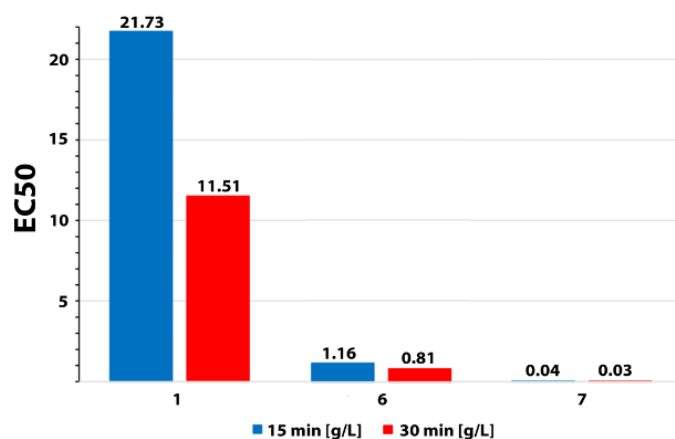


Figure 15: EC₅₀ values for fluoromethyl phosphonium salt **1**, [PMe₄]I and [P(CH₂OH)₄]SO₄ measured after 15 min (blue) and after 30 min (red).

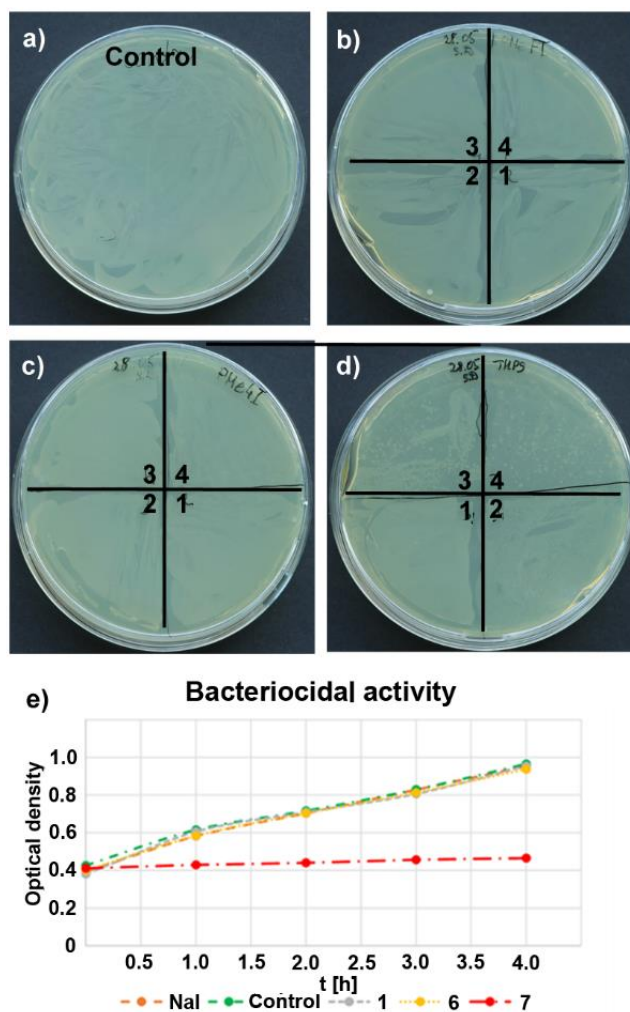


Figure 16: E-coli bacteria colonies on a culture medium at four different substrate concentrations; a) Control, b) Compound **1**. (1): 24.7 mmol/L; (2): 52.9 mmol/L; (3): 105.9 mmol/L; (4): 211.8 mmol/L; c) [PMe₄]I. (1): 26.7 mmol/L; (2): 57.3 mmol/L; (3): 114.6 mmol/L; (4): 229.3 mmol/L; d) [P(CH₂OH)₄]₂SO₄. (1): 1.35 mmol/L; (2): 2.71 mmol/L; (3): 5.42 mmol/L; (4): 10.8 mmol/L; e) Inhibited colony growth of Control, NaI, **1**, [PMe₄]I and [P(CH₂OH)₄]₂SO₄.

8.3 Conclusion

In summary, we have reported an efficient and facile synthesis method for a series of new fluoromethyl phosphonium salts in high purity. Single crystal X-ray diffraction gives an insight in the influence of the substituents at the phosphorus on the structural parameters of the P-CH₂F group. The C-F bond length stays unaffected by substitution at phosphorus and corresponds to a typical C-F single bond. The P-C bond length fits well to that reported for bioisosteric P-CH₂OH derivatives. In all cases investigated weak intermolecular H···I and H···F interactions are observed. They have been studied by Hirshfeld analysis. In particular, the H···F interactions favor the formation of hydrogen bonded chains in the crystal, which represent the structural motive for the fluoromethyl phosphonium salts **1**, **2** and **4**. The H···I contacts are characteristic for the cation/anion interaction. Toxicological tests were carried out on the most water soluble phosphonium salt **1**. In contrast to the toxic P-CH₂OH structural motive the bioisosteric P-CH₂F group showed no toxicity in the case of the bacteria investigated. This finding is anticipated to be useful for adjusting the toxicity of P-CH₂OH based biocides.

8.4 Acknowledgement

Financial support by Ludwig-Maximilian University is grateful acknowledged. We are thankful to F-Select GmbH for a generous donation of fluoroiodomethane. The authors thank Prof. Dr. T. M. Klapötke, Ludwig-Maximilian University, for the generous allocation of diffractometer time. Dr. Peter Mayer is thanked, for the help of solving the crystal structure of compound **1**.

8.5 Experimental Section

8.5.1 General Procedure

All compounds were handled using *Schlenk* techniques under dry argon. The phosphines were obtained from BASF, Hoechst AG and VWR. Fluoroiodomethane was distilled under inert conditions before use. The samples for infrared spectroscopy were placed under ambient conditions without further preparation onto an Smith DuraSamplIR II ATR device and measured with a Perkin Elmer BX II FR-IR System spectrometer. Raman spectra was measured with a Bruker MultiRam FT Raman spectrometer. Melting/decomposition points were determined with a OZM DTA 552-Ex instrument. The samples for NMR spectroscopy were prepared under inert atmosphere using Ar as protective gas. The solvent used was dried using 3 Å mol sieve and stored under Ar atmosphere. Spectra were recorded with a Bruker Avance III spectrometer operating at 400.1 MHz (¹H), 376.4 MHz (¹⁹F), 100.6 MHz (¹³C) and 162 MHz (³¹P). Chemical shifts are referred to TMS (¹H, ¹³C), CFCl₃ (¹⁹F) and H₃PO₄ (³¹P). All spectra were recorded at 299.15 K. Mass spectrometric data were acquired with a Jeol MStation sectorfield instrument in the FAB⁺ mode. Elemental burning analysis was performed using an Elementar vario EL instrument. Single crystals, suitable for X-ray diffraction, were obtained by slow evaporation of a solution in acetonitrile. Data collection was performed with an Oxford Xcalibur 3 diffractometer equipped with a Spellman generator (50 kV, 40 mA) and a Kappa CCD detector, operating with Mo-K_α radiation ($\lambda = 0.71073 \text{ \AA}$). Data collection and data reduction were performed with the CrysAlisPro

software.^[23] Absorption correction using the multiscan method^[23] was applied. The structures were solved with SHELXS-97,^[24] refined with SHELXL-97^[25] and finally checked using PLATON.^[26]

8.5.2 Synthesis and Characterization

(Fluoromethyl)trimethylphosphonium iodide (1)

Caution, this reaction is very exothermic! Trimethylphosphine (7.06 g, 92.8 mmol) was condensed in a flask and cooled to -78 °C. To this fluoroiodomethane (6.24 mL, 92.8 mmol) was carefully added. After 30 min the reaction mixture was allowed to warm up to ambient temperature. The precipitate was dried *in vacuo* and **1** was obtained as white powder (21.7 g, 0.09 mol, 99 %). Phas. trans. 54 °C; 128 °C; Dec.p. 209 °C; ¹H NMR (400 MHz, D₂O, 26 °C): δ = 5.44 (d, ²J_{H,F} = 45.3 Hz, 2H; CH₂F), 2.05 (d, ²J_{H,P} = 15.0 Hz, 9H; CH₃); ¹³C{¹H} NMR (100.6 MHz, D₂O, 26 °C): δ = 77.1 (dd, ¹J_{C,F} = 183.8 Hz, ¹J_{C,P} = 64.6 Hz; CH₂F), 4.9 (d, ¹J_{C,P} = 53.6 Hz; CH₃); ³¹P{¹H} NMR (162 MHz, D₂O, 26 °C): δ = 27.2 (d, ²J_{P,F} = 60.3 Hz); ³¹P NMR (162 MHz, D₂O, 26 °C): δ = 27.2 (d of dezetts of t, ²J_{P,F} = 60.3 Hz, ²J_{P,H} = 15.0 Hz to CH₃, ²J_{P,H} = 1.6 Hz to CH₂F) ¹⁹F{¹H} NMR (376 MHz, D₂O, 26 °C): δ = -242.8 (d, ²J_{F,P} = 60.3 Hz); ¹⁹F NMR (376 MHz, D₂O, 26 °C): δ = -242.8 (dt, ²J_{F,P} = 60.3 Hz, ²J_{F,H} = 45.3 Hz); IR (ATR): $\tilde{\nu}$ = 2993 (s), 2957 (m), 2919 (m), 2899 (m), 2886 (w), 1627 (w), 1567 (w), 1524 (w), 1440 (w), 1418 (w), 1397 (w), 1321 (w), 1304 (w), 1291 (m), 1224 (m), 1021 (s), 962 (s), 883 (s), 809 (m), 779 (m), 745 (w), 643 cm⁻¹ (m); Raman (1000 mW): $\tilde{\nu}$ = 2992 (s), 2958 (s), 2917 (s), 2900 (s), 2889 (s), 2791 (m), 1441 (w), 1418 (w), 1324 (w), 1290 (w), 1225 (w), 1025 (w), 972 (w), 940 (w), 885 (w), 783 (w), 746 (w), 646 (m), 379 (w), 272 (m), 250 cm⁻¹ (w); HRMS (FAB) (m/z): calcd for C₄H₁₀FP: 109.0582 [M⁺]; found, 109.0567; elemental analysis calcd (%) for C₄H₁₀FIP: C 20.36 H 4.70; found C 20.40 H 4.66.

Tris(diethylamino)(fluoromethyl)phosphonium iodide (2)

Tris(diethylamino)phosphine was synthesized as described in literature.^[27] To a solution of fluoroiodomethane (0.676 mL, 10.0 mmol) in diethylether (90 mL) cooled to 0 °C, a solution of tris(diethylamino)phosphine (2.73 mL, 10.0 mmol) in diethylether (10 mL) was added slowly with stirring during 3 h. The solution was concentrated and cooled to -10 °C. The precipitate was filtrated off and compound **2** was obtained as colorless crystals (3.25 g, 0.008 mol, 80 %). M.p. 70 °C; Dec.p. 130 °C; ¹H NMR (400 MHz, CDCl₃, 26 °C): δ = 5.77 (d, ²J_{H,F} = 45.9 Hz, 2H; CH₂F), 3.24 (dq, ³J_{H,P} = 11.2 Hz, ³J_{H,H} = 7.1 Hz, 12H; NCH₂), 1.26 (t, ³J_{H,H} = 7.1 Hz, 18H; CH₃); ¹³C {¹H} NMR (100.6 MHz, CD₃CN, 26 °C): δ = 78.2 (dd, ¹J_{C,F} = 182.6, ¹J_{C,P} = 130.3 Hz; CH₂F), 40.1 (d, ²J_{C,P} = 4.1 Hz, NCH₂), 13.6 (s, CH₃); ³¹P{¹H} NMR (162 MHz, CDCl₃, 26 °C): δ = 48.1 (d, ²J_{P,F} = 59.9 Hz); ¹⁹F{¹H} NMR (376 MHz, CDCl₃, 26 °C): δ = -241.1 (d, ²J_{F,P} = 59.9 Hz); ¹⁹F NMR (376 MHz, CDCl₃, 26 °C): δ = -241.1 ppm (dt, ²J_{F,P} = 59.9 Hz, ²J_{F,H} = 45.9 Hz); FT-IR (ATR): $\tilde{\nu}$ = 2972 (m), 2925 (m), 2887 (m), 2840 (m), 1747 (w), 1643 (w), 1575 (w), 1465 (w), 1449 (w), 1385 (m), 1369 (m), 1292 (s), 1249 (s), 1209 (s), 1153 (s), 1112 (w), 1059 (w), 1016 (s), 971 (s), 928 (w), 801 (m), 764 (w), 704 (w), 625 cm⁻¹ (w); Raman (1000 mW): $\tilde{\nu}$ = 2974 (s), 2929 (s), 2896 (s), 2840 (s), 1451 (m), 1371 (w), 1371 (w), 1294 (w), 1207

(w), 1082 (w), 1023 (w), 981 (w), 953 (w), 928 (w), 795 (w), 625 (w), 412 (w), 316 cm^{-1} (w); HRMS (FAB): (m/z) calcd for $\text{C}_{13}\text{H}_{32}\text{FN}_3\text{P}$: 280.2318 [M^+], found, 280.2316; elemental analysis calcd (%) for $\text{C}_{13}\text{H}_{32}\text{FIN}_3\text{P}$: C 38.34 H 7.92 N 10.32; found C 37.06 H 8.13 N 10.01.

Tributyl(fluoromethyl)phosphonium iodide (3)

To a solution of tributylphosphine (1.92, 9.50 mmol) in diethylether (15 mL), fluoriodomethane (0.65 mL, 9.50 mmol) was added in small portions over a period of 5 min. The solution was heated to 35 °C for 32 h, the precipitate formed was filtrated off, washed with diethylether (2 × 15.0 mL) and dried *in vacuo*. Compound **3** was obtained as white powder (2.34 g, 6 mmol, 68 %). M.p. 58 °C; ^1H NMR (400 MHz, CDCl_3 , 26 °C): δ = 5.92 (d, $^2J_{\text{H,F}}=45.9$ Hz, 2H; CH_2F), 2.71 – 2.56 (m, 6H, CH_2), 1.70 – 1.45 (m, 12H, CH_2), 1.00 (t, $^3J_{\text{H,H}}=7.1$ Hz, 9H; CH_3); ^{13}C NMR (100.6 MHz, CDCl_3 , 26 °C): δ = 76.1 (dd, $^1J_{\text{C,F}}=190.4$ Hz, $^1J_{\text{C,P}}=58.1$ Hz; CH_2F), 24.1 (d, $^2J_{\text{C,P}}=15.4$ Hz; PCH_2CH_2), 23.8 (dd, $^3J_{\text{C,P}}=4.6$ Hz, $^5J_{\text{C,F}}=0.7$ Hz; $\text{PCH}_2\text{CH}_2\text{CH}_2$), 18.1 (d, $^1J_{\text{C,P}}=44.6$ Hz; PCH_2), 13.6 (d, $^4J_{\text{C,P}}=0.8$ Hz; CH_3); $^{31}\text{P}\{^1\text{H}\}$ NMR (162 MHz, CDCl_3 , 26 °C): δ = 32.8 (d, $^2J_{\text{P,F}}=51.6$ Hz); $^{19}\text{F}\{^1\text{H}\}$ NMR (376 MHz, CDCl_3 , 26 °C): δ = -247.9 (d, $^2J_{\text{F,P}}=51.6$ Hz); ^{19}F NMR (376 MHz, CDCl_3 , 26 °C): δ = -247.9 (dt, $^2J_{\text{F,P}}=51.6$ Hz, $^2J_{\text{F,H}}=45.9$ Hz); FT-IR (ATR): $\tilde{\nu}$ = 2960 (s), 2934 (m), 2872 (w), 1572 (m), 1463 (m), 1379 (m), 1340 (m), 1313 (m), 1283 (m), 1231 (m), 1208 (m), 1099 (m), 1078 (m), 1011 (w), 968 (m), 916 (m), 866 (m), 801 (m), 746 (m), 712 (m), 661 cm^{-1} (w); Raman (1000 mW): $\tilde{\nu}$ = 2965 (s), 2937 (s), 2904 (s), 2874 (s), 2734 (w), 1447 (m), 1399 (w), 1315 (w), 1100 (w), 1052 (w), 890 (w), 661 (w), 245 cm^{-1} (w); HRMS (FAB): (m/z) calcd for $\text{C}_{13}\text{H}_{29}\text{FIP}$: 235.1985 [M^+], found, 235.2005; elemental analysis calcd (%) for $\text{C}_{13}\text{H}_{29}\text{FIP}$: C 43.10 H 8.07; found C 42.97 H 8.05.

Tris(2-cyanoethyl)(fluoromethyl)phosphonium iodide (4)

To a solution of tris(2-cyanoethyl)phosphine (0.915 g, 4.74 mmol) in acetonitrile (20 mL), fluoriodomethane (0.35 mL, 4.74 mmol) was added. The solution was stirred for 7 d and then concentrated *in vacuo*. The precipitate was filtrated off and dried *in vacuo*. Crystalline colorless **4** was obtained (1.10 g, 3 mmol, 66 %). M.p. 138 °C; ^1H NMR (400 MHz, CD_3CN , 26 °C): δ = 5.85 (d, $^2J_{\text{H,F}}=44.8$ Hz, 2H; CH_2F), 3.19 – 2.78 ppm (m, 12H, CH_2); ^{13}C NMR (100.6 MHz, CD_3CN , 26 °C): δ = 76.0 (dd, $^1J_{\text{C,F}}=188.3$, $^1J_{\text{C,P}}=56.1$ Hz; CH_2F), 15.6 (d, $^1J_{\text{C,P}}=46.0$ Hz; PCH_2), 11.9; $^{31}\text{P}\{^1\text{H}\}$ NMR (162 MHz, CDCl_3 , 26 °C): δ = 35.3 (d, $^2J_{\text{P,F}}=56.8$ Hz); $^{19}\text{F}\{^1\text{H}\}$ NMR (376 MHz, CDCl_3 , 26 °C): δ = -249.5 (d, $^2J_{\text{F,P}}=56.8$ Hz); ^{19}F NMR (376 MHz, CDCl_3 , 26 °C): δ = -249.5 ppm (dt, $^2J_{\text{F,P}}=56.8$, $^2J_{\text{F,H}}=44.8$ Hz); FT-IR (ATR): $\tilde{\nu}$ = 3001 (w), 2958 (m), 2927 (s), 2899 (m), 2251 (s), 1571 (w), 1411 (s), 1362 (s), 1311 (m), 1243 (m), 1229 (m), 1191 (w), 1028 (s), 1005 (m), 978 (s), 940 (m), 880 (w), 804 (s), 781 (s), 707 (m), 690 (m), 675 (m), 516 cm^{-1} (m); Raman (1000 mW): $\tilde{\nu}$ = 2999 (w), 2960 (w), 2923 (s), 2901 (s), 2250 (s), 1411 (w), 1395 (w), 1311 (w), 1246 (w), 1005 (w), 915 (w), 806 (w), 692 (w), 676 (w), 484 (w), 411 (w), 369 (w), 250 (w), 201 cm^{-1} (w); HRMS (FAB): (m/z) calcd for $\text{C}_{10}\text{H}_{14}\text{FIN}_3\text{P}$: 226.2146 [M^+], found, 226.0922; elemental analysis calcd (%) for $\text{C}_{10}\text{H}_{14}\text{FIN}_3\text{P}$: C 34.01 H 4.00 N 11.90; found C 34.12 H 4.10 N 11.90.

5-(diphenylphosphino)-1-fluoromethyldiphenyl phosphonium iodide (5)

1,1'-(Oxydi-2,1-phenylene)bis(1,1'-diphenylphosphine) (0.30 g, 0.576 mmol) was dissolved in toluene (25.0 mL) and fluoroiodomethane (0.1 mL, 1.5 mmol) was added. The solution was heated to 110 °C for 1 d and the resulting precipitate was filtrated off, washed with toluene (3 × 15.0 mL) and dried *in vacuo* to yield colorless crystals of **5** (0.41 g, 0.58 mmol, 55 %). Dec.p. 231 °C; ¹H NMR (400 MHz, CDCl₃, 26 °C): δ = 7.95 – 7.89 (m, 2H; ArH), 7.85 – 7.81 (m, 1H; ArH), 7.79 – 7.75 (m, 1H; ArH), 7.72 – 7.61 (m, 8H; ArH), 7.56 – 7.47 (m, 6H; ArH), 7.44 – 7.38 (m, 3H; ArH), 7.33 – 7.29 (m, 2H; ArH), 7.23 – 7.17 (m, 2H; ArH), 7.03 – 6.98 (m, 2H; ArH), 6.82 – 6.79 (m, 1H; ArH), 6.28 ppm (dd, ²J_{H,F}=46.0, ²J_{H,P}=12.8 Hz, 2H; CH₂F); Due to the low solubility no ¹³C NMR spectrum of acceptable quality could be obtained. ³¹P{¹H} NMR (162 MHz, CDCl₃, 26 °C): δ = 18.7 (d, ²J_{P,F} = 62.2 Hz; 1P, PCH₂F), 30.7 ppm (s; 1P, PPh₂); ¹⁹F{¹H} NMR (376 MHz, CDCl₃, 26 °C): δ = -240.3 ppm (d, ²J_{F,P} = 62.2 Hz); ¹⁹F NMR (376 MHz, CDCl₃, 26 °C): δ = -240.3 (dt, ²J_{F,P} = 62.2 Hz, ²J_{F,H} = 45.3 Hz); FT-IR (ATR): $\tilde{\nu}$ = 3145 (w), 3048 (w), 2988 (w), 2887 (w), 1580 (m), 1563 (m), 1520 (m), 1475 (s), 1458 (s), 1435 (s), 1342 (w), 1314 (w), 1264 (m), 1233 (s), 1188 (m), 1157 (m), 1133 (w), 1110 (m), 1100 (m), 1076 (w), 1029 (s), 996 (w), 907 (w), 886 (m), 793 (m), 754 (m), 744 (s), 721 (w), 702 (s), 688 (w), 620 (w), 542 (s), 505 cm⁻¹ (m); Raman (1000 mW): $\tilde{\nu}$ = 3143 (w), 3051 (s), 2884 (w), 2832 (w), 1584 (s), 1189 (w), 1164 (w), 1110 (w), 1098 (w), 1030 (m), 999 (s), 794 (w), 692 (w), 671 (w), 615 (w), 584 (w), 306 (w), 262 (w), 225 (w), 177 cm⁻¹ (w); HRMS (EI): (m/z) calcd for C₃₇H₃₀FIOP₂: 698.4964 [M⁺], found, 571.1760; elemental analysis calcd (%) for C₃₇H₃₀FIOP₂: C 63.62 H 4.33; found C 63.91 H 4.36.

(Fluoromethyl)diphenylphosphine (6)

Diphenylphosphine (0.499 mL, 2.87 mmol) was solved in THF (15 mL) and cooled to 0 °C. *n*Butyllithium (2.43 mL, 1.30 M, 3.16 mmol) was added and the solution was stirred for 1 h. The deep red solution was cooled to -78 °C and fluoroiodomethane (0.194 mL, 2.87 mmol) was added in portions over a period of 10 min. The reaction mixture was allowed to warm up to ambient temperature overnight. Degassed water (0.50 mL) was added and THF was removed *in vacuo*. The product was extracted with pentane (15.0 mL) and the solvent removed *in vacuo*. A colorless oil was obtained. (0.41 g, 2 mmol, 65 %). M.p. -32 °C; Dec. p. 235 °C; ¹H NMR (400 MHz, CDCl₃, 26 °C): δ = 7.54 – 7.47 (m, 4H; ArH), 7.41 – 7.34 (m, 6H; ArH), 5.28 (dd, ²J_{H,F} = 49.0 Hz, ²J_{H,P} = 8.4 Hz, 6H; CH₂F); ¹³C NMR (100.6 MHz, CDCl₃, 26 °C): δ = 133.5 (dd, ¹J_{C,P} = 17.7 Hz, ³J_{C,F} = 0.8 Hz; C-*i*), 129.3, 128.7, 128.6, 84.6 (dd, ¹J_{C,F} = 199.9, ¹J_{C,P} = 21.3 Hz; CH₂F); ³¹P{¹H} NMR (162 MHz, CDCl₃, 26 °C): δ = -11.9 (d, ²J_{P,F} = 114.0 Hz); ¹⁹F{¹H} NMR (376 MHz, CDCl₃, 26 °C): δ = -230.4 (d, ²J_{F,P} = 114.0 Hz); ¹⁹F NMR (376 MHz, CDCl₃, 26 °C): δ = -230.4 (dt, ²J_{F,P} = 114.0, ²J_{F,H} = 49.0 Hz); FT-IR (ATR): $\tilde{\nu}$ = 3054 (m), 2918 (s), 1958 (m), 1889 (m), 1809 (m), 1586 (m), 1481 (m), 1433 (m), 1306 (m), 1236 (m), 1184 (m), 1123 (m), 1096 (m), 1069 (m), 977 (m), 914 (w), 843 (m), 740 (w), 721 (m), 691 (m), 618 (m), 544 (m), 506 cm⁻¹ (m); Raman (1000 mW): $\tilde{\nu}$ = 3142 (s), 3056 (m), 2958 (m), 2919 (m), 1587 (m), 1572 (w), 1435 (w), 1186 (w), 1159 (w), 1099 (w), 1029 (m), 1000 (s), 684 (w), 668 (w), 618 (w), 377 (w), 262 (w), 204 cm⁻¹ (w); HRMS (EI): (m/z) calcd for C₁₃H₁₂FP: 218.2112 [M⁺], found 218.0653; elemental analysis calcd (%) C₁₃H₁₂FP: C 71.56 H 5.54; found C 71.74 H 5.78.

Determination of TEP value

Ni(CO)₄ (1.56 g, 9.17 mmol) was condensed into a flask and pentane (25 mL) was added. The solution was cooled to -78 °C and a solution of (fluoromethyl)diphenylphosphine (0.20 g, 0.91 mmol) in pentane (10 mL) was slowly added. The reaction mixture was warmed to room temperature within 2 h, the solvent and the excess of Ni(CO)₄ were removed *in vacuo* and a colorless solid was obtained. FT-IR-TEP (ATR): $\tilde{\nu}$ = 3060 (m), 2919 (m), 2068 (s), 1988 (m), 1943 (m), 1568 (m), 1488 (m), 1431 (m), 1334 (m), 1100 (m), 995 (m), 850 (m), 798 (m), 745 (m), 737 (m), 689 cm⁻¹ (m).

Reaction of fluoroiodomethane with (fluoromethyl)diphenyl phosphine

Freshly prepared fluoromethyldiphenyl phosphine (0.41 g, 1.88 mmol) was dissolved in toluene (20 mL) and fluoroiodomethane (0.127 mL, 1.88 mmol) was added dropwise at ambient temperature. The reaction mixture was stirred over night. The ³¹P{¹H} NMR spectrum showed no indication for the formation of bis(fluoromethyl)diphenyl phosphonium iodide. The reaction mixture was heated to reflux for 1 d. Again the ³¹P{¹H} NMR spectrum showed no indication for the formation of bis(fluoromethyl)diphenyl phosphonium iodide; instead in addition to the starting phosphine **6** the formation of small amounts of some unidentified phosphorus containing products (δ ³¹P = 45 - 22) was observed. Applying an analogous procedure no reaction was observed also when using diethylether and acetonitrile as solvents.

8.6 References

- [1] a) G. Wittig, W. Haag, *Chem. Ber.* **1955**, *88*, 1654-1666; b) G. Wittig, U. Schöllkopf, *Chem. Ber.* **1954**, *87*, 1318-1330; c) H. Schmidbaur, *Inorg. Synth.* **1978**, *18*, 135-140.
- [2] Y. L. Yagupolskii, N. V. Pavlenko, S. V. Shelyazhenko, A. A. Filatov, M. M. Kremlev, A. I. Mushta, I. I. Gerus, S. Peng, V. A. Petrov, M. Nappa, *J. Fluorine Chem.* **2015**, *179*, 134-141.
- [3] a) M. Reichel, J. Martens, E. Woellner, L. Huber, A. Kornath, K. Karaghiosoff, *Eur. J. Inorg. Chem.* **2019**, *2019*, 2530-2534; b) J. Hu, W. Zhang, F. Wang, *Chem. Commun. (Cambridge, U. K.)* **2009**, 7465-7478.
- [4] J. Hu, B. Gao, L. Li, C. Ni, J. Hu, *Org. Lett.* **2015**, *17*, 3086-3089.
- [5] a) N. A. Meanwell, *J. Med. Chem.* **2018**, *61*, 5822-5880; b) N. A. Meanwell, *J. Med. Chem.* **2011**, *54*, 2529-2591; c) G. A. Showell, J. S. Mills, *Drug Discovery Today* **2003**, *8*, 551-556.
- [6] a) C. C. Okoro, *Pet. Sci. Technol.* **2015**, *33*, 1366-1372; b) Y. Xue, G. Voordouw, *Front Microbiol* **2015**, *6*, 1387; c) P. Bajpai, *Pulp and Paper Industry: Microbiological Issues in Papermaking*, Elsevier Science, **2015**.
- [7] a) S. P. Denyer, *Int. Biodeterior. Biodegrad.* **1995**, *36*, 227-245; b) A. Kanazawa, T. Ikeda, T. Endo, *J. Appl. Bacteriol.* **1995**, *78*, 55-60.
- [8] M. Pohanka, *Biomed. Pap.* **2011**, *155*, 219-230.

- [9] a) T. Liang, C. N. Neumann, T. Ritter, *Angew. Chem., Int. Ed.* **2013**, *52*, 8214–8264; *Angew. Chem.* **2013**, *125*, 8372–8423; b) P. Kirsch, *Modern Fluoroorganic Chemistry: Synthesis, Reactivity, Applications*, Wiley, **2006**.
- [10] a) C. A. Tolman, *Chem. Rev.* **1977**, *77*, 313–348; b) D. G. Gusev, *Organometallics* **2009**, *28*, 6458–6461; c) G. Landelle, J.-F. Paquin, John Wiley & Sons, Ltd., **2011**, 1–2.
- [11] a) W. v. E. Doering, A. K. Hoffmann, *J. Am. Chem. Soc.* **1955**, *77*, 521–526; b) L. V. Nesterov, A. Y. Kessel, R. I. Mutalapova, *Zh. Obshch. Khim.* **1969**, *39*, 2453–2456; c) W. C. Davies, W. J. Jones, *J. Chem. Soc.* **1929**, 33–35; d) M. M. Rauhut, I. Hechenbleikner, H. A. Currier, F. C. Schaeffer, V. P. Wystrach, *J. Am. Chem. Soc.* **1959**, *81*, 1103–1107.
- [12] a) D. J. Burton, D. M. Wiemers, *J. Fluorine Chem.* **1985**, *27*, 85–89; b) R. Mazurkiewicz, T. Gorewoda, A. Kuznik, M. Grymel, *Tetrahedron Lett.* **2006**, *47*, 4219–4220.
- [13] G. Prakash, I. Ledneczki, S. Chacko, G. A. Olah, *Org. Lett.* **2008**, *10*, 557–560.
- [14] a) F. H. Allen, O. Kennard, D. G. Watson, L. Brammer, A. G. Orpen, R. Taylor, *J. Chem. Soc., Perkin Trans. 2* **1987**, 1–19; b) A. Kornath, F. Neumann, H. Oberhammer, *Inorg. Chem.* **2003**, *42*, 2894–2901.
- [15] R.-X. Li, L. Zhou, P.-P. Shi, X. Zheng, J.-X. Gao, Q. Ye, D.-W. Fu, *New J. Chem.* **2019**, *43*, 154–161.
- [16] T. Steiner, *Angew. Chem., Int. Ed.* **2002**, *41*, 48–76; *Angew. Chem.* **2002**, *114*, 50–80.
- [17] M. C. Davis, D. A. Parrish, *Synth. Commun.* **2008**, *38*, 3909–3918.
- [18] H. Schmidbaur, R. Pichl, G. Mueller, *Z. Naturforsch., B: Anorg. Chem., Org. Chem.* **1986**, *41B*, 395–397.
- [19] F. Dornhaus, M. Bolte, H.-W. Lerner, M. Wagner, *Eur. J. Inorg. Chem.* **2006**, 5138–5147.
- [20] N. J. Goodwin, W. Henderson, B. K. Nicholson, *Inorg. Chim. Acta* **2002**, *335*, 113–118.
- [21] a) *Vol. DIN EN ISO 11348-2:2009-05*; b) *Vol. DIN EN ISO 11348-1:2009-05*.
- [22] P. Broxton, P. M. Woodcock, P. Gilbert, *J. Appl. Bacteriol.* **1983**, *54*, 345–353.
- [23] Program package CrysAlisPro 1.171.38.46 Rigaku OD, **2015**.
- [24] G. M. Sheldrick, SHELXS-97: Program for Crystal Structure Solution, University of Göttingen, Germany, **1997**.
- [25] G. M. Sheldrick, SHELXL-97: Program for the Refinement of Crystal Structures, University of Göttingen, Germany, **1997**.
- [26] A. L. Spek, PLATON: A Multipurpose Crystallographic Tool, Utrecht University, Utrecht, The Netherlands, **1999**.
- [27] G. Bencivenni, R. Cesari, D. Nanni, H. El Mkami, J. C. Walton, *Org. Biomol. Chem.* **2010**, *8*, 5097–5104.

8.7 Supporting Information

Table 1: Structure refinement data of compound **1** (left) and compound **2** (right).

Empirical formula	C ₄ H ₁₁ F I P	C ₁₃ H ₃₂ F I N ₃ P
Formula weight	236.00	407.28
Temperature	143(2) K	173(2) K
Wavelength	0.71073 Å	0.71073 Å
Crystal system	Orthorhombic	Triclinic
Space group	<i>Pnma</i>	<i>P</i> -1
Unit cell dimensions	a = 12.1430(5) Å b = 7.3397(3) Å c = 9.2655(5) Å α = 90° β = 90° γ = 90°	a = 10.0648(3) Å b = 10.1439(5) Å c = 18.6453(8) Å α = 93.292(4)° β = 92.580(3)° γ = 90.104(3)°
Volume	825.80(7) Å ³	1898.53(14) Å ³
Z	4	4
Density (calculated)	1.898 mg/m ³	1.425 mg/m ³
Absorption coefficient	3.993 mm ⁻¹	1.774 mm ⁻¹
F(000)	448	832
Crystal size	0.100 x 0.050 x 0.050 mm ³	0.100 x 0.100 x 0.020 mm ³
Theta range for data collection	4.356 - 30.493°	4.151 - 28.282°
Index ranges	-17 ≤ h ≤ 17, -10 ≤ k ≤ 10, -13 ≤ l ≤ 11	-13 ≤ h ≤ 13, -13 ≤ k ≤ 13, -24 ≤ l ≤ 24
Reflections collected	8368	30663
Independent reflections	1346 [R _{int} = 0.0395]	9397 [R _{int} = 0.0592]
Data / restraints / parameters	1346 / 0 / 43	9397 / 0 / 367
Goodness-of-fit on F ²	1.102	1.013
Final R indices [I > 2σ(I)]	R ₁ = 0.0223, wR ₂ = 0.0460	R ₁ = 0.0430, wR ₂ = 0.0717
R indices (all data)	R ₁ = 0.0313, wR ₂ = 0.0504	R ₁ = 0.0826, wR ₂ = 0.0860
Largest diff. peak and hole	1.020 and -0.573 e Å ⁻³	1.020 and -0.588 e Å ⁻³

Table 2: Structure refinement data of compound **4** (left) and compound **5** (right).

Empirical formula	C ₁₀ H ₁₄ F I N ₃ P	C ₃₇ H _{30.57} F I O _{1.28} P ₂
Formula weight	353.11	703.57
Temperature	143(2) K	123(2) K
Wavelength	0.71073 Å	0.71073 Å
Crystal system	Monoclinic	Triclinic
Space group	<i>P2</i> ₁ / <i>c</i>	<i>P</i> -1
Unit cell dimensions	a = 8.7566(2) Å b = 9.3257(3) Å c = 17.2049(5) Å α = 90° β = 100.741(2)° γ = 90°	a = 11.3894(4) Å b = 13.0313(6) Å c = 13.4302(4) Å α = 64.227(4)° β = 66.641(3)° γ = 68.195(4)°
Volume	1380.36(7) Å ³	1599.41(13) Å ³

Z	4	2
Density (calculated)	1.699 mg/m ³	1.461 mg/m ³
Absorption coefficient	2.427 mm ⁻¹	1.136 mm ⁻¹
F(000)	688	710
Crystal size	0.393 x 0.307 x 0.165 mm ³	0.250 x 0.100 x 0.080 mm ³
Theta range for data collection	4.226 - 30.505°	4.110 - 30.507°
Index ranges	-12 ≤ h ≤ 12, -13 ≤ k ≤ 13, -24 ≤ l ≤ 24	-16 ≤ h ≤ 16, -18 ≤ k ≤ 18, -19 ≤ l ≤ 19
Reflections collected	27409	32102
Independent reflections	4202 [R _{int} = 0.0388]	9734 [R _{int} = 0.0358]
Data / restraints / parameters	4202 / 0 / 152	9734 / 3 / 422
Goodness-of-fit on F ²	1.021	1.041
Final R indices [I > 2σ(I)]	R ₁ = 0.0241, wR ₂ = 0.0497	R ₁ = 0.0410, wR ₂ = 0.0929
R indices (all data)	R ₁ = 0.0351, wR ₂ = 0.0547	R ₁ = 0.0555, wR ₂ = 0.1020
Largest diff. peak and hole	0.916 and -0.561 e.Å ⁻³	2.846 and -0.832 e.Å ⁻³

Table 3: Structure refinement data of compound **6**.

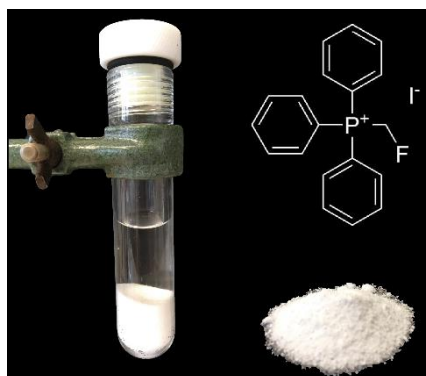
Empirical formula	C ₁₃ H ₁₂ F O P
Formula weight	234.20
Temperature	143(2) K
Wavelength	0.71073 Å
Crystal system	Triclinic
Space group	<i>P</i> -1
Unit cell dimensions	a = 11.5552(17) Å b = 13.7077(16) Å c = 17.2666(11) Å α = 69.635(9)° β = 78.081(9)° γ = 65.391(13)°
Volume	2325.0(5) Å ³
Z	8
Density (calculated)	1.338 mg/m ³
Absorption coefficient	0.224 mm ⁻¹
F(000)	976
Crystal size	0.200 x 0.200 x 0.100 mm ³
Theta range for data collection	4.104 - 26.372°
Index ranges	-14 ≤ h ≤ 14, -17 ≤ k ≤ 17, -21 ≤ l ≤ 21
Reflections collected	34798
Independent reflections	9439 [R _{int} = 0.0508]
Data / restraints / parameters	9439 / 0 / 624
Goodness-of-fit on F ²	1.016
Final R indices [I > 2σ(I)]	R ₁ = 0.0489, wR ₂ = 0.1157
R indices (all data)	R ₁ = 0.0929, wR ₂ = 0.1424
Largest diff. peak and hole	0.470 and -0.289 e.Å ⁻³

9 Synthesis and Properties of the Fluoromethylating Agent – (Fluoromethyl)triphenylphosphonium Iodide

Marco Reichel, Jörn Martens, Eduart Wöllner, Laura Huber, Andreas Kornath, Konstantin Karaghiosoff*

Published in *Eur. J. Inorg. Chem.* **2019**, 226, 109351–109354.

DOI: 10.1002/ejic.201900165



Abstract: (fluoromethyl)triphenylphosphonium iodide has been prepared in a simple and high yield synthesis. The salt was characterized by vibrational, NMR-spectroscopy and a single crystal X-ray structure analysis. The salt crystallizes in an orthorhombic space group $Pna2_1$ with four formula units in the unit cell. The experimental data are discussed together with quantum chemically calculated values. The title compound is the first example of a phosphonium salt containing a P-CH₂F moiety. Hydrogen bonding in the crystal of the fluoromethyl phosphonium iodide is discussed.

9.1 Introduction

Nowadays, around 20 % of all pharmaceuticals and 30 - 40% of all agrochemicals contain fluorine.^[1] Due to their unique physical, chemical and biological properties, fluorinated organic compounds are widely used in drugs, agrochemicals, dyes, polymers or surfactants.^[2] Fluoromethylated compounds, especially compounds with a monofluoromethyl moiety CH₂F are of considerable pharmaceutical importance.^[3] Many of these molecules are biologically active (Figure 1).^[1,4] Afloqualone (**1**) is a muscle-relaxant and sedative with clinical use.^[5] Sevofluran (**2**) is a volatile anesthetic with great significance in pediatric anesthesia due to its good hypnotic, only weak analgesic and muscle relaxing properties.^[4,6] Fluticasone propionate (**3**) – a widely used drug against inflammatory diseases and as analgesic in the treatment of certain cancers^[1] – is one of the industrially most important drugs. Beta-fluorinated amino acids (**4**, **6**) act as so called “suicide substrates” being able to inactivate decarboxylase enzymes and can be used against Parkinson diseases.^[7] The Androsta-1,4-diene-3,17-dione (**5**) acts as aromatase inhibitor and is suitable for the treatment of estrogen-dependent diseases such as anovulatory infertility, prostate hyperplasia, mammary carcinoma and many more.^[8]

There are only a few possible synthetic methods to generate the fluoromethyl group reported in literature. One strategy starts from a suitably substituted functionality CH₂X (X = Cl, Br, I or

another electronegative group) and involves the exchange of X by F using CsF or an appropriate reagent delivering fluoride anions. A second pathway is the direct fluoromethylation using a fluoromethylating agent like CH₂FBr or CH₂FI.^[9] Recently a nucleophilic fluoromethylation strategy involving the fluoromethyl anion as the lithium derivative was reported to yield α -fluoromethyl alcohols, -ketones and -amines.^[10]

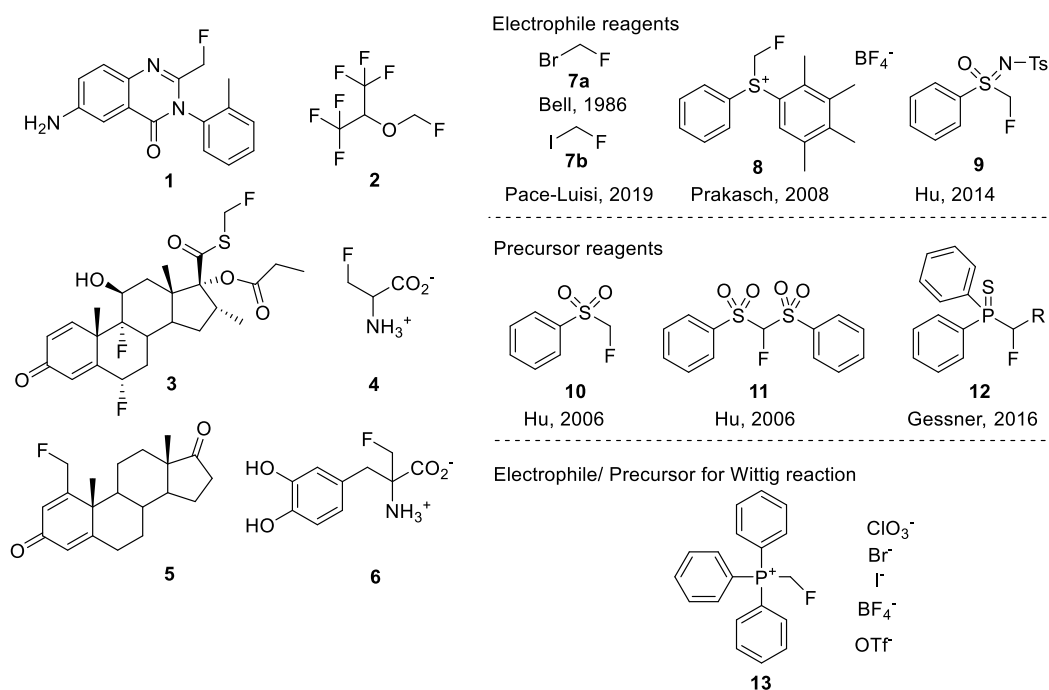


Figure 1: Representative CH₂F-containing drugs (left). Fluoromethylating agents (right).

Very recently new techniques for the transfer of “CHF” and “CIF” units to organic substrates starting from diarylfluoromethyl sulfonium salts or CH₂FI in combination with the use of special bases have been reported.^[11] In addition to the fluoromethyl halides CH₂FBr and CH₂FI other more effective fluoromethylating agents have been developed in the last years (Figure 1).^[3,10,12] *Emilia Leitao* et al. reported, that monofluoromethyl-*S*-phenyl-*S*-2,3,4,5-tetramethylphenyl sulfonium tetrafluoroborate, mono-fluoromethyl ammonium salts and monofluoromethyl-phosphonium salts **13** (Figure 2) are suitable for monofluoromethylation. Thus, fluoromethylation of the precursor **14** with the phosphonium salts **13** proceeds under mild conditions (room temperature) with caesium carbonate yielding Fluticasone **3**. This synthesis avoids the use of ozone depleting CH₂FBr.^[12c] Furthermore, the phosphonium cation in **13** is used to generate a *Wittig* reagent with a CHF-group attached to phosphorus. Reaction with carbonyl compounds results in the formation of fluoroethenes. This route has been applied to synthesize isofagomine analogs as glucocerebrosidase modulator having therapeutic uses^[13] or SSAO inhibitors.^[14] In the special case of **16**, formation of the C=C double bond is followed by hydrogen shift, resulting in an overall fluoromethylation at the carbonyl carbon atom (Figure 2).^[1] The fluoromethyl triphenylphosphonium reagent **13** can be prepared by a series of different routes.^[15] The synthesis of **13**, X = BF₄, involves for instance fluoromethylation of triphenylphosphine by the sulfonium derivative described by *Prakash*.^[3] The iodide **13**, X = I, is readily obtained by fluoromethylation of triphenylphosphine with CH₂FI. Unfortunately this straightforward reaction requires long reaction times (e.g. 63 h reflux in benzene).^[4,13,15] In

particular, the long reaction time makes the synthesis of larger amounts of **13** ($X = I$) problematic.^[16] In the course of our recent investigations on fluoromethylating agents we recognized that to our best knowledge structural deformations on PCH_2F moiety has not been reported in literature. This prompted us to investigate the phosphonium salt more closely.

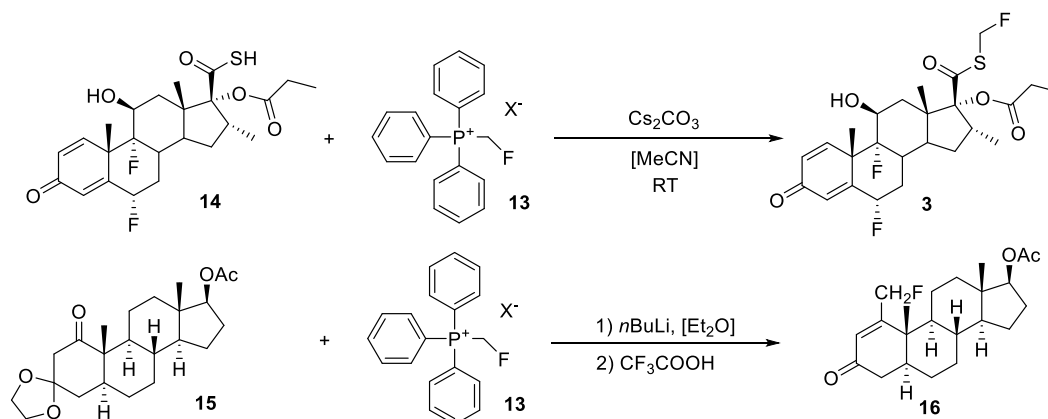


Figure 2: Reaction of monofluoromethyl phosphonium salt **13** with Androstrane derivate **14** and **15**.

9.2 Results and Discussion

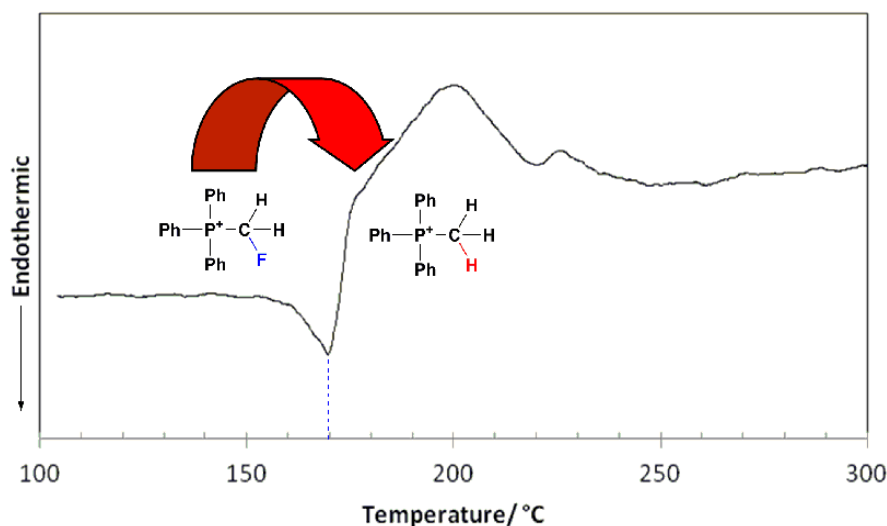
9.2.1 Synthesis and Properties

For the synthesis of **13** ($X = I$) we choose the reaction of triphenylphosphine with CH_2FI . The specific challenge of this fluoromethylation of triphenylphosphine with CH_2FI is the slow reaction rate. We observed, that heating of the reaction mixture in toluene at $110\text{ }^\circ\text{C}$ for a prolonged time (63 h) results in the formation of a brown solution, most probably due to decomposition of CH_2FI . However, if a solution of triphenylphosphine and the equimolar amount of CH_2FI is heated in a pressure tube to temperatures up to $120\text{ }^\circ\text{C}$, the reaction time is reduced considerably (6 h in DME) yielding **13** ($X = I$) up to 61 %. Different reaction solvents and times have been tested (Table 1). Temperatures higher than $120\text{ }^\circ\text{C}$ result in decomposition of CH_2FI . Reaction time can be further reduced by using an excess of CH_2FI . The excess of CH_2FI can be readily recovered by distillation during workup (see Experimental). The best conditions with DME or acetonitrile as solvent (entries 8 and 9) yield the phosphonium iodide **13** as a colorless microcrystalline powder (yield up to 99.8 %) in a high purity as determined by 1H and ^{19}F NMR spectroscopy.

Table 1: Fluoromethylation of triphenylphosphine to **13** (X = I) under various reaction conditions.

Entry	Solvent	t[h]	T[°C]	X(eq)	pressure	Yield [%]
1	Pentane	6	36	1	No	10
2	Diethylether	6	35	1	No	29
3	DME/Dioxane	6	85	1	No	37
4	DME	12	84	1	No	60
5	Toluene	63	110	1	No	70
6	Acetonitrile	6	120	1	Yes	59
7	DME	6	120	1	Yes	61
8	Acetonitrile	4	120	3	Yes	94
9	DME	3	120	3	Yes	99.8

The phosphonium iodide **13** (X = I) is slightly light sensitive changing its color from colorless to slightly brownish on prolonged exposure to light. The differential thermal analysis (DTA) curve of **13** (X = I) is shown in Figure 3. It shows the melting point at 170 °C with an onset point of 155 °C (the melting behavior was confirmed by DSC measurement). Literature values are in range of 168 – 171 °C.^[15d,16] The phosphonium iodide **13** is reported to decompose at its melting point (Figure 3), changing its color to brown. NMR spectroscopic (in CD₃CN) and single X-ray analysis of the resulting brown solid shows by surprise the formation of the triphenylmethyl - phosphonium cation Ph₃P(CH₃)⁺.^[17] This cannot be explained for us, but one cannot doubt the identity.

**Figure 3:** Thermal behavior (DTA) of **13**.

9.2.2 Crystal Structure

Single crystals of **13** (X = I), suitable for X-ray diffraction, were obtained by slow evaporation of an acetonitrile solution. The compound crystallizes in the orthorhombic space group *Pna*2₁ with four formula units in the unit cell. The asymmetric unit of **13** is shown in Figure 4.

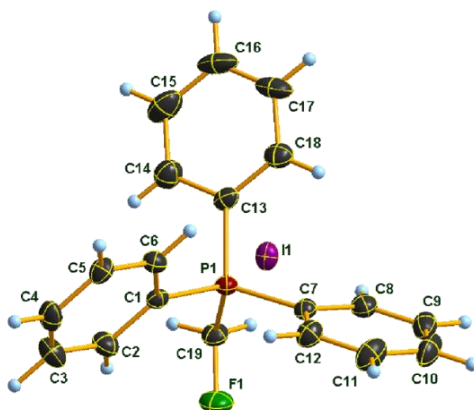


Figure 4: Molecular structure of compound **13** in the solid state, DIAMOND representation, thermal ellipsoids shown at 50 % probability level.

The phosphorus atom displays a slightly distorted tetrahedral surrounding. The phenyl moieties show a propeller like arrangement. The P1-C19 distance to the carbon atom of the CH₂F group corresponds with 1.810(4) Å to a P-C single bond.^[18] The C19-F1 distance of 1.379(5) Å compares to the value of 1.399 Å (C_{sp}³-F), found in literature.^[18] The most interesting feature of the structure is the PCH₂F moiety. The P1-C19 bond length of 1.810(4) Å is elongated compared to a P-CH₃ moiety [1.776(2) Å]. The C19-F1 bond length of 1.379(5) Å is unaffected by the phosphonium substituent and in the region of a typical C-F single bond observed for CH₂FI [1.380(17) Å] or CH₂BrF [1.377(4) Å].^[19] In order to obtain information on the structural behavior of the P-CH₂F unit, weak interactions in the crystal structure of **13** (X = I) are of interest. The iodide anions show weak hydrogen bonding to the CH₂-protons of the phosphonium cation, which results in the formation of chains along the a-axis (Figure 5).

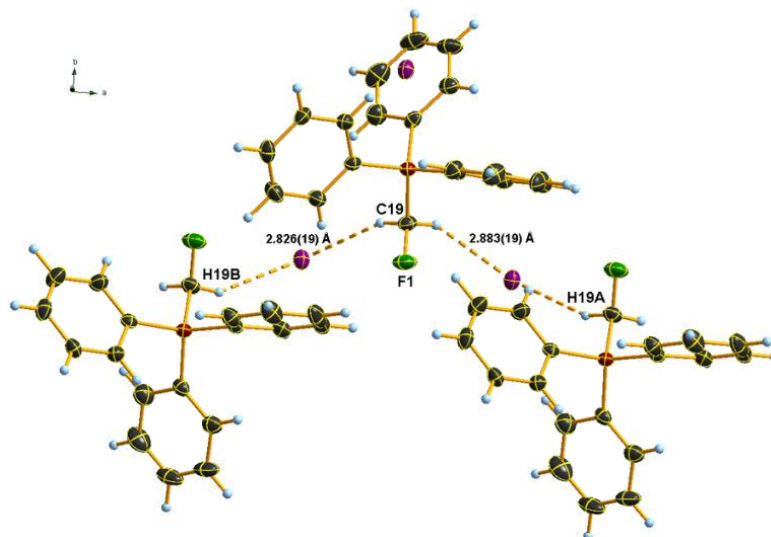


Figure 5: Hydrogen bonding in the crystal structure of compound **13**, DIAMOND representation. Thermal ellipsoids are shown at 50 % probability level. Symmetry code for the left phosphonium cation: $-0,5+x, -0,5-y, z$; for the left iodide anion: $1,5,-x, 0,5+y, -0,5+z$; for the right phosphonium cation: $0,5+x, -0,5-y, z$; for the right iodide anion: $2-x, -y, -0,5+z$.

There are no significant fluorine-hydrogen interactions (shortest distance 2.51(3) Å). In contrast, the crystal structure of the related triphenylphosphonium hydroxymethyl iodide (CH₂F replaced by the bioisosteric CH₂OH)^[20] is dominated by a $-\text{OH}\cdots\text{I}$ hydrogen bond; the

interactions of I to the CH₂ protons are in this case (as expected) weaker (CH \cdots I distances of 3.0923(2) and 3.2070(2) Å).^[21]

9.2.3 Vibrational Spectra

The experimental and calculated Raman spectra of **13** in the range of 150 – 3500 cm⁻¹ are shown in Figure 6. The assignments were made on the basis of literature data and quantum chemical calculations (B3LYP/ 6-311G+(d,p)) of the phosphonium cation.^[22]

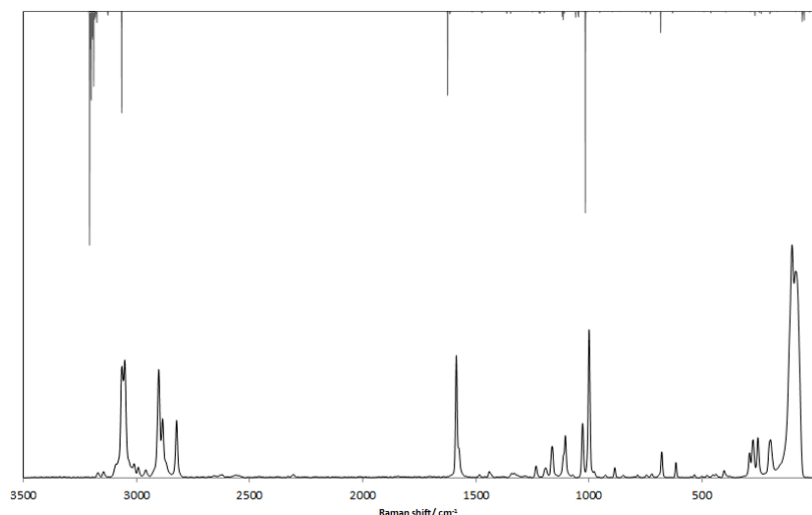


Figure 6: Experimental Raman spectrum of **13** (bottom) and calculated vibrational spectrum of the cation of **13** (top).

The characteristic line in the Raman spectra of **13** (999 cm⁻¹) corresponds to the skeleton vibration mode of the aromatic carbon atoms. The asymmetric $\nu_{as}(\text{CH}_2)$, symmetric $\nu_s(\text{CH}_2)$ and rocking $\varrho(\text{CH}_2)$ vibration modes of the fluoromethyl group account for the lines at 2901, 2884 and 1233 cm⁻¹, respectively. The C-F stretching mode is calculated to appear at 1056 cm⁻¹, but compared to other –CH₂F compounds of poor intensity and therefore not observable in the Raman spectrum. The bands 1110 cm⁻¹ $\nu(\text{CF})$ and 719 cm⁻¹ $\nu(\text{CF})$ in the IR-spectra are assigned to the CF stretch- and PCF deformation vibration. The band at 883 cm⁻¹ is assigned to the rocking vibration of the CH₂F group.

9.3 Conclusion

In conclusion we have developed an efficient and facile synthesis method for the monofluoromethylating agent **13** (X = I) in high purity. Single crystal X-ray diffraction reveals first structural information of a phosphorus bonded CH₂F group. The P-CH₂F moiety has an elongated P-C bond compared to that of a P-CH₃ moiety whereas the C-F bond lengths of **13** (X = I) is in the region of a typical C-F single bond observed for example in CH₂FI. Stronger hydrogen bonds are resulted between CH₂F and I than with the bioisoster CH₂OH moiety and I. The compound forms CH \cdots I hydrogen bonded chains in the crystal along the a-axis, while only very weak fluorine hydrogen interactions are observed.

Table 2: Selected vibrational frequencies [cm^{-1}], intensities and assignments for **13** (experimental and calculated), PPh₃ and CH₂FI (FIM).

13 Experimental	13 Calculated	PPh ₃	FIM	Assignments
3064 (50)	3205 (100)		2976	$\nu_s(\text{C}_{\text{arom}}\text{H})$, $\nu(\text{CH})$
3051 (52)	3191 (20)	3048		$\nu_{\text{as}}(\text{C}_{\text{arom}}\text{H})$
2901 (47)	3125 (10)			$\nu_{\text{as}}(\text{CH}_2)$
2884 (25)	3064 (50)			$\nu_s(\text{CH}_2)$
1586 (49)	1623 (35)	1584		$\nu_{\text{as}}(\text{C}_{\text{arom}}\text{C}_{\text{arom}})$
1233 (5)	1248 (1)		1266	$\vartheta(\text{CH}_2)$, $\nu(\text{CF})$
1191 (11)	1195 (2)	1180		$\zeta(\text{C}_{\text{arom}}\text{H})$, $\nu(\text{CH})$,
1162 (15)	1116 (2)	1158		$\nu_{\text{as}}(\text{C}_{\text{arom}}\text{P})$
1104 (20)	1109 (5)	1095		$\nu_s(\text{C}_{\text{arom}}\text{C}_{\text{arom}})$
1028 (25)	1044 (11)	1027		$\delta(\text{C}_{\text{arom}}\text{C}_{\text{arom}})$
999 (55)	1012 (20)	1000		$\delta(\text{C}_{\text{arom}}\text{C}_{\text{arom}})$
615 (10)	628 (8)	618	561	$\delta(\text{C}_{\text{arom}}\text{C}_{\text{arom}})$, $\nu(\text{Cl})$
290 (15)	282 (3)			$\nu_{\text{as}}(\text{PC})$

The intensities for the Raman spectra are shown in parentheses and scaled relative to the intensity of the strongest peak in each spectrum, which is assigned to a value of 100. The symbols ν_s , ν_{as} , ϑ , ζ and δ denote symmetric-, asymmetric-, rock-, scissor- and in plane vibration mode respectively.

9.4 Acknowledgement

We are thankful to F-Select GmbH for a generous donation of CH₂FI. We thank Prof. Dr. T. M. Klapötke for the generous allocation of diffractometer time and for his continuous support. We thank Thomas Schnappinger for the help with the DFT calculations

9.5 Experimental Section

9.5.1 General Procedures

All compounds were handled using Schlenk techniques under dry Ar. Triphenylphosphine (BASF) was dried *in vacuo* at room temperature for 15 min and fluoroiodomethane (donation from F-Select GmbH) was distilled under inert conditions before use. Solvents were purchased from ABCR, dried and distilled before use. The samples for NMR spectroscopy were prepared under inert atmosphere using Ar as protective gas. The solvent CDCl₃ was dried using CaCl₂, distilled and stored under Ar atmosphere. Spectra were recorded on a Bruker Avance III spectrometer operating at 400.1 MHz (¹H), 376.4 MHz (¹⁹F), 161.9 MHz (³¹P) and 100.6 MHz (¹³C). Chemical shifts are referred to TMS (¹H, ¹³C), CFC₃ (¹⁹F) and 85 % H₃PO₄ (³¹P). The samples for Raman spectroscopy were sealed in glass tubes under Argon. The Raman spectrum of **13** was recorded with a Bruker MultiRam

FT Raman spectrometer using a neodymium doped yttrium aluminium garnet (Nd:YAG) laser ($\lambda = 1064$ nm) with 1074 mW. The samples for Infrared spectroscopy were placed under ambivalent conditions without further preparation onto an ATR unit using a Perkin Elmer Spectrum BX II FT-IR System spectrometer. Melting and/or decomposition points were detected with a Linseis DSC-PT10 instrument and with a OZM DTA 552-Ex instrument under inert atmosphere and ambivalent conditions, respectively. For the DSC, the powder sample was pelletized into an aluminium crucible with a sample weight of 1 mg. The sample was placed into the instrument chamber filled with N₂ as protective gas. The scanning temperature range was set from 293 K to 673 K at a scanning rate of 5 K min⁻¹. The DTA was recorded under ambivalent conditions. Therefore, 25 mg of the sample was filled into a tube, which was placed into the instrument. The scanning temperature range was set from 293 K to 673 K at a scanning rate of 5 K min⁻¹. The samples were prepared under N₂ atmosphere. High resolution mass spectral data were acquired using a Jeol MStation Sectorfield in FAB⁺ mode. The sample was prepared under N₂ atmosphere. Elemental analysis was done with a Vario EL instrument and a Metrohm 888 Titando device. The calculations were performed with the Gaussian09 program.^[22b] The structure was optimized and frequencies calculated at the DFT B3LYP level of theory using a 6-311G+(d,p) basis set. Single crystals of compound **13** (X = I), suitable for X-ray diffraction, were obtained by slow evaporation of a solution in acetonitrile. The crystals were introduced into perfluorinated oil and a suitable single crystal was carefully mounted on the top of a thin glass wire. Data collection was performed with an Oxford Xcalibur 3 diffractometer equipped with a Spellman generator (50 kV, 40 mA) and a Kappa CCD detector, operating with Mo-K α radiation ($\lambda = 0.71073$ Å).

Data collection and data reduction were performed with the CrysAlisPro software.^[23] Absorption correction using the multiscan method^[24] was applied. The structures were solved with SHELXS-97,^[25] refined with SHELXL-97^[25] and finally checked using PLATON.^[26] Details for data collection and structure refinement are summarized in the supplementary information.

CCDC-1892768 contains supplementary crystallographic data for this compound. These data can be obtained free of charge from The Cambridge Crystallographic Data Centre *via* www.ccdc.cam.ac.uk/data_request/cif.

9.5.2 Preparation

Synthesis (Method A)

A solution of triphenylphosphine (1.14 g, 4.33 mmol) in DME (6 mL) was inserted into a pressure tube and CH₂FI (0.879 mL, 13.0 mmol) was added quickly. The pressure tube was sealed under Ar and heated for 3 h at 120 °C. The white precipitate was separated by vacuum filtration, dried *in vacuo* yielding **13** as colorless crystalline solid (2.28 g, 99.8 %). From the filtrate, the excess of CH₂FI was recovered by distillation.

Synthesis (Method B)

A solution of triphenylphosphine (1.42 g, 5.41 mmol) in acetonitrile (6 mL) was inserted into a pressure tube and CH₂FI (1.10 mL, 16.2 mmol) was added quickly. The pressure tube was

sealed under Argon and heated for 4 h at 120 °C. The solvent and the excess of CH₂FI was removed using a rotary evaporator, the resulting white solid was washed with 3 × 20 mL toluene and dried *in vacuo*. Yield: 2,15 g (94 %). Excess of CH₂FI was recovered by distillation of the collected solution from the rotary evaporator.

¹H-NMR (400 MHz, CDCl₃, 26°C): δ = 7.92 – 7.83 (m, 9H), 7.77 – 7.72 (m, 6H), 6.88 (d, ²J_{F,H} = 45.0 Hz, 2H, -CH₂F) ppm. ¹³C{¹H}-NMR (100.6 MHz, CDCl₃, 26°C): δ = 136.2 (d, ⁴J_{P,C} = 3.1 Hz, C-4), 134.5 (dd, ²J_{P,C} = 10.4, ⁴J_{FC} = 1.2 Hz, C-2), 130.9 (d, ³J_{P,C} = 13.0 Hz, C-3), 114.8 (d, ¹J_{P,C} = 86.5 Hz, C-1), 78.3 (dd, ¹J_{F,C} = 197.7, ¹J_{PC} = 63.8 Hz, -CH₂F) ppm. ³¹P{¹H}-NMR (162 MHz, CDCl₃, 26°C): δ = 19.3 (d, ²J_{P,F} = 57.6 Hz) ppm. ¹⁹F{¹H}-NMR (376 MHz, CDCl₃, 26°C): δ = -242.87 (d, ²J_{P,F} = 57.6 Hz) ppm. ¹⁹F-NMR (376 MHz, CDCl₃, 26°C): δ = -242.87 (dt, ²J_{P,F} = 57.6, ²J_{F,H} = 45.0 Hz) ppm. Raman: (see Table 2). FT-IR (ATR): $\tilde{\nu}$ = 3050(w), 2896(m), 2879(m), 2818(m), 2625(w), 2303(w), 2215(w), 2012(w), 1906(w), 1823(w), 1677(w), 1585(m), 1483(w), 1435(s), 1338(w), 1315(w), 1185(w), 1163(w), 1110(s, v(CF)), 1023(s), 995(m), 926(w), 883(m, ν CH₂F), 846(w), 785(w), 752(m), 739(s), 719(s, v(CF)), 681(s), 614(w), 530(s) cm⁻¹. Elemental analysis: Calcd. for C₁₉H₁₇FIP: C 54.05 H 4.06, found: C 53.86 H 4.12 %. HRMS-FAB (m/z) [M⁺]: Calcd. for C₁₉H₁₇FP: 295.1052, found: 295.1038. Mp.: 170 °C (Dec.).

9.6 References

- [1] W. Zhang, J. Hu, F. Wang, *Chem. Commun.* **2009**, 7465 - 7478.
- [2] D. K. Kölmel, *Chemische Biologie von Peptoiden und Synthese fluoriger Farbstoffe*, Vol. 25, Logos, Berlin, **2013**.
- [3] G. K. S. Prakash, I. Ledneczi, S. Chacko, G. A. Olah, *Org. Lett.* **2008**, *10*, 557-560.
- [4] J. Hu, B. Gao, L. Li, C. Ni, J. Hu, *Org. Lett.* **2015**, *17*, 3086-3089.
- [5] T. Ochiai, R. Ishida, *Jpn. J. Pharmacology* **1982**, *32*, 427-438.
- [6] L. V. Kudzma, C. G. Huang, R. A. Lessor, L. A. Rozov, S. Afrin, F. Kallashi, C. McCutcheon, K. Ramig, *J. Fluorine Chem.* **2001**, *111*, 11-16.
- [7] a) C. Walsh, *Tetrahedron* **1982**, *38*, 871-909; b) T. Tsushima, K. Kawada, *Tetrahedron Lett.* **1985**, *26*, 2445-2448.
- [8] R. Bohlmann, *DE 4330237 A1* (Ed.: S. AG), Germany, **1995**.
- [9] S. Monticelli, V. Pace, *Aust. J. Chem.* **2018**, *71*, 473-475.
- [10] G. Parisi, M. Colella, S. Monticelli, G. Romanazzi, W. Holzer, T. Langer, L. Degennaro, V. Pace, R. Luisi, *J. Am. Chem. Soc.* **2017**, *139*, 13648-13651.
- [11] a) J. Veliks, A. Kazia, *Chem Eur. J.* **2019**, *25*, 3786-3789; b) S. Monticelli, M. Colella, V. Pillari, A. Tota, T. Langer, W. Holzer, L. Degennaro, R. Luisi, V. Pace, *Org. Lett.* **2019**, *21*, 584-588.
- [12] a) M. Zhou, X. Shen, C. Ni, W. Zhang, J. Hu *Chem. Sci.* **2014**, *5*, 117 - 122 b) F. Swarts, *Bull. Cl. Sci., Acad. R. Belg.* **1910**, 113 - 123 c) E. P. T. Leitao, C. R. Turner, *WO 2011151624 A1*, Hovione Inter Limited, Switz, **2011** d) D. J. Burton, P. E. Greenlimb, *J. Fluorine Chem.* **1974**, *3*, 447-449 e) R. Bohlmann, D. Bittler; M. Gottwald, P. Muhn, Y. Nishino, B. Schoenecker, G. Hobe, *DE 4330237 A1*, Germany, **1995**.
- [13] R. M. Kaul, J. Ernest, J. Sun, D. Vocadlo, Y. Zhou, Y. Zhu, *WO 2015095963 A1*, Alectos Therapeutics Inc., Can, **2015**.

- [14] M. F. Deodhar, D. Alison, J. S. Foot, W. Jarolimek, I. A. McDonald, A. Robertson, C. I. Turner, *WO 2013163675 A1*, Pharmaxis Ltd., Australia, **2013**.
- [15] a) D. J. Burton, D. M. Wiemers, *J. Fluorine Chem.* **1985**, *27*, 85-89 b) G. Landelle, J.-F. Paquin, *e-EROS Encycl. Reagents Org. Synth.*, John Wiley & Sons, Ltd, Chichester, UK, **2011** c) D. G. Cox, D. J. Burton, *J. Org. Chem.* **1988**, *53*, 366-374 d) M. Schlosser, M. Zimmermann, *Synthesis* **1969**, Thieme, Stuttgart, 75 - 76.
- [16] D. J. Burton, P. E. Greenlimb, *J. Org. Chem.* **1975**, *40*, 2796.
- [17] J. Adamek, J. Mrowiec-Białoń, A. Październiak-Holewa, R. Mazurkiewicz, *Thermochim. Acta* **2011**, *512*, 22-27.
- [18] F. H. Allen, D. G. Watson, L. Brammer, A. G. Orpen, R. Taylor, *J. Chem. Soc., Perkin Trans. 2* **1987**, 1 - 19.
- [19] M. Feller, K. Lux, A. Kornath, *Eur. J. Inorg. Chem.* **2015**, 5357.
- [20] C. Siebert, *Chem. Unserer Zeit* **2004**, 38.
- [21] M.C Davis, D. A. Parrish, *Synth. Commun.* **2008**, *38*, 3909.
- [22] a) M. Hesse, H. Meier, B. Zeeh, *Spektroskopische Methoden in der organischen Chemie*, Thieme, **2005** b) A. F. Izmaylov, G. Zheng, J. L. Sonnenberg, M. Hada, , K. T. M. Ehara, R. Fukuda, J. Hasegawa, M. Ishida, T. Nakajima, , O. K. Y. Honda, H. Nakai, T. Vreven, J. A. Montgomery, Jr., , F. O. J. E. Peralta, M. Bearpark, J. J. Heyd, E. Brothers, , V. N. S. K. N. Kudin, T. Keith, R. Kobayashi, J. Normand, , A. R. K. Raghavachari, J. C. Burant, S. S. Iyengar, J. Tomasi, , N. R. M. Cossi, J. M. Millam, M. Klene, J. E. Knox, J. B. Cross, , C. A. V. Bakken, J. Jaramillo, R. Gomperts, R. E. Stratmann, , A. J. A. O. Yazyev, R. Cammi, C. Pomelli, J. W. Ochterski, , K. M. R. L. Martin, V. G. Zakrzewski, G. A. Voth, , J. J. D. P. Salvador, S. Dapprich, A. D. Daniels, , J. B. F. O. Farkas, J. V. Ortiz, J. Cioslowski, , a. D. J. Fox, Gaussian, Inc., Wallingford CT, **2010**.
- [23] Program package CrysAlisPro 1.171.38.46 Rigaku OD, **2015**.
- [24] G. M. Sheldrick, SHELXS-97: Program for Crystal Structure Solution, University of Göttingen, Germany, **1997**.
- [25] G. M. Sheldrick, SHELXL-97: Program for the Refinement of Crystal Structures, University of Göttingen, Germany, **1997**.
- [26] A. L. Spek, PLATON: A Multipurpose Crystallographic Tool, Utrecht University, Utrecht, The Netherlands, **1999**.

9.7 Supporting Information

Table 1: Structure refinement parameter of **13**.

Empirical formula	C ₁₉ H ₁₇ FIP
Formula weight	422.19
Temperature	143(2) K
Wavelength	0.71073 Å
Crystal system	Orthorhombic
Space group	<i>Pna</i> 2 ₁
Unit cell dimensions	a = 11.7439(4) Å

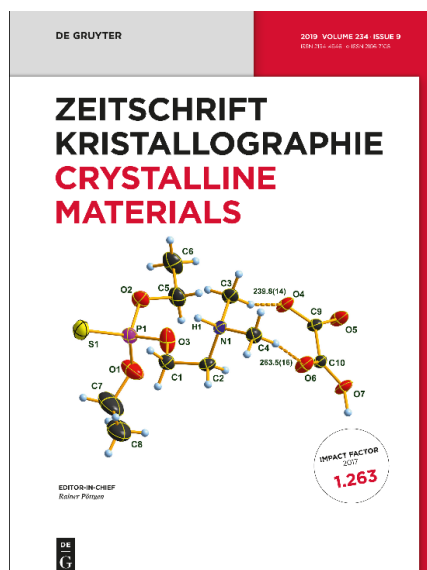
	$b = 9.1986(4) \text{ \AA}$
	$c = 16.6342(6) \text{ \AA}$
	$\alpha = 90^\circ$
	$\beta = 90^\circ$
	$\gamma = 90^\circ$
Volume	$1796.95(12) \text{ \AA}^3$
Z	4
Density (calculated)	1.561 mg/m^3
Absorption coefficient	1.874 mm^{-1}
F(000)	832
Crystal size	$0.100 \times 0.080 \times 0.050 \text{ mm}^3$
Theta range for data collection	$4.25 - 25.24^\circ$
Index ranges	$-16 \leq h \leq 16, -13 \leq k \leq 13, -23 \leq l \leq 15$
Reflections collected	19153
Independent reflections	4583 [$R_{\text{int}} = 0.0417$]
Goodness-of-fit on F^2	0.981
Final R indices [$I > 2\sigma(I)$]	$R_1 = 0.0297, wR_2 = 0.0476$
R indices (all data)	$R_1 = 0.0491, wR_2 = 0.0540$
Largest diff. peak and hole	$0.456 \text{ and } -0.476 \text{ e\AA}^{-3}$

10 *O,O*-Diethyl *O*-[2-(dimethylamino)ethyl] Phosphorothioate: Structural Evidence of the Decomposition Product and its Oxalate Salt

Marc André Althoff, Jörn F. Martens, Marco Reichel, Manfred Metzulat, Thomas M. Klapötke, Konstantin L. Karaghiosoff*

Published in *Z. Kristallogr.* **2019**, *234*, 613–621.

DOI: 10.1515/zkri-2019-0025



Abstract: The molecular and single crystal structure of *O,O*-diethyl *O*-[2-(dimethylamino)ethyl] phosphorothioate oxalate, as determined by single crystal X-ray diffraction studies, is described for the first time; although this compound is well-known by industry and research from the mid-20th century. The known decomposition product of pure *O,O*-diethyl *O*-[2-(dimethylamino)ethyl] phosphorothioate could also be structurally characterized. Additionally, the compounds are characterized by recent analytical methods e.g. NMR. The findings of our study support the thesis that the isolated decomposition product must be a by-product of the thiono-thiolo rearrangement process of the title compound.

10.1 Introduction

Phosphoric acid esters are a widely studied class of compounds with a broad range of applications. They range from fertilizers over drugs and pesticides to the deadly chemical warfare agents and many more.^[1,2] Our recent research is mainly aimed at a better understanding of organo(thio)phosphates (OTP's) closely related to chemical warfare agents, namely Amiton,^[3] which is controlled under the Chemical Weapons Convention.^[4-7] Since, not all scientifically interesting issues of OTP's have been addressed and solved at the time of their discovery we want to assist closing some of the remaining gaps. As an example the still unresolved mechanism of the thiono-thiolo rearrangement of TP's may be mentioned.^[8-13] The two most important ones of the many proposed rearrangement pathways are shown in Figure 1. The first one has an ionic intramolecular transition state and was postulated by Fukuto and Stafford.^[14] The second one is an ionic intermolecular process and was developed by Tammelin.^[15] All of the many suggested pathways work very well for the respective compound investigated but no general rule could be derived so far. Another noteworthy fact is the OTP's ability to alkylate suitable reaction partners, which in part supports the above theories.^[16] Furthermore, Cadogan and Thomas as well as Tammelin reported independently on the formation of solid degradation products during the storage of pure Amiton and comparable compounds.^[15,17] These degradation products are said to contain the respective 1,1,4,4-tetraalkylpiperazinium salts. Cadogan and Thomas postulate their formation via dimerization of the threemembered immonium ions, whereas Tammelin is of the opinion those are formed via a different immonium ion (c.f. Figure 1). We were also challenged with the above mentioned issues and are of the opinion that both processes, rearrangement and decomposition, are related with each other. This must be the case since both reactions are not observed if the respective quaternary ammonium salts are prepared.^[18-21] Although *O,O*-diethyl *O*-[2-(dimethylamino)ethyl] phosphorothioate (**1**) and several salts thereof were described decades ago, no single crystal structure of these compounds has been reported yet. The same holds true for the decomposition products. However, the identity of those compounds was so far only proven by means of IR spectroscopy and synthesis of the postulated molecules to proof for identity.^[17,22] Consequently, this class of compounds is also lacking a description by recent analytical methods like NMR spectroscopy or mass spectrometry.

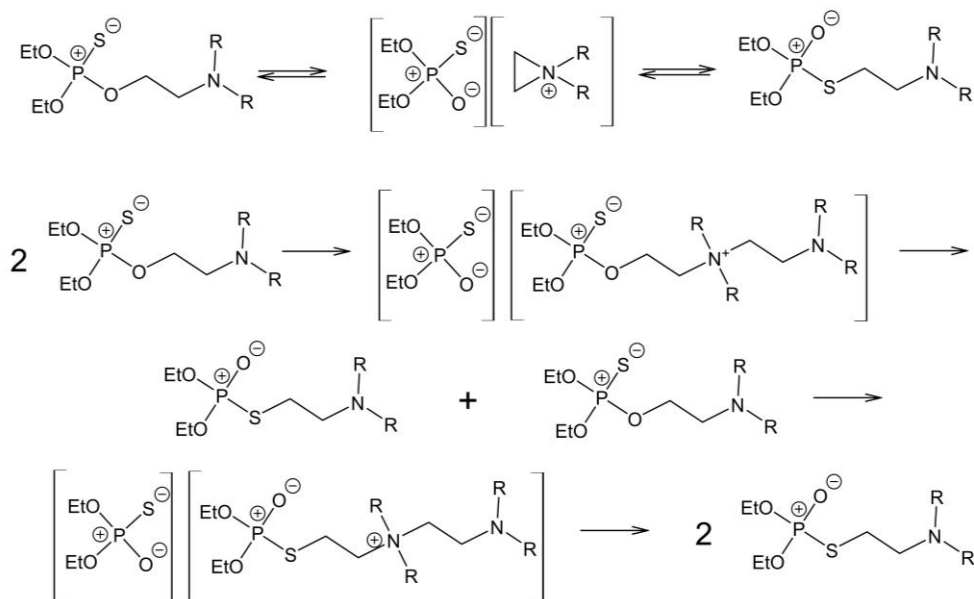


Figure 1: Proposed mechanisms for the thiono–thiol rearrangement of organo(thio)phosphates.

10.2 Results and Discussion

10.2.1 Synthesis

The synthesis of *O,O*-diethyl *O*-[2-(dimethylamino)ethyl] phosphorothioate (**1**) is relatively smooth to perform and results in good yield. A depiction of the reaction scheme can be found in Figure 2. The same holds true for the preparation of its oxalate salt **3** which forms quite rapidly as white powder upon mixing of the two educts. On the contrary the preparation of the required single crystals of compounds **2** and **3** suitable for single X-ray crystallography studies is more time consuming. The powder needs to be recrystallized from an excess of acetone. The identity of the found crystal of compound **2** in the NMR tube with the synthesized one was done by comparison of the respective crystallographic cell parameters; they fitted very well. While we prepared the ^{31}P -NMR spectra of compound **1** for the first time after the synthesis we found a single signal at 69.0 ppm. After finding of the crystal in the NMR-tube we run another ^{31}P -NMR experiment which revealed the presence of an additional signal at 29.6 ppm belonging to the thio isomer of compound **1**. This means that we found three different molecules in the NMR tube at the same time. Moreover, it is strong evidence for the close relation of the thiono-thiolo rearrangement and the decomposition process of *O,O*-diethyl *O*-[2-(dimethylamino)ethyl] phosphorothioate (**1**) and related compounds.

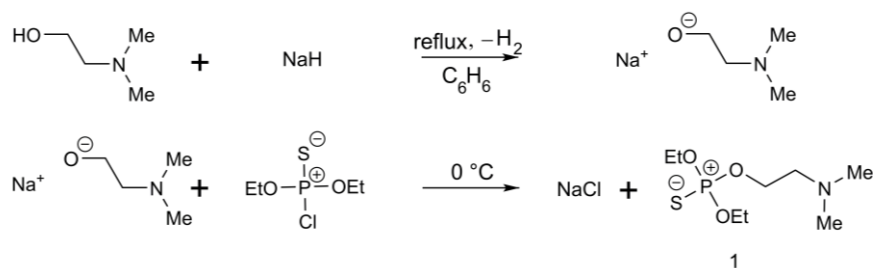


Figure 2: Reaction pathway for the synthesis of compound **1**.

10.2.2 NMR Spectroscopy

In general, all couplings of phosphorus, carbon atoms and protons could be clearly identified and resolved. In the ^{31}P NMR spectrum of compound **1** a signal at 69.0 ppm is observed. It is coupled to a septet of 9.5 Hz coupling constant. Interestingly the two different sets of CH_2 -groups have coincidentally the same coupling constant to the phosphorus. Regularly it would be expected to observe a triplicated pentet. This single signal at the same time proves the purity of the sample. The spin system of the two ethoxy groups can be denoted as an A3MNX-spin system and result in a *qdt* coupling pattern at 15.8 ppm. The two diastereomeric protons, denoted M and N, of the methylene group cannot be distinguished since their coupling constants do not differ sufficiently from each other.

Accordingly, the two methyl groups at the nitrogen show a *qtt* coupling pattern in the ^{13}C NMR at 45.6 ppm having 1J , 2J and 4J couplings to adjacent protons. The six methyl protons themselves result in a singlet at 2.18 ppm. All other protons show additional coupling to phosphorus and thus have an additional doublet splitting. Furthermore, the three methylene carbons bound to the oxygen atoms have a very similar chemical shift of 65.6 ppm for the two belonging to the ethoxy moiety and 65.7 ppm for the side chain methylene group. They could be clearly differentiated from each other by the geminal quartet splitting of the methyl protons in the ethoxy moiety, compared to the triplet coupling for the other one. The most complicated coupling could be observed for the carbon NMR of the methylene group neighboring the nitrogen, since it couples to four different nuclei. All discussed spectra are presented in the supporting information.

10.2.3 Vibrational Spectroscopy

In the IR spectra of all compounds a strong band can be assigned to the CH_3 asymmetric vibration at 2966-2979 cm^{-1} . In the spectrum of compound **1** also the respective CH_2 vibration at 2822 and 2771 cm^{-1} can be identified. Some weak CH deformation vibrations in the region of 1448-1476 cm^{-1} can also be found along all three compounds. Additionally, the stretching vibration of the N-C-H groups of the tertiary amine is observed at 2771 cm^{-1} for compound **1**. Moreover, the signal at 1162 cm^{-1} can be assigned to the tertiary aliphatic amine moiety. These findings are in very good agreement with common literature values.^[33] The P=S valance vibrations can be found in the region of 820 cm^{-1} and 780 cm^{-1} as a strong doublet band for all compounds. The doublet structure of the P=S stretching vibration absorption maxima in the IR can be accounted to the presence of two rotational isomers of the molecule.^[34] An additional strong signal at 1703 cm^{-1} can be found in the IR spectrum of compound **2** which can be clearly assigned to the carbonyl stretching vibration of the oxalic acid part of the crystal.^[35] Due to the strong fluorescence of compounds **1** and **3** no Raman spectra could be obtained. The Raman spectrum of compound **2** shows fewer vibrational modes compared to the IR spectrum. The CH deformation vibrations of the piperazine ring can be found at 1435 cm^{-1} and the CH_3 rocking vibrations of the P-O CH_2CH_3 moiety at 1186 cm^{-1} , respectively. Finally, at 1037 cm^{-1} the respective P-O-C stretching vibrations can be identified and at 809 cm^{-1} , the C-C vibrations of the piperazine ring occur. Obtained spectra can be found in the supplement to this work.

10.2.4 Mass Spectrometry

The ESI-MS spectrum of compound **1** shows a clear $[M-H]^+$ signal of 242.1 m/z and a stronger fragment signal at 72.0 m/z . Compared to this the MS (EI) spectra does not show a molecule peak but two signals at m/z 58.0 and 71.1. The latter one is representing the same fragment as the m/z 72.0 signal in the ESI-MS spectra. This fragment is resulting from bond breaking between the oxygen and the methylene group of the nitrogen containing side chain of the molecule. The respective spectra can be found in the supporting information.

10.3 Molecular and Crystal Structure

10.3.1 Compound 2

The molecular structure of the asymmetric unit with grown fragments of compound **2** is presented in Figure 3. As can be seen the structure is comprised of two individual fragments being the respective counter ion of one another. The two-fold axis of the Laue-group becomes obvious to be sitting in the center of the cationic ring. The former bond between C5 and O2 of the parent molecule, compound **1**, has been broken and instead the nitrogen moiety has formed a 1,1,4,4-tetra-methyl-substituted piperazine cation by joining a second nitrogen moiety of another compound **1** molecule. The N-C bond lengths in the ring are close to tabulated values of a standard C-N bond being 1.47 Å.^[36] Compared to an unsubstituted piperazine molecule the observed bond lengths are shortened by 0.02 Å.^[37] The ring formed has chair configuration. The nitrogen atom exhibits a distorted tetrahedral configuration with bond angles in the range of 108.5-111.7°.

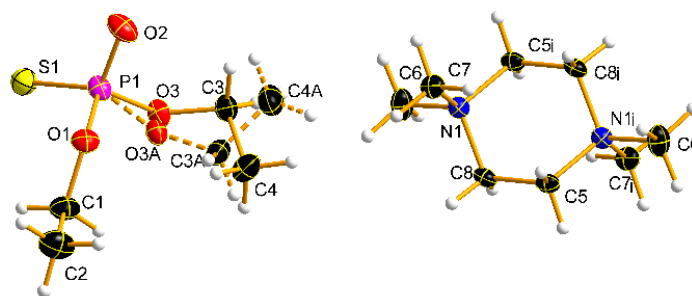


Figure 3: Molecular structure of compound **2** in the crystal (asymmetric unit with grown fragment), DIAMOND^[31] representation; displacement ellipsoids are drawn at 50% probability level. The broken bonds indicate a split position of the respective atoms. The index *i* stands for the atoms not belonging to the asymmetric unit. The symmetry operations to describe the indexed atoms of the cation are: 2 - *x*, -*y*, 2 - *z*.

The anionic part of the crystal is formed by the *O,O*-diethyl-thio-phosphorus acid moiety. The phosphorus as the central atom of this part has also a distorted tetrahedral configuration. The S1-P1-O2 angle being 119.3° is large compared to the other S-P-O angles of 104.4° and 111.3°. The bond lengths of the respective atoms are also of great importance. As known from the parent compound **1** O2 was bound to a CH₂-group and thus would be expected to have the character of a single bond. On the contrary in the crystal structure the P-O₂ bond has the length of a P-O double bond being 1.48 Å long, whereas the character of the P-S bond length with 1.97 Å lies somewhere in between that of a single and a double bond of 2.11 Å and 1.91 Å,

respectively.^[36] Additionally, the P1-O1 and P1-O3 bonds are also shorter than expected for a single bond. The shorter carbon-carbon bonds can be accounted to the strong electron withdrawing properties of the neighboring oxygen atom. Moreover, one ethoxy moiety (O3-C3-C4) bonded to the phosphorus exhibits strong molecular disorder and thus needed to be split into a second position which is indicated by an additional letter A at the corresponding carbon and oxygen atoms. This split position is always depicted by broken bonds in the graphical illustrations. By growing the unit cell (c.f. Figure 4) one can see that each of the nitrogen containing rings sits on the corners as well as the center of the unit cell. Figure 4 also shows that four formula units are the content of the unit cell. The six-membered piperazine ring itself forms a sub-lattice comparable to tungsten in the body-centered cubic (A2) structure.^[38] The four negatively charged counterions can be easily seen from Figure 4. No hydrogen bonds could be found in the crystal structure.

Table 1: Selected bond length (Å) of compound **2**.

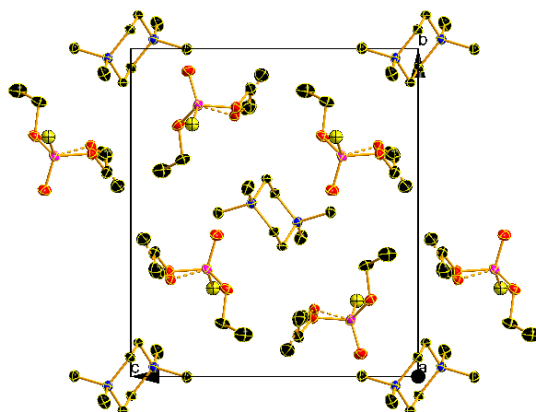
S1 - P1	1.967(5)	C3A - C4A	1.497(5)
P1 - O1	1.606(3)	C3 - O3	1.436(10)
P1 - O2	1.483(4)	C3A - O3A	1.477(11)
P1 - O3	1.585(9)	C5 - C8	1.508(8)
P1 - O3A	1.638(10)	N1 - C5	1.507(6)
O1 - C1	1.443(6)	N1 - C6	1.502(6)
C1 - C2	1.498(2)	N1 - C7	1.503(6)
C3 - C4	1.493(5)	N1 - C8	1.507(6)

Table 2: Selected bond angles (°) of compound **2**.

O1 - P1 - S1	111.3(1)	C1 - O1 - P1	121.3(1)
O2 - P1 - S1	119.2(1)	C3 - O3 - P1	119.8(6)
O3 - P1 - S1	104.4(3)	C3A - O3A - P1	120.9(7)
O3A - P1 - S1	106.4(3)	C6 - N1 - C7	108.0(1)
O1 - P1 - O3	110.2(2)	C6 - N1 - C8	108.5(1)
O1 - P1 - O3A	96.6(2)	C6 - N1 - C5	108.5(1)
O2 - P1 - O1	103.9(1)	C7 - N1 - C8	111.6(1)
O2 - P1 - O3	107.6(3)	C7 - N1 - C5	111.7(1)
O2 - P1 - O3A	116.9(3)	C8 - N1 - C5	108.5(2)
O1 - C1 - C2	108.2(2)	N1 - C5 - C8	112.3(1)
O3 - C3 - C4	112.0(4)	N1 - C8 - C5	112.2(1)
O3A - C3A - C4A	111.3(4)		

Table 3: Details for X-ray data collection and structure refinement for compound **2** (CCDC 1908795) and **3** (CCDC 1908796).

Empirical formula	C ₈ H ₂₀ NO ₃ PS (Compound 2)	C ₁₀ H ₂₂ NO ₇ PS (Compound 3)
Formula weight	241.28	331.31
Temperature	173(2) K	173(2) K
Wavelength	0.71073 Å	0.71073 Å
Crystal system	monoclinic	triclinic
Space group	<i>P</i> 2 ₁ / <i>n</i> ,	<i>P</i> -1
Unit cell dimensions	<i>a</i> = 7.4660(2) Å <i>b</i> = 13.5370(4) Å <i>c</i> = 11.8560(4) Å α = 90° β = 92.861(3)° γ = 90°	<i>a</i> = 5.5611(4) Å <i>b</i> = 8.4383(5) Å <i>c</i> = 18.307(2) Å α = 98.090(6)° β = 93.525(7)° γ = 105.213(5)°
Volume	1196.76(6) Å ³	816.36(11) Å ³
Z	4	2
Density (calculated)	1.339 mg/m ³	1.348 mg/m ³
Absorption coefficient	0.389 mm ⁻¹	0.323 mm ⁻¹
F(000)	520	352
Crystal size	0.460 x 0.340 x 0.260 mm ³	0.350 × 0.100 × 0.050 mm ³
Theta range for data collection	4.36 – 25.24°	4.12 – 25.24°
Index ranges	-9 ≤ <i>h</i> ≤ 9, -18 ≤ <i>k</i> ≤ 18, -15 ≤ <i>l</i> ≤ 15	-6 ≤ <i>h</i> ≤ 6, -10 ≤ <i>k</i> ≤ 10, -22 ≤ <i>l</i> ≤ 22
Reflections collected	10777	11935
Independent reflections	2943 [R _{int} = 0.046]	3304 [R _{int} = 0.052]
Goodness-of-fit on F ²	1.041	1.043
Final R indices [I > 2σ(I)]	R ₁ = 0.0293, wR ₂ = 0.0727	R ₁ = 0.0467, wR ₂ = 0.1102
R indices (all data)	R ₁ = 0.0374, wR ₂ = 0.0779	R ₁ = 0.0707, wR ₂ = 0.1253
Largest diff. peak and hole	0.303 and -0.259 e Å ⁻³	0.609 and -0.447 e Å ⁻³

**Figure 4:** Representation of the unit cell of compound **2** with grown fragments of the positive counter ion in the crystal, DIAMOND^[31] representation; displacement ellipsoids are drawn at 50% probability level. The broken bonds indicate a split position of the respective atoms. View along *a*-axis; hydrogen atoms are omitted for better oversight.

10.3.2 Compound 3

The molecular structure of the asymmetric unit of compound **3** is presented in Figure 5. As can be seen one protonated molecule of compound **1** is coordinated by one deprotonated molecule oxalic acid. They are coordinated via two hydrogen bridges from the oxalic acid towards the methyl groups bound to the nitrogen of compound **1**. The observed bond length and bond angles of compound **3** are given in Tables 4 and 5, respectively. The bond lengths are all in the expected range and do agree with reported literature values.^[36]

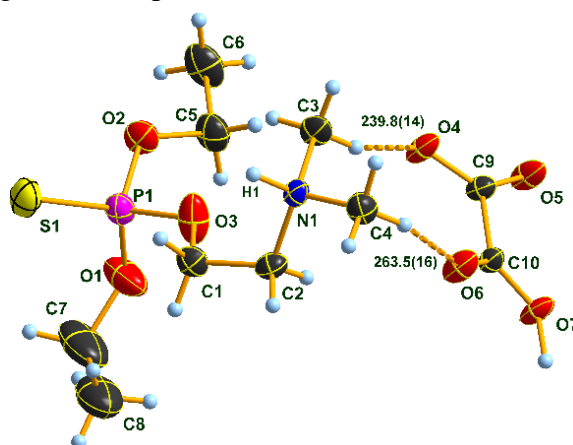


Figure 5: Molecular structure of compound **3** in the crystal (asymmetric unit), DIAMOND^[31] representation; displacement ellipsoids are drawn at 50% probability level. The broken bonds indicate hydrogen bonds.

According to the observed bond angles it can be seen that the sulfur is demanding in space and thus forces the three oxygens which are bound to the phosphorus to get closer to each other. The S–P–O angles range from 113° to 117°, whereas the respective O–P–O angles vary from 102° to 104°.

Table 4: Selected bond length (Å) of compound **3**.

P1 - O1	1.558(2)	O1 - C7	1.390(4)
P1 - O2	1.564(2)	C5 - C6	1.499(4)
P1 - O3	1.570(2)	C8 - C7	1.417(5)
P1 - S1	1.913(1)	N1 - C4	1.486(3)
O4 - C9	1.263(3)	N1 - C3	1.490(3)
O5 - C9	1.232(3)	N1 - C2	1.495(3)
O2 - C5	1.465(3)	O3 - C1	1.443(3)
O6 - C10	1.217(3)	C2 - C1	1.498(4)
O7 - C10	1.304(3)		

The crystal structure shows several hydrogen bonds. The shortest one can be found to coordinate the oxalic acid anions as a flat layered chain structure along the a-b-plane. Those anions coordinate the cations by weaker hydrogen bonds (c.f. Table 6 and Figure 6). Two oxygens (O5 and O7) of the oxalic acid are coordinated with the nitrogen's hydrogen atom of the next neighboring compound **1** molecule, being the cation. The remaining oxygens (O4 and

O6) of the oxalic acid interact with the two methyl groups bound to the protonated nitrogen of another compound **1** cation.

Table 5: Selected angles (°) of compound **3**.

O1 - P1 - O2	103.5(1)	O5 - C9 - O4	126.6(2)
O1 - P1 - O3	103.8(1)	O5 - C9 - C10	118.8(2)
O2 - P1 - O3	101.7(1)	O4 - C9 - C10	114.6(2)
O1 - P1 - S1	116.8(1)	O3 - C1 - C2	110.3(2)
O2 - P1 - S1	113.3(1)	C7 - O1 - P1	127.4(2)
O3 - P1 - S1	115.8(1)	O2 - C5 - C6	106.9(2)
C5 - O2 - P1	122.7(2)	O1 - C7 - C8	115.8(4)
C4 - N1 - C3	109.9(2)	N1 - C2 - C1	113.7(2)
C4 - N1 - C2	110.3(2)	O6 - C10 - O7	125.5(2)
C3 - N1 - C2	113.4(2)	O6 - C10 - C9	121.9(2)
C1 - O3 - P1	121.9(2)	O7 - C10 - C9	112.7(2)

Table 6: Parameters of the hydrogen bonds of compound **3**.

D--H...A	D--H [Å]	H--A [Å]	D--A [Å]	D--H----A
O7 ^{iv} ...H7 ^{iv} ...O4 ⁱ	1.10	1.36	2.459	174.1°
N1 ⁱⁱ ...H1 ⁱⁱ ...O5 ^v	0.94	1.88	2.759	154.2°
N1 ⁱⁱⁱ ...H1 ⁱⁱⁱ ...O5 ^{vi}	0.94	1.88	2.759	154.2°
O7 ^{iv} ...H7 ^{iv} ...O4 ^{vii}	1.10	1.36	2.459	174.1°

At the same time the structure of compound **3** is the first report of a single crystal structure of this compound class.

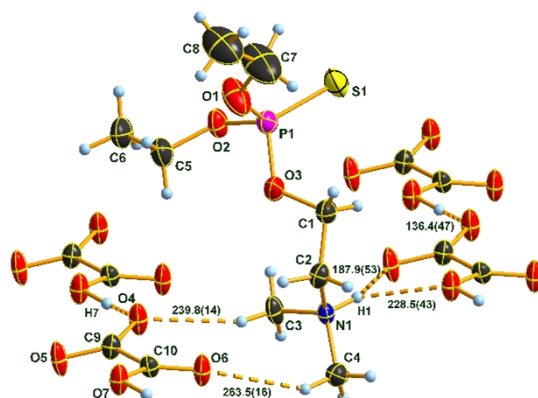


Figure 6: Molecular structure of compound **3** in the crystal (enhanced asymmetric unit with all hydrogen bonds in the crystal), DIAMOND^[31] representation; displacement ellipsoids are drawn at 50% probability level. The broken bonds indicate hydrogen bonds.

10.4 Conclusion

To the best of our knowledge the decomposition products of Amiton and Amiton-like compounds have only been characterized by their infrared spectroscopy data. The oxalate salt **3** of *O,O*-diethyl *O*-[2-(dimethylamino)ethyl] phosphorothioate **1** is described for the first time by its molecular and crystal structure. The habitus of the crystals (plates) is nicely reflected by the layered structure resulting from single X-ray crystal structure analysis. Furthermore, we conclude that the decomposition and thiono-thiol rearrangement of this class of compounds are related processes since all three compounds could be found in a stored NMR-tube which initially only contained pure compound **1**. These findings support the studies from Fukuto and Stafford and thus we were able to definitely proof the existence of the postulated compound by its crystal structure.^[14] However, it still remains unclear whether the process of the isomerization proceeds via a three-membered immonium ion or via the process described by Tammelin.^[15] Additionally, for the title compound a full set of NMR spectra is presented along with other so far unreported spectral data.

10.5 Acknowledgement

We acknowledge the collaboration between the German Armed Forces (Bundeswehr) and the Ludwig-Maximilian University (LMU) according to the official collaboration agreement between the two institutions. Financial support of this work by the LMU and the German Armed Forces is gratefully acknowledged.

10.6 Experimental Section

10.6.1 General Procedure

¹H, ¹³C and ³¹P NMR spectra were recorded with a Bruker AV400TR FTNMR spectrometer, using TMS for ¹H (400.1 MHz) and ¹³C (100.6 MHz), and 85% H₃PO₄ for ³¹P (161.9 MHz) as external standards. A Thermo Scientific™ Trace GC 1310 with PTV injector and an Agilent J&W GCcolumn (CP-Sil 8 CB Low Bleed/MS, 30 m 0.25 μm), Triplus RSH™ auto sampler and TSQ Duo triple quadrupole mass spectrometer was used in single quad mode. Chromeleon™ 7.2 Chromatography Management Software was used for system control and data processing. HPLC-Separations were performed on a modular DIONEX UltiMate™ 3000HPLC system (Thermo Scientific™) equipped with a SRD-3400 (4-channel degasser) solvent racks, HPG-3400SD gradient pump, WPS-3000TSL (Analytical) auto sampler, TCC-3000SD column oven, DAD-3000 photometer, MSQ-Plus mass detector. An Accucore RP-MS column (3.0 × 150.0 mm, particle size 2.6 μm Thermo Scientific™ Part. No. 17626-153030) was used for separation. Chromeleon™ 7.2 Chromatography Management Software was used for system control and data processing. The IR-spectra were recorded with a Spectrum One FT-IR spectrometer from Perkin Elmer, equipped with a Golden Gate ATR™ unit from Specac. The spectra were recorded from 600 to 4000 cm⁻¹. As a rule, before and after each easurement a blank was taken and 4 spectra were accumulated to give a good average. Raman spectra were recorded on a First Defender RMX Instrument from Analyticon. For IR and Raman data

processing, the OMNIC 8 software from Thermo Scientific™ was used. Differential scanning calorimetry (DSC) measurements were performed on a Linseis PT-10 instrument at a heating rate of 5 °C/min. The refractive index was determined on an Abbe-refractometer with a temperature controlled water bath. A single crystal suitable for diffraction studies was introduced into perfluorinated oil and was carefully mounted on the top of a thin glass wire. Data collection was performed with an Oxford Xcalibur 3 diffractometer equipped with a Spellman generator (50 kV, 40 mA) and a κ CCD detector, operating with Mo-K α radiation ($\lambda = 0.71073$ Å). Data collection was performed with the CrysAlis CCD software;^[23] CrysAlis RED software^[24] was used for data reduction. Absorption correction using the SCALE3 ABSPACK multiscan method^[25] was applied. The structures were solved by direct methods with SHELXS-97,^[26] refined with SHELXL-97^[27] and SHELXL-2014^[28] in the last step and finally checked using PLATON.^[29] All above mentioned programs were embedded in the WINGX software.^[30] Diamond software, program version 3.2k, was used to prepare the drawings of the crystal structure^[31] Details for data collection and structure refinement are summarized in Table 1. Selected bondlength and angles are given in Tables 2 and 3, respectively. Hydrogen atoms were treated with HFIX commands when they could not be clearly identified during the refinement process. Although the ellipsoids of C7 and C8 in compound (**3**) are looking quite large compared to those of C1 and C2 a refinement by splitting them into two individual positions did not result in better fit parameters.

10.6.2 Preparation

O,O-diethyl *O*-[2-(dimethylamino)ethyl] phosphorothioate (**1**)

Sodium hydride (0.85 g, 35 mmol) was weighed into a 100 mL three-neck round-bottom flask under nitrogen atmosphere. 40 mL of anhydrous benzene were added and the solution was stirred and refluxed. Carefully 2-(dimethylamino) ethanol (3.14 g, 35 mmol) was added dropwise to the solution. Upon the formation of 2-(dimethylamino) ethanolate anion the solution turned almost transparent. The reaction mixture was cooled with an ice bath and *O,O'*-diethyl chlorothiophosphate (6.85 g, 35 mmol) was added dropwise with stirring. The reaction mixture was allowed to warm to room temperature overnight and was carefully extracted three-times with 10 mL of distilled water to which hydrochloric acid was added to reach pH 2. Then ammonia solution (8% v/v) was added to this fraction until a pH value of >10 was reached. This solution was washed three-times with 5 mL of diethylether and dried over anhydrous sodium sulfate. Finally, the solvent was removed by rotary evaporation, resulting in a slightly yellowish liquid. Yield: 6.60 g, 27 mmol (77.1%). Elemental analysis: calcd.: C(39.82%), H(8.35%), N(5.80%), S(13.29%), found: C(39.79%), H(8.32%), N(5.82%), S(13.24%). n_{D20} : 1.4394. IR (ATR, ν , cm^{-1}): 2979, 2822, 2771, 1457, 1390, 1283, 1162, 1099, 1010, 954, 819, 783, 617. NMR: ^{13}C NMR (100.6 MHz, CDCl_3 , 299.0 K, TMS): δ 65.7 (*tdt*, $^1J_{\text{CH}} = 147.5$ Hz, $^2J_{\text{PC}} = 5.8$ Hz, $^2J_{\text{CH}} = 3.0$ Hz, CH_2), 65.6 (*tdq*, $^1J_{\text{CH}} = 148.1$ Hz, $^2J_{\text{PC}} = 5.6$ Hz, $^2J_{\text{CH}} = 4.4$, CH_2), 58.7 (*tdqt*, $^1J_{\text{CH}} = 132.6$ Hz, $^2J_{\text{CH}} = 2.7$ Hz, $^3J_{\text{PC}} = 8.0$ Hz, $^3J_{\text{CH}} = 5.1$ Hz, CH_2), 45.6 (*qtt*, $^1J_{\text{CH}} = 133.0$ Hz, $^3J_{\text{CH}} = 5.5$ Hz, $^4J_{\text{CH}} = 0.9$ Hz, CH_3), 15.8 (*qdt*, $^1J_{\text{CH}} = 127.2$ Hz, $^2J_{\text{CC}} = 2.6$ Hz, $^3J_{\text{PC}} = 7.5$ Hz, CH_3) ppm. ^1H NMR (400.1 MHz, CDCl_3 , 299.0 K, TMS): δ 4.03 (*dq*, $^3J_{\text{PH}} = 9.6$ Hz, $^3J_{\text{HH}} = 7.1$ Hz, 4H, CH_2), 4.03 (*dt*, $^3J_{\text{PH}} = 9.3$ Hz, $^3J_{\text{HH}} = 6.0$ Hz, 2H, CH_2), 2.51 (*dt*, $^3J_{\text{HH}} = 6.0$ Hz, $^4J_{\text{PH}} =$

0.6 Hz, 2H, CH₂), 2.18 (s, 6H, CH₃), 1.23 (dt, ⁴J_{PH} = 0.8 Hz, ³J_{HH} = 7.1 Hz, 6H, CH₃) ppm. ³¹P NMR (161.9 MHz, CDCl₃, 299.0 K, 85% H₃PO₄): δ 69.0 (sep, ³J_{PH} = 9.5 Hz, 1P) ppm. GC-MS (70eV EI): m/z (%) = 58.0 (100) [CH₂-N-(CH₃)₂]⁺, 71.1 (98) [CH₂-CH₂-N-(CH₃)₂]⁺, 97.0 (10) [(HS)P(O)(OH)₂]⁺. HPLC-MS (ESI): m/z (%) = 242.1 (58) [M-H]⁺, 72.0 (100) [CH₂-CH₂-NH-(CH₃)₂]⁺.

1,1,4,4-tetramethylpiperazinium di-*O,O*-diethylphosphorothioate (2)

In the first stance 1,1,4,4-tetramethylpiperazinium di-*O,O*-diethylphosphorothioate (**2**), as the decomposition product of the compound **1**, was found as a tiny single crystal in a stored NMR tube which was kept at 4 °C in the fridge for about 1 year. The NMR solvent was *d*8-toluene. Direct synthesis of compound **2** was successful by adopting standard text book procedures as follows: Step A (synthesis of the cation): anhydrous piperazine (0.67 g, 7.8 mmol) was dissolved in 15 mL dried acetonitrile. Iodmethane (4.65 g, 31.2 mmol) was dissolved in 10 mL of dried acetonitrile. Both solutions were carefully mixed upon which a white powder was forming under the production of excess heat. The intermediate A (1,1,4,4-tetramethylpiperazinediium diiodide) was filtered and washed three times with dried acetonitrile. Step B (synthesis of the anion according to Friedrich et al.^[32]): *O,O*-diethyl thiophosphoryl chloride (3.05 g, 16 mmol) was added to 40 mL of 1N sodium hydroxid solution and the solution was allowed to react for 12 h under stirring at room temperature. The solid intermediates were isolated by vacuum evaporation of the remaining water. The obtained white powder was dissolved in methanol and the product was separated from insoluble sodium chloride by filtration. The methanol was vacuum evaporated and intermediate B (sodium *O,O*-diethylthiophosphate) obtained as white powder. Equal molar amounts of intermediate A and B were dissolved in distilled water and mixed together in a round bottom flask. The water was allowed to evaporate over time so that crystallization starts forming the title compound (**2**). Yield: 3.86 g, 8 mmol (50.0%) with respect to piperazine. Elemental analysis: calc.: C(39.82%), H(8.35%), N(5.80%), S(13.29%), found: C(39.78%), H(8.37%), N(5.75%), S(13.21%). Melting point (DSC): 180.2°C. IR (ATR, ν, cm⁻¹): 3214, 2966, 1615, 1448, 1366, 1306, 1168, 1115, 1076, 1042, 953, 914, 852, 816. Raman (ν, cm⁻¹): 1435, 1401, 1333, 1301, 1186, 1037, 809, 438.

Oxalate of *O,O*-diethyl *O*-[2-(dimethylamino)ethyl] phosphorothioate (3)

The oxalate of *O,O*-diethyl *O*-[2-(dimethylamino)ethyl] phosphorothioate (**3**) was prepared by the following procedure: compound **1** (2.41 g, 10 mmol) was dissolved in 10 mL of methanol. To this solution oxalic acid (0.45 g, 5 mol) was added. The solution was poured on a watch glass to evaporate the solvent. 2.0 g of the obtained white powder were dissolved in acetone and filtered hot to remove remaining impurities. Upon cooling white needle-like crystals are formed. To obtain crystals suitable for X-ray investigation 1.0 g of the needles were dissolved in an excess of acetone in a small vial. The vial was placed in a flask with the bottom covered with n-pentane and allowed to stand in the lab upon which a single crystal formed in the acetone phase. Yield: 2.44 g, 4 mmol (85.3%). Elemental analysis: calc.: C(36.25%), H(6.69%),

N(4.23%), S(9.68%), found: C(35.80%), H(6.17%), N(3.74%), S(9.45%). Melting Point (DSC): 90.6°C. IR (ATR, ν , cm^{-1}): 2977, 1703, 1476, 1391, 1152, 1088, 957, 809, 640.

10.7 References

- [1] B. P. Paudyal, Organophosphorus poisoning. *J. Nepal Med. Assoc.* **2008**, *47*, 251.
- [2] K. Than, Organophosphates: a common but deadly pesticide. *Natl. Geogr.* **2013**. <http://news.nationalgeographic.com/news/2013/07/130718-organophosphates-pesticides-indianfood-poisoning/>.
- [3] G. L. Baldit, Amiton – a new acaricide and scabicide. *J. Sci. Food Agric.* **1958**, *9*, 516.
- [4] OPCW, Convention on the prohibition of the development, production, stockpiling and use of chemical weapons and on their destruction, OPCW, Paris and New York City, **1997**.
- [5] M. A. Althoff, A. Bertsch, M. Metzulat, O. Kalthoff, K. Karaghiosoff, New aspects of the detection and analysis of organo(thio)phosphates related to the chemical weapons convention. *Phosphorus Sulfur*. **2016**, *192*, 149.
- [6] M. A. Althoff, A. Bertsch, M. Metzulat, T. M. Klapotke, K. L. Karaghiosoff, Application of headspace and direct immersion solid-phase microextraction in the analysis of organothiophosphates related to the chemical weapons convention from water and complex matrices. *Talanta* **2017**, *174*, 295.
- [7] M. A. Althoff, K. Grieger, M. A. C. Hartel, K. L. Karaghiosoff, T. M. Klapotke, M. Metzulat, Application of the transpiration method to determine the vapor pressure and related physico-chemical data of low volatile, thermolabile, and toxic organo(thio)phosphates. *J. Phys. Chem. A*. **2017**, *121*, 2603.
- [8] K. Bruzik, W. J. Stec, Thiono-thiolo rearrangement and solvolysis of the secondary alkyl phosphorothionates. 3. *J. Org. Chem.* **1981**, *46*, 1618.
- [9] K. Bruzik, W. J. Stec, Stereochemistry and product distribution in the thiono-thiolo rearrangement of phosphorothioic esters. 4. Role of leaving-group solvation. *J. Org. Chem.* **1981**, *46*, 1625.
- [10] K. Bruzik, W. J. Stec, Stereochemistry of thiono-thiolo rearrangement of phosphorothioic esters. 2. *J. Org. Chem.* **1979**, *44*, 4488.
- [11] W. Reimschuessel, J. Adamus, Mechanism of thiono-thiolo isomerization of thiophosphates – kinetic evidence for Hilgetag hypothesis. *Phosphorus Sulfur*. **1990**, *49*, 77.
- [12] Y. Yamada, K. Mukai, H. Yoshioka, Y. Tamaru, Z. Yoshida, Palladium catalyzed thiono-thiolo allylic rearrangement of O-allyl phosphorothionates and phosphonothionates. *Tetrahedron Lett.* **1979**, *52*, 5015.
- [13] Y. Yamada, G. Suzukamo, H. Yoshioka, Y. Tamaru, Z. Yoshida, Palladium(II) catalyzed thiono-thiolo rearrangement of propargyl thionophosphates. *Tetrahedron Lett.* **1984**, *25*, 3599.
- [14] T. R. Fukuto, E. M. Stafford, The isomerization of *O,O*-diethyl *O*-2-diethylaminoethyl phosphorothionate. *J. Am. Chem. Soc.* **1957**, *79*, 6083.
- [15] L. E. Tammelin, Isomerisation of omega-dimethylaminoethyldiethylthiophosphate. *Acta Chem. Scand.* **1957**, *11*, 1738.

- [16] C. Fest, K. J. Schmidt, *The chemistry of organophosphorus pesticides*. Springer, Berlin Heidelberg, Berlin, **2012**.
- [17] J. I. G. Cadogan, L. C. Thomas, *The reactivity of organophosphorus compounds*. 3. The decomposition of 2-diethylaminoethyldiethyl phosphate and of S-2-diethylaminoethyl diethylphosphorothioate (Amiton). *J. Chem. Soc.* **1960**, 2248.
- [18] H. M. Fitch, inventor; Campbell Pharmaceuticals, Inc.; assignee, Quaternary ammonium salts of dialkylaminoalkylthiophosphate Esters. GB819735A patent GB819735, **1959**.
- [19] M. Markowitz, A convenient method for preparation of quaternary ammonium salts. *J. Org. Chem.* **1957**, 22, 83.
- [20] H. Z. Sommer, L. L. Jackson, Alkylation of amines – a new method for the synthesis of quaternary ammonium compounds from primary and secondary amines. EATR 4311 ed. USA: Department of the Army Edgewood Arsenal, **1969**.
- [21] H. Martin, E. Habicht, inventors; Cilag AG, assignee, Verfahren zur Herstellung von spasmolytisch wirksamen basischen Estern, ihren Saeureadditionssalzen und quartaren Salzen. DE1055546B, **1959**.
- [22] J. I. G. Cadogan, *Reactivity of organophosphorus compounds*. 11. High-temperature decomposition of S-2-diethylaminoethyldiethyl phosphorothioate (Amiton). *J. Chem. Soc.* **1962**, 18.
- [23] CrysAlis Ccd. 1.171.27p5beta (release 01-04-2005 CrysAlis171. NET (compiled Apr 1 2005, 17:53:34) ed., Oxford Diffraction Ltd., **2005**.
- [24] CrysAlis Red. Version 1.171.27p5 beta (release 01-04-2005 CrysAlis171.NET) (compiled Apr 1 2005, 17:53:34) ed., Oxford Diffraction Ltd., **2005**.
- [25] Scale3 Abspack – an Oxford Diffraction Program. Version 1.0.4, gui: 1.0.3 ed., Oxford Diffraction Ltd., **2005**.
- [26] G. M. Sheldrick, Shelxl-97: program for crystal structure solution. University of Gottingen, Gottingen, Germany, **1997**.
- [27] G. M. Sheldrick, Shelxl-97: program for the refinement of crystal structures. University of Gottingen, Gottingen, Germany, **1997**.
- [28] G. M. Sheldrick, Crystal structure refinement with Shelxl. *Acta Crystallogr. C.* **2015**, 71, 3.
- [29] A. L. Spek, PLATON: a multipurpose crystallographic tool. Utrecht University, Utrecht, The Netherlands, **1999**.
- [30] L. Farrugia, WinGX and ORTEP for windows: an update. *J. Appl. Crystallogr.* **2012**, 45, 849.
- [31] K. Brandenburg, Diamond. Version 3.2k ed. Crystal ImpactGbR, Bonn, Germany, **2014**.
- [32] H. D. Friedrich, K. D. Egon, inventors, *O,O*-dialkyl thiophosphoric acid salts intermeds for – insecticides. DE 1805159A1 patent DE 1805159A1, **1970**.
- [33] G. Socrates, *Infrared and Raman characteristic group frequencies: tables and charts*, Wiley, London, **2004**.
- [34] M. M. Halmann, *Analytical chemistry of phosphorus compounds*. Wiley-Interscience, New York, **1972**.
- [35] M. Otto, *Analytische Chemie*. Wiley-VCH, Weinheim, **2011**.

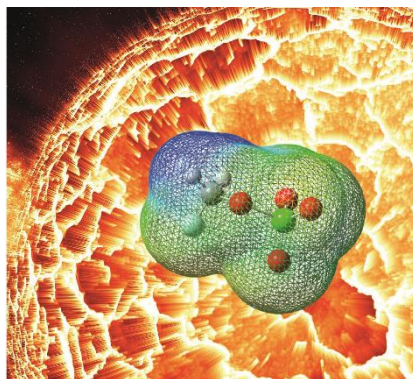
- [36] A. F. Holleman, E. Wiberg, N. Wiberg, Lehrbuch Der Anorganischen Chemie. Walter de Gruyter, Berlin and New York, **2007**.
- [37] S. Gunasekaran, B. Anita. Spectral Investigation and Normal Coordinate Analysis of Piperazine. *Indian J. Pure Appl. Phys.* **2008**, 46, 833.
- [38] R. J. D. Tilley, Understanding solids: the science of materials. Wiley, Hoboken, **2005**.

11 Synthesis and Investigation of Highly Energetic and Shock-sensitive Fluoromethyl Perchlorate

Marco Reichel, Burkhard Krumm, Konstantin Karaghiosoff*

Published in *J. Fluorine Chem.* **2019**, 226, 109351–109354.

DOI: 10.1016/j.jfluchem.2019.109351



Abstract: Small covalent organic perchlorates are a less investigated class of compounds, due to the risk of serious explosions. Apart from the simplest alkyl ester, methyl perchlorate, only the trifluoro-substituted ester is known to date. With the synthesis and isolation of fluoromethyl perchlorate (FMP) another member of this class of compounds has been studied, and properties spectroscopically and theoretically investigated. In addition, the energetic properties of FMP were studied and are discussed.

11.1 Introduction

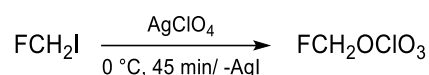
With the discovery of the first organic perchlorate ester, ethyl perchlorate, in 1841, its unusually violent explosive properties were at that time so unexpected, it was assumed that there was no substance of comparable explosive power.^[1] Because organic perchlorates have a notorious reputation for being extremely treacherous materials that are unstable and highly explosive, extensive investigations of these compounds are absent.^[2] In the 1970s, alkyl perchlorates were regarded as extremely strong alkylation agents and thus also as excellent polymerization catalysts.^[1b, 3] The high reactivities of these covalently bound compounds result from is given by the fact that the perchlorate anion is an excellent leaving group. Thus, solvents such as ethanol, acetonitrile, anisole or other aromatic compounds are easily alkylated.^[1b] However, interest in this possible practical application was quickly lost and other reagents were used instead.^[4] The simplest representative of alkyl perchlorates is methyl perchlorate (CH_3OCIO_3 ,

MP), which has already been extensively investigated.^[1a, 5] However, only trifluoromethyl perchlorate (CF₃OCIO₃, TFMP) has been investigated in the series of fluorine substituted analogues of MP.^[2b] The partially fluorinated fluoromethyl perchlorate (FCH₂OCIO₃, FMP) was not reported until now. Apart from this, few organic perchlorates with larger substituents have been structurally characterized by X-ray crystallography.^[6] The comparison of MP and FMP, however, provides added insight into the influence of fluorine substitution on the energetic, reactive and spectroscopic properties of such esters.

11.2 Results and Discussion

11.2.1 Synthesis

The synthesis of unsubstituted alkyl perchlorates from alkyl halides and anhydrous silver perchlorate is well known.^[7] However, the trifluoromethyl derivative TFMP was synthesized by treatment of chlorine perchlorate ClOCIO₃ with CF₃I.^[2b] Fluoromethyl perchlorate (FMP) can be obtained by a solvent-free procedure by treating anhydrous AgClO₄ with fluoroiodomethane (Scheme 1).



Scheme 1: Synthesis of fluoromethyl perchlorate (FMP).

Similar to methyl perchlorate MP, FMP is a colorless, volatile liquid. FMP is highly sensitive and explodes with the slightest degree of mechanical shock. When attempting to record a Raman spectrum, adjustment of the glass sample vessel resulted in a violent explosion, that was accompanied by a remarkable blast wave and white flash of light. The resulting decomposition products, similar to what was reported for FOCIO₃,^[8] caused irritation of pharynx and lungs, which resulted in respiratory distress for several days. Measurements of impact and friction sensitivities were not possible, because an initial experiment indicated values below the possible measuring range of 5 J (impact sensitivity) and 1 N (friction). Consequently, also no elemental analysis was performed.^[5b,9] However, unambiguous identity, purity and structural characterization of FMP are provided by NMR spectroscopy.

11.2.2 NMR Spectroscopy

A thorough NMR spectroscopical investigation was performed by means of multi-nuclear NMR spectroscopy. In the ¹H NMR spectrum the resonance of the methylene hydrogen atoms of FMP occurred as a doublet at 4.61 ppm with a ²J_{H,F} coupling of 51.4 Hz. This is a high-frequency shift compared to the methyl group of MP,^[10] as expected due to the electron-withdrawing effect of the fluorine atom. The corresponding ¹⁹F NMR resonance of FMP occurred at -152.1 ppm as a triplet (Figure 1). Additionally, the ³⁵Cl and ³⁷Cl isotopomers were resolved and allowed the determination of the isotopic shift ³Δ¹⁹F(^{37/35}Cl).

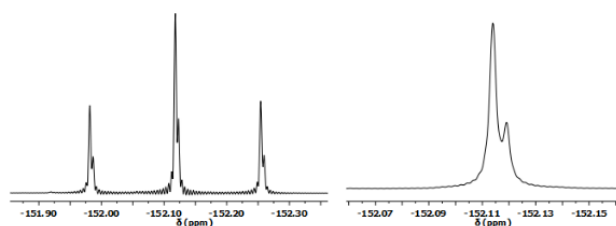


Figure 1: ^{19}F NMR spectrum ($^{19}\text{F}\{^1\text{H}\}$ right) showing chlorine isotopomers $\text{FCH}_2\text{O}^{35}\text{ClO}_3$ and $\text{FCH}_2\text{O}^{37}\text{ClO}_3$ (C_6D_6 , 26°C).

The chlorine isotope shift for FMP is 5.5 ppb (2.4 Hz), which is significantly greater than those of other $^3\Delta^{19}\text{F}(^{37}/^{35}\text{Cl})$ shifts for selected HCFCs or CFCs (-1.1 to -2.5 ppb).^[11] The substitution of a heavier Cl isotope leads to increased shielding and thus to a low-frequency shift of the signal. The intensity distribution is 3:1, which corresponds to the natural isotopic abundance ratio of $^{35}\text{Cl}:^{37}\text{Cl}$. Both the chemical shift and the coupling pattern of the ^{19}F signal in combination with the isotopic shift confirm that the fluoromethyl group is covalently bound to the perchlorate group *via* oxygen. The carbon resonance of FMP in the proton decoupled ^{13}C NMR spectrum is observed as a doublet at 100.2 ppm with $^1J_{\text{C,F}} = 241.3$ Hz. A highly concentrated solution of FMP in C_6D_6 enabled the detection of the ^{17}O resonances. The ^{17}O resonance of the fluoromethoxy moiety is detected at $\delta = 354$ ppm and that of the ClO_3 unit at 296 ppm. The latter is in good agreement with that of silver perchlorate at $\delta = 294$ ppm (HClO_4 and LiClO_4 $\delta = 290$ ppm^[12]). In the ^{35}Cl NMR spectrum the resonance is detected at 986 ppm, slightly shifted to low frequency compared to the perchlorate anion at 1010 ppm in a saturated solution of AgClO_4 in benzene- D_6 (26°C). Due to the lower symmetry of the Cl atom environment, the signal is broadened due to increased quadrupolar relaxation with a line width of 220 Hz, compared to the highly symmetric ClO_4^- with a linewidth of 65 Hz.

11.2.3 IR Spectroscopy

The IR spectrum of FMP was tentatively assigned according to the data of MP and TFMP, assisted by quantum-mechanical calculations (Table 1).^[2b, 5b, 13]

Table 1: Characteristic IR vibrations of MP^[10] (experimental), FMP (experimental and calculated) and TFMP^[2b] (experimental).

	CH_3OCIO_3 (MP)	$\text{FCH}_2\text{OCIO}_3$ (FMP)	Calc.	CF_3OCIO_3 (TFMP)
$\nu_{\text{as}}(\text{ClO}_3)$	1280 (vs)	1277 (s)	1151 (s)	1308 (vs)
$\nu_{\text{as}}(\text{ClO}_3)$	1250 (vs)	1254 (s)	1131 (s)	1308 (vs)
$\nu(\text{CF})$	—	1074 (m)	1038 (m)	1265/1241/1171 (s)
$\nu(\text{CO})$	1045 (s)	1037 (w)	1010 (m)	914 (m)
$\nu_{\text{s}}(\text{ClO}_3)$	965 (s)	961 (s)	918 (s)	1028 (vs)
$\nu(\text{OCl})$	700 (s)	670 (s)	574 (s)	615 (s)
$\delta_{\text{as}}(\text{ClO}_3)$	—	621 (m)/586 (w)	519 (w)/487 (w)	568 (mw)/560 (sh)
$\delta_{\text{s}}(\text{ClO}_3)$	—	490 (s)	604 (w)	512 (w)

For FMP, the asymmetric stretching absorption band $\nu_{as}(ClO_3)$ at 1277 cm^{-1} is assigned to the ClO_3 moiety at the ClO_4 group and the symmetric stretching vibration $\nu_s(ClO_3)$ was observed at 961 cm^{-1} . The characteristic $\nu(CO)$ stretching vibration of the perchloric acid ester was observed at 1037 cm^{-1} and the CF stretching band $\nu(CF)$ was found at 1074 cm^{-1} . Compared to MP, the CO vibration of FMP is shifted to lower wavenumbers, because of the electron withdrawing effect of the fluorine atom.

11.2.4 Mass Spectrometry

The mass spectrum of FMP does not show a molecular ion peak and also no fragment for the FCH_2O moiety, which is typical behavior for alkyl perchlorates. The molecular fragments ClO_3^+ and ClO_2^+ were detected. The absence of the ClO_4^+ fragment in the mass spectrum is mentioned in the literature as evidence of a covalent, organic bound perchlorate.^[1b, 9]

11.2.5 Energetic Properties

In order to determine the energetic behavior of FMP, the thermodynamic properties were predicted and compared to MP (Table 2). The heat of formation was calculated at the CBS-4 M level of theory using Gaussian 09.^[14] The heat of formation is considerably more negative for FMP than for MP (Table 2). This indicates that the F-C-O moiety is more stable than H-C-O, as this is the only significant difference between the two molecules.^[5b]

Table 2: Physical and thermodynamic properties of MP and FMP.

	MP	FMP
formula	CH_3ClO_4	CH_2FCIO_4
M_r [g mol ⁻¹]	114.48	132.47
O + F + Cl ^[a] [%]	86.9	89.4
Ω_{CO} ^[b] [%]	28.1	36.4
Ω_{CO_2} ^[b] [%]	14.1	24.2
T_{boil} ^[c] [°C]	52	49
ρ_{293K} ^[d] [g cm ⁻³]	1.5	1.6
ΔH_f° ^[e] [kJ mol ⁻¹]	-30.2	-217.4
EXPLO5 V6.03		
ΔU_f° ^[f] [kJ kg ⁻¹]	-5893	-3896
T_{C-J} ^[g] [K]	4912	3966
P_{C-J} ^[h] [GPa]	16.9	15.9
V_{det} ^[i] [ms ⁻¹]	6601	6278
V_g ^[j] [dm ³ kg ⁻¹]	756.5	735.1

[a] combined oxygen fluorine and chlorine content; [b] absolute oxygen balance assuming the formation of CO or CO₂ and HF, HCl; [c] boiling point from Siwoloboff method; [d] experimental determined density at 293 K; [e] heat of formation calculated at the CBS-4 M level of theory; [f] detonation energy; [g] detonation temperature; [h] detonation pressure; [i] detonation velocity; [j] volume of detonation gases at standard temperature and pressure conditions.

Based on the heats of formation and the corresponding densities at ambient temperature, the detonation parameters of FMP and MP were calculated using EXPLO5 V6.03 computer code.^[15] The detonation parameters were calculated at the C-J point (Chapman-Jouguet point) with the help of the stationary detonation model using a modified Becker-Kistiakowski-Wilson state equation for the system. The C-J point was found by the

Hugoniot curve of the system by its first derivative.^[16] The calculated detonation parameters are all below the values of nitroglycerine ($\Delta H_f^\circ -6099 \text{ kJ kg}^{-1}$, $T_{C-J} 4316 \text{ K}$, $P_{C-J} 23.7 \text{ GPa}$, $V_{\text{det}} 7850 \text{ ms}^{-1}$, $V_o 781 \text{ dm}^3 \text{ kg}^{-1}$). Except for the detonation pressure, MP is a more powerful energetic material than FMP. Although the friction and impact sensitivity could not be determined experimentally (outside the possible measuring range), the electrostatic potential (Figure 2) can be used to make a general comparison of FMP and MP.^[17]

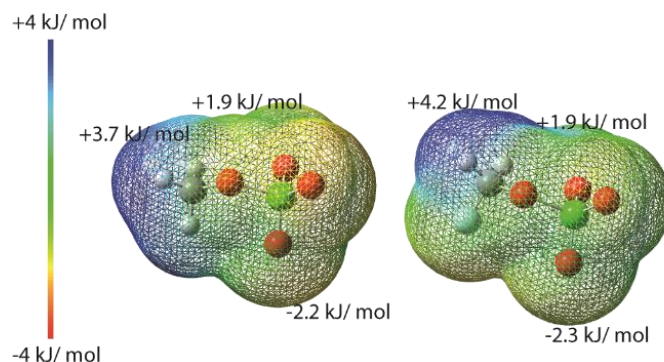


Figure 2: ESP of MP (left) and FMP (right). Isovalue: 0.02.

The ESP surfaces of MP and FMP are very similar in principle (Figure 2). Both have an equally pronounced positive potential in the center of the molecule. Furthermore, the positive potentials of both are stronger than their negative potentials (MP: +3.7 vs -2.2; FMP: +4.2 vs -2.3). This already indicates high impact sensitivities for both compounds.^[17a] Additionally, calculations showed that the LUMO of FMP is energetically 3.34 kJ/mol lower than that of MP. This, combined with the literature knowledge that alkyl perchlorates are likely to alkylate according to a S_N^2 mechanism, strongly suggests that fluoromethylation with FMP would also occur *via* a S_N^2 mechanism.^[18]

11.3 Acknowledgement

Financial support by Ludwig–Maximilian University is grateful acknowledged. We thank Professor Thomas M. Klapötke for his support and continuous interest in our work. We are thankful to F–Select GmbH for a generous donation of fluoroiodomethane.

11.4 Experimental Section

11.4.1 General Procedures

All compounds were handled using *Schlenk* techniques under dry argon. Anhydrous silver perchlorate was purchased from VWR. Fluoroiodomethane was distilled under inert conditions before use. The boiling point of FMP was determined using the Siwoloboff method in a Büchi B-540 apparatus with a heating rate of $1 \text{ }^\circ\text{C min}^{-1}$ (boiling point capillary immersed in a drop of liquid placed in a boiling point tube; upon heating bubbles rise forming a bubble chain; at the boiling point bubbles are released with a frequency of 0.6 Hz).^[19] The sample for infrared spectroscopy was placed directly onto an Smith DuraSamplIR II ATR device using a Perkin Elmer BX II FT-IR System spectrometer. The samples for NMR spectroscopy were prepared under inert atmosphere using Ar as protective gas. The solvent benzene- D_6 was dried using 3 \AA

mol sieve and stored under Ar atmosphere. Spectra were recorded at 26 °C on a Bruker Avance III spectrometer operating at 400.1 MHz (¹H), 376.4 MHz (¹⁹F), 100.6 MHz (¹³C), 54.2 MHz (¹⁷O) and 39.2 MHz (³⁵Cl). Chemical shifts are referenced to TMS (¹H, ¹³C), CFC1₃ (¹⁹F), H₂O (¹⁷O), 0.1M NaCl/D₂O (³⁵Cl). The mass spectrum was recorded on a Thermo Fisher GC/MS instrument.

11.4.2 Preparation

Caution! *FMP is a highly energetic material with high sensitivity towards impact and friction. A violent explosion occurred during work with this compound. Additional proper protective precautions like ear plugs, Kevlar gloves, face shield, shatterproof jacket and helmet, Kevlar arm guards and heavy armored blast shields should be used when handling this compound. It is therefore advisable to avoid as much as possible manipulation of neat material, as well as exposure to vapor.*

Finely powdered anhydrous AgClO₄ (10.0 g, 48.2 mmol, 16eq) was placed under argon in a narrow Schlenk tube to form a column. Fluoroiodomethane (0.2 mL, 2.96 mmol, 1eq) was slowly injected on top of the AgClO₄ under cooling and allowed to react for 45 min at room temperature. Afterwards, the product was condensed into a cold trap. The immersion tube of the cold trap extended to just above the bottom of the cold trap to keep the drip distance as short as possible during defrosting. The product was obtained in quantitative yield (0.39 g, 99%) as a colorless liquid. B.p. 49 °C; ¹H NMR (C₆D₆): δ 4.63 ppm (d, ²J(H,F) = 51.4 Hz, FCH₂); ¹⁹F NMR (C₆D₆): δ -152.1 ppm (t, ²J(F,H) = 51.4 Hz, FCH₂); ¹³C{¹H} NMR (C₆D₆): δ 100.2 ppm (d, ¹J(C,F) = 241.3 Hz, FCH₂); ¹⁷O NMR (C₆D₆): δ 354 (br, 1O, FCH₂O), 296 ppm (br, 3O, ClO₃); ³⁵Cl NMR (C₆D₆): δ 986 ppm (br, ClO₃). IR(ATR): ν̄ 1277, 1254, 1074, 1037, 961, 670, 621, 586, 490 cm⁻¹. MS (70eV): *m/z* (%): 82.9531 (100) [³⁵ClO₃⁺], 66.9582 (30) [³⁵ClO₂⁺].

11.5 References

- [1] a) J. Meyer, W. Spormann, Zur Kenntnis der Ester der Überchlorsäure, Z. Anorg. Allg. Chem. 228 (1936) 341–351; b) N. S. Zefirov, V. V. Zhdankin, A. S. Koz'min, Synthesis and properties of covalent organic perchlorates, Russ. Chem. Rev. 57 (1988) 1815–1839.
- [2] a) H. Burton, P. F. G. Praill, Perchloric acid and some organic perchlorates, Analyst 80 (1955) 4–15; b) C. J. Schack, K. O. Christie, Infrared and Raman spectra of trifluoromethyl perchlorate, Inorg. Chem. 13 (1974) 2374–2377.
- [3] G. N. Dorofeenko, S. V. Krivuch, V. I. Dulenko, Y. A. Zhdanov, Perchloric acid and its compounds in organic synthesis, Usp. Khim. 34 (1965) 219–252.
- [4] C. D. Beard, K. Baum, Aliphatic perchlorates and trifluoromethanesulfonates, US4165332 (1979).
- [5] a) N. S. Zefirov, A. S. Koz'min, V. V. Zhdankin, V. N. Kirin, N. M. Yur'eva, V. D. Sorokin, Competitive binding of super-weak nucleophiles in carbocationic-like processes, Chem. Scr. 22 (1983) 195–200; b) S. L. Brunswick, D. W. Ball, Organic chlorate and perchlorate derivatives as high energy materials: High-level computations

- on methyl chlorate and methyl perchlorate, *J. Mol. Struct.: THEOCHEM* 866 (2008) 1–4.
- [6] a) J. Engberts, H. Morssink, A. Vos, Crystal and molecular structure of a covalent perchloric acid ester: p-tolylsulfonylmethyl perchlorate, *J. Am. Chem. Soc.* 100 (1978) 799–802; b) D. Yufit, V. Rau, Y. Struchkov, A. Koz'min, V. Kirin, V. Zhdankin, N. Zefirov, 4-exo-(2,4-Dinitrophenylthio)-anti-6-perchloryloxy-9,10-cis-endo-dimethyltetracyclo[5.3.0.02,5.03,8]decane, C₁₈H₁₉ClN₂O₈S, *Cryst. Struct. Commun.* 10 (1981) 1539–1544; c) V. Bondar, T. Rau, V. Rau, Y. Struchkov, V. Zhdankin, A. Koz'min, V. Kirin, N. Zefirov, 9(RS)-Iodo-6(SR)-perchlorato-3,4-dimethoxycarbonyltetracyclo[6.1.1.02,7.05,10]dec-3-ene, C₁₄H₁₄ClIO₈, *Cryst. Struct. Commun.* 10 (1981) 587–590; d) K. Potekhin, V. Rau, Y. Struchkov, V. Zhdankin, A. Koz'min, N. Zefirov, 4-exo-Iodo-anti-6-perchloryloxy-9,10-cis-dimethyltetracyclo[5.3.0.02,5.03,8]decane, C₁₂H₁₆ClIO₄, *Cryst. Struct. Commun.* 11 (1982) 211–214; e) T. Rau, V. Rau, K. Potekhin, Y. Struchkov, V. Zhdankin, A. Koz'min, V. Kirin, N. Zefirov, 9(RS)-Iodo-6-(SR)-perchloryloxy-3(RS),4(RS)-dimethoxycarbonyltetracyclo[6.1.1.02,7.05,10]decane, C₁₄H₁₆ClIO₈, *Cryst. Struct. Commun.* 11 (1982) 207–210; f) N. Zefirov, A. Koz'min, V. Zhdankin, V. Kirin, K. Potekhin, Y. Struchkov, 4-Exo-(2,4-Dinitrophenylthio)-anti-6-perchloryloxy-9,10-cis-endo-dimethoxycarbonyltetracyclo[5.3.0.02,5.03,8]decane, C₂₀H₁₉ClN₂O₁₂S, *Cryst. Struct. Commun.* 11 (1982) 1921–1924; g) D. Yufit, Y. Struchkov, N. Yur'eva, A. Koz'min, N. Zefirov, 6(SR)-perchloryloxy-9-(RS)-hydroxy-3,4-dimethoxycarbonyltetracyclo[6.1.1.02,7.05,10]dec-3-ene, C₁₄H₁₅ClO₉, *Cryst. Struct. Commun.* 11 (1982) 1903–1908; h) V. Sorokin, I. Plokhikh, V. Yashkir, K. Potekhin, A. Koz'min, Y. Struchkov, N. Zefirov, *Proc. Nat. Acad. Sci. USSR* 332 (1993) 606; i) N. Yashin, E. Averina, V. Rybakov, T. Kuznetsova, N. Zefirov, *CSD Communication* (2015); j) N. Yashin, E. Averina, Y. Grishin, V. Rybakov, T. Kuznetsova, N. Zefirov, Oxidative nucleophilic substitution reaction of alkyl iodides upon treatment with perchlorate and dinitramide anions. Synthesis of alkyl-substituted perchlorates, *Russ. Chem. Bull.* 65 (2016) 451–455.
- [7] J. Radell, J. W. Connolly, A. J. Raymond, Alkyl perchlorates: Preparation, study, and stabilization, *J. Am. Chem. Soc.* 83 (1961) 3958–3960.
- [8] a) P. Patnaik, *A comprehensive guide to the hazardous properties of chemical substances*, 3rd ed., Wiley-Interscience, 2007; b) R. A. Lewis, *Lewis' dictionary of toxicology*, CRC Press, 1998, p. 508.
- [9] C. J. Schack, D. Pilipovich, K. O. Christe, Halogen perchlorates. Reactions with fluorocarbon halides, *Inorg. Chem.* 14 (1975) 145–151.
- [10] a) K. Baum, C. D. Beard, Reactions of dichlorine heptoxide with alcohols, 96 (1974) 3233–3237; b) N. S. Zefirov, V. V. Zhdankin, G. V. Makhon'kova, Y. V. Dan'kov, A. S. Koz'min, Oxidatively assisted nucleophilic substitution of iodine in alkyl iodides by nucleofugic anions, *J. Org. Chem.* 50 (1985) 1872–1876.
- [11] A. Foris, *Magn. Reson. Chem.* 38 (2000) 813–819.
- [12] a) W. G. Klemperer, 17O-NMR Spectroscopy as a Structural Probe, *Angew. Chem. Int. Ed. Engl.* 17 (1978) 246–254; b) I. P. Gerathanassis, Oxygen-17 NMR spectroscopy:

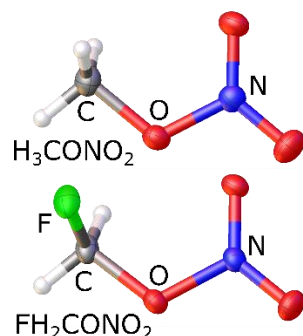
- Basic principles and applications (Part I), *Prog. Nucl. Magn. Reson. Spectrosc.* 56 (2010) 95–197.
- [13] D. N. Kevill, H. S. Posselt, Perchlorate esters. Part 8. Kinetics and mechanism of the methanolysis of methyl perchlorate in benzene, *J. Chem. Soc., Perkin Trans. 2* (1984), 909–914.
- [14] GAUSSIAN 09, revision C.01, G. W. T. M. J. Frisch, H. B. Schlegel, G. E. Scuseria, M. A. Robb, J. R. Cheeseman, G. Scalmani, V. Barone, B. Mennucci, G. A. Petersson, H. Nakatsuji, M. Caricato, X. Li, H. P. Hratchian, A. F. Izmaylov, J. Bloino, G. Zheng, J. L. Sonnenberg, M. Hada, M. Ehara, K. Toyota, R. Fukuda, J. Hasegawa, M. Ishida, T. Nakajima, Y. Honda, O. Kitao, H. Nakai, T. Vreven, J. A. Montgomery, Jr., J. E. Peralta, F. Ogliaro, M. Bearpark, J. J. Heyd, E. Brothers, K. N. Kudin, V. N. Staroverov, R. Kobayashi, J. Normand, K. Raghavachari, A. Rendell, J. C. Burant, S. S. Iyengar, J. Tomasi, M. Cossi, N. Rega, J. M. Millam, M. Klene, J. E. Knox, J. B. Cross, V. Bakken, C. Adamo, J. Jaramillo, R. Gomperts, R. E. Stratmann, O. Yazyev, A. J. Austin, R. Cammi, C. Pomelli, J. W. Ochterski, R. L. Martin, K. Morokuma, V. G. Zakrzewski, G. A. Voth, P. Salvador, J. J. Dannenberg, S. Dapprich, A. D. Daniels, Ö. Farkas, J. B. Foresman, J. V. Ortiz, J. Cioslowski, D. J. Fox, Gaussian, Inc., Wallingford, CT, 2009.
- [15] a) M. Sućeska, Calculation of the detonation properties of C-H-N-O explosives, *Propellants, Explos., Pyrotech.* 16 (1991) 197–202; b) M. Sućeska, Evaluation of detonation energy from EXPLO5 computer code results, *Propellants, Explos., Pyrotech.* 24 (1999) 280–285.
- [16] T. M. Klapötke, B. Krumm, F. X. Steemann, K.-D. Umland, Bis(1,3-dinitratoprop-2-yl) nitramine, a new sensitive explosive combining a nitrate ester with a nitramine, *Z. Anorg. Allg. Chem.* 636 (2010) 2343–2346.
- [17] a) T. M. Klapötke, *Chemistry of High-Energy Materials*, De Gruyter, 2017; b) Z. Friedl, M. Jungova, S. Zeman, A. Husarova, Friction sensitivity of nitramines. Part IV: links to surface electrostatic potentials, *Hanneng Cailiao* 19 (2011) 613–615.
- [18] T. Engel, P. J. Reid, *Physikalische Chemie*, Pearson Studium, 2006.
- [19] a) *Laborpraxis Band 2: Messmethoden*, Springer International Publishing, 2016; b) A. Siwoloboff, Ueber die Siedepunktbestimmung kleiner Mengen Flüssigkeiten, *Ber. Dtsch. Chem. Ges.* 19 (1886) 795–796; c) https://static1.buchi.com/sites/default/files/shortnotes/Short_Note_0.pdf.

12 Solid/Gas Phase Structures and Energetic Properties of the Dangerous Methyl and Fluoromethyl Nitrates

Marco Reichel, Burkhard Krumm, Yury V. Vishnevskiy, Sebastian Blomeyer, Jan Schwabedissen, Hans-Georg Stammler, Konstantin Karaghiosoff,* and Norbert W. Mitzel*

Published in *Angew. Chem.* **2019**, *58*,18557–18561.

DOI: 10.1002/ange.201911300



Abstract: An improved synthesis for the simplest nitric acid ester, methyl nitrate, and a new synthesis of fluoromethyl nitrate use the metathesis of the corresponding iodomethanes with silver nitrate. Both compounds were identified by spectroscopy and structure determination in the solid on in-situ grown crystals by X-ray diffraction as well as in the gas phase by electron diffraction. Fluorination leads to structures with shorter C-O and N-O bonds, has an energetically destabilizing effect and increases friction sensitivity, but decreases detonation performance.

12.1 Introduction

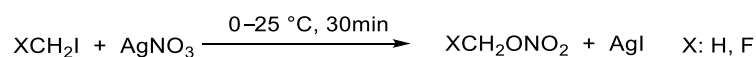
Potential energetic material candidates are commonly screened for density, performance, stability and sensitivity towards friction and impact, among others.^[1] In general, high density contributes to high performance.^[2] The influence of fluorine substituents on energetic materials is well documented, but almost nothing is known on the important parameter sensitivity towards impact and friction. These sensitivities were frequently rationalized with numerous and short inter- and intramolecular open shell interactions.^[3] Understanding the mutual interactions between atoms and functional groups is crucial to develop safe-to-handle energetic materials. Small and simple, yet highly energetic molecules are particularly suitable for exploring the effect of H/F exchange on the sensitivities due to the limited number of intermolecular interactions.^[4] They are often highly sensitive to impact and friction. The challenge is to find suitable molecules whose sensitivities can be determined by conventional methods and to compare them with non- and polyfluorinated derivatives, as was recently demonstrated for perchloric acid esters.^[5] Fluoromethyl nitrate (FCH₂ONO₂, FMN) is one of three fluorine-containing derivatives of methyl nitrate, CH₃ONO₂ (MN),^[6] besides F₂CHONO₂ (DFMN)^[8] and F₃CONO₂ (TFMN).^[9] Organic nitrates are important energetic compounds widely used in military and

aviation industries, but FMN (and also DFMN) was so far only studied by ab initio calculations.^[7,10] In contrast, TFMN (m.p. -163°C , b.p. -18°C) is isolable, but unstable even at low temperatures.^[8,9] The ‘mysterious’ MN (m.p. -82°C , b.p. 65°C), so called *Schießwasser* (German for shooting water), was used as early as 1420, though then not recognized as this material.^[11a,b] It was assigned to mysterious accidents between 1933 and 1955 and again in the 1980s.^[11c-g] Despite its unflattering reputation, various synthetic protocols, properties and applications were reported.^[6,10,12] The first structure elucidation of this toxic and consciousness-altering substance dates back until 1937 with theoretical and initial gas-phase electron diffraction (GED) studies.^[13] Solid state structures from single crystal X-ray diffraction of MN and FMN are so far unavailable, but could serve to compute electrostatic potentials, often used to explain changes in sensitivity and for comparison with quantum-mechanical results.^[2,14]

12.2 Results and Discussion

12.2.1 Synthesis

The original synthesis of MN, the nitration of methanol with nitric acid, cannot be adopted for FMN. This would require starting from fluoromethanol, known to be unstable and to readily decompose into HF and formaldehyde under ambient conditions.^[6,15] However, successful is the adaptation of an ethyl nitrate synthesis via silver catalyzed heterolysis,^[16] by reacting iodomethane or fluoroiodomethane, with silver nitrate (Scheme 1). Both, MN and FMN (m.p. -91°C , b.p. 58°C), were isolated as water-clear, volatile liquids with strong odors. They cause severe headache upon exposure.



Scheme 1: Synthesis of MN and FMN.

12.2.2 NMR Spectroscopy

Identification and characterization is possible by NMR spectroscopy. Compared to the methyl group ^1H NMR resonance of MN, the methylene group of FMN results in a doublet at 5.98 ppm ($^2J_{\text{F,H}} = 52.0$ Hz); the high frequency shift is due to the strong electron-withdrawing effect of fluorine. FMN shows a triplet ^{19}F NMR signal at -155.9 ppm, and a doublet of triplets ^{13}C NMR resonance at 99.1 ppm ($^1J_{\text{F,C}} = 228.8$, $^1J_{\text{C,H}} = 182.4$ Hz). The ^{15}N NMR signal at -52.4 ppm is a triplet of doublets ($^3J_{\text{N,H}} = 6.7$, $^3J_{\text{F,N}} = 1.7$ Hz; Figure 1), i.e. substitution of MN (-39.4 ppm, quartet $^3J_{\text{N,H}} = 3.9$ Hz) by one fluorine atom leads to a low frequency shift. The ^{17}O resonances (obtained using highly concentrated solutions, Figure 1) of the FCH_2O unit in FMN at 363 ppm is significantly high-frequency shifted relative to methoxy resonance in MN at 310 ppm. In contrast, the NO_2 resonance at 446 ppm remains unaffected upon H/F exchange. Values of CD_3CN solutions are similar to those of neat ethyl nitrate (340, 470 ppm).^[17]

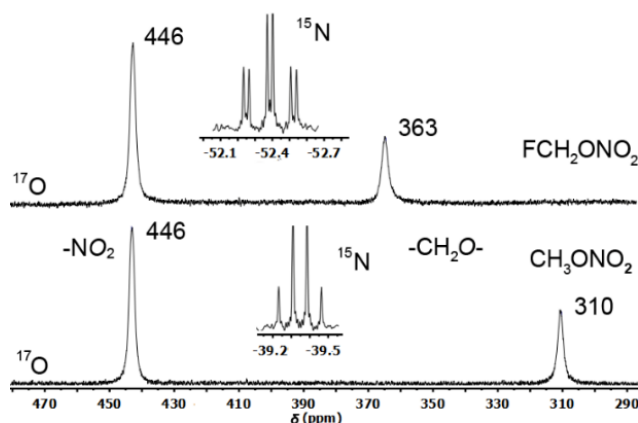


Figure 1: ^{15}N and ^{17}O NMR spectra of FMN (top) and MN (bottom) in CD_3CN (26 °C).

12.2.3 Vibrational Spectroscopy

Selected vibrations of the IR and Raman spectra of MN and FMN are listed in Table 1. The IR stretching vibrations of the NO_2 group for FMN are found at 1670 cm^{-1} ($\nu_{\text{as}}\text{NO}_2$) and 1291 cm^{-1} ($\nu_{\text{s}}\text{NO}_2$). Compared to MN, these vibrational modes are shifted to higher wavenumbers due to the electronegative F substituent. The lower values of the ν_{NO} stretching vibration of FMN (IR, 811 cm^{-1}) indicates a weaker N-O(CH_2F) bond upon F/H substitution. The experimental data differ in part from earlier calculated data, likely due to the liquid state.^[7]

Table 1: Selected IR/Raman vibrations of MN and FMN (liquids/25 °C, calcd DFT/6311G(d,p), cm^{-1}).

	MN				FMN			
	IR		Raman		IR		Raman	
	exp.	cal.	exp.	cal.	exp.	cal.	exp.	cal.
$\nu_{\text{as}}\text{NO}_2$	1622 (s)	1714 (s)	1636 (w)	1714 (w)	1670 (s)	1767 (s)	1689 (w)	1767 (w)
$\nu_{\text{s}}\text{NO}_2$	1281 (s)	1324 (s)	1285 (m)	1324 (w)	1291 (s)	1340 (m)	1296 (m)	1340 (w)
ν_{CF}	–	–	–	–	1047 (m)	1032 (w)	1049 (w)	1032 (w)
ν_{CO}	989 (s)	1015 (m)	991 (m)	1015 (m)	996 (s)	1023 (s)	1005 (w)	1023 (w)
ν_{NO}	854 (s)	862 (s)	860 (m)	862 (m)	811 (s)	824 (s)	822 (m)	824 (m)
δNO_2	652 (m)	661 (m)	664 (w)	661 (m)	654 (m)	647 (w)	660 (w)	647 (m)

12.2.4 Structural Properties

MN and FMN were structurally characterized in the gas phase by electron diffraction (GED, Table 2) and in case of MN additionally by combining GED data with rotational constants (Table 3; details see Supporting Information). Figure 3 shows the radial distribution curves for the GED experiments. While MN adopts C_s symmetry with one of the hydrogen atoms in anti-periplanar position to the nitrogen atom, the fluorine atom in FMN resides *gauche* relative to the planar NO_2 unit ($\phi(\text{F1C1O1N1}) = 74.7(8)^\circ$). Fluorination has severe effects on the structure parameters: in FMN the C-O1 and N-O2/O3 distances are shortened by 0.04 \AA (MN $1.425(3)$, FMN $1.385(3)\text{ \AA}$) and 0.01 \AA (MN $1.205(1)$, $1.198(1)\text{ \AA}$, FMN $1.190(2)$, $1.185(1)\text{ \AA}$), respectively. In variance, the O1-N distance in FMN is about 0.05 \AA longer than in MN (MN $1.403(2)$, FMN $1.454(2)\text{ \AA}$). This is likely due to negative hyperconjugation of the oxygen lone pairs into

the antibonding orbitals of the C-F and NO bonds. The C-O1-N angle in FMN at 115.3° is wider by 2° than in MN.

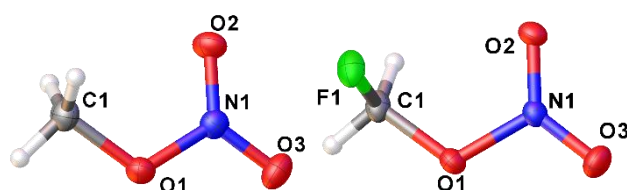


Figure 2: Molecular structures of MN (left) and FMN (right) in the solid state. Ellipsoids are set at 50% probability level. Numbering holds for the gas-phase structures as well.

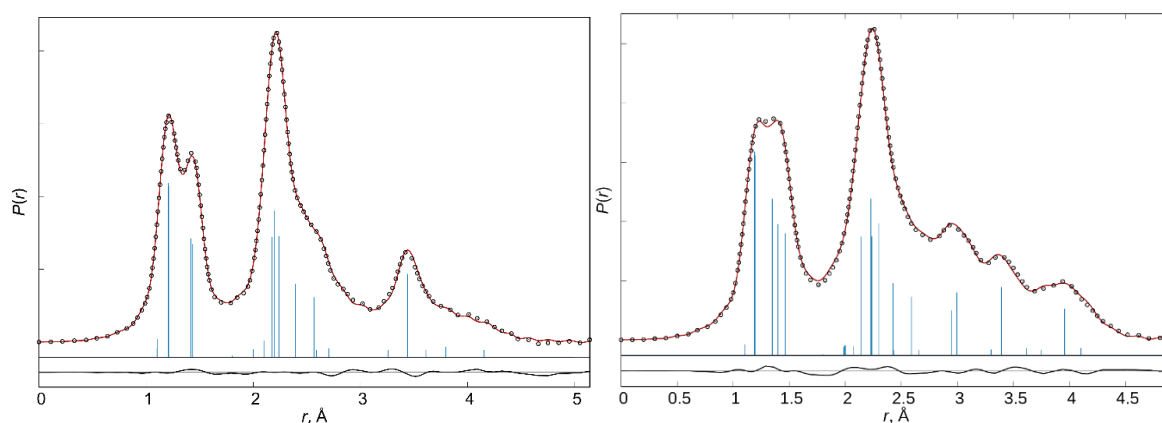


Figure 3: Experimental (circles) and model (line) radial distribution functions of MN (left) and FMN (right). The line below is the difference curve. Vertical bars indicate interatomic distances in the molecule.

Thus, both crystal structures feature pseudo-trigonal-bipyramidally coordinated nitrogen atoms with intermolecular contacts in axial position.

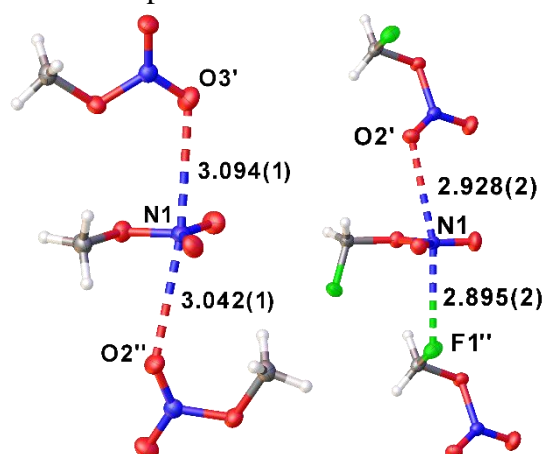


Figure 4: Molecular assembly in the solid state of methyl nitrate and fluoromethyl nitrate. Symmetry operations generating equivalent positions for MN: $(-\frac{1}{2}+x, y, \frac{3}{2}-z)$ for (') and $(\frac{1}{2}+x, \frac{1}{2}-y, 1-z)$ for (''), for FMN: $(+x, 1-y, \frac{1}{2}+z)$ for (') and $(-\frac{1}{2}+x, \frac{1}{2}-y, -\frac{1}{2}+z)$ for ('').

Table 2: Selected structural parameters for the solid-state (XRD) and the gas-phase structures (GED or GED+RotC) for methyl nitrate (MN) and fluoromethyl nitrate (FMN). Distances are given in Å and angles in degree.

Parameter	MN		FMN	
	XRD	GED+RotC	XRD	GED
C-O	1.451(1)	1.425(3)	1.412(2)	1.385(3)
O1-N	1.388(1)	1.403(2)	1.433(2)	1.454(2)
N-O2	1.204(1)	1.205(1)	1.208(2)	1.190(2)
N-O3	1.212(1)	1.198(1)	1.200(2)	1.185(1)
C-F			1.379(2)	1.336(2)
C-O-N	113.3(1)	113.6(3)	113.3(1)	115.3(2)
O1-N-O2	118.5(1)	116.3(3)	118.1(1)	115.1(3)
O1-N-O3	112.9(1)	112.3(2)	111.9(1)	111.9(11)
O2-N-O3	128.6(1)	131.4(4)	130.1(1)	133.0(13)
F-C-O-N			79.7(1)	74.7(8)

The solid-state structures of both nitrates were determined by X-ray diffraction of *in-situ* grown crystals. An unexpectedly obtained small crystal of oxonium nitrate dihydrate during crystallization of MN was also structurally characterized (details in the Supporting Information). MN crystallizes in the space group *Pbca* and FMN in *Cc*. Both contain one molecule per asymmetric unit.^[18] In both molecules, the carbon, nitrogen and oxygen atoms are almost coplanar, the root mean square deviation is 0.001 Å. *C_s* symmetry for MN is broken by the torsion angles of the methyl group $\phi(\text{NOCH})$: 175.6(7)°, 65.9(7)° and 60.0(7)°. FMN adopts a *gauche*-conformation with a torsion angle $\phi(\text{NOCF})$ of 79.7(1)°; $\phi(\text{NOCH})$ are 169(2)° and 40(2)°. As in the gas phase, structural changes upon fluorination result in a shorter C1-O1 bond (MN 1.451(1) Å; FMN 1.412(2) Å), a longer O1-N1 bond (MN 1.388(1) Å; FMN 1.433(2) Å) and slightly shorter N1-O2/O3 bonds (MN 1.204(1) / 1.212(1) Å, FMN 1.208(2) / 1.200(2) Å). Solid MN and FMN contain N...O and N...F contacts below or near the van der Waals distances (3.07 / 3.02 Å) (Figure 4). Two independent N...O contacts in MN have lengths of 3.094(1) (N1...O3') and 3.042(1) Å (N1...O2'') and a corresponding angle O3'...N1...O2'' of 171.9(1)°. Comparable contacts in FMN are significantly shorter at 2.928(2) Å (N1...O2') and 2.895(2) Å (N1...F1'') and the angle O2'...N1...F1'' at 168.1(1)° is narrower.

12.2.5 Energetic Properties

The influence of H/F substitution on the energetic properties was determined and results for MN^[11e,11f,21] and FMN are listed in Table 4. Sensitivity towards friction and impact of MN and FMN was determined experimentally according to standards of the German Federal Institute for Material Research and Testing (BAM).^[22] Both nitrates show equal sensitivities to impact of 0.2 J. However, the friction sensitivity of FMN is significantly higher than that of MN. Thus, the UN recommendations on transport of dangerous goods require FMN to be classified as very sensitive towards impact and sensitivity towards friction.^[23]

Table 3: Theoretical and refined structural parameters (in Å, degrees) from GED intensities and rotational constants of MN.

Parameter	MP2(full)/cc-pwCVTZ	GED+RotC ^[a]	wGED ^[b] , %
C1-O1	1.426	1.425(3)	48
O1-N1	1.407	1.403(2)	40
N1-O2	1.207	1.205(1)	64
N1-O3	1.201	1.198(1)	64
Average C-H	1.084	1.080(5)	49
C1-O1-N1	112.2	113.6(3)	14
O1N1O2	117.1	116.3(3)	17
O1N1O3	112.6	112.3(2)	7
O2N1O3	130.3	131.4(4)	8
wRMSD ^[c] , MHz	15.9	2.7	
R-factor ^[d] , %	7.0 ^[e]	4.8	

[a] Values correspond to equilibrium structure. In parentheses are one total standard deviations obtained from *Monte-Carlo* simulations as described earlier.^[19] [b] Contribution of GED data into refined value, estimated according to the method W2.^[20] [c] Weighted root-mean-square deviation of model rotational constants from experimental. [d] Factor of disagreement model and experimental electron diffraction intensities. [e] Model refined against GED data with geometrical parameters fixed at *ab initio* values.

Table 4: Physical and thermodynamic properties of MN and FMN.

	MN	FMN
formula	CH ₃ NO ₃	CH ₂ FNO ₃
<i>M</i> [g mol ⁻¹]	77.04	95.03
<i>IS</i> ^[a] [J]	0.2	0.2
<i>FS</i> ^[b] [N]	353	108
<i>N</i> ^[c] [%]	18.18	14.74
<i>N</i> + <i>O</i> + <i>F</i> ^[d] [%]	80.48	85.24
Ω_{CO} ^[e] [%]	10.4	25.3
Ω_{CO_2} ^[e] [%]	-10.4	8.4
<i>T</i> _{melt} ^[f] [°C]	-83.0	-90
<i>T</i> _{boil} ^[g] [°C]	65.0	58.0
$\rho_{100\text{K}}$ ^[h] [g cm ⁻³] (XRD)	1.579	1.838
$\rho_{293\text{K}}$ ^[i] [g cm ⁻³]	1.21	1.28
ΔH_f^0 ^[j] [kJ mol ⁻¹]	-162.3	-361.7
EXPLO5 V 6.03		
ΔU_f^0 ^[k] [kJ kg ⁻¹]	-6021	-4450
<i>T</i> _{C-J} ^[l] [K]	4151	3827
<i>P</i> _{C-J} ^[m] [GPa]	14.2	12.3
<i>V</i> _{det} ^[n] [ms ⁻¹]	6653	6133
<i>V</i> _o ^[o] [dm ³ kg ⁻¹]	923.7	836.8

[a] Impact sensitivity (BAM drop-hammer, method 1 of 6); [b] friction sensitivity (BAM friction tester, method 1 of 6); [c] nitrogen content; [d] combined nitrogen, oxygen and fluorine content; [e] absolute oxygen balance assuming the formation of CO or CO₂ and HF; [f] melting point; [g] boiling point from Siwoloboff method; [h] density determined by X-ray diffraction at 100 K; [i] experimentally determined density at 293 K; [j] heat of formation calculated at the CBS-4M level of theory [k] detonation energy; [l] detonation temperature; [m] detonation pressure; [n] detonation velocity; [o] volume of detonation gases at standard temperature and pressure conditions.

In contrast to impact or shock sensitivity, friction sensitivity usually attracts only little attention of theoreticians, but there seems to be a relationship between friction sensitivity and electronic potential (ESP).^[24] Compared to MN the ESP of FMN is different to an extent, explaining the significantly larger impact sensitivity (Figure 5).^[2] For FMN the positive region (blue) is larger

and the positive potential (max. +100 kJ/mol) is stronger than for MN. The maximum negative potentials at the NO₂ unit (-44 kJ/mol) and the F atom (-52 kJ/mol) in FMN are much less negative in FMN. This is in contrast to the situation in MN with a stronger negative (max. -84 kJ/mol) than positive region. This and the fact that there is a higher positive potential in the molecular centre, indicates FMN to be more friction sensitive.^[2,14b] The weaker negative potential (maximum: -44/-52 vs. -84 kJ/mol) is probably the main reason for the increased friction sensitivity.^[24] A destabilizing effect of fluorine substitution explained already the high instability of trifluoromethyl nitrate TFMN.^[9] Initial results on methylene dinitrate CH₂(ONO₂)₂,^[25] prepared in analogy to FMN, confirm this increased instability (see Supporting Information).^[26] Consequently, it is not surprising that attempts to synthesise the multiply fluorine/nitrate substituted FCH(ONO₂)₂ from FCHI₂ were not successful. An immediate decomposition into N₂O₅ (hydrolyzing to HNO₃) and “FCHO” was proven by NMR spectroscopy.^[27]

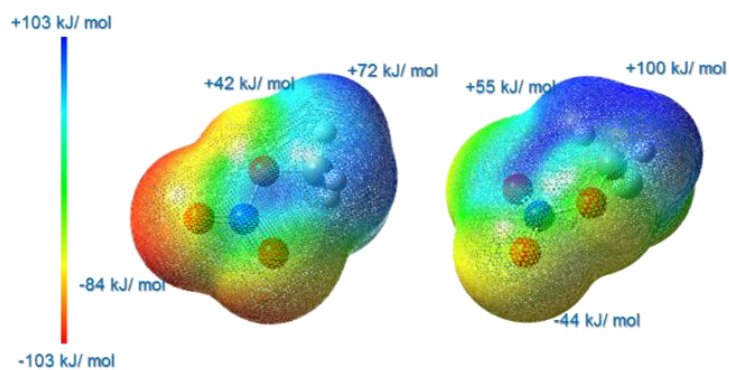


Figure 5: ESP of MN (left) and FMN (right), isovalue = 0.02.

Quantum-chemical calculations were carried out for MN and FMN. Heats of formation were computed using optimised structures^[28] and are considerably more negative for FMN than for MN (Table 4). Based on these values and the corresponding densities at ambient temperature, detonation parameters of MN and FMN were calculated using the EXPLO5 V6.03 code^[30] (Table 4). Calculations at the *Chapman-Jouguet* (C-J) point applied a stationary detonation model with a modified *Becker-Kistiakowski-Wilson* state equation. The C-J point was located using the first derivative of the *Hugoniot* curve of the system.^[31] The calculated detonation parameters are comparable with those of glycerine trinitrate (ΔU_f^0 -6099 kJ kg⁻¹, T_{C-J} 4316 K, P_{C-J} 23.7 GPa, V_{det} 7850 ms⁻¹, V_o 781 dm³ kg⁻¹). The heat of detonation, detonation pressure, velocity and temperature of glycerine trinitrate are all higher than those of MN and FMN, but smaller than the gas volumes released from MN and FMN.

12.3 Conclusion

In conclusion, we have synthesized and characterized fluoromethyl nitrate for comparison with methyl nitrate in order to learn about the effect of fluorine substitution on various structural and energetic parameters. We find shorter C-O and N-O bonds and a wider C-O-N angle in the fluorinated species. Fluorine substitution has a destabilizing effect, it increases friction sensitivity but decreases detonation performance.

12.4 Acknowledgement

This work was funded by the Deutsche Forschungsgemeinschaft (DFG, German Research Foundation): the core facility GED@BI (project no. 324757882) and a grant for structure elucidation of MN and FMN (project no. 416982996). Financial support by Ludwig-Maximilian University is gratefully acknowledged. We thank F-Select GmbH for a generous donation of fluoroiodomethane, and Mr. A. Harter for participating on this project.

12.5 Experimental Section

12.5.1 General Procedures

All compounds were handled using *Schlenk* techniques under dry Ar. Silver nitrate, purchased from VWR, was dried in *vacuo* at room temperature for 30 min and fluoroiodomethane (donation from F-Select GmbH) was distilled under inert conditions before use. Melting points T_{melt} were determined on the X-ray diffractometer with an Oxford Cryosystem/ Cryostream controller of the 700 series. Boiling points were determined using the *Siwoloboff* method in a Büchi B-540 apparatus using a heating rate of 1 °C min⁻¹.^[1] The sensitivities towards impact and friction were determined with a BAM ball-drop and a BAM friction tester, respectively (method 1 out of 6).^[2] The samples for infrared spectroscopy were placed under ambivalent conditions without further preparation onto an Smith DuraSampLIR II ATR device using a Perkin Elmer BX II FR-IR System spectrometer. Samples for Raman spectroscopy were sealed in glass tubes. The measurement was carried out on a Bruker MultiRam FT Raman device using a neodymium-doped yttrium aluminum garnet (Nd:YAG) laser ($\lambda = 1064$ nm) with 1074 mW. The samples for NMR spectroscopy were prepared under inert atmosphere using Ar as protective gas. The solvent CD₃CN was dried using 3 Å mol sieve and stored under Ar atmosphere. Spectra were recorded on a Bruker Avance III spectrometer operating at 400.1 MHz (¹H), 376.4 MHz (¹⁹F), 100.6 MHz (¹³C), 54.2 MHz (¹⁷O), 40.6 MHz (¹⁵N) and 28.9 MHz (¹⁴N). Chemical shifts are referred to TMS (¹H/¹³C), CFC₃ (¹⁹F), H₂O (¹⁷O), MeNO₂ (¹⁴N/¹⁵N). All spectra were recorded at 299.15 K (26 °C). Elemental analyses were performed with an Elemental Vario EL Analyzer.

12.5.2 Preparation

Caution! *MN and FMN are highly energetic materials with high sensitivities towards impact and friction. Even if no accident has occurred during the synthesis and manipulation of these compounds, additional proper protective precautions like ear plugs, Kevlar gloves, face shield, shatterproof jacket and helmet, Kevlar arm guards and heavy armored blast shields should be used when undertaking work with these compounds.*

Fluoromethyl nitrate (FMN)

The reaction was performed under Argon as inert gas. Finely mortared AgNO₃ (9.42 g, 55.5 mmol, 15 eq) was placed into a small *Schlenk* tube. Fluoroiodomethane (0.25 mL, 3.7 mmol, 1 eq) was slowly injected through a septum on top of the silver nitrate under cooling

at 0 °C. The mixture was reacted without stirring for 45 min at room temperature. Then the septum was replaced by another *Schlenk* tube, into which the product was condensed. The product was obtained in quantitative yield (0.35 g, 99.7%) as a colorless liquid with high vapor pressure. $T_{\text{melt}} -91^{\circ}\text{C}$; $T_{\text{boil}} 58^{\circ}\text{C}$; $^1\text{H NMR}$: $\delta = 5.99$ (d, $^2J(\text{F,H}) = 52.0$ Hz, 2H, CH_2F); $^{13}\text{C NMR}$: $\delta = 99.1$ (dt, $^1J(\text{F,C}) = 228.8$ Hz, $^1J(\text{C,H}) = 182$ Hz, CH_2F); $^{13}\text{C}\{^1\text{H}\}$ NMR: $\delta = 99.1$ (d, $^1J(\text{F,C}) = 228.8$ Hz, CH_2F); $^{19}\text{F}\{^1\text{H}\}$ NMR: $\delta = -155.9$ (s, CH_2F); $^{19}\text{F NMR}$: $\delta = -155.9$ (t, $^2J(\text{F,H}) = 52.0$ Hz, CH_2F); $^{17}\text{O NMR}$: $\delta = 446$ (2O, NO_2), 363 (1O, FCH_2O); $^{15}\text{N}\{^1\text{H}\}$ NMR: $\delta = -52.3$ (d, $^3J(\text{F,N}) = 1.7$ Hz, ONO_2); $^{15}\text{N NMR}$: $\delta = -52.3$ (td, $^3J(\text{N,H}) = 7.0$ Hz, $^3J(\text{F,N}) = 1.7$ Hz, ONO_2); IR (ATR): $\tilde{\nu} = 1670$ (s, $\nu_{\text{as}}\text{NO}_2$), 1461 (w), 1291 (s, $\nu_{\text{s}}\text{NO}_2$), 1047 (m, νCF), 997 (s), 811 (s, νNO), 760 (m, $\gamma_{\text{w}}\text{NO}_2$), 654 (m, δNO_2), 575 (m), 456 (w) cm^{-1} ; Raman (1074 mW): $\tilde{\nu} = 3054$ (w), 2997 (s), 2906 (w), 2799 (w), 1689 (w, $\nu_{\text{as}}\text{NO}_2$), 1462 (w), 1412 (w), 1296 (m, $\nu_{\text{s}}\text{NO}_2$), 1143 (w), 1049 (w, νCF), 1005 (w), 822 (m, νNO), 660 (w, δNO_2), 581 (m), 458 (m), 364 (m) cm^{-1} ; EA calcd (%) for CH_2FNO_3 : C 12.64, H 2.12, N 14.74; found: C 12.83, H 2.17, N 15.03.

Methyl nitrate (MN)

The reaction was performed analogous to the above for FMN, by using AgNO_3 (10.6 g, 62.6 mmol, 15 eq) and iodomethane (0.26 mL, 4.1 mmol, 1 eq) instead of fluoroiodomethane. The product was obtained in nearly quantitative yield (0.32 g, 99.5%) as a colorless liquid. $T_{\text{melt}} -83^{\circ}\text{C}$; $T_{\text{boil}} 65^{\circ}\text{C}$; $^1\text{H NMR}$: $\delta = 4.10$ (s, CH_3); $^{13}\text{C}\{^1\text{H}\}$ NMR: $\delta = 61.1$ (s, CH_3); $^{17}\text{O NMR}$: $\delta = 446$ (2O, NO_2), 310 (1O, H_3CO); $^{15}\text{N}\{^1\text{H}\}$ NMR: $\delta = -39.9$ (s, ONO_2); $^{15}\text{N NMR}$: $\delta = -39.9$ (q, $^3J(\text{N,H}) = 3.9$ Hz, ONO_2); IR (ATR): $\tilde{\nu} = 1622$ (s, $\nu_{\text{as}}\text{NO}_2$), 1428 (w), 1281 (s, $\nu_{\text{s}}\text{NO}_2$), 989 (s), 854 (s, νNO), 760 (m, $\gamma_{\text{w}}\text{NO}_2$), 652 (m, δNO_2), 578 (w) cm^{-1} ; Raman (1074 mW): $\tilde{\nu} = 3041$ (w), 2963 (s), 2902 (w), 2833 (w), 1636 (w, $\nu_{\text{as}}\text{NO}_2$), 1525 (w), 1438 (w), 1285 (m, $\nu_{\text{s}}\text{NO}_2$), 1176 (w), 991 (w), 860 (m, νNO), 664 (w, δNO_2), 579 (m), 354 (w) cm^{-1} ; EA calcd (%) for CH_3NO_3 : C 15.59, H 3.93, N 18.18; found: C 15.77, H 3.89, N 18.55.

Methylene dinitrate (MDN)

The reaction was performed under Argon as inert gas. Finely mortared AgNO_3 (0.807 g, 4.75 mmol, 2.5 eq) was placed into a *Schlenk* flask containing 5 mL dry acetonitrile. Subsequently, diiodomethane (0.15 mL, 1.9 mmol, 1 eq) was slowly added under cooling. The solution was reacted at 50°C for 48 h. Acetonitrile was removed under reduced pressure and MDN was obtained as a slightly yellowish liquid. $^1\text{H NMR}$: $\delta = 6.29$ (s, CH_3); $^{13}\text{C}\{^1\text{H}\}$ NMR: $\delta = 89.7$ (s, CH_3); $^{14}\text{N NMR}$: $\delta = -18$ (ONO_2); IR (ATR): $\tilde{\nu} = 3056$ (w), 2947 (w), 1759 (w), 1657 (s, $\nu_{\text{as}}\text{NO}_2$), 1422 (m), 1276 (s, $\nu_{\text{s}}\text{NO}_2$), 1227 (w), 1118 (w), 1071 (w), 1015 (m), 958 (s, νCON), 838 (w, νNO), 782 (s, νNO), 745 (s, $\gamma_{\text{w}}\text{NO}_2$) cm^{-1} ; Raman (1074 mW): $\tilde{\nu} = 3056$ (w), 2998 (s), 2946 (w), 1685 (w, $\nu_{\text{as}}\text{NO}_2$), 1426 (w), 1298 (m, $\nu_{\text{s}}\text{NO}_2$), 1023 (w), 840 (s, νNO), 605 (s, δNO_2), 569 (m), 419 (w), 250 (m) cm^{-1} .

12.6 References

- [1] D. S. Viswanath, T. K. Ghosh, V. M. Boddu, *Emerging Energetic Materials: Synthesis, Physicochemical, and Detonation Properties*, Springer, Netherlands, **2018**.
- [2] T. M. Klapötke, *Chemistry of High-Energy Materials*, De Gruyter, **2017**.

- [3] a) T. M. Klapötke, P. Mayer, A. Schulz, J. J. Weigand, *J. Am. Chem. Soc.* **2005**, *127*, 2032–2033; b) C. J. Eckhardt, A. Gavezzotti, *J. Phys. Chem. B* **2007**, *111*, 3430–3437; c) E. A. Zhurova, A. I. Stash, V. G. Tsirelson, V. V. Zhurov, E. V. Bartashevich, V. A. Potemkin, A. A. Pinkerton, *J. Am. Chem. Soc.* **2006**, *128*, 14728–14734; d) Y. Tang, J. Zhang, L. A. Mitchell, D. A. Parrish, J. M. Shreeve, *J. Am. Chem. Soc.* **2015**, *137*, 15984–15987.
- [4] a) C. Zhang, X. Wang, H. Huang, *J. Am. Chem. Soc.* **2008**, *130*, 8359–8365; b) Y. Ma, A. Zhang, C. Zhang, D. Jiang, Y. Zhu *Cryst. Growth Des.* **2014**, *14*, 4703–4713; c) Y. Ma, A. Zhang, X. Xue, D. Jiang, Y. Zhu, C. Zhang, *Cryst. Growth Des.* **2014**, *14*, 6101–6114; d) J. Zhang, Q. Zhang, T. T. Vo, D. A. Parrish, J. M. Shreeve, *J. Am. Chem. Soc.* **2015**, *137*, 1697–1704.
- [5] a) J. Meyer, W. Spormann, *Z. Anorg. Allg. Chem.* **1936**, *228*, 341–351; b) M. Reichel, B. Krumm, K. Karaghiosoff, *J. Fluorine Chem.* **2019**, in press (<https://doi.org/10.1016/j.jfluchem.2019.109351>).
- [6] A. P. Black, F. H. Babers, *Org. Synth.* **1939**, *19*, 64–66.
- [7] X. D. Gong, H. M. Xiao, *J. Mol. Struct. Theochem* **1999**, *488*, 179–185.
- [8] A. M. Kosmas, Z. Salta, A. Lesar, *J. Phys. Chem. A* **2009**, *113*, 3545–3554.
- [9] S. Sander, H. Willner, H. Oberhammer, G. A. Argüello, *Z. Anorg. Allg. Chem.* **2001**, *627*, 655–661.
- [10] T. Urbanski, *Chemistry of Technology of Explosives*, Pergamon Press, New York, **1984**.
- [11] a) J. Gartz, *Vom griechischen Feuer zum Dynamit: Eine Kulturgeschichte der Explosivstoffe*, E. S. Mittler & Sohn, Hamburg, **2015**; b) *Feuerwerkbuch von 1420* (anonymous), Stainer, Augsburg, **1529**; c) A. Stettbacher, *Spreng- und Schießstoffe: Atomzerfallselemente u. ihre Entladungerscheinungen*, Rascher-Verlag, Zürich, **1948**; d) G. Mauz, in *Spiegel*, Feb 1st 1988, *5*, 98. e) T. Ammann, in *Stern*, June 13th 2015, *25*, (<https://www.stern.de/auto/news/le-mans-1955---das-rennen-in-den-tod-6292490.html>); f) P. Gray, P. L. Smith, *J. Chem. Soc.* **1953**, 2380–2385; g) E. G. Cowley, J. R. Partington, *J. Chem. Soc.* **1933**, 1252–1254.
- [12] a) J. Kames, U. Schurath, F. Flocke, A. Volz-Thomas, *J. Atmos. Chem.* **1993**, *16*, 349–359; b) G. Desseigne, *Meml. Poudres* **1957**, *39*, 147–156.
- [13] a) L. Pauling, L. O. Brockway, *J. Am. Chem. Soc.* **1937**, *59*, 13–20; b) N. Milgram, *Food Aversion Learning*, Springer US, **2013**; c) A. P. Cox, S. Waring, *Trans. Faraday Soc.* **1971**, *67*, 3441–3450; d) J. Shao, X. Cheng, X. Yang, *Struct. Chem.* **2005**, *16*, 457–460; e) Y. Zhao, K. N. Houk, L. P. Olson, *J. Phys. Chem. A* **2004**, *108*, 5864–5871; f) X. M. Pan, Z. Fu, Z. S. Li, C. C. Sun, H. Sun, Z. M. Su, R. S. Wang, *Chem. Phys. Lett.* **2005**, *409*, 98–104; g) W. B. Dixon, E. B. Wilson, Jr., *J. Chem. Phys.* **1961**, *35*, 191–198.
- [14] a) Y. Tang, C. He, G. H. Imler, D. A. Parrish, J. M. Shreeve, *J. Mater. Chem. A* **2018**, *6*, 8382–8387; b) J. S. Murray, M. C. Concha, P. Politzer, *Mol. Phys.* **2009**, *107*, 89–97.
- [15] G. Olah, A. Pavlath, *Acta Chim. Acad. Sci. Hung.* **1953**, *3*, 203–207.
- [16] D. N. Kevill, E. K. Fujimoto, *J. Chem. Soc., Chem. Commun.* **1983**, 1149–1150.
- [17] L. Anderson, J. Mason, *J. Chem. Soc., Dalton Trans.* **1974**, 202–205.
- [18] CCDC 1936406 (FMN), 1936407 (MN) and 1936408 (oxonium nitrate) contain the supplementary crystallographic data for this paper. These data can be obtained free of

- charge from The Cambridge Crystallographic Data Centre via www.ccdc.cam.ac.uk/conts/retrieving.html.
- [19] Y. V. Vishnevskiy, J. Schwabedissen, A. N. Rykov, V. V. Kuznetsov, N. N. Makhova, *J. Phys. Chem. A* **2015**, *119*, 10871–10881.
- [20] T. Baše, J. Holub, J. Fanfrlík, D. Hnyk, P. D. Lane, D. A. Wann, Yu. V. Vishnevskiy, D. Tikhonov, C. G. Reuter, N. W. Mitzel, *Chem. - Eur. J.* **2019**, *25*, 2313–2321.
- [21] a) J. Köhler, R. Meyer, A. Homburg, *Explosivstoffe*, Wiley-VCH, **2008**; b) J. D. Ray, R. A. Ogg, Jr., *J. Phys. Chem.* **1959**, *63*, 1522–1523; c) G. Desseigne, *Meml. Poudres* **1948**, *30*, 59–68; d) D. R. Lide, *CRC Handbook of Chemistry and Physics, Standard Thermodynamic Properties of Chemical Substances, Vol. 90*, Taylor and Francis, Boca Raton, FL, **2009**.
- [22] a) T. M. Klapötke, B. Krumm, F. X. Steemann, G. Steinhauser, *Safety Science* **2010**, *48*, 28–34; b) D. Pollock, R. F. Gentner, *Impact Sensitivity of Wetted Primary Explosives as Determined by the Ball Drop Test*, PN, Dover, **1972**.
- [23] a) www.reichel-partner.de; b) Test methods according to the UN Manual of Tests and Criteria, Recommendations on the Transport of Dangerous Goods, N. Y. United Nations Publication, Geneva, 4th revised ed., 2003: Impact: insensitive >40 J, less sensitive ≥ 35 J, sensitive ≥ 4 J, very sensitive ≤ 3 J; friction: insensitive >360 N, less sensitive: 360 N, sensitive <360 N and >80 N, very sensitive ≤ 80 N, extremely sensitive ≤ 10 N.
- [24] Z. Friedl, M. Jungova, S. Zeman, A. Husarova, *Chin. J. Energ. Mater* **2011**, *19*, 613–615.
- [25] a) A. F. Ferris, K. W. McLean, I. G. Marks, W. D. Emmons, *J. Am. Chem. Soc.* **1953**, *75*, 4078; b) T. Urbanski, M. Witanowski, *Trans. Faraday Soc.* **1963**, *59*, 1039–1045; c) Z. Fang, L. Chen, S. Wang, J. Chen, F. Li, *Propellants, Explos., Pyrotech.* **1995**, *20*, 83–86.
- [26] G. Travagli, *Gazz. Chim. Ital.* **1938**, *68*, 718–721.
- [27] N. Muller, D. T. Carr, *J. Phys. Chem.* **1963**, *67*, 112–115.
- [28] a) GAUSSIAN 09, revision C.01, G. W. T. M. J. Frisch et al., Gaussian, Inc., Wallingford, CT, 2009; b) GaussView 5, V5.0.8, T. K. R. Dennington, J. Millam, Semichem Inc., Shawnee Mission, 2009.
- [29] a) T. Helgaker, J. Gauss, P. Joergensen, J. Olsen, *J. Chem. Phys.* **1997**, *106*, 6430–6440; b) J.-H. Lii, N. I. Allinger, *J. Mex. Chem. Soc.* **2009**, *53*, 96–107; c) S. R. Saraf, W. J. Rogers, M. S. Mannan, M. B. Hall, L. M. Thomson, *J. Phys. Chem. A* **2003**, *107*, 1077–1081.
- [30] a) M. Sućeska, *Propellants, Explos., Pyrotech.* **1991**, *16*, 197–202; b) M. Sućeska, *Propellants, Explos., Pyrotech.* **1999**, *24*, 280–285.
- [31] T. M. Klapötke, B. Krumm, F. X. Steemann, K.-D. Umland, *Z. Anorg. Allg. Chem.* **2010**, *636*, 2343–2346.

12.7 Supporting Information

12.7.1 Crystal Growth

Crystals of CH_3NO_3 (MN) were grown *in-situ* inside of a sealed capillary. At 245 K, a small crystal could be manually grown. It turned out to be oxonium nitrate, see below. Slowly chilling with 10 K/h to 100 K methyl nitrate crystallizes as oligocrystalline material.

A twinned crystal of FMN was grown *in situ* inside of a sealed capillary at 182.5 K by manually growing a crystal seed, chilling to 162 K with 1 K/h and to 100 K with 20 K/h.

A crystal of $\text{H}_3\text{O}^+ \text{NO}_3^- \cdot 2 \text{H}_2\text{O}$ was grown *in-situ* inside of a sealed capillary at 245 K. Chilling fast to 180 K the methylnitrate acted as undercooled solvent.

12.7.2 Structure Refinement Data

All measurements were examined on a Rigaku Supernova diffractometer using $\text{MoK}\alpha$ ($\lambda = 0.71073 \text{ \AA}$) radiation. Using Olex2,^[1] the structures were solved with the ShelXT^[2] structure solution program using Intrinsic Phasing and refined with the ShelXL^[3] refinement package using Least Squares minimization. All hydrogen atoms were refined isotropically. For MN seven domains were indexed and taken into account for data reduction, only none or minor overlapping reflections of the main domain (quota ca. 27%) were used for structure solution and refinement. The crystal of FMN was twinned by a rotation of 180° around 100 with ratio 58:42. Both domains were taken into account during data reduction and refinement.

Table 1: Structure refinement data of MN, FMN and $\text{H}_3\text{O}^+ \text{NO}_3^- \cdot 2 \text{H}_2\text{O}$.

Empirical formula	$\text{CH}_3 \text{NO}_3$	CH_2FNO_3	H_7NO_6
Formula weight	77.04	95.04	117.07
Temperature	100.0(1) K	100.0(1) K	180.0(1) K
Wavelength	0.71073 \AA	0.71073 \AA	0.71073 \AA
Crystal system	Orthorhombic	Monoclinic	Orthorhombic
Space group	<i>Pbca</i>	<i>Cc</i>	<i>P2₁2₁2₁</i>
Unit cell dimensions	$a = 4.6169(2) \text{ \AA}$ $b = 11.2184(6) \text{ \AA}$ $c = 12.5130(7) \text{ \AA}$ $\alpha = 90^\circ$ $\beta = 90^\circ$ $\gamma = 90^\circ$	$a = 5.0962(16) \text{ \AA}$ $b = 14.286(3) \text{ \AA}$ $c = 4.8520(10) \text{ \AA}$ $\alpha = 90^\circ$ $\beta = 103.57(3)^\circ$ $\gamma = 90^\circ$	$a = 3.48643(15) \text{ \AA}$ $b = 9.5040(4) \text{ \AA}$ $c = 14.7100(5) \text{ \AA}$ $\alpha = 90^\circ$ $\beta = 90^\circ$ $\gamma = 90^\circ$
Volume	$648.10(6) \text{ \AA}^3$	$343.40(16) \text{ \AA}^3$	$487.42(3) \text{ \AA}^3$
Z	8	4	4
Density (calculated)	1.579 mg/m^3	1.838 mg/m^3	1.595 mg/m^3
Absorption coefficient	0.161 mm^{-1}	0.211 mm^{-1}	0.180 mm^{-1}
F(000)	320	320	248
Crystal size	$0.510 \times 0.320 \times 0.270 \text{ mm}^3$	$0.630 \times 0.330 \times 0.270 \text{ mm}^3$	$0.240 \times 0.150 \times 0.100 \text{ mm}^3$
Theta range for data collection	$6.5 - 61.7^\circ$	$5.7 - 73.6^\circ$	$5.1 - 64.5^\circ$

Index ranges	-6≤h≤6, -15≤k≤16, -17≤l≤17	-8≤h≤8, -23≤k≤23, -8≤l≤8	-5≤h≤5, -14≤k≤13, -21≤l≤21
Reflections collected	8968	13818	9655
Independent reflections	1002 [R _{int} = 0.0576]	3370 [R _{int} = 0.0214]	1638 [R _{int} = 0.0339]
Data / restraints / parameters	1002 / 0 / 59	3370 / 2 / 64	1638 / 0 / 93
Goodness-of-fit on F ²	0.929	1.061	1.079
Final R indices [I>2σ(I)]	R ₁ = 0.0283, wR ₂ = 0.0645	R ₁ = 0.0329, wR ₂ = 0.1007	R ₁ = 0.0307, wR ₂ = 0.0603
R indices (all data)	R ₁ = 0.0407, wR ₂ = 0.0670	R ₁ = 0.0349, wR ₂ = 0.1074	R ₁ = 0.0411, wR ₂ = 0.0649
Largest diff. peak and hole	0.13 and -0.20 e Å ⁻³	0.36 and -0.30 e Å ⁻³	0.16 and -0.21 e Å ⁻³

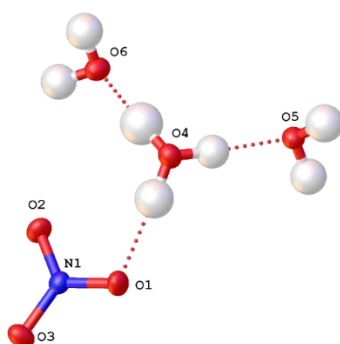


Figure 1: Asymmetric unit of H₃O⁺ NO₃⁻ · 2-H₂O.

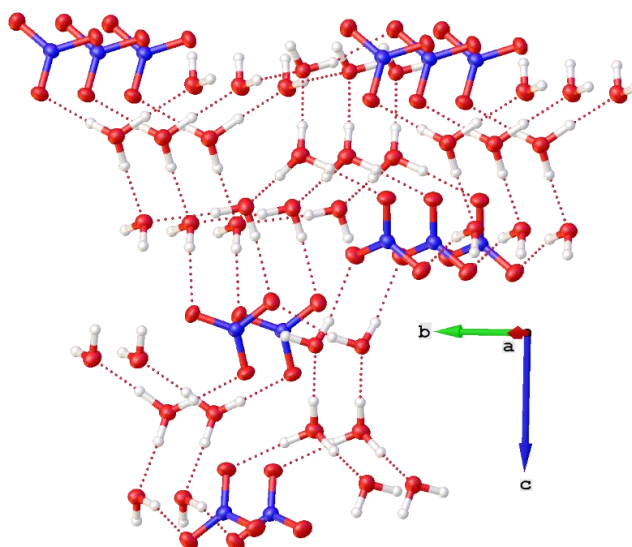


Figure 2: Hydrogen bond network of H₃O⁺ NO₃⁻ · 2-H₂O.

12.7.3 References

- [1] O. V. Dolomanov, L. J. Bourhis, R. J. Gildea, J. A. K. Howard, H. Puschmann, *J. Appl. Crystallogr.* **2009**, *42*, 339–341.
- [2] G. M. Sheldrick, *Acta Crystallogr.* **2015**, *A71*, 3–8.
- [3] G. M. Sheldrick, *Acta Crystallogr.* **2015**, *C71*, 3–8.

12.7.4 Gas-phase Electron Diffraction

12.7.4.1 General Information

The electron diffraction patterns were recorded on the heavily improved Balzers Eldigraph KD-G2 gas-phase electron diffractometer at Bielefeld University. Experimental details are listed in Table 2, instrumental details are reported elsewhere.^[1]

Table 2: Details of the gas-phase electron diffraction experiment for methyl nitrate and fluoromethyl nitrate.

Parameters	Methyl nitrate		Fluoromethyl nitrate					
	short distance	detector	long distance	detector	short distance	detector	long distance	detector
nozzle-to-plate distance, mm	250.0		500.0		250.0		500.0	
accelerating voltage, kV	60		60		60		60	
fast electron current, μA	1.54		1.53		1.54		1.53	
electron wavelength, ^a \AA	0.048672		0.048629		0.048672		0.048629	
nozzle temperature, K	297		298		297		298	
Sample pressure, ^b mbar	2.8×10^{-6}		4.2×10^{-6}		5.0×10^{-6}		4.7×10^{-6}	
residual gas pressure ^c , mbar	7.0×10^{-7}		1.2×10^{-6}		7.0×10^{-7}		1.2×10^{-6}	
exposure time, s	10		10		10		10	
used s range, \AA^{-1}	7.4-32.2		2.0-16.4		9.2-30.0		3.0-16.0	
number of inflection points ^d	7		4		7		5	
R_f factor	6.3		3.2		6.9		1.9	

^a Determined from CCl_4 diffraction patterns measured in the same experiment. ^b During the measurement.

^c Between measurements. ^d Number of inflection points on the reduced background lines.

The electron diffraction patterns, four for each, long and short nozzle-to-plate distance (with the exception of only three for the medium distance for FMN) were measured on the Fuji BAS-IP MP 2025 imaging plates, which were scanned by using calibrated Fuji BAS 1800II scanner. The intensity curves (see below) were obtained by applying the method described earlier.^[2] Electron wavelengths were refined^[3] using carbon tetrachloride diffraction patterns, recorded in the same experiment as the substance under investigation.

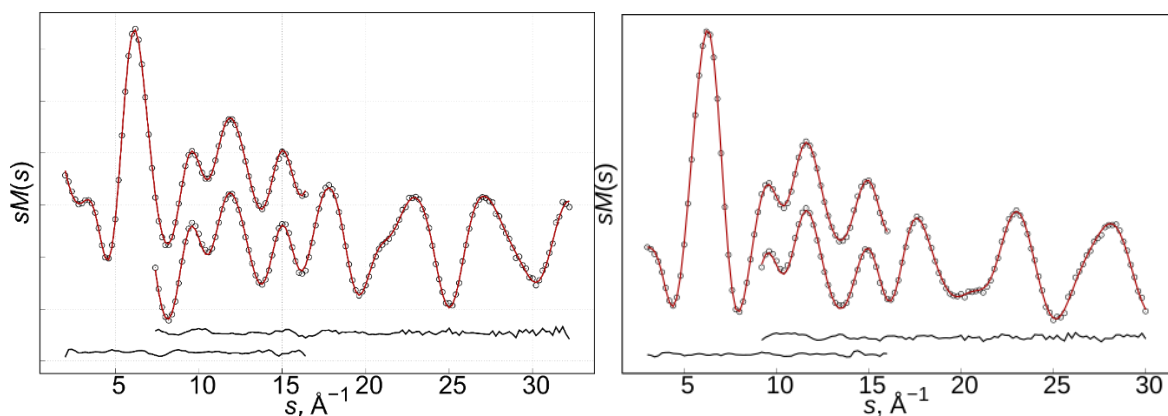


Figure 3: Experimental and model molecular electron diffraction intensities of MN (left) and FMN (right) in the main refinement; in case of MN combined with rotational constants.

12.7.4.2 Structural Analysis of MN

Two types of experimental data were available for structural analysis: (a) electron diffraction intensities measured in this work and (b) published earlier rotational constants.^[4]

Molecular structure of methyl nitrate has been refined from published rotational constants for eight isotopologues. The parameters were refined unconstrained within C_s symmetry point group. The experimental B_0 rotational constants have been corrected to equilibrium geometry using theoretically computed differences ($B_e - B_0$) at the DFT level and VPT2 theory as implemented in Gaussian program package.^[5] The obtained results are listed in Table 3. Interestingly, the differences between results obtained with PBE0 and TPSSh corrections were negligible, although the corrections themselves deviated by 5-10%. To assess the influence of uncertainties in corrections ($B_e - B_0$) onto the errors of refined molecular structure parameters *Monte-Carlo* simulations have been done as described earlier.^[6] Assumed standard deviations for rotational constants were 5% of their respective corrections. The obtained in this way total errors are provided in Table 3.

Table 3: Structural parameters of methyl nitrate (Å and degrees) refined from experimental B_0 rotational constants using theoretical corrections ($B_e - B_0$) from VPT2 calculations with PBE0 and TPSSh DFT functionals. Uncertainties are standard deviations from least squares method (LSQ) or total errors from *Monte-Carlo* simulations.

Parameter	PBE0/def2-TZVP, LSQ errors	TPSSh/def2-TZVP, LSQ errors	TPSSh/def2-TZVP, total errors
C1-O1	1.433(5)	1.433(5)	1.433(22)
O1-N1	1.399(8)	1.397(8)	1.397(38)
N1-O2	1.206(5)	1.205(5)	1.207(22)
N1-O3	1.203(6)	1.203(6)	1.203(29)
Average C-H	1.078(4)	1.078(4)	1.079(21)
C1-O1-N1	112.6(2)	112.5(2)	112.5(11)
O1N1O2	117.7(7)	117.8(7)	117.8(33)
O1N1O3	112.8(4)	112.7(4)	112.7(21)
O2N1O3	129.5(9)	129.5(9)	129.5(45)
wRMSD, MHz	0.42	0.41	0.41

Next, molecular structure of MN has been refined from electron diffraction intensities. The procedure was as follows. Background procedure has been applied for each of the measured total intensity functions, extracting molecular intensity. The individual intensities, four from each nozzle-to-detector distance, were averaged. The averaged molecular intensity functions $sM(s)$, one from middle and one from the long camera setting, were used in structural analysis. The geometry of the molecule has been defined using a Z-matrix (see Attachment). The initial values of parameters have been taken from MP2(fc)/cc-pVTZ calculations. The differences between parameters in groups were fixed on the values also taken from this level of theory. In preliminary calculations of anharmonic vibrational frequencies using VPT2 theory it was found that TPSSh/def2-TZVP level of theory reproduces experimental values most closely. Therefore, force fields from this level were used to calculate interatomic vibrational mean square

amplitudes and corrections, required in structural analysis. The corrections were calculated for equilibrium structure taking into account cubic force fields. This type of calculations was done in VibModule program. [7] In the refinement amplitudes have been divided into four groups (see Attachment). The ratios of amplitudes in each group were fixed at the theoretical values. Thus scale factors for theoretical amplitudes have been refined to the values 1.06(1), 1.13(7), 0.99(5), 1.19(7). The values of refined geometrical parameters are listed in the attachment. The largest correlation 0.81 was between the first scale factor for the amplitudes and the scale factor for the molecular intensity from middle camera measurements. Finally, a combined refinement of molecular model has been done utilizing both GED data and rotational constants. The model and grouping of parameters was the same as in the refinement based on only GED data. The relative weighting of the rotational constants has been adjusted manually so that their average contributions to the refined parameters were possibly similar to those from GED data. In the least squares method the maximal correlation -0.83 was between parameters in groups 7 and 8 (see Z-matrix attachment). As expected, the quality of fit for GED data and rotational constants was worse than in case of using only one type of data in the least squares refinement. However, it is expected that the overall accuracy of the refined parameters in this model was higher. The refined geometrical parameters of MN are listed in Tables 1 in section 4.2.4. Note, the final values were corrected by the *Monte-Carlo* procedure, which was used to assess the influence of uncertainties in different parameters of the model and in data and also for calculation of total errors. For this reason, a series of quantum-chemical calculations has been performed for computing the possible ranges of geometrical constraints. The approximations were MP2(fc)/cc-pVTZ, MP2(full)/cc-pwCVTZ, B3LYP-D3/def2-TZVP, B3PW91-D3/def2-TZVP, M06-2X/def2-TZVP, TPSSh/def2-TZVP, PBE0-D3/def2-TZVP. The obtained from these calculations ranges for constraints were additionally extended by 30%. The same procedure was used for obtaining ranges of possible values for vibrational amplitudes and corrections, where the tested quantum-chemical approximations were PBE0-D3/def2-TZVP, B3LYP-D3/def2-TZVP, M06-2X/def2-TZVP, B3PW91-D3/def2-TZVP and TPSSh/def2-TZVP.

12.7.4.3 Structural Analysis of FMN

Even the lowest predicted energy difference of 14.5 kJ mol⁻¹ (see chapter above) between the two possible conformers would result in a *Boltzmann* distribution based ratio of 99.99:0.01 favoring the *gauche* conformer. Therefore, and due to an insufficient agreement of the experimental data with the *anti*-conformer, we decided to refine the structure of FMN taking into account only the *gauche* conformer. The refinement procedure based on the electron diffraction intensities was in close analogy to the one described for MN with the following differences: For the medium distance only three individual intensities were used for averaging, the initial values of parameters have been taken from MP2(full)/cc-pwCVTZ calculations and the Z-matrix was modified (see attachment). In the refinement amplitudes have been divided into five groups (see Table below). The ratios of amplitudes in each group were fixed at the theoretical values. Thus, scale factors for theoretical amplitudes have been refined to the values 0.95(2), 1.12(4), 0.92(2), 1.40(5), 1.21(6). The values of refined geometrical parameters are listed in the attachment. The largest correlation 0.88 was between the first scale factor for the amplitudes and the scale factor for the molecular intensity from middle camera measurements.

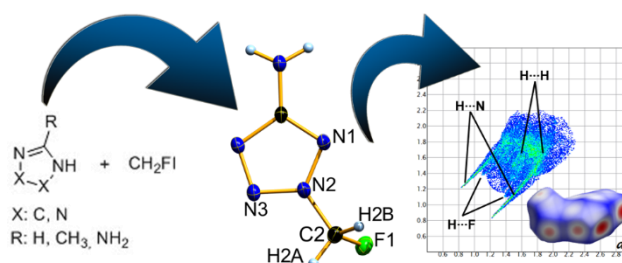
12.7.4.4 References

- [1] a) R. J. F. Berger, M. Hoffmann, S. A. Hayes, N. W. Mitzel, *Z. Naturforsch.* **2009**, *64b*, 1259; b) C. G. Reuter, Y. V. Vishnevskiy, S. Blomeyer, N. W. Mitzel, *Z. Naturforsch.* **2016**, *71b*, 1.
- [2] Y. V. Vishnevskiy, *J. Mol. Struct.* **2007**, *833*, 30.
- [3] Y. V. Vishnevskiy, *J. Mol. Struct.* **2007**, *871*, 24.
- [4] A. P. Cox, S. Waring, *Trans. Faraday Soc.* **1971**, *67*, 3441–3450.
- [5] Frisch, M. J., Trucks, G. W., Schlegel, H. B., Scuseria, G. E., Robb, M. A., Cheeseman, J. R., Scalmani, G., Barone, V., Mennucci, B., Petersson, G. A., Nakatsuji, H., Caricato, M., Li, X., Hratchian, H. P., Izmaylov, A. F., Bloino, J., Zheng, G., Sonnenberg, J. L., Hada, M., Ehara, M., Toyota, K., Fukuda, R., Hasegawa, J., Ishida, M., Nakajima, T., Honda, Y., Kitao, O., Nakai, H., Vreven, T., Montgomery, J. J. A., Peralta, J. E., Ogliaro, F., Bearpark, M., Heyd, J. J., Brothers, E., Kudin, K. N., Staroverov, V. N., Kobayashi, R., Normand, J., Raghavachari, K., Rendell, A., Burant, J. C., Iyengar, S. S., Tomasi, J., Cossi, M., Rega, N., Millam, J. M., Klene, M., Knox, J. E., Cross, J. B., Bakken, V., Adamo, C., Jaramillo, J., Gomperts, R., Stratmann, R. E., Yazyev, O., Austin, A. J., Cammi, R., Pomelli, C., Ochterski, J. W., Martin, R. L., Morokuma, K., Zakrzewski, V. G., Voth, G. A., Salvador, P., Dannenberg, J. J., Dapprich, S., Daniels, A. D., Farkas, O., Foresman, J. B., Ortiz, J. V., Cioslowski, J., Fox, D. J., Gaussian 09, Revision D.01. Gaussian, Inc., Wallingford CT, 2016.
- [6] Y. V. Vishnevskiy, J. Schwabedissen, A. N. Rykov, V. V. Kuznetsov, N. N. Makhova, *J. Phys. Chem. A* **2015**, *119*, 10871–10881.
- [7] Y. V. Vishnevskiy, Y. A. Zhabanov, *J. Phys.: Conf. Series* **2015**, *633*, 012076.

13 Monofluoromethylated Nitrogen Rich Heterocycles: Synthesis, Characterization and Fluorination Effect

Marco Reichel, Maximilian Wurzenberger, Jörg Stierstorfer, Andreas Kornath, Konstantin Karaghiosoff*

To be submitted



Abstract: A straight forward synthesis and efficient introduction of fluoromethyl group in nitrogen heterocycles is reported. Starting from the respective NH heterocycles fluoromethylation is performed with fluoriodomethane and proceeds under mild reaction conditions. Structural information of monofluoromethylated nitrogen-containing cyclic

compounds containing the biologically active NCH₂F moiety are reported. The particularly impressively change of physical and spectroscopic properties by the substitution of a methyl group by a monofluoromethyl group is discussed based on these examples.

13.1 Introduction

Nitrogen containing heterocycles with a fluoromethyl group directly bonded to nitrogen are of great interest due to their application in different areas. While heterocycles with the NCH₂F structural motive have been used as reagents in nickel catalyzed cross coupling reactions^[1], most of their applications are related to biologically active compounds. Five membered nitrogen heterocycles with an N-bonded CH₂F group are used for agro chemicals, especially for microbiocides and herbicides.^[2] In addition, based on the bioisosteric relationship between CH₂F and a variety of functional groups, they are essential for the pharmaceutical industry. Thus, NCH₂F containing heterocycles act as biologically active building blocks in endothelial lipase inhibitors (**1**),^[3] in agents for the treatment of CRF-1 related disorders (**2**)^[4] or acting as choline transporter inhibitors (**3**).^[5]

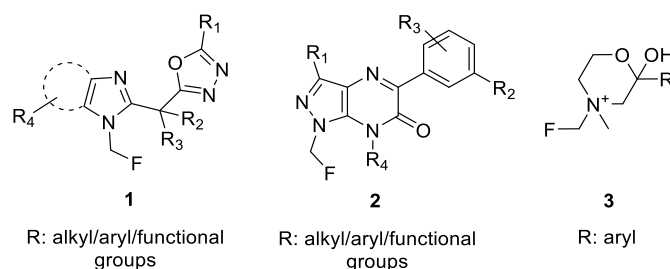


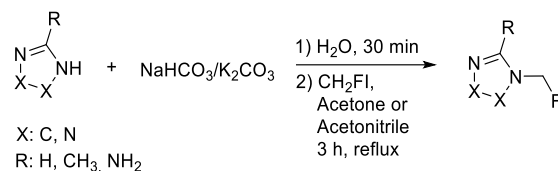
Chart 1: Biological active NCH₂F containing heterocycles.

Due to the strong and polar C-F bond the introduction of fluorine in organic compounds changes (in part dramatically) their physical properties and compounds with unique physical and properties can be obtained.^[6] Monofluoromethyl diaalkylamines are a good example; unlike the corresponding chloro-, bromo- and iodomethyl analogues they no longer have a salt-like character.^[7] This affects the boiling/melting points as well as the solubility and reaction behavior. The synthesis of amines with a fluoromethyl group attached to nitrogen is still a challenge, however. It is well known, that fluoromethyl halides CH₂FCl, CH₂FBr and CH₂FI can be used for electrophilic fluoromethylation of various oxygen-, sulfur-, carbon- and nitrogen- nucleophiles.^[8] While secondary fluoromethyl amines are likely to eliminate hydrogen fluoride and are of limited stability, tertiary fluoromethyl amines and N-CH₂F ammonium salts are stable and are prepared starting from the corresponding secondary or tertiary amines by reaction mostly with CH₂FCl.^[8-9] However the use of cheap CH₂FCl and CH₂FBr as fluoromethylating agents becomes increasingly problematic due to the ozone depleting properties of these compounds. In addition, handling of volatile CH₂FCl and CH₂FBr is challenging, particularly taking into account the harsh reaction conditions necessary.^[6, 8]

Structural information is of crucial importance in development and design of new pharmaceutically active agents. Although a large number of nitrogen compounds with a N-bonded CH₂F group have been prepared and many of them are used as pharmaceutical drugs,

surprisingly practically no structural information is available for the NCH₂F motive. Only one crystal structure - that of Me₃NCH₂F⁺ PbI₃^{-10]} - has been described in the literature so far.

Herein, we report a simple and practical method to synthesize new monofluoromethylated nitrogen heterocycles under mild reaction conditions with high yields using fluoriodomethane (Scheme 1).



Scheme 1: Method to generate monofluoromethylated nitrogen heterocycles.

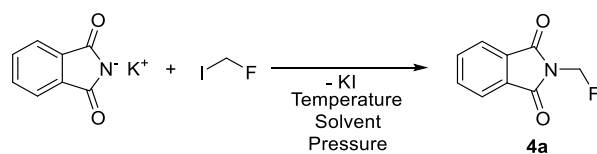
The change in physical properties and the influence of fluorine has been investigated by comparing the CH₂F containing new nitrogen heterocycles with the corresponding methyl derivatives. The molecular and crystal structures of selected nitrogen heterocycles containing the NCH₂F group have been determined by single crystal X-ray diffraction and offer an insight on the structural properties of this fascinating building block.

13.2 Results and Discussion

N-Fluormethyl phthalimide (**4**) is an important intermediate in the production of agrochemicals acting as herbicides or microbiocides.^[11] Its synthesis starting from phthalimide and introducing the CH₂F group by reaction with CH₂FCl is unattractive due to the low yield (23 %), while alternative routes are more complicated and more expensive.^[12]

For the synthesis of **4** we have used potassium phthalimide as the starting material, which was readily prepared from phthalimide according to a modified literature known procedure.^[14] Reaction of potassium phthalimide with CH₂FI results in the formation of **4**, which can be readily isolated by crystallization. The reaction conditions were optimized to give the best yield of 71 %. (Table 1).

Table 1: Optimization of the reaction conditions for the synthesis of **4**.



entry	T [°C]	p [bar]	solvent	t [h]	yield (%)
1	35.6	1	Et ₂ O	3h	5
2	40	1	DCM	3h	12
3	82	1	CH ₃ CN	3h	34
4	100	7	Et ₂ O	3h	9
5	100	6.1	DCM	3h	39
6	100	1,9	CH ₃ CN	3h	52
7	120	3,3	CH ₃ CN	3h	71

Potassium phthalimide was refluxed at ambient pressure in different solvents. The resulting yields were nearly as poor as for CH₂FCl (23%), the reaction in acetonitrile giving the best results (Table 1). In a previous study it was shown that fluoromethylation under increased pressure can lead to better yields.^[6, 13] Following this experience we performed the synthesis in a pressure tube and in fact for all solvents the yields of **4** were higher at 100 °C as compared to ambient conditions (Table 1). This further confirms the great impact of the pressure for fluoromethylation reactions with CH₂FI. Acetonitrile as solvent led to the highest yield (52%). The yield could be further improved to 71 % by performing the reaction in acetonitrile at 120 °C. Higher temperatures resulted in a brownish color of the reaction solution most probably indicating decomposition.

Single crystals of compound **4** were obtained by slow evaporation of the acetonitrile solution. Unexpectedly single crystals of the corresponding hydroxymethyl derivative **5** formed in the crystallization batch after one month at ambient temperature, most probably due to slow hydrolysis of the NCH₂F group. A similar behavior has been observed in the case of primary fluoromethyl amines.^[8] The molecular structures of **4** and **5** in the crystal are shown in Figure 1.

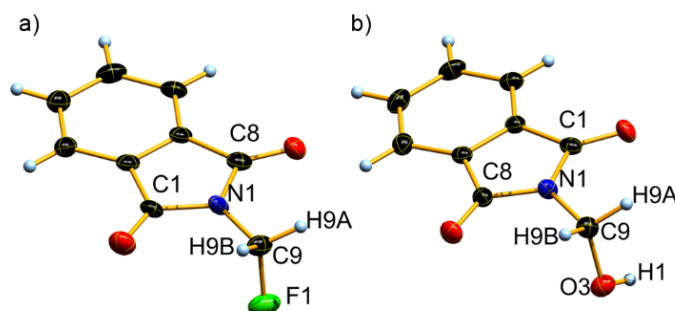


Figure 1: Molecular structure of **4** (a) and **5** (b) in the crystal. DIAMOND representation, thermal ellipsoids are shown with 50 % probability. Selected bond length and angles of **4**: N1-C9, 1.427(4); C9-F1, 1.388(3); F1-C9-N1, 109.3(2); F1-C9-N1-C1, 95.6(3).

The crystal structures of **4** and **5** offer the unique possibility to compare the structural behavior of two molecules differing only in F / OH at the same position. In both cases the molecules are completely planar and only the functional groups (F and OH) are positioned out of the molecular plane. The most interesting feature of the molecular structure of **4** is the NCH₂F group. The nitrogen atom in **4** and **5** displays a trigonal planar environment. The N1-C9 distance of 1.427(4) Å in **4** is somewhat shorter as compared to the N1-C9 distance of 1.456(3) Å in **5** and significantly shorter as compared to the distance of 1.51(2) Å reported for the Me₃NCH₂F cation.^[10] In this last case, however, the CH₂F group is disordered and structural parameters are less accurate. The C9-F1 bond length (1.388(3) Å) compares well to the value of a 1.399 Å for a C_{sp}³-F single bond, found in the literature^[14] and also to the C,F distance reported for the PCH₂F group (1.379(5) Å) (Figure 1).^[6] However, the CH₂-F bond length is shorter than the C,O distance in the bioisoster CH₂-OH moiety of 1.402(3) Å and the Me₃NCH₂F cation with 1.43(2) Å.^[10] There are considerable differences in the physical properties between **4** and **5**. For example, with a melting point of 82 °C, **4** is melting much lower than **5** (168 °C)^[15] or the analogous methyl derivative (CH₃ in place of CH₂F, 134 °C).^[16] In order to understand the difference in physical properties of the fluoromethyl compound **4**

and the hydroxymethyl compound **5** it is necessary to look into the interactions in the crystal (Figure 2).

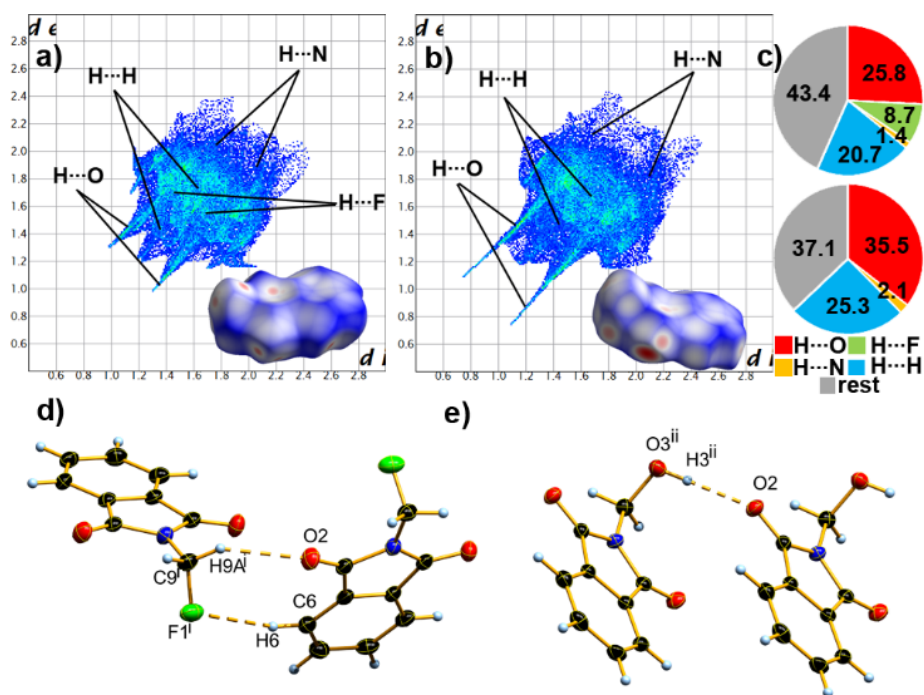


Figure 2: Two-dimensional fingerprint plot as well as the corresponding Hirshfeld surface (bottom right in 2D plot) of **4** (a) and **5** (b). Color coding: white, distance d equals VDW distance; blue, d exceeds VDW distance, red, d , smaller than VDW distance). Population of close contacts of **4** (top) and **5** (bottom) in crystal stacking. View of hydrogen bonding in **4** (d) and **5** (e), showing the strongest interactions. DIAMOND representation. Thermal ellipsoids are drawn at 50 % probability level. Symmetry code: *i*) $1-x, 0.5+y, -z$; *ii*) $1+x, y, z$.

In the case of **5** the OH group acts as a H-donor and undergoes hydrogen bonding with the oxygen atom of one of the carbonyl groups. This results in the formation of chains of hydrogen bonded molecules of **5** in the crystal. In the case of **4** the electronegative fluorine atom can act only as a H-acceptor in hydrogen bonding and interactions are less strong as compared to **5**. The strongest interactions are between a proton of CH₂ and the oxygen atom of C=O of another molecule, followed by the interaction between fluorine of the same CH₂F group and an aromatic proton of the same second molecule. This also results in the formation of chains in the crystal of **4** with the only difference of weaker interactions. This behavior is confirmed also by the Hirshfeld analysis of the structures of **4** and **5**. For strong O-H bonding the 2D fingerprint plot exhibits two distinct spikes.^[17] Comparing Figures 2a and 2b it becomes obvious, that O-H hydrogen bonding in **5** is much stronger than in **4**. Evaluation of the population of the close contacts (Figure 2c) shows, that **5** with 35.5 % O...H close contacts displays more H-bridges than **4**. With respect to $d_i + d_e$ (d_i : distance from the Hirshfeld surface to the nearest atom interior; d_e : distance from the Hirshfeld surface to the nearest atom exterior) we can follow that 8.7 % F...H contacts for **4** are weak due to their long distance and so these interactions cannot compensate the lower number of O...H contacts in **4**. The hydrogen bonding in Figures 2d and 2e shows the shortest contacts in the crystal. Considering these short contacts as well as the angles at the respective hydrogen atoms of 175(3)° in **5** and of (150(1)°, 163(2)°) in **4** (Table 2) the intermolecular interactions in **5** are considered to be stronger than in **4**.^[18] This is in accord with and explains the dramatic difference of the melting points of both compounds.

Table 2: Bond length [Å] and bond angles [°] of selected H-bonds.

Compound	Bond	d(D-H)	d(H...A)	d(D...A)	<(D-H...A)
4	C9 ⁱ -H9A ⁱ ...O2	0.96(2)	2.416(2)	3.284(4)	150(1)
	C6-H6...F1 ⁱ	0.99(4)	2.68(3)	3.651(5)	163(2)
5	O3 ⁱⁱ -H3 ⁱⁱ ...O2	0.86(3)	1.98(4)	2.835(3)	175(3)
6b	C4-H4B...F1 ⁱ	0.98(2)	2.584(2)	3.148(3)	143(2)
6a	C1 ⁱⁱ -H1 ⁱⁱ ...F1	0.98(2)	2.63(2)	3.561(2)	157(2)
	O2-H3...N1 ⁱⁱ	0.81(2)	1.99(2)	2.796(2)	175(2)
7	C2-H2...O2	0.96(2)	2.39(2)	3.329(2)	166(2)
	C6-H6B...F2 ⁱⁱⁱ	0.94(2)	2.36(2)	3.055(3)	130.5(8)
	C6-H6A...I1	0.94(2)	3.59(2)	4.007(2)	110.1(7)
	C1 ⁱⁱ -H1 ⁱⁱ ...I1	0.92(3)	3.15(2)	3.952(3)	148(2)
8a	C6 ⁱⁱⁱ -H6B ⁱⁱⁱ ...I1	0.94(2)	3.47(2)	4.158(3)	131.6(7)
	N5-H5B...N4 ⁱ	0.89(3)	2.963(4)	2.963(4)	168(3)
	N5 ⁱ -H5B ⁱ ...N4	0.89(3)	2.963(4)	2.963(4)	168(3)
8b	C4-H4A...F1	0.97(3)	2.37(3)	3.098(3)	131(3)
	N5-H5A...F1 ⁱⁱⁱ	0.86(2)	2.60(2)	2.939(2)	105(2)
	N5 ⁱⁱ -H5B ⁱⁱ ...N1	0.89(2)	2.23(2)	3.095(2)	165(2)

Symmetry code: **4**) *i*) 1-x, 0.5+y, -z; **5**) *ii*) 1+x, y, z; **6b**) *i*) 0.5+x, 0.5-y, 1-z; **6a**) *ii*) 1-x, 0.5+y, 0.5-z; **7**) *iii*) 1.5-x, 0.5+y, z; **8a**) *i*) 2-x, 1-y, -z; **8b**) *ii*) 0.5+x, 0.5-y, 0.5+z; *iii*) 0.5-x, 0.5+y, 0.5-z

Another pair of heterocycles, which can be compared and display the effect of fluorine are 1*H*-2-methylimidazole^[19] and the new 1*H*-1-fluoromethyl-2-methylimidazole **6**. Similar to the synthesis of **4**, the fluoromethyl derivative **6** was obtained by reaction of potassium 2-methylimidazolate with CH₂FI. Potassium 2-methylimidazolate is readily prepared starting from 1*H*-2-methylimidazole by reaction with potassium carbonate (Scheme 1).^[20] Fluoromethyl imidazole **6** is isolated as a slightly yellowish oil (63 % yield), which tends to form a super cooled melt. Single crystals of **6a** and its monohydrate **6b** (Figure 2) were formed by slow evaporation of a solution of **6** in chloroform. The nitrogen atom in **6a** and **6b** displays a trigonal planar environment, as observed for **4** (Figure 3). The N2-C5 distance to the fluoromethyl group in both, **6a** (1.422(3) Å) and the hydrate **6b** (1.424(2) Å) is almost the same and in good agreement with that found in **4** (1.427(4) Å). The crystal water seems to not affect the C5-F1 bond length. With values of 1.400(3) Å (**5**) and 1.394(2) Å (**6b**) these distances fit well to that observed in the case of **4** (1.388(3) Å). However, somewhat shorter C,F distances are reported for PCH₂F (1.379(5) Å),^[6] CH₂FI (1.38(2) Å),^[21] and CH₂FBr (1.377(4) Å).^[21] Compounds **6a** and **6b** mainly differ in the intermolecular interactions in the crystal (Figure 3).

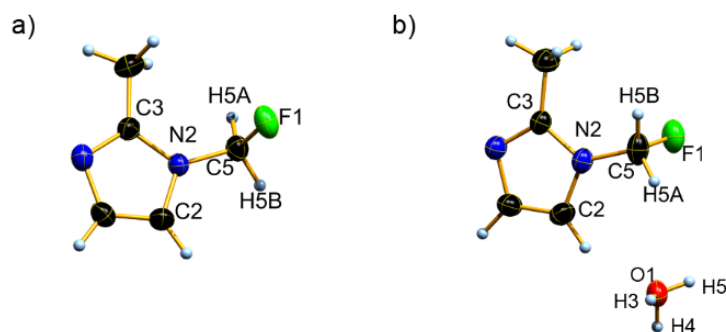


Figure 3: Molecular structure of **6a** (a) and of the monohydrate **6b** (b) in the crystal. In the case of **6b** one proton of the H₂O molecule is disordered over two positions (50 % disorder). DIAMOND representation, thermal ellipsoids are drawn with 50 % probability. Selected bond length and angles of **6a**: C5-F1, 1.400(3); C5-N2, 1.422(3); N2-C5-F1, 109.2(2); F1-C5-N2-C3, -84.3(3). **6b**: C5-F1, 1.394(2); C5-N2, 1.424(2); F1-C5-N2, 109.5(2); F1-C5-N2-C3, -85.3(2).

Looking at the Hirshfeld analysis of the structures of **6a** and **6b**, from the distinct spikes of **6b** in the 2D Plot it becomes evident, that the H \cdots F interactions in the sum are less but stronger,^[17] as compared to **6a** (Figures 3a-c). The larger angle at hydrogen of 157(2) $^\circ$ in **6b** as compared to (143(2) $^\circ$) in **6a** (Table 2) confirms that intermolecular H \cdots F interactions in **5b** are stronger than in **6a** (Figures 3f,g).^[18] The sum $d_i + d_e$ (d_i : distance from the Hirshfeld surface to the nearest atom interior; d_e : distance from the Hirshfeld surface to the nearest atom exterior) indicates, that for **6a** in general all interactions in the crystal are very weak (Table 2), due to the long distances of the H \cdots N and H \cdots F contacts (Figure 5a) and the angles at hydrogen with values of 143(2) $^\circ$ -175(2) $^\circ$.^[17-18] The low melting point of 27 $^\circ$ C observed for **6b** is in accord with these weak interactions. Compared to its methyl analogue (m.p. 51 $^\circ$ C b.p. 206 $^\circ$ C),^[22] **6b** shows lower melting and boiling points. This is in good agreement with the observation made for **4**, the melting point of which is about 50 $^\circ$ C lower than that of the corresponding methyl derivative.

Fluoromethyl imidazole **6a** was allowed to react with CH₂FI yielding 76 % of the corresponding 1*H*-1,3-di(fluoromethyl)-2-methyl imidazolium iodide (**7**). Single crystals of **7** were obtained by slow evaporation of a solution of **7** in acetonitrile. The molecular structure of **7** in the crystal is shown in Figure 4.

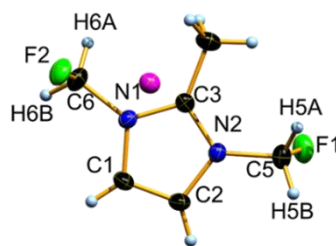


Figure 4: Molecular structure of **7** in the crystal. DIAMOND representation, thermal ellipsoids are drawn with 50 % probability. Selected bond length and angles of **7**: F1-C5, 1.371(3); C5-N2, 1.440(3); F2-C6, 1.374(3); C6-N1, 1.445(3); F1-C5-N2, 108.7(2); F2-C6-N1, 108.6(2); F1-C5-N2-C3, -92.0(3); F2-C6-N1-C3, -84.5(3).

Both nitrogen atoms in compound **7** display a trigonal planar environment. As compared to **6a** (N2-C5: 1.422(3) Å, 1.424(2) Å), the N-C bond length in **7** (N2-C5: 1.440(3) Å, N1-C6 (1.445(3) Å)) are slightly longer. However, the C5-F1 and C6-F2 distances of 1.371(3) Å and 1.374(3) Å, respectively, are significantly shorter than in **6a** (1.400(3) Å, 1.394(2) Å) and are similar to those reported for PCH₂F (1.379(5) Å),^[6] CH₂FI (1.380(17) Å),^[21] or CH₂FBr (1.377(4) Å).^[21] The intermolecular interactions also change dramatically, due to the introduction of ionic charges and of the iodide anion. The H \cdots N close contacts, which are characteristic for **6a**, are replaced by H \cdots I and H \cdots F contacts (Figures 5c,e). As a result, about 62 % attractive contacts are present in **7**, in contrast to 42.5 % in **6b**. This is in accord with the fact, that **7** can be heated up to 252 $^\circ$ C without observable decomposition. The non-distinct spikes for the H \cdots F and H \cdots I contacts (Figure 3g) and the sum $d_i + d_e$ (d_i : distance from the Hirshfeld surface to the nearest atom interior; d_e : distance from the Hirshfeld surface to the nearest atom exterior) indicate, that these interactions are weak (Table 2).^[17-18]

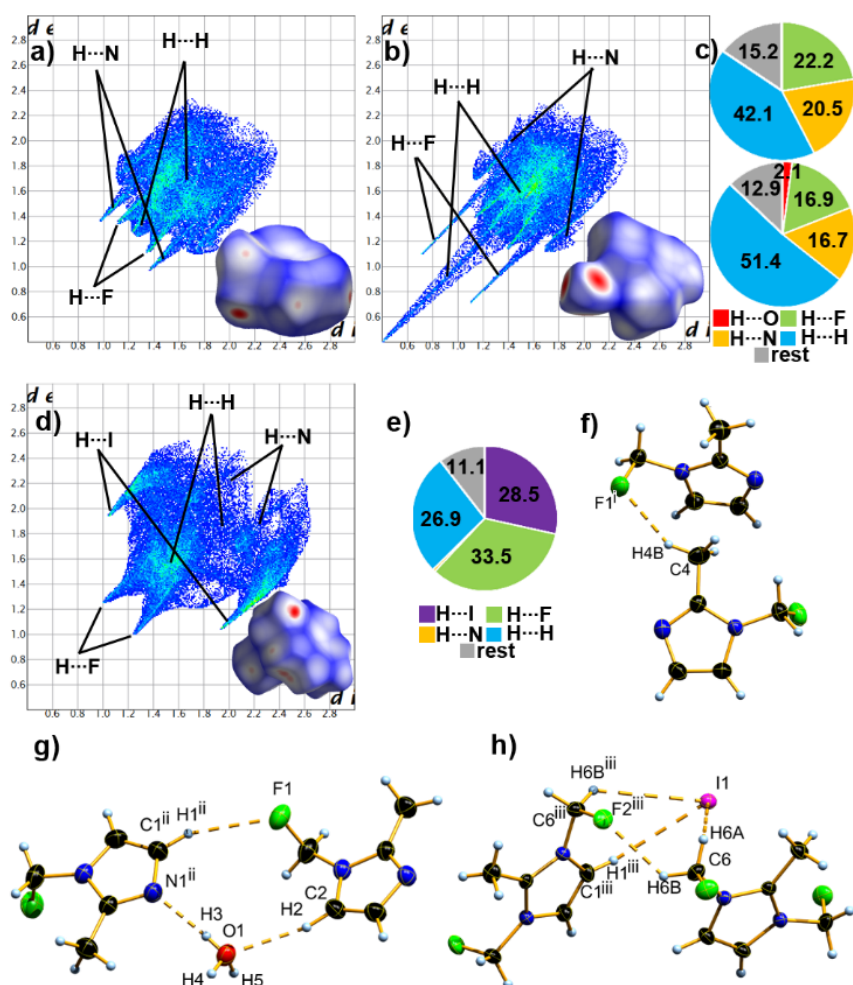
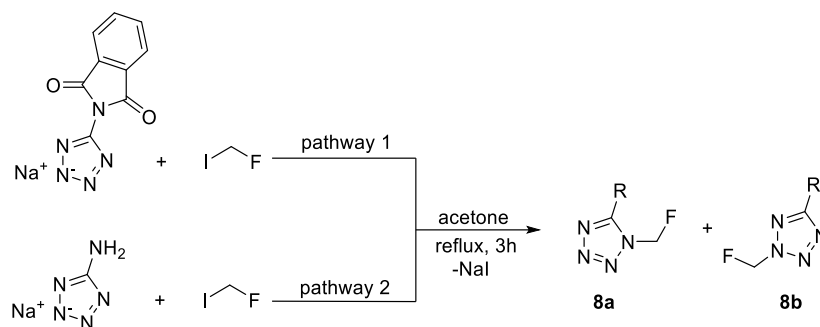


Figure 5: Two-dimensional fingerprint plot as well as the corresponding Hirshfeld surface (bottom right in 2D plot) of **6a** (a), **6b** (b) and **7** (d). Color coding: white, distance d equals VDW distance; blue, d exceeds VDW distance, red, d smaller than VDW distance. Population of close contacts of **6a** (c) top, **6b** (c) bottom and **7** (e) in crystal stacking. Strongest hydrogen bonds in **6a** (f), **6b** (g) and **7** (h). DIAMOND representation. Thermal ellipsoids are drawn at 50% probability level. Symmetry codes: *i*) 0.5+x, 0.5-y, 1-z; *ii*) 1-x, 0.5+y, 0.5-z; *iii*) 1.5-x, 0.5+y, z.

As an example, the strongest H...I contact (Figure 3h), with a distance of 3.15(2) Å is by far longer than the only weak interaction with a distance of 2.83(2) Å found in [PPh₃CH₂F]I.^[6] A similar weak contact was observed in [PPh₃CH₂OH]I, where the CH...I interaction corresponds to a distance of 3.092(2) Å.^[23] The melting point of **7** is by approx. 50 °C lower as compared to its methyl analogue (312 °C). Decomposition for **6** occurs at 252 °C without melting.^[24]

Tetrazoles with small substituents at nitrogen and carbon are an intriguing class of compounds, in particular with respect to their rich coordination chemistry and their tunable energetic properties. Fluoromethyl tetrazoles are not described in the literature. Methyl tetrazoles are known, their selective synthesis is quite challenging, however, and isomers are obtained by most of the synthetic procedures. As a consequence tedious and complicated purification steps have to be applied in order to obtain pure compounds.^[25] Since 1- and 2-methyl 5-aminotetrazoles have a great importance in high energetic materials research, we attempted the synthesis of the corresponding 1- and 2-fluoromethyl derivatives with the scope to study the influence of fluorine on their energetic properties and their sensitivity towards friction and impact.^[26]



Scheme 2: Synthesis of monofluoromethylated aminotetrazole.

Initial experiments along reaction pathway 1 (Scheme 2) did not result in the exclusive formation of **8b**, as described for the methyl analogue.^[25a] The synthesis of **8** was attempted along pathway 2, which also results in the formation of the two isomers **8a** and **8b**, but in which the additional two steps of protection with phthalic acid anhydride and deprotection to fluoromethyl aminotetrazole **8** are not necessary. Unlike for the reaction of sodium 5-aminotetrazole (NaAT) with CH₃I or SO₄(CH₃)₂,^[27] water or ethanol should be avoided as solvent for the synthesis of **8**, as using these solvents lead to extensive decomposition during the reaction. The reaction of NaAT with CH₂FI in acetone provided 83% of a 2 : 1 mixture of **8a** and **8b**. From this mixture **8a** was isolated with 51 % and **8b** with 24 % yield. Single crystals of the two compounds were obtained by solving the products in water and cooling the solution to 3 °C for several days. The molecular structures of **8a** and **8b** in the crystal are shown in Figure 6.

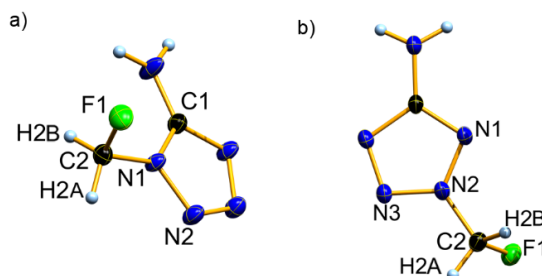


Figure 6. Molecular structure of **8a** (a) and **8b** (b) in the crystal. DIAMOND representation, thermal ellipsoids are drawn with 50 % probability. Selected bond length and angles of **8a**: F1-C2, 1.382(3); C2-N1, 1.429(4); F1-C2-N1, 109.3(2); F1-C2-N1-C1, -82.7(4). **8b**: F1-C2, 1.380(2); C2-N2, 1.439(2); F1-C2-N2, 108.6(2); F1-C2-N2-N1, -70.0(2).

The nitrogen atom bonded to the CH₂F group in **8a** and **8b** displays a trigonal planar environment, as observed for **4**, **6a** and **7**. The corresponding N1-C2 and N2-C2 bond lengths of 1.429(4) and 1.439(2) Å, respectively, compare well to the values observed in **4** (1.427(4) Å) and **5** (1.422(3) Å) and are somewhat shorter than the value observed in **7** (1.445(3) Å). The C2-F1 distance of 1.382(3) Å (**8a**) and 1.380(2) Å (**8b**) is in line with the corresponding distances in **4** (1.388(3) Å) and **7** (1.371(3) Å) and is shorter than in **6a** (1.400(3) Å). Also in this case the C-F distances compare well with those reported for PCH₂F (1.379(5) Å),^[6] CH₂FI (1.38(2) Å),^[21] and CH₂FBr (1.377(4) Å).^[21]

Noteworthy is the different thermal behavior observed for **8a** and **8b**. The melting points of these two compounds differ by almost 60 °C. An analogous behavior is reported for the methyl derivatives.^[28]

Crystal structure data are available only for the 2-methyl-5-aminotetrazole.^[25a] For 1-methyl-5-aminotetrazole^[29] only the unit cell dimensions are reported.

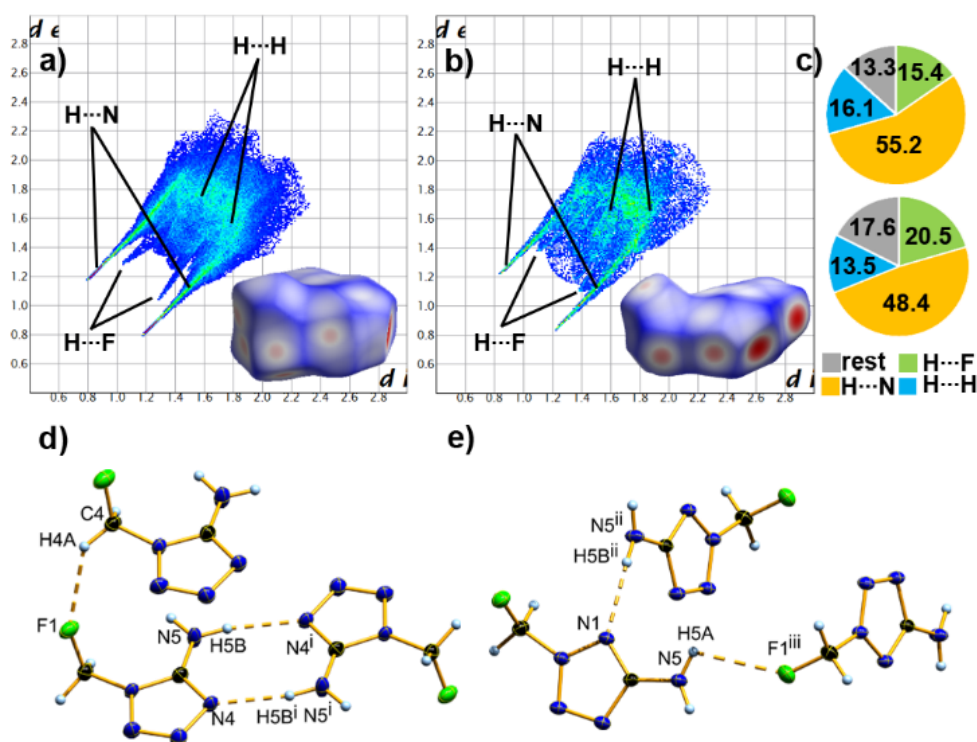


Figure 7: Two-dimensional fingerprint plot as well as the corresponding Hirshfeld surface (bottom right in 2D plot) of **8a** (a) and **8b** (b). Color coding: white, distance d equals VDW distance; blue, d exceeds VDW distance, red, d , smaller than VDW distance). Population of close contacts of **8a** (c) top and **8b** (c) bottom in crystal stacking. Strongest hydrogen bonds in **8a** (d) and **8b** (e). DIAMOND representation. Thermal ellipsoids are drawn at 50 % probability level. Symmetry codes: *i*) 2-x, 1-y, -z; *ii*) 0.5+x, 0.5-y, 0.5+z; *iii*) 0.5-x, 0.5+y, 0.5-z.

In order to obtain an insight into the intermolecular interactions in the crystal a Hirshfeld analysis was performed on the crystal structures of **8a** and **8b** (Figure 7). The sum $d_i + d_e$ (d_i : distance from the Hirshfeld surface to the nearest atom interior; d_e : distance from the Hirshfeld surface to the nearest atom exterior) in the 2D plot of **8a** and **8b** reveals, that the spikes for N...H contacts are similarly wide for both compounds and only slightly longer for **8a**. Thus for both compounds, the N...H contacts in this range are similarly strong and the strong interactions occur with a similar frequency. However, there are clear differences regarding the F...H contacts. These are clearly stronger for **8a** (distinct long spikes) than for **8b** (Figure 7), as indicated also by the shorter hydrogen bridges in the crystal structure (Figures 7d,e). With H...F contact distances of 2.37(3) Å (**8a**) vs. 2.60(3) Å (**8b**) the attractive forces in the crystal of 1-fluoromethyl-5-aminotetrazole **8a** are clearly stronger than for **8b** (Table 2). The sum of the attractive interactions for **8a** (70.6 %) and for **8b** (68.9 %) is almost the same. In all intermolecular interactions in the crystal of **8a** are stronger than in crystalline **8b**.

Experimentally this results in dramatic differences in the thermal behavior of the two isomers **8a** and **8b**. Compound **8a** decomposes while melting at 131 °C, while the isomer **8b** melts at 75 °C and decomposes at 166 °C. It is interesting to compare these thermal properties with

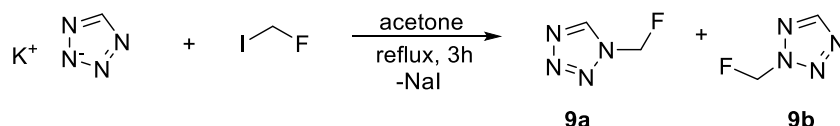
those of the corresponding methyl derivatives. The 5-amino-1-methyl tetrazole (m.p. 226 °C^[28a]) and 5-amino-2-methyl tetrazole (m.p. 105 °C^[28b]) show in both cases a higher melting point than their fluorine containing derivative.

The sensitivities towards friction and impact of **8a** and **8b** was determined experimentally according to standards of the German Federal Institute for Material Research and Testing (BAM).^[30] According to the UN recommendations on transport of dangerous goods, **8a** and **8b** has to be classified as non sensitive towards impact and friction (Table 3).^[31] *Ab initio* calculations were carried out to compute the heat of formation for **8**, using the optimized geometry of the molecules starting from the X-ray diffraction experiment.^[32] The heat of formation is more positive for **8a** than for **8b** (see Table 3). Based on the heats of formation and the corresponding densities determined from the X-ray experiment, the detonation parameters of **8a** and **8b** were calculated using EXPLO5 V6.03 code.^[33] The detonation parameters were calculated at the *Chapman-Jouguet* (C-J) point with the help of a stationary detonation model using a modified *Becker-Kistiakowski-Wilson* state equation for the system. The C-J point was located using the first derivative of the *Hugoniot* curve of the system.^[30] These indicate, that the detonation parameters for **8a** exceed those of **8b** (Table 3).

Table 3: Physical and thermodynamic properties of **8a** and **8b**.

	8a	8b	9a
formula	C ₂ H ₄ FN ₅	C ₂ H ₄ FN ₅	C ₂ H ₃ FN ₄
<i>M</i> [g mol ⁻¹]	117.04	117.04	102.03
<i>IS</i> ^[a] [J]	>40	>40	>40
<i>FS</i> ^[b] [N]	>360	>360	>360
<i>N</i> ^[c] [%]	59.81	59.81	54.89
<i>T</i> _{mel} / <i>T</i> _{boil} ^[d] [°C]	131	75	160
<i>ρ</i> _{273K} ^[e] [g cm ⁻³]	1.648	1.637	1.581
<i>ΔH</i> _f ⁰ [f] [kJ mol ⁻¹]	24.0	13.4	51.5
EXPLO5 V 6.03			
<i>ΔU</i> _f ⁰ [g] [kJ kg ⁻¹]	-2605	-2521	-3051
<i>T</i> _{C-J} ^[h] [K]	2136	2093	2443
<i>P</i> _{C-J} ^[i] [GPa]	19.8	19.1	17.0
<i>V</i> _{det} ^[j] [ms ⁻¹]	7596	7500	7085
<i>V</i> _o ^[k] [dm ³ kg ⁻¹]	859	859	826

[a] Impact sensitivity (BAM drop-hammer, method 1 of 6); [b] friction sensitivity (BAM friction tester, method 1 of 6); [c] nitrogen content; [d] melting point for **7** boiling point for **8**; [e] density determined by X-ray diffraction at 130 K for **7** and at room temperature for **8**; [f] heat of formation calculated at the CBS-4M level of theory [g] detonation energy; [h] detonation temperature; [i] detonation pressure; [j] detonation velocity; [k] volume of detonation gases at standard temperature and pressure conditions.



Scheme 3: Synthesis of monofluoromethylated 5H-tetrazole.

We also attempted the synthesis of fluoromethyl tetrazoles unsubstituted in 5-position by reaction of potassium tetrazolate with CH₂FI. Potassium tetrazolate was readily prepared from tetrazole with potassium carbonate. After workup only one isomer, the 1-fluoromethyltetrazole (**9a**), was isolated as colorless oil with a yield of 12 %. Compound **9a** has a boiling point of 160 °C and a melting point of 0 °C. Both are lower as compared to the corresponding methyl

derivative, which has an extrapolated boiling point of 213 °C (145 °C, 118 Torr) and a melting point of 10 °C.^[34] The detonation energy and detonation temperature calculated for **9a** exceed the values for compounds **8a** and **8b**. In contrast, the performances of **8a** and **8b** with respect to detonation pressure, detonation velocity and released gas surpass those of compound **9a** (Table 3).

13.3 Conclusion

In summary we have synthesized new fluoromethylated nitrogen containing heterocycles, which can act as interesting and versatile ligands for transition metals. Single crystal X-ray diffraction studies reveal for the first time reliable structural information on CH₂F bonded to nitrogen. Only weak fluorine hydrogen interactions were observed in the structures of all compounds investigated. However, the intermolecular interactions in the crystal were identified to be responsible for the low melting points of the fluoromethyl derivatives. Thus, as a general trend, the introduction of a CH₂F group in place of a CH₃ group lowers the boiling and melting point by about 10-90 °C. In 2-fluoromethyl-5-aminotetrazole the reduced number of stronger N···H contacts as compared to the 1-fluoromethyl isomer is the main reason for the dramatic difference of the thermal behavior of the two isomers. The same situation results from the comparison of fluoromethyl- and hydroxymethyl phthalimide. Lowering the number of strong O···H contacts decreases the melting point of the fluoromethyl derivative. Fluoromethyl imidazole derivatives show almost negligible interactions in the crystal, the melting points of those are low.

13.4 Acknowledgement

Financial support by Ludwig–Maximilian University is grateful acknowledged. We are thankful to F–Select GmbH for a generous donation of fluoroiodomethane.

13.5 Experimental Section

13.5.1 General Procedure

Fluoroiodomethane was a donation from F-Select GmbH and distilled before use. All other chemicals were commercially available from abcr. For NMR spectroscopy the solvents were dried using 3 Å molesive. Spectra were recorded on a Bruker Avance III spectrometer operating at 400.1 MHz (¹H), 100.6 MHz (¹³C), 376.4 MHz (¹⁹F), and 40.6 MHz/ 28.9 MHz (^{15/14}N). Chemical shifts are referred to TMS (¹H, ¹³C), CFCI₃ (¹⁹F) and MeNO₂ (¹⁵N). Raman spectra were recorded with a Bruker MultiRam FT Raman spectrometer using a neodymium doped yttrium aluminium garnet (Nd:YAG) laser ($\lambda = 1064$ nm) with 1074 mW. The samples for Infrared spectroscopy were placed under ambivalent conditions onto an ATR unit using a Perkin Elmer Spectrum BX II FT-IR System spectrometer. Melting and / or decomposition points were detected with a OZM DTA 552-Ex or Linseis DSC instrument. The scanning temperature range was set from 293 K to 673 K at a scanning rate of 5 K min⁻¹. Elemental analysis was done with a Vario EL instrument and a Metrohm 888 Titrando device. The mass spectrum was recorded on a Thermo Fischer GC/MS instrument. Crystallographic Data collection was performed with an Oxford Xcalibur 3 diffractometer

equipped with a Spellman generator (50 kV, 40 mA) and a Kappa CCD detector, operating with Mo-K α radiation ($\lambda = 0.71073 \text{ \AA}$). Data collection and data reduction were performed with the CrysAlisPro software.^[1] Absorption correction using the multiscan method^[1] was applied. The structures were solved with SHELXS-97,^[2] refined with SHELXL-97^[3] and finally checked using PLATON.^[4] Details for data collection and structure refinement are summarized in the supplementary information.

13.5.2 Preparation

Monofluoromethylphthalimide (4)

Potassium hydroxide (3.81 g, 67.9 mmol) was dissolved in ethanol (50 mL) and to the boiling solution subsequent phthalimide (10.0 g, 67.9 mmol) was added and refluxed overnight. Afterwards the solvent was removed the crude salt was washed with ethanol (3×50 mL) yielding the potassium salt as white solid (12.0 g, 64.5 mmol). In a pressure tube, the potassium salt (0.88 g, 4.79 mmol) was solved in acetonitrile (15 mL) and fluoroiodomethane (0.320 mL, 4.79 mmol) was added in one portion. The reaction was heated to 120 °C for 3 h. Afterwards, the solvent was removed in *vacuo* and the product extracted with a water dichloromethane mixture (1:1, 50 mL). Afterwards the organic solvent was removed in *vacuo* 4 was obtained as colorless powder (610 mg, 71%). M.p. 82 °C; ¹H NMR (400 MHz, CDCl₃): $\delta = 7.97 - 7.95$ (m, 2H), 7.81 (dd, $J = 5.4 \text{ Hz}$, 3.1 Hz, 2H), 5.77 (d, $J = 52.1 \text{ Hz}$, 2H) ppm. ¹⁹F{¹H} NMR (376 MHz, CDCl₃): $\delta = -174.2$ (s) ppm. ¹⁹F NMR (376 MHz, CDCl₃): $\delta = -174.2$ (t, $J = 52.1 \text{ Hz}$) ppm. ¹³C{¹H} NMR (101 MHz, CDCl₃): $\delta = 166.6, 135.0, 131.8, 124.3, 74.9$ (d, $J = 198 \text{ Hz}$) ppm. IR (ATR): $\tilde{\nu} = 3504$ (w), 3351 (w), 3212 (w), 3064 (w), 2979 (w), 2938 (w), 2352 (w), 1773 (m), 1722 (s), 1704 (s), 1608 (m), 1464 (m), 1437 (m), 1406 (m), 1361 (s), 1322 (s), 1310 (s), 1219 (m), 1187 (m), 1153 (w), 1088 (w), 1069 (w), 1054 (w), 954 (s), 852 (w), 795 (w), 708 (s), 646 (w), 616 (s), 560 (m), 531 (s); Raman (1074 mW): $\tilde{\nu} = 3089$ (s), 2987 (m), 1737 (m), 1611 (s), 1466 (w), 1365 (w), 1199 (s), 1173 (m), 1155 (m), 990 (m), 970 (m), 854 (w), 800 (w), 730 (w), 714 (m), 620 (w), 562 (w), 534 (w), 415 (w), 389 (w), 240 (w), 164 (w), 107 (vs), 77 (vs); Anal. Calcd for C₉H₆FNO₂: C, 61.29; H, 4.01; N, 7.82. Found: C, 61.29; H, 4.01; N, 7.52. HRMS (GC/EI) m/z: [M] Calcd for C₉H₆FNO₂ 179.0383; Found: 179.0377.

1-fluoromethyl-2methyl-imidazole (6a)

2-Methylimidazole (1.00 g, 12.2 mmol) was dissolved in acetonitrile (15 mL) and potassium carbonate (0.84 g, 6.10 mmol) was added in one portion. The suspension was stirred for 30 min and fluoroiodomethane (0.82 mL, 12.2 mmol) was added dropwise. The reaction mixture was stirred overnight. After the solvent was removed in *vacuo*, the product was extracted from a mixture of water and chloroform (1:1, 100 mL). The organic solvent was removed yielding a yellowish oil (0.45 g, 63 %). M.p. 27 °C; B.p. 192 °C; ¹H NMR (400 MHz, CD₃CN): $\delta = 7.12$ (d, $J = 1.5 \text{ Hz}$, 1H), 6.84 (s, 1H), 5.91 (d, $J = 52.9 \text{ Hz}$), 2.38 (s, 3H) ppm. ¹⁹F{¹H} NMR (376 MHz, CD₃CN): $\delta = -164.3$ (s) ppm. ¹⁹F NMR (376 MHz, CD₃CN): $\delta = -164.3$ (t, $J = 52.9 \text{ Hz}$, 2H) ppm. ¹³C{¹H} NMR (101 MHz, CD₃CN): $\delta = 146.9, 121.3, 118.4, 84.4$ (d, $J = 194.0 \text{ Hz}$), 12.6 ppm. ¹⁴N{¹H} NMR (28.9 MHz, CD₃CN): $\delta = -120$ (s, 1N), -210 (s, 1N) ppm. IR (ATR): $\tilde{\nu} = 3114$ (w), 3000 (w), 2934 (w), 1676 (m), 1539 (m), 1506 (m), 1422 (m), 1396 (m), 1377

(m), 1282 (s), 1187 (w), 1130 (w), 1086 (w), 969 (s), 856 (w), 765 (s), 734 (s), 680 (s), 662 (s), 626 (w), 566 (w); Raman (1074 mW): $\tilde{\nu}$ = 3143 (m), 3120 (m), 2998 (m), 2936 (s), 1506 (s), 1485 (s), 1457 (w), 1426 (w), 1392 (w), 1369 (w), 1285 (w), 1131 (m), 1088 (w), 989 (w), 914 (w), 769 (m), 682 (w), 664 (w), 260 (m).; HRMS (GC/EI) m/z: [M] Calcd for C₅H₇FN₂ 114.0593; Found: 114.0586.

Bisfluoromethyl-2methyl-imidazolium iodide (7)

Compound **6a** (0.20 g, 1.75 mmol) was dissolved in acetonitrile (6 mL) and fluoroiodomethane (0.12 mL, 1.75 mmol) was added dropwise. After the reaction mixture was stirred overnight, the precipitate was filtered off yielding a white solid (0.36 g, 76%). Dec.p. 252 °C; ¹H NMR (400 MHz, D₂O): δ = 7.80 (s, 2H), 6.32 (d, *J* = 49.1 Hz, 4H) ppm. ¹⁹F{¹H} NMR (376 MHz, D₂O): δ = -175.7 (s) ppm. ¹⁹F NMR (376 MHz, D₂O): δ = -175.7 (t, *J* = 49.1 Hz) ppm. ¹³C{¹H} NMR (101 MHz, D₂O): δ = 149.3, 122.2, 84.7 (d, *J* = 204.6 Hz), 9.5 ppm. ¹⁴N{¹H} NMR (28.9 MHz, D₂O): δ = -197 (s, 1N) ppm. IR (ATR): $\tilde{\nu}$ = 3132 (w), 3088 (m), 2955 (w), 2866 (w), 1745 (w), 1634 (w), 1597 (m), 1534 (m), 1469 (m), 1350 (m), 1270 (s), 1217 (s), 1136 (s), 1011 (s), 970 (m), 782 (s), 760 (s), 660 (s), 488 (w), 441 (s); Raman (1074 mW): $\tilde{\nu}$ = 3087 (s), 3034 (m), 2998 (m), 2926 (s), 1527 (s), 1399 (m), 1376 (m), 1351 (m), 1108 (m), 1020 (m), 763 (s), 674 (m), 662 (m), 443 (m), 412 (m), 331 (m), 304 (m), 254 (m), 178 (s); Anal. Calcd for C₆H₉F₂IN₂: C, 26.30; H, 3.31; N, 10.22. Found: C, 26.14; H, 3.10; N, 10.01. HRMS (DEI) m/z: [M-H]⁺ Calcd for C₆H₈F₂N₂⁺ 146.0650; Found: 146.0661.

1-Fluoromethyl-5-aminotetrazole (8a)

5-Aminotetrazole (10.2 g, 120 mmol) were solved in water (50 mL) and sodium hydrogen carbonate (10.8 g, 120 mmol) was added slowly in small portions. After the solution was stirred for 30 min, the solvent was removed. The obtained sodium 5-aminotetrazole (12.6 g, 117 mmol), was slurried in acetone (50 mL) and fluoroiodomethane (7.94 mL, 117 mmol) was added dropwise. After the reaction mixture was refluxed for 3h, the solvent was removed in vacuo. The in water (70 mL) slurried beige crude product, was filtrated and washed with diethylether (200 mL). Pure product **8a** was obtained (7.05 g, 51 %). Dec.p. 131 °C; ¹H NMR (400 MHz, (CD₃)₂SO): δ = 7.31 (s, 2H), 6.26 (d, *J* = 51.8 Hz, 2H) ppm. ¹⁹F{¹H} NMR (376 MHz, (CD₃)₂SO): δ = -170.8 (s) ppm. ¹⁹F NMR (376 MHz, (CD₃)₂SO): δ = -170.8 (t, *J* = 51.8 Hz) ppm. ¹³C{¹H} NMR (101 MHz, (CD₃)₂SO): δ = 156.1 (d, *J* = 1.1 Hz), 81.3 (d, *J* = 189.2 Hz) ppm. ¹⁵N NMR (40.6 MHz, (CD₃)₂SO): δ = 9.3 (d, *J* = 0.8 Hz, 1N), -23.8 (s, 1N), -94.2 (s, 1N), -171.3 (d, *J* = 19.6 Hz, 1N), -333.8 (t, *J* = 89.0 Hz, 1N) ppm. IR (ATR): $\tilde{\nu}$ = 3319 (w), 3137 (w), 2798 (w), 2750 (w), 1652 (m), 1591 (m), 1485 (w), 1459 (w), 1400 (w), 1342 (w), 1305 (w), 1284 (w), 1183 (w), 1104 (w), 1007 (m), 960 (m), 805 (m), 752 (w), 720 (m), 472 (m); Raman (1074 mW): $\tilde{\nu}$ = 3057 (w), 2996 (w), 1593 (w), 1464 (w), 1403 (w), 1342 (w), 1309 (w), 1141 (w), 1100 (w), 1011 (w), 964 (w), 807 (s), 753 (w), 722 (w), 480 (w), 443 (w), 299 (w), 164 (w), 143 (m), 102 (s); Anal. Calcd for C₂H₄FN₅: C, 20.52; H, 3.44. Found: C, 20.30; H, 3.45; HRMS (DEI) m/z: [M] Calcd for C₂H₄FN₅ 117.0451; Found: 117.0446.

2-Fluoromethyl-5-aminotetrazole (8b)

The solvent of the received filtrate from the synthesis of **8a**, was removed *in vacuo*. The obtained solid – containing **8a** and **8b** – was purified via sublimation at 80 °C. Compound **8b** was sublimated as a white solid onto the cooling finger (3.32 g, 24%). M.p. 75 °C; Dec.p. 166 °C; ¹H NMR (400 MHz, (CD₃)₂SO): δ = 6.42 (d, *J* = 50.9 Hz, 2H), 6.39 (s, 2H) ppm. ¹⁹F{¹H} NMR (376 MHz, (CD₃)₂SO): δ = -170.2 (s) ppm. ¹⁹F NMR (376 MHz, (CD₃)₂SO): δ = -170.2 (t, *J* = 50.9 Hz) ppm. ¹³C{¹H} NMR (101 MHz, (CD₃)₂SO): δ = 167.9, 86.5 (d, *J* = 202.2 Hz) ppm. ¹⁵N NMR (40.6 MHz, (CD₃)₂SO): δ = 2.1 (t, *J* = 2.2 Hz, 1N), -72.0 (s, 1N), -108.1 (d, *J* = 17.5 Hz, 1N), -120 (s, 1N), -337.5 (t, *J* = 84.6 Hz, 1N) ppm. IR (ATR): $\tilde{\nu}$ = 3387 (w), 3310 (w), 3237 (w), 3177 (w), 3049 (w), 2996 (w), 2005 (w), 1633 (w), 1565 (w), 1442 (w), 1409 (w), 1369 (w), 1213 (w), 1027 (w), 983 (w), 820 (w), 759 (w), 711 (w), 533 (w) 464 (w); Raman (1074 mW): $\tilde{\nu}$ = 3310 (w), 3047 (w), 2994 (m), 1544 (w), 1463 (w), 1410 (w), 1234 (w), 1212 (w), 1105 (w), 1088 (w), 1022 (w), 986 (s), 713 (w), 661 (w), 467 (m), 339 (w), 294 (w), 142 (s), 115 (m) 102 (s); Anal. Calcd for C₂H₄FN₅: C, 20.52; H, 3.44. Found: C, 20.21; H, 3.34; HRMS (DEI) *m/z*: [M] Calcd for C₂H₄FN₅ 117.0451; Found: 117.0443.

2-Fluoromethyltetrazole (9a)

1*H*-5*H*-tetrazole (0.83 mg, 11.8 mmol) was solved in acetone (35 mL) and potassium carbonate (0.82 g, 5.70 mmol) was added in one portion. After 30 min, fluoroiodomethane (0.8 mL, 11.8 mmol) was added dropwise and refluxed overnight. After the precipitate was filtered off, the solvent distilled off. The crud liquid product was distilled in high vacuum to obtain **9a** as a colorless liquid (0.145 g, 12%). M.p. 0 °C; B.p. 160 °C; ¹H NMR (400 MHz, CDCl₃): δ = 8.09 (s, 1H), 5.60 (d, *J* = 50.0 Hz, 2H) ppm. ¹⁹F{¹H} NMR (376 MHz, CDCl₃): δ = -171.2 (s) ppm. ¹⁹F NMR (376 MHz, CDCl₃): δ = -171.2 (t, *J* = 50.0 Hz) ppm. ¹³C{¹H} NMR (101 MHz, CDCl₃): δ = 103.2, 34.8 (d, *J* = 209.5 Hz) ppm. ¹⁵N NMR (40.6 MHz, CDCl₃): δ = 5.5 (s, 1N), -40.4 (d, *J* = 11.9 Hz, 1N), -73.6 (d, *J* = 15.1 Hz, 1N), -96.9 (dd, *J* = 17.3 Hz, 6.4 Hz, 1N) ppm. IR (ATR): $\tilde{\nu}$ = 3150 (w), 3058 (w), 3000 (w), 2404 (w), 2361 (w), 2129 (w), 1704 (w), 1545 (w), 1461 (w), 1403 (m), 1367 (s), 1323 (w), 1283 (s), 1224 (m), 1184 (s), 1118 (m), 1046 (s), 1019 (s), 995 (s), 890 (m), 768 (s), 707 (s), 680 (s); Raman (1074 mW): $\tilde{\nu}$ = 3153 (m), 3056 (w), 3001 (s), 2921 (w), 1461 (m), 1403 (m), 1370 (m), 1320 (m), 1285 (s), 1226 (m), 1186 (m), 1120 (w), 1053 (w), 1023 (m), 998 (s), 772 (m), 683 (m), 440 (m), 156 (s); HRMS (GC/EI) *m/z*: [M+H] Calcd for C₂H₄FN₄ 103.0420; Found: 103.0414.

13.6 References

- [1] L. An, Y.-L. Xiao, Q.-Q. Min, X. Zhang, *Angew. Chem., Int. Ed.* **2015**, *54*, 9079–9083.
- [2] a) K. Makino, H. Yoshioka, Institute of Physical and Chemical Research, JP63179866A, **1988**; b) Y. L. Chen, Pfizer Inc., EP276942A1, **1988**.
- [3] K. Masuda, S. Kida, N. Yoshikawa, M. Katou, T. Kato, M. Nakajima, E. Kojima, M. Yonehara, Shionogi & Co. Ltd., WO2011074560A1, **2011**.
- [4] J. Stehouwer, M. Goodman, C. Kilts, C. Nemeroff, Emory University, WO2010096426A2, **2010**.

- [5] Q.-H. Zheng, M. Gao, B. H. Mock, S. Wang, T. Hara, R. Nazih, M. A. Miller, T. J. Receveur, J. C. Lopshire, W. J. Groh, D. P. Zipes, G. D. Hutchins, T. R. DeGrado, *Bioorg. Med. Chem. Lett.* **2007**, *17*, 2220–2224.
- [6] M. Reichel, J. Martens, E. Woellner, L. Huber, A. Kornath, K. Karaghiosoff, *Eur. J. Inorg. Chem.* **2019**, *2019*, 2530–2534.
- [7] H. Boehme, M. Hilp, *Chem. Ber.* **1970**, *103*, 104–111.
- [8] W. Zhang, L. Zhu, J. Hu, *Tetrahedron* **2007**, *63*, 10569–10575.
- [9] K. G. Grozinger, R. W. Kriwacki, S. F. Leonard, T. P. Pitner, *J. Org. Chem.* **1993**, *58*, 709–713.
- [10] X.-N. Hua, W.-Q. Liao, Y.-Y. Tang, P.-F. Li, P.-P. Shi, D. Zhao, R.-G. Xiong, *J. Am. Chem. Soc.* **2018**, *140*, 12296–12302.
- [11] K. Makino, H. Yoshioka, Institute of Physical and Chemical Research, JP63179866A, **1988**.
- [12] a) M. Rueda-Becerril, C. Chatalova Sazepin, J. C. T. Leung, T. Okbinoglu, P. Kennepohl, J.-F. Paquin, G. M. Sammis, *J. Am. Chem. Soc.* **2012**, *134*, 4026–4029; b) F. Yin, Z. Wang, Z. Li, C. Li, *J. Am. Chem. Soc.* **2012**, *134*, 10401–10404; c) K. Makino, H. Yoshioka, *J. Fluorine Chem.* **1987**, *35*, 677–683.
- [13] M. Reichel, J. Martens, C. C. Unger, K. Karaghiosoff, *Phosphorus, Sulfur Silicon Relat. Elem.* **2019**, *194*, 467–468.
- [14] F. H. Allen, O. Kennard, D. G. Watson, L. Brammer, A. G. Orpen, R. Taylor, *J. Chem. Soc., Perkin Trans. 2* **1987**, S1–S19.
- [15] Z.-J. Quan, R.-G. Ren, X.-D. Jia, Y.-X. Da, Z. Zhang, X.-C. Wang, *Tetrahedron* **2011**, *67*, 2462–2467.
- [16] K. Zheng, C. Yao, *Shiyong Huagong* **2004**, *33*, 145–148.
- [17] C. Zhang, X. Xue, Y. Cao, Y. Zhou, H. Li, J. Zhou, T. Gao, *CrystEngComm* **2013**, *15*, 6837–6844.
- [18] T. Steiner, *Angew. Chem., Int. Ed.* **2002**, *41*, 48–76.
- [19] G. Laus, A. Schwaerzler, G. Bentivoglio, M. Hummel, V. Kahlenberg, K. Wurst, E. Kristeva, J. Schutz, H. Kopacka, C. Kreutz, G. Bonn, Y. Andriyko, G. Nauer, H. Schottenberger, *Z. Naturforsch., B: Chem. Sci.* **2008**, *63*, 447–464.
- [20] M. Lissel, S. Schmidt, B. Neumann, *Synthesis* **1986**, 382–383.
- [21] M. Feller, K. Lux, A. Kornath, *Eur. J. Inorg. Chem.* **2015**, *2015*, 5357–5362.
- [22] a) H. Tian, Z. Yu, A. Hagfeldt, L. Kloo, L. Sun, *J. Am. Chem. Soc.* **2011**, *133*, 9413–9422; b) J. Sarasin, E. Wegmann, *Helv. Chim. Acta* **1924**, *7*, 720–723.
- [23] M. C. Davis, D. A. Parrish, *Synth. Commun.* **2008**, *38*, 3909–3918.
- [24] A. Fuerstner, M. Alcarazo, R. Goddard, C. W. Lehmann, *Angew. Chem., Int. Ed.* **2008**, *47*, 3210–3214.
- [25] a) T. M. Klapoetke, C. M. Sabate, A. Penger, M. Rusan, J. M. Welch, *Eur. J. Inorg. Chem.* **2009**, 880–896; b) Y.-H. Joo, J. n. M. Shreeve, *Org. Lett.* **2008**, *10*, 4665–4667.
- [26] a) M. H. H. Wurzenberger, N. Szimhardt, J. Stierstorfer, *Inorg. Chem.* **2018**, *57*, 7940–7949; b) M. H. H. Wurzenberger, N. Szimhardt, J. Stierstorfer, *J. Am. Chem. Soc.* **2018**, *140*, 3206–3209; c) M. Reichel, B. Krumm, K. Karaghiosoff, *J. Fluorine Chem.* **2019**, *226*, 109351–109355.

- [27] a) S. V. Voitekhovich, A. S. Lyakhov, V. E. Matulis, L. S. Ivashkevich, O. A. Ivashkevich, *Polyhedron* **2019**, *162*, 100–110; b) E. Vieira, J. Huwyler, S. Jolidon, F. Knoflach, V. Mutel, J. Wichmann, *Bioorg. Med. Chem. Lett.* **2005**, *15*, 4628–4631; c) C. Stadler, J. Daub, J. Koehler, R. W. Saalfrank, V. Coropceanu, V. Schuenemann, C. Ober, A. X. Trautwein, S. F. Parker, M. Poyraz, T. Inomata, R. D. Cannon, *J. Chem. Soc., Dalton Trans.* **2001**, 3373–3383.
- [28] a) K. Karaghiosoff, T. M. Klapoetke, P. Mayer, C. M. Sabate, A. Penger, J. M. Welch, *Inorg. Chem.* **2008**, *47*, 1007–1019; b) R. A. Henry, W. G. Finnegan, *J. Am. Chem. Soc.* **1954**, *76*, 923–926; c) T. M. Klapoetke, N. K. Minar, J. Stierstorfer, *Polyhedron* **2009**, *28*, 13–26.
- [29] J. H. Bryden, *Acta Crystallogr.* **1953**, *6*, 669–670.
- [30] T. M. Klapötke, B. Krumm, F. Xaver Steemann, G. Steinhauser, *Safety Science* **2010**, *48*, 28–34.
- [31] a) www.reichel-partner.de; b) Test methods according to the UN Manual of Tests and Criteria, Recommendations on the Transport of Dangerous Goods, N. Y. United Nations Publication, Geneva, 4th revised ed., 2003: Impact: insensitive >40 J, less sensitive ≥ 35 J, sensitive ≥ 4 J, very sensitive ≤ 3 J; friction: insensitive >360 N, less sensitive: 360 N, sensitive <360 N and >80 N, very sensitive ≤ 80 N, extremely sensitive ≤ 10 N.
- [32] GAUSSIAN 09, revision C.01, G. W. T. M. J. Frisch, H. B. Schlegel, G. E. Scuseria, M. A. Robb, J. R. Cheeseman, G. Scalmani, V. Barone, B. Mennucci, G. A. Petersson, H. Nakatsuji, M. Caricato, X. Li, H. P. Hratchian, A. F. Izmaylov, J. Bloino, G. Zheng, J. L. Sonnenberg, M. Hada, M. Ehara, K. Toyota, R. Fukuda, J. Hasegawa, M. Ishida, T. Nakajima, Y. Honda, O. Kitao, H. Nakai, T. Vreven, J. A. Montgomery, Jr., J. E. Peralta, F. Ogliaro, M. Bearpark, J. J. Heyd, E. Brothers, K. N. Kudin, V. N. Staroverov, R. Kobayashi, J. Normand, K. Raghavachari, A. Rendell, J. C. Burant, S. S. Iyengar, J. Tomasi, M. Cossi, N. Rega, J. M. Millam, M. Klene, J. E. Knox, J. B. Cross, V. Bakken, C. Adamo, J. Jaramillo, R. Gomperts, R. E. Stratmann, O. Yazyev, A. J. Austin, R. Cammi, C. Pomelli, J. W. Ochterski, R. L. Martin, K. Morokuma, V. G. Zakrzewski, G. A. Voth, P. Salvador, J. J. Dannenberg, S. Dapprich, A. D. Daniels, Ö. Farkas, J. B. Foresman, J. V. Ortiz, J. Cioslowski, D. J. Fox, Gaussian, Inc., Wallingford, CT, 2009;
- [33] a) M. Suceca, *Propellants, Explos., Pyrotech.* **1999**, *24*, 280–285; b) M. Suceca, *Propellants, Explos., Pyrotech.* **1991**, *16*, 197–202.
- [34] a) O. Gryzkiewicz-Trochimowski, *Compt. rend.* **1958**, *246*, 2627–2629; b) E. Oliveri-Mandala, T. Passalacqua, *Gazz. Chim. Ital.* **1914**, *43*, 465–475.

13.7 Supporting Information

Table 1: Structure refinement data of compound **4** (left) and hydroxymethylphthalimide (right).

Empirical formula	C ₉ H ₆ F N O ₂	C ₉ H ₇ N O ₃
Formula weight	179.15	177.16
Temperature	123(2) K	143(2) K
Wavelength	0.71073 Å	0.71073 Å
Crystal system	Monoclinic	Monoclinic

Space group	<i>P2₁</i>	<i>P2₁</i>
Unit cell dimensions	a = 5.8214(11) Å b = 6.4085(9) Å c = 10.3135(13) Å α = 90° β = 97.131(15)° γ = 90°	a = 5.5869(3) Å b = 6.6791(4) Å c = 10.4013(6) Å α = 90° β = 96.387(6)° γ = 90°
Volume	381.78(10) Å ³	385.72(4) Å ³
Z	2	2
Density (calculated)	1.558 mg/m ³	1.525 mg/m ³
Absorption coefficient	0.127 mm ⁻¹	0.117 mm ⁻¹
F(000)	184	184
Crystal size	0.150 x 0.100 x 0.100 mm ³	0.150 x 0.100 x 0.100 mm ³
Theta range for data collection	4.261 - 28.269°	4.356 - 28.281°
Index ranges	-7 ≤ h ≤ 4, -7 ≤ k ≤ 8, -13 ≤ l ≤ 13	-7 ≤ h ≤ 6, -8 ≤ k ≤ 8, -13 ≤ l ≤ 13
Reflections collected	3314	3164
Independent reflections	1773 [R _{int} = 0.0354]	1717 [R _{int} = 0.0262]
Data / restraints / parameters	1773 / 1 / 123	1717 / 1 / 127
Goodness-of-fit on F ²	1.008	1.045
Final R indices [I > 2σ(I)]	R ₁ = 0.0434, wR ₂ = 0.0844	R ₁ = 0.0363, wR ₂ = 0.0693
R indices (all data)	R ₁ = 0.0604, wR ₂ = 0.0932	R ₁ = 0.0432, wR ₂ = 0.0725
Largest diff. peak and hole	0.176 and -0.215 e Å ⁻³	0.205 and -0.149 e Å ⁻³

Table 2: Structure refinement data of 1-fluoromethyl-2-methyl-imidazole (left) and 1-fluoromethyl-2-methyl-imidazole hydrate (right).

Empirical formula	C ₅ H ₇ F N ₂	C ₅ H ₉ F N ₂ O
Formula weight	114.13	132.14
Temperature	143(2) K	143(2) K
Wavelength	0.71073 Å	0.71073 Å
Crystal system	Orthorhombic	Monoclinic
Space group	<i>P2₁2₁2₁</i>	<i>P2₁/c</i>
Unit cell dimensions	a = 6.7291(5) Å b = 7.3965(4) Å c = 11.5727(7) Å α = 90° β = 90° γ = 90°	a = 4.4208(4) Å b = 13.1213(8) Å c = 11.6886(8) Å α = 90° β = 91.772(7)° γ = 90°
Volume	575.99(6) Å ³	677.69(9) Å ³
Z	4	4
Density (calculated)	1.316 mg/m ³	1.295 mg/m ³
Absorption coefficient	0.106 mm ⁻¹	0.110 mm ⁻¹
F(000)	240	280
Crystal size	0.200 x 0.100 x 0.100 mm ³	0.200 x 0.100 x 0.100 mm ³
Theta range for data collection	4.094 - 30.233°	4.613 - 28.280°

Index ranges	-9≤h≤9, -9≤k≤10, -16≤l≤15	-5≤h≤4, -17≤k≤17, -15≤l≤14
Reflections collected	5115	5569
Independent reflections	1573 [R _{int} = 0.0484]	1667 [R _{int} = 0.0342]
Data / restraints / parameters	1573 / 0 / 82	1667 / 0 / 122
Goodness-of-fit on F ²	1.028	1.066
Final R indices [I>2σ(I)]	R ₁ = 0.0448, wR ₂ = 0.1016	R ₁ = 0.0391, wR ₂ = 0.0871
R indices (all data)	R ₁ = 0.0592, wR ₂ = 0.1118	R ₁ = 0.0571, wR ₂ = 0.1003
Largest diff. peak and hole	0.163 and -0.171 e Å ⁻³	0.166 and -0.163 e Å ⁻³

Table 3: Structure refinement data of bisfluoromethyl-2-methyl-imidazole iodide (left) and 1-fluoromethyl-5-aminotetrazole (right).

Empirical formula	C ₆ H ₉ F ₂ I N ₂	C ₂ H ₄ F N ₅
Formula weight	274.05	117.10
Temperature	133(2) K	143(2) K
Wavelength	0.71073 Å	0.71073 Å
Crystal system	Orthorhombic	Triclinic
Space group	<i>Pbca</i>	<i>P</i> -1
Unit cell dimensions	a = 10.9927(2) Å b = 7.4181(2) Å c = 22.0714(5) Å α = 90° β = 90° γ = 90°	a = 5.9640(8) Å b = 11.3520(11) Å c = 13.9347(11) Å α = 100.396(7)° β = 91.285(9)° γ = 96.475(9)°
Volume	1799.81(7) Å ³	921.14(17) Å ³
Z	8	8
Density (calculated)	2.023 mg/m ³	1.689 mg/m ³
Absorption coefficient	3.532 mm ⁻¹	0.152 mm ⁻¹
F(000)	1040	480
Crystal size	0.200 x 0.100 x 0.050 mm ³	0.200 x 0.100 x 0.100 mm ³
Theta range for data collection	4.132 - 30.498°	3.441 - 28.856°
Index ranges	-15≤h≤15, -10≤k≤10, -31≤l≤31	-7≤h≤7, -14≤k≤15, -17≤l≤17
Reflections collected	33060	6967
Independent reflections	2737 [R _{int} = 0.0461]	4138 [R _{int} = 0.0358]
Data / restraints / parameters	2737 / 0 / 116	4138 / 0 / 353
Goodness-of-fit on F ²	1.080	1.012
Final R indices [I>2σ(I)]	R ₁ = 0.0222, wR ₂ = 0.0446	R ₁ = 0.0562, wR ₂ = 0.0971
R indices (all data)	R ₁ = 0.0321, wR ₂ = 0.0484	R ₁ = 0.1136, wR ₂ = 0.1247
Largest diff. peak and hole	1.272 and -0.503 e Å ⁻³	0.273 and -0.303 e Å ⁻³

Table 4: Structure refinement data of 2-fluoromethyl-5-aminotetrazole (left) and 1-fluoromethyl-5-aminotetrazole CuClO₃ complex (right).

Empirical formula	C ₂ H ₄ F N ₅	C ₂ H ₄ F N ₅ · CuClO ₃
Formula weight	117.10	498.30
Temperature	133(2) K	133(2) K

Wavelength	0.71073 Å	0.71073 Å
Crystal system	Monoclinic	Hexagonal
Space group	$P2_1/n$	$P6_3$
Unit cell dimensions	a = 4.0877(3) Å b = 14.1054(8) Å c = 8.0338(4) Å $\alpha = 90^\circ$ $\beta = 92.394(5)^\circ$ $\gamma = 90^\circ$	a = 12.3154(5) Å b = 12.3154(5) Å c = 6.6489(9) Å $\alpha = 90^\circ$ $\beta = 90^\circ$ $\gamma = 120^\circ$
Volume	462.81(5) Å ³	873.33(14) Å ³
Z	4	2
Density (calculated)	1.681 mg/m ³	1.895 mg/m ³
Absorption coefficient	0.151 mm ⁻¹	1.484 mm ⁻¹
F(000)	240	500
Crystal size	0.200 x 0.100 x 0.100 mm ³	0.100 x 0.020 x 0.010 mm ³
Theta range for data collection	3.846 - 30.494°	3.308 - 26.368°
Index ranges	-5 ≤ h ≤ 5, -20 ≤ k ≤ 20, -11 ≤ l ≤ 11	-15 ≤ h ≤ 15, -15 ≤ k ≤ 15, -8 ≤ l ≤ 8
Reflections collected	8680	13355
Independent reflections	1407 [R _{int} = 0.0512]	1202 [R _{int} = 0.0456]
Data / restraints / parameters	1407 / 0 / 89	1202 / 1 / 88
Goodness-of-fit on F ²	1.073	1.151
Final R indices [I > 2σ(I)]	R ₁ = 0.0410, wR ₂ = 0.0996	R ₁ = 0.0255, wR ₂ = 0.0669
R indices (all data)	R ₁ = 0.0509, wR ₂ = 0.1087	R ₁ = 0.0281, wR ₂ = 0.0685
Largest diff. peak and hole	0.259 and -0.241 e Å ⁻³	0.771 and -0.195 e Å ⁻³

14 Appendix

14.1 List of Abbreviations

A	Hydrogen bond acceptor
Å	Angström (10 ⁻¹⁰ m)
°C	Degree Celsius
D	Hydrogen bond donor
δ	Chemical shift in ppm
DCM	Dichloromethane
EI	Electron ionization
ESI	Electrone Spray Ionisation
FAB	Fast Atom Bombardement
FMN	Fluoromethyl Nitrate
FMP	Fluoromethyl Perchlorate
g	gram
Goof	Goodness of fit
h	hour
Hz	Hertz (s ⁻¹)
<i>in vacuo</i>	Underpressure
IR	Infrared
K	Kelvin

m	medium (IR/Raman)
mL	milliliter
mm	millimeter
MN	Methyl Nitrate
MP	Methyl Perchlorate
v	wavenumber (cm ⁻¹)
NMR	Nuclear Magnetic Resonance
ppm	parts per million
q	quartet (NMR)
s	strong (IR/Raman), singlet (NMR)
t	triplet (NMR)
w	weak (IR/Raman)

14.2 Computations

Using the atomization energy method, based on the atomization energies in Table 1, the enthalpy of formation of the molecule in the gas phase can first be calculated.^[1]

$$\Delta H_{f(gas,298K,Molecule)}^{\circ} = H_{(Molecule,298K)} - \sum n \cdot H_{(Atom,298K)}^{\circ} + \sum n \cdot \Delta H_{f(Atom,298K)}^{\circ}$$

$\Delta H_{f(gas,298K,Molecule)}^{\circ}$ = Enthalpy of formation of the gas phase species molecule

$H_{Molecule,298K}$ = Total energy of the gas phase (formation from atomic nuclei and electrons)

$H_{(Atom,298K)}^{\circ}$ = CBS – 4M electronic enthalpies

$\Delta H_{f(Atom,298K)}^{\circ}$ = Standard enthalpy of formation of gaseous atoms

n = atomic number

Table 1: CBS-4M electronic enthalpies and literature-known standard enthalpies of formation of gaseous atoms.

	$H_{(Atom, 298 K)}^{\circ}$ [a.u.]	$\Delta H_{f(Atom,298 K)}^{\circ}$ [kJ mol ⁻¹]
H	-0.500991	217.998
C	-37.786156	716.68
N	-54.522462	472.68
O	-74.991202	249.18
F	-99.649394	79.38

Enthalpy of sublimation / vaporization:

In order to obtain the energy of formation at the condensed (liquid/ solid) phase, the corresponding enthalpy of sublimation must first be calculated (Trouton's Rule).^[2]

$$\Delta H_v^{\circ} = 90 \cdot T_{boil}$$

ΔH_v° = Enthalpy of vaporisation

T_{boil} = Boiling point of the compound

Heat of formation (Enthalpy of formation):

The heat of formation of the compound results from the subtraction of the heat of formation vaporization from the heat of formation of the gas phase species.^[2]

$$\Delta H^{\circ}_{f(\text{liquid})} = \Delta H^{\circ}_{f(\text{gas},298\text{K},\text{Molecule})} - \Delta H^{\circ}_v$$

$\Delta H^{\circ}_{f(\text{liquid})}$ = Heat of formation of the liquid product

The results of the calculation for the heat of formation are shown in Table 2. The theoretical value of MN is in good agreement compared to the experimentally determined value of $\Delta H^{\circ}_{f(\text{liquid})}$ of MN ($-156.3 \text{ kJ mol}^{-1}$).^[3]

Table 2: Heat of formation calculation results.

M	$H_{(\text{molecule},298\text{K})}$ [a. u.]	$\Delta H^{\circ}_{f(\text{gas},298\text{K},\text{molecule})}$ [kJ mol^{-1}]	ΔH°_v [kJ mol^{-1}]	$\Delta H^{\circ}_{f(\text{liquid})}$ [kJ mol^{-1}]	Δn	ΔU_f° [kJ mol^{-1}]
FMN	-418.994048	-331.9	29.8	-361.7	-3.5	-353.1
MN	-319.822235	-131.8	30.4	-162.3	-3.5	-153.6

14.3 References

- [1] a) L. A. Curtiss, K. Raghavachari, P. C. Redfern, J. A. Pople, *J. Chem. Phys.* **1997**, *106*, 1063-1079; b) E. F. C. Byrd, B. M. Rice, *J. Phys. Chem. A* **2006**, *110*, 1005–1013.
- [2] T. M. Klapötke, *Chemie der hochenergetischen Materialien*, De Gruyter, **2009**.
- [3] D. R. Lide, *CRC Handbook of Chemistry and Physics, Standard Thermodynamic Properties of Chemical Substances, Vol. 90*, Taylor and Francis, Boca Raton, FL, **2009**.

14.4 List of Publications

- 1) **M. Reichel**, M. Egenhöfer, B. Krumm, K. Karaghiosoff, *Z. Anorg. Allg. Chem.* **2020**, *646*, 328–331.
- 2) **M. Reichel**, K. Karaghiosoff, *Angew. Chem. Int. Ed.* **2020**, accepted article DOI: 10.1002/anie.201913175
- 3) **M. Reichel**, D. Dosch, T. M. Klapötke, K. Karaghiosoff *J. Am. Chem. Soc.* **2019**, *141*, 19911–19916.
- 4) **M. Reichel**, B. Krumm, S. Blomeyer, Y. Vishnevskiy, J. Schwabedissen, H.-G. Stämmler, K. Karaghiosoff, N. W. Mitzel *Angew. Chem., Int. Ed.* **2019**, *58*, 18557–18561.
- 5) **M. Reichel**, B. Krumm, K. Karaghiosoff *J. Fluorine Chem.* **2019**, *226*, 109351–109355.
- 6) **M. Reichel**, J. Martens, E. Wöllner, L. Huber, A. Kornath, K. Karaghiosoff *Eur. J. Inorg. Chem.* **2019**, 2530–2534.

7) **M. Reichel**, J. Martens, C.C. Unger, K. Karaghiosoff *Phosphorus, Sulfur Silicon and the Related Elements* **2018**, 467–468.

8) M. A. Althoff, J. Martens, **M. Reichel**, M. Metzulat, T. M. Klapötke, K. Karaghiosoff *Z. Kristallogr.* **2019**, 234, 613–621.

9) M. A. Althoff, A. Bertsch, J. Martens, **M. Reichel**, M. Metzulat, K. Karaghiosoff *Phosphorus, Sulfur Silicon and the Related Elements* **2018**, 307–308.

14.5 List of Presentations

1) **M. Reichel**, C. Unger, S. Dubrovnik, A. Roidl, K. Karaghiosoff *Tuning the toxicity of phosphonium based biocides using the bioisosteric fluoromethyl moiety*, Conference PBSi-Phosphorus, Boron, Silicon, Italy, Rome, **2019**. Poster presenter.

2) **M. Reichel**, K. Karaghiosoff *Large Scale Synthesis and Properties of a Phosphorus Based Fluoromethylating Agent*, Conference ICHAC-International Conference on Heteroatom Chemistry, Czech Republic, Prague, **2019**. Poster presenter.

3) **M. Reichel**, F. Saunders, J. Martens, K. Karaghiosoff *New coordination polymeres from tris(2-cyanoethyl)phosphine and Cu(I)X (X = Cl, Br, CN)*, KCT-Koordinationschemie Treffen, Deutschland, München, **2019**. Poster presenter.

4) **M. Reichel** *Fluoromethyl nitrate – The Influence of Fluorine on Small Molecules*, Deutscher Fluortag, Deutschland, Schmitten, **2018**. Oral presenter.

5) **M. Reichel**, J. Martens, C. C. Unger, K. Karaghiosoff *Reactivity of Phosphines with Iodomethane Analogue Fluoroiodomethane*, ICPC-International Conference on Phosphorus Chemistry, Hungary, Budapest, **2018**. Poster presenter.

6) **M. Reichel** *Modern NMR Analytics*, Symposium fachübergreifender, moderner Analytik – Innovative Nutzung analytischer Verfahren, Hexal AG, Deutschland, Holzkirchen, **2017**. Oral presenter.

7) C. Kirst, **M. Reichel**, K. Karaghiosoff *Neue Di(2-Pyridyl)Keton-Komplexe mit Cu(I)-Bildung von zyklischen sechsgliedrigen seitenverknüpften Cu₃X₃-Clustern (X = Hal)*, KCT-Koordinationschemie Treffen, Deutschland, München, **2019**. Poster presentation.

8) M. Althoff, A. Bertsch, J. Martens, **M. Reichel**, M. Metzulat, K. Karaghiosoff *Thiono-Thiolo Rearrangement vs. In-Situ Decomposition Reactions*. ICPC-International Conference on Phosphorus Chemistry, Hungary, Budapest, **2018**. Poster presentation.